Molecular effects of fermentation in the gut and its relevance for metabolism and satiety

Daniëlle Haenen

Thesis committee

Promotor
Prof. Dr Michael R. Müller
Professor of Nutrition, Metabolism and Genomics
Wageningen University

Co-promotors
Dr Guido J.E.J. Hooiveld
Assistant professor, Division of Human Nutrition
Wageningen University

Prof. Dr Bas Kemp
Professor of Adaptation Physiology
Wageningen University

Other members
Prof. Dr Renger F. Witkamp, Wageningen University
Prof. Dr Wouter H. Hendriks, Wageningen University
Prof. Dr Michiel Kleerebezem, Wageningen University
Prof. Dr Albert K. Groen, University of Groningen

Molecular effects of fermentation in the gut and its relevance for metabolism and satiety

Daniëlle Haenen

Abstract

Dietary fibres, the edible parts of plants that are resistant to digestion and absorption in the human small intestine, were shown to be important in the prevention of obesity and the metabolic syndrome. This association can partially be attributed to a fibre-induced increase in satiety. Dietary fibres can be fermented by bacteria, collectively referred to as the microbiota, in the large intestine (i.e. caecum and colon), resulting in the production of the short-chain fatty acids (SCFAs) acetate, propionate and butyrate. Part of the effect of dietary fibres on satiety is thought to be mediated via the production of SCFAs.

The objective of the research described in this thesis was to reveal the effects of fermentation in the large intestine using comprehensive approaches with focus on metabolism and satiety.

The effect of 2-wk-consumption of resistant starch (RS), a dietary fibre highly fermentable by the gut microbiota, was studied in 2 pig experiments. In the first experiment, performed in adult female pigs, intestinal samples were collected from different areas of the gastrointestinal tract to measure luminal microbiota composition, luminal SCFA concentrations and the expression of host genes involved in SCFA uptake, SCFA signalling, and satiety regulation in mucosal tissue. In an additional study the effects of RS were investigated in young growing pigs fitted with a cannula in the proximal colon for repeated collection of tissue biopsies for whole-genome expression profiling and luminal content for measurement of SCFA concentrations and microbiota composition. To limit inter-individual variation, the RS diet was provided to the pigs in a 2 x 2 crossover design for 2 wk per diet. Furthermore, the behaviour of the pigs was monitored and the postprandial plasma response of satiety-related hormones and metabolites was measured at the end of each 2 wk period using repeated peripheral blood sampling via catheters.

In order to determine the potential differences in post-prandial plasma protein profiles, minipigs were assigned to a control (C) diet or a diet containing the bulky fibre lignocellulose (LC), the viscous and fermentable fibre pectin (PEC) or RS for periods of 8 d in a 4 x 4 Latin square design. Portal and carotid blood samples were collected from catheters on d 8 of each treatment, both before and at several time points after an ad libitum morning meal.

Male C57BL/6J mice were used to study the effect of background diet and SCFAs on colonic gene expression. Mice were fed a semi-synthetic low fat or high fat diet starting 2 wk before the treatment period. During treatment, mice received a

rectal infusion of either an acetate, propionate, butyrate, or a control saline solution on 6 consecutive days, after which colon was collected to perform comprehensive gene expression profiling.

RS enhanced satiety based on behavioural observations, as RS-fed pigs showed less feeder-directed and drinking behaviours than pigs fed a digestible starch (DS) diet. In both caecum and colon, differences in microbiota composition were observed between RS-fed pigs and DS-fed pigs. In the colon these included the induction of the healthy gut-associated butyrate-producing *Faecalibacterium prausnitzii*, whereas potentially pathogenic members of the *Gammaproteobacteria* were reduced in relative abundance in RS-fed pigs. Caecal and colonic SCFA concentrations were significantly higher in RS-fed pigs. Gene expression profiling of the proximal colon revealed a shift upon RS consumption from the regulation of immune response towards lipid and energy metabolism. The nuclear receptor *PPARG* was identified as a potential key upstream regulator. At plasma level, SCFA concentrations were higher in RS-fed pigs throughout the day. Postprandial glucose, insulin and glucagon-like peptide 1 (GLP-1) responses were lower in RS-fed than in DS-fed pigs, whereas triglyceride levels were higher in RS-fed than in DS-fed pigs.

In minipigs, plasma protein profiles were found to be most similar with C and LC consumption and with PEC and RS consumption, indicating that the consumption of diets with fermentable fibres results in a different plasma protein profile compared to a diet containing non-fermentable fibres or a diet without fibres.

In mice we observed that dietary fat content had a major impact on colonic gene expression responses to SCFAs, especially after propionate treatment. Moreover, the diet- and SCFA-dependent gene expression changes pointed towards the modulation of several metabolic processes. Genes involved in oxidative phosphorylation, lipid catabolism, lipoprotein metabolism and cholesterol transport were suppressed by acetate and butyrate treatment, whereas propionate resulted in changes in fatty acid and sterol biosynthesis, and in amino acid and carbohydrate metabolism. Furthermore, SCFA infusion on the high fat diet background appeared to partially reverse the gene expression changes induced by high fat feeding without SCFA infusion.

In conclusion, this thesis showed that the consumption of RS changed the microbiota composition in the colonic lumen, with a decrease in the abundance of potentially pathogenic bacteria and an increase in the abundance of SCFA-producing populations. Furthermore, colonic gene expression changes were observed after RS consumption and after colonic administration of SCFAs. With both treatments,

among the changes in the transcriptional profile of the host were adaptations in metabolic processes, such as energy and lipid metabolism, and immune response. We also showed that fat content in the background diet had a major impact on gene expression responses to SCFAs in colon. Overall, this thesis supports the implementation of fermentable dietary fibres into the human diet to improve colonic health and to reduce energy intake and body weight gain, which ultimately may prevent obesity and type 2 diabetes. Additional research is required to further elucidate the mechanisms via which fermentable dietary fibres can improve human health.

Table of contents

General introduction and outline

Background

Obesity and metabolic syndrome

Obesity has become a major public health issue, affecting a large part of the global population. According to the World Health Organization, the worldwide prevalence of obesity nearly doubled between 1980 and 2008, with more than 1.4 billion adults (age ≥20) being overweight (BMI ≥25) in 2008. Of these adults, over 200 million men and nearly 300 million women were obese (BMI ≥30) (1). In Europe, over 50% of men and women were overweight in 2008, of which approximately 23% of women and 20% of men were obese (2). In addition, overweight and obesity cause more than 1 million deaths and 12 million life-years of ill health each year, and obesity is responsible for up to 6% of national health care costs in Europe (3).

Obesity is associated with the metabolic syndrome, a combination of risk factors that act together and can ultimately lead to chronic diseases such as cardiovascular disease and type 2 diabetes. The main risk factors are central obesity (defined as waist circumference), dyslipidemia, increased blood pressure and increased fasting plasma glucose. In the United States, the prevalence of metabolic syndrome has increased as the prevalence of obesity increased, affecting over 30% of the population (4, 5). The development of metabolic syndrome is a complex process involving various lifestyle factors, of which diet is a major one (6). During the agricultural revolution and industrialization of food production, the composition of foods dramatically changed, which has been linked to some of the problems of overeating. Modification of dietary patterns can have tremendous impact on health outcomes.

Dietary fibres

Dietary fibre is an extensively studied food component regarding its potential health benefits. Fibres have been shown to be protective against cardiovascular disease and important for normal laxation (7). Fibres are mostly known for their importance for colonic health and functionality because of their fermentation by bacteria in the colon. In addition, fibres are considered to be useful in the prevention of obesity and metabolic syndrome. A number of studies provided evidence that the consumption of dietary fibre increases insulin sensitivity (8, 9) and that it can help with the reduction of body weight in overweight and obese subjects (10, 11). Part of these observations can be attributed to effects on appetite control, since dietary fibre consumption has been linked to an increase in satiety (12-14).

Because there is no universally agreed and reliable method to quantify all of the dietary fibre components, there is still a lot of debate about its definition (15). A highly accepted definition was formulated by the American Association of Cereal

Chemists (AACC) in 2000: *Dietary fibre is the edible parts of plants or analogous carbohydrates that are resistant to digestion and absorption in the human small intestine with complete or partial fermentation in the large intestine. Dietary fibre includes polysaccharides, oligosaccharides, lignin, and associated plant substances. Dietary fibres promote beneficial physiological effects including laxation, and/or blood cholesterol attenuation, and/or blood glucose attenuation* (16).

Many different types of dietary fibre have been identified and characterised. One of the means by which fibres can be classified is according to their physicochemical properties. There are for instance viscous fibres, which form a gel-like paste in the stomach, bulky fibres with a high water-binding capacity and fibres that are highly fermentable by bacteria in the large intestine (17). Identification of the physicochemical properties of a fibre is essential, especially when studying satiety regulation.

Satiety

The modern Westernized human diets provide the majority of calories from fat and carbohydrates (18). These nutrients are rapidly digested and absorbed as fatty acids and monosaccharides in the small intestine and provide a relatively short period of satiety (19, 20). For developing nutritional advice regarding the control of food intake, knowledge on satiety regulation is required.

Satiety is defined as the state of fullness, resulting from the combined action of regulatory feedback mechanisms throughout the gastrointestinal tract. Variation in the regulation of satiety is caused by diet- and subject-related factors. Diet-related factors are for instance the nutritional composition of a diet and the physicochemical properties of food components. Examples of subject-related factors are level of energy expenditure and the presence of obesity or metabolic syndrome. Currently, the interplay between dietary feedback mechanisms and diet- and subject-related factors is poorly understood.

Satiety signals arise from multiple sites in the gastrointestinal tract. These nutrient sensing signals can be mediated by multiple signalling molecules including intestinal peptides, hormones and their corresponding receptors. Also post-absorptive actions of products of digestion and fermentation play an important role. The stomach and small intestine have been extensively studied, whereas information on the potential contribution of the large intestine, i.e. caecum and colon, to regulation of satiety is limited.

Dietary fibres can affect energy intake and satiety in several ways. First of all, fibres decrease the energy density of foods, which may reduce energy intake (21). In addition, it usually takes longer to chew food products with a high fibre content, which may enhance sensory satiety and reduce meal size (22). Moreover, fibres may

reduce intestinal passage rate, which slows down nutrient absorption and prolongs feelings of satiety (23). Fibres may also decrease energy absorption by reducing the bioavailability of nutrients (24). Last but not least, dietary fibres can be fermented by bacteria in the large intestine, which may result in a shift in composition and activity of the microbiota, and concomitant increased production of short-chain fatty acids (SCFAs). These SCFAs can enhance satiety via various mechanisms (25).

Satiety-related hormones

It has been suggested that gut hormones play a key role in appetite, satiety and glucose homeostasis. Examples of these hormones are amylin, cholecystokinin (CCK), ghrelin, glucose-dependent insulinotropic polypeptide (GIP) and pancreatic polypeptide (PP). These hormones may be influenced by specific dietary fibres. Numerous studies have been performed on the effect of dietary fibres on gut hormone release (26-30). Because this thesis primarily focusses on events occurring in the large intestine, the 2 main hormones that are released in the large intestine are described in more detail: glucagon-like peptide 1 (GLP-1) and peptide tyrosine-tyrosine (PPY).

GLP-1 and PYY are gut hormones released by endocrine L-cells in the distal small intestine and colon in response to food intake. Both hormones play an important role in the 'ileal brake', a mechanism that regulates the flow of nutrients from the stomach to the small intestine. This ileal brake eventually slows gastric emptying and promotes digestive activities to increase nutrient absorption. Furthermore, there is strong evidence that GLP-1 and PYY are involved in the regulation of satiety (20, 31, 32).

GLP-1 is an incretin hormone that enhances glucose-dependent insulin release, inhibits glucagon secretion, and increases pancreatic β-cell growth. Food intake results in a rapid increase in GLP-1 concentrations in plasma. A number of studies have shown that dietary fibres can modify this postprandial GLP-1 response. However, the direction and the degree of this changed response depend on the type and the amount of dietary fibre. Elevated (29), inhibited (33) and unaffected GLP-1 responses (34) have been reported.

Like GLP-1, PYY is involved in the regulation of insulin secretion and glucose homeostasis. Plasma concentrations of PYY increase after a meal and decrease upon fasting. PYY secretion already occurs before nutrients have reached the PYY-releasing cells and is proportional to caloric intake. Meal composition, including the presence of dietary fibre, also affects postprandial PYY release. However, the direction and the magnitude of the effect of fibres on PYY levels highly depend on the fibre type used (31).

Microbiota

The microorganisms that inhabit the intestine of an organism, including bacteria, viruses, fungi and Archaea, are collectively referred to as the gut microbiota. The human gut contains an enormous amount and variety of these microorganisms, including at least 10^{14} bacteria belonging to approximately 1000 species (35). The general awareness that the microbial composition is an important factor in health and disease is increasing. Modulation of microbial composition by probiotics was shown to attenuate the development of inflammatory bowel disease and irritable bowel syndrome (36). Besides the consumption of probiotics, faecal transplantation of microbiota from a healthy individual was found to be a useful therapy for these gastrointestinal disorders (37).

Evidence suggesting that gut microbiota are also highly important in the regulation of energy homeostasis and fat storage is accumulating (38, 39). For instance, it was shown that conventionally raised mice have 42% more total body fat than germ-free mice. After conventionalizing the germ-free mice, a 57% increase in total body fat was observed (40). In addition, germ-free mice were found to be protected from the development of obesity after consuming a high fat diet (41). The relationship between microbiota composition and fat storage was also studied in humans, showing that the Firmicutes/Bacteroidetes ratio is related to adiposity, as obese people have fewer Bacteroidetes compared to lean controls. In addition, the relative abundance of Bacteroidetes increased while the abundance of Firmicutes decreased with weight loss in obese subjects (42).

One of the main factors affecting intestinal microbiota composition is diet composition (35, 43-50). For example, mice consuming a Western-type diet rich in saturated fat had a different gut microbiota composition compared to mice consuming diets rich in unsaturated fat (51). It has also been reported that mice fed a high fat diet have reduced numbers of Bacteroidetes and increased numbers of Firmicutes and Proteobacteria (43). In turn, the microbial composition might determine how an individual responds to a diet. Recently, it was suggested that the human gut microbiome can be classified into so-called enterotypes. This finding indicates that a number of well-balanced symbiotic states between microbiota and host exist, which might respond differently to diet (52).

Although the total microbial profile of the intestine can provide information on the health status of the gut, the exact function of many microbial species is poorly understood. However, for some particular microbial groups the role in gut health is elucidated rather well. For instance, within the group of Proteobacteria several species are known to be pathogenic. These pathogenic bacteria include

1

Escherichia, *Salmonella*, and *Vibrio*. Among the bacteria known to be beneficial for health are Bifidobacteria and *Lactobacillus*, which are therefore frequently used as probiotics.

Microbiota can also be classified into saccharolytic and proteolytic bacteria, according to the substrates they preferably ferment. Saccharolytic bacteria metabolise carbohydrates, which mainly yields SCFAs, lactate, pyruvate, and ethanol. This process and especially the production of SCFAs is regarded as beneficial for the host (53). Proteolytic bacteria can metabolise undigested and endogenous proteins, peptides, and amino acids present in the large intestine. This process mainly occurs in the distal colon, where carbohydrates are depleted. The fermentation of proteins results in the production of metabolites such as SCFAs and branched-chain fatty acids, but also the potentially toxic substances ammonia, amines, phenols and indols are produced (54).

Short-chain fatty acids

As mentioned previously, some dietary fibres can be fermented by bacteria in the large intestine, resulting in the production of SCFAs. SCFAs are absorbed by enterocytes either via facilitated diffusion, or mediated by transporters such as monocarboxylate transporter type 1 (MCT1) and sodium-coupled MCT1 (SMCT1). More than 95% of the SCFAs are rapidly absorbed from the colonic lumen and metabolised by the host (55). However, data on the exact production and uptake rates of SCFAs is limited, in particular in mice and humans.

An increasing amount of evidence suggests that the health benefits observed with dietary fibre consumption are partly due to the action of SCFAs (53). For instance, SCFAs are agonists for FFAR2 and FFAR3, G protein-coupled receptors (GPCRs) highly present in enteroendocrine cells in the gut epithelium. It is suggested that SCFAs can stimulate the production and release of GLP-1 and PYY by enteroendocrine L-cells via FFAR2 and FFAR3 (56-58), thereby playing a role in satiety regulation.

Acetate, propionate and butyrate are the main SCFAs produced. Butyrate is almost entirely utilised by colonocytes as their preferred energy substrate (59), while acetate and propionate are also transported to the liver via the portal vein (60). Propionate is metabolized by the liver and used for gluconeogenesis, while acetate may serve as a substrate for cholesterol synthesis and lipogenesis (61). In addition, acetate is taken up by muscle and adipose tissue (62). Since these individual SCFAs have very distinct properties, their effects on metabolism and health outcomes are under current review.

Animal models

To gain knowledge on the effect of nutrition on biological processes in humans, animal experiments have proven to be highly valuable. Use of animal models allows standardization of experimental factors such as age, body weight and food intake. The advantages of the 2 animal models used in this thesis, namely mice and pigs, are described below.

Mice
Mice are a frequently used animal model, because they are cheap, small, easy to house and to handle, and they have a high reproduction rate. Furthermore, inbred strains to limit inter-individual genetic variation and transgenic mouse models are available (63, 64). Although mice share 99% of their genes with humans, data obtained from mouse experiments may not be directly translated to humans because of large contributions of the genetic background caused by the breeding selection (65). However, to comprehensively understand basal mechanisms of metabolism and the role of nutrition and nutrient-activated transcription factors in metabolic regulation, mouse models are indispensable.

Pigs
For answering certain research questions, the pig can be a more suitable model for humans compared to mice. The use of the pig as an experimental model allows precise and highly relevant dietary intervention studies for humans. First of all, the domestic pig is a valuable invasive model for the digestive function in humans, because the anatomy and physiology of the gastrointestinal tract of pigs has a lot of similarities with those in humans (66). In addition, extensive conservation exists between the pig and human genome sequence (67-70) and recently developed techniques are available for the pig including industry standard Affymetrix porcine microarrays (71).

Tools

Several techniques are available to increase our understanding of physiological and molecular mechanisms. In this paragraph some background information will be given about the techniques that were applied to obtain the results described in this thesis.

With so-called 'omics technologies' it is possible to make a snapshot of the entire genome, transcriptome, proteome or metabolome of an organism or tissue. Previous studies have shown the value of these techniques in identifying new potential mechanisms via which nutrients can affect health outcomes (72-75). In the studies described in this thesis, transcriptomics, proteomics and metabolomics techniques were applied to gain knowledge on the host response, of which transcriptomics is the most unbiased methodology. Furthermore, a metagenomics technique was used in order to measure the microbiota composition of the pig intestine.
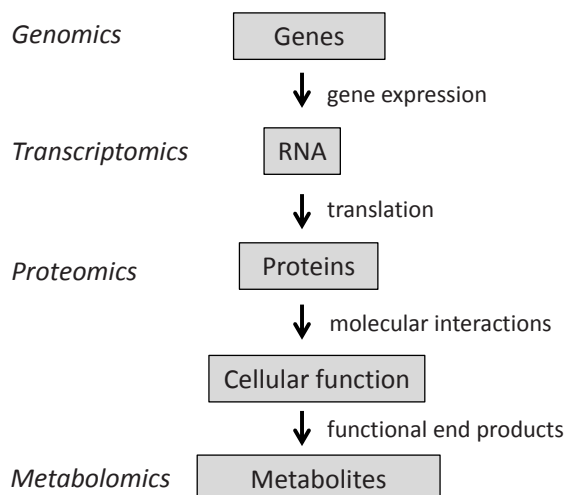

Figure 1 Overview of the 4 main omics technologies.

Metagenomics

Several methods have been developed to determine the intestinal microbiota composition of an organism. With these techniques the metagenome, the collective genome of the microbial community, is studied. In principal, 2 techniques can be applied to study the gut metagenome: sequencing techniques such as deep of 16S rRNA gene fragments or next-generation parallel sequencing, and the phylogenetic microarray.

Phylogenetic microarrays have been developed to analyse the intestinal microbiota composition of several species, including humans (HITChip), mice (MITChip) and pigs (PITChip). In the pig experiments described in this thesis, the PITChip (Pig Intestinal Tract Chip) was used, which contains oligonucleotides targeting the 16S rRNA gene sequences of porcine intestinal microbial species-level phylotypes. It provides a very deep and reproducible phylogenetic analysis. Compared with deep pyrosequencing of 16S rRNA gene fragments (76) and next-generation parallel sequencing of intestinal metagenomes (77), PITChip has a similar resolution and a higher sensitivity.

Chapter 2 and **3** of this thesis describe the results of PITChip analysis. In **Chapter 2**, the first generation PITChip, containing >2,900 oligonucleotides based on 16S rRNA gene sequences of 627 porcine intestinal microbial species-level phylotypes, was used. In **Chapter 3**, samples were analysed on the second generation PITChip. This is an updated version of the original phylogenetic microarray, comprised of >3,200 oligonucleotides targeting the 16S rRNA gene sequences of 781 porcine intestinal microbial phylotypes.

Transcriptomics

The transcriptome is the complete and dynamic set of RNA transcripts produced by the genome. Characterization of the transcriptome via measurement of mRNA levels has long been of interest to researchers. Basically, 2 techniques are available to measure gene expression levels of large numbers of genes simultaneously.

The first technique is the DNA microarray, currently the most frequently used method. By comparing the gene expression profile of samples obtained after different treatments, it is possible to determine which genes are differentially expressed. The arrays used for microarray analysis consist of DNA oligonucleotides, each containing a specific DNA sequence called a probe. The oligonucleotide probes were synthesised *in situ* using photolithography. The mRNA present in the samples of interest can hybridise to these probes. Subsequently, probe-target hybridization is detected and quantified by fluorescence to determine the relative abundance of nucleic acid sequences in the target.

The second technique is called RNA-Seq, a recently developed approach for transcriptome profiling that uses high-throughput deep-sequencing technologies. In principle, a population of RNA is converted to a library of cDNA fragments with adaptors attached to one or both ends. Each molecule is then sequenced in a high-throughput manner to obtain short sequences. The resulting reads are either aligned to a reference genome or reference transcripts, or assembled *de novo* without the genomic sequence to produce a genome-scale transcription map that consists of both the transcriptional structure and/or level of expression for each gene (78).

Compared with microarray, RNA-Seq has lower background noise and the possibility to distinguish the different isoforms and allelic expression. Moreover, a limitation of microarrays is that sequence information is required in order to detect and evaluate transcripts (78). On the other hand, the microarray technique has a number of advantages compared to RNA-Seq. The amount of time to retrieve results is shorter, RNA-Seq protocols still suffer from unknown biases and with RNA-Seq high abundance transcripts are responsible for the majority of the sequencing data.

In **Chapter 3**, the Affymetrix Porcine Gene 1.0 ST array was used to measure the full gene expression profile in colonic tissue of pigs. This array contains 595,966 probes, representing 17,116 unique genes. The Affymetrix Mouse Gene 1.1 ST array, containing 828,268 probes representing 21,225 unique genes, was used to measure the gene expression profile in colonic tissue of mice as described in **Chapter 4**.

Proteomics
The proteome is the entire set of proteins expressed by a genome, cell, tissue or organism. Several techniques can be applied to measure this highly dynamic proteome. Methods to determine the proteome can be separated into 2 groups: Gel-based proteomics and mass spectrometry (MS)-based proteomics (79).

Among the gel-based approaches are one-dimensional and two-dimensional polyacrylamide gel electrophoresis (1D-PAGE and 2D-PAGE respectively). For simple pre-separation of complex protein mixtures before mass spectrometric analysis, 1D-PAGE is often used. 2D-PAGE allows the separation of up to 10,000 protein species for global differential proteome analysis. In MS-based proteomics, the chemical compounds of a sample are ionized and the resulting charged molecules (ions) are analysed according to their mass-to-charge (*m/z*) ratios (79).

The proteomics results described in **Chapter 6** of this thesis were obtained by using the SELDI-TOF-MS technique. SELDI-TOF-MS is the abbreviation of Surface-enhanced laser desorption/ionization time-of-flight mass spectrometry. It is an ionization method in MS that is especially used for the high-throughput analysis

of protein mixtures, such as blood or urine. For analysis of plasma, samples are first processed to get rid of highly abundant proteins (e.g. albumin) that complicate the detection of medium and low abundance proteins. Subsequently, the samples are spotted on the surface of ProteinChip arrays. Some proteins in the sample bind to the surface of the array while others are removed by washing. Usually each sample is analysed on multiple arrays, with each array having the capacity to bind specific proteins. For instance, CM10 arrays are used to analyse molecules that have a positive charge on the surface, H50 arrays capture larger proteins through hydrophobic interactions and IMAC30 arrays capture molecules that bind polyvalent metal ions. Each array is irradiated with a laser, resulting in ionization of the adherent molecules. The ions travel through a vacuum flight tube and their *m/z* ratios are calculated from their time of flight through the vacuum chamber.

Metabolomics

The metabolome refers to the complete and dynamic set of small-molecule metabolites found in a biological sample. The 2 most commonly used techniques to measure the metabolome are MS and ^{1}H-nuclear magnetic resonance (^{1}H-NMR) spectroscopy. MS is a very sensitive technique which is usually performed after separation of the metabolites by gas chromatography (GC) or high-performance liquid chromatography (HPLC).

NMR spectroscopy is a technique that applies the magnetic properties of certain atomic nuclei. It determines the physical and chemical properties of atoms or the molecules in which they are contained, relying on the phenomenon of nuclear magnetic resonance.

When NMR active nuclei (e.g. ^{1}H or ^{13}C) are placed in a magnetic field, they absorb electromagnetic radiation at a frequency characteristic of the isotope. The resonant frequency, the energy of the absorption, and the intensity of the signal are proportional to the strength of the magnetic field. The chemical environment determines the position of the metabolite. With NMR spectroscopy, all kinds of small molecule metabolites can be measured simultaneously. Therefore, this technique does not require pre-separation of the metabolites, making sample preparation relatively simple. Another advantage of NMR is its high analytical reproducibility.

We used ^{1}H-NMR spectroscopy to measure the metabolome of plasma collected from pigs (**Chapter 3**, **5** and **6**). Plasma samples were first ultra-filtrated to remove large molecules and then metabolites were determined by using an Avance III NMR spectrometer.

Thesis outline and aims

The work presented in this thesis was embedded in a larger IP/OP funded program entitled "Satiety & Satisfaction". The main objective of the subproject 'Fermentation in the gut prolongs satiety' was to estimate the potential contribution of fermentable dietary fibres to the regulation of satiety and to elucidate their mode of action, using the pig as a model for humans. Therefore, a number of experiments was conducted at the research facilities of Wageningen University in Wageningen and Lelystad.

Three fibre types, i.e. lignocellulose, pectin and resistant starch, were screened for satiating properties in pigs using behavioural tests. Since pigs consuming a diet high in resistant starch (RS) showed the highest degree of satiety, this fibre type was selected for more detailed analysis at the level of the intestine. Pigs were either assigned to an RS diet or a digestible starch (DS) diet for 2 wk, after which intestinal samples along the proximal-distal axis were collected for measuring luminal microbiota composition, luminal SCFA concentrations and the expression of host genes involved in SCFA uptake, SCFA signalling, and satiety regulation in mucosal tissue. Study outcomes of this experiment are described in **Chapter 2**.

Because the results from the first study were promising, an additional experiment was performed on the effects of RS, in which 10 young growing pigs were fitted with catheters for repeated blood sampling and with a cannula in the proximal colon for repeated collection of tissue biopsies and luminal content. Peripheral blood samples were collected before and at several time points after the morning meal, and luminal content (microbiota composition, SCFAs) and colon biopsies (whole-genome expression profiling) were collected from the cannula. To limit inter-individual variation, the DS and RS diet were provided to the pigs in a 2 x 2 crossover design for 2 wk per diet. Results from this study are described in **Chapter 3** and **5**, with each chapter having a specific focus. In **Chapter 3**, we aimed to identify genes regulated by RS in the proximal colon using microarray analysis, to elucidate which metabolic pathways were affected, and to correlate gene expression changes with alterations in microbiota composition and SCFA concentrations. The objective of **Chapter 5** was to assess the time-course of RS-induced changes in physical activity and behaviour, satiety-related hormones and metabolites in peripheral blood, and to relate those to feeding behaviour and meal size during an *ad libitum* meal. In addition, satiating effects of RS were evaluated in the presence of extra dietary fat.

The results of a proteomics analysis of portal and arterial plasma samples are described in **Chapter 6**. This study was performed in minipigs provided with 4 different fibre diets (Control, Lignocellulose, Pectin and Resistant starch) in a 4x4

Latin square design. The main study objective was to determine the effect of fibres with different physicochemical properties on postprandial plasma protein and metabolite profiles.

In addition to the pig studies that have been performed, an experiment was conducted in mice. **Chapter 4** describes the results of this mouse study, which aimed to determine the effect of dietary fat content on colonic gene expression profile after colonic acetate, propionate and butyrate administration. Mice on a low fat or a high fat diet background received a rectal infusion of a control solution or a solution containing acetate, propionate or butyrate for 6 consecutive days, after which colon was collected for whole-genome expression profiling.

1

A diet high in resistant starch modulates microbiota composition, SCFA concentrations and gene expression in pig intestine

Daniëlle Haenen, Jing Zhang, Carol Souza da Silva, Guido Bosch, Ingrid M. van der Meer, Jeroen van Arkel, Joost J.G.C. van den Borne, Odette Pérez Gutiérrez, Hauke Smidt, Bas Kemp, Michael Müller and Guido J.E. J. Hooiveld

Abstract

Resistant starch (RS) is highly fermentable by microbiota in the colon, resulting in the production of SCFAs. RS is thought to mediate a large proportion of its health benefits, including increased satiety, through the actions of SCFAs. The aim of this study was to investigate the effects of a diet high in RS on luminal microbiota composition, luminal SCFA concentrations and the expression of host genes involved in SCFA uptake, SCFA signalling and satiety regulation in mucosal tissue obtained from small intestine, caecum and colon. Twenty adult female pigs were either assigned to a digestible starch (DS) diet or a diet high in RS (34%) for a period of 2 wk. After the intervention, luminal content and mucosal scrapings were obtained for detailed molecular analysis. RS was completely degraded in caecum. In both the caecum and colon, differences in microbiota composition were observed between DS- and RS-fed pigs. In the colon these included the stimulation of the healthy gut-associated butyrate-producing *Faecalibacterium prausnitzii*, whereas potentially pathogenic members of the *Gammaproteobacteria*, including *Escherichia coli* and *Pseudomonas* spp., were reduced in relative abundance. Caecal and colonic SCFA concentrations were significantly greater in RS-fed pigs, and caecal gene expression of monocarboxylate transporter 1 (*SLC16A1*) and glucagon (*GCG*) was induced by RS. In conclusion, our data show that RS modulates microbiota composition, SCFA concentrations and host gene expression in pig intestine. Combined, our data provide an enhanced understanding of the interaction between diet, microbiota and host.

Introduction

Obesity and related disorders, such as cardiovascular diseases and type 2 diabetes, have become major public health issues (4, 5). Various lifestyle factors, of which diet is a major one, play an important role in the development of these disorders (6, 80). A large amount of research has reported an inverse relationship between fibre consumption and the risk of obesity and diabetes (81). Moreover, consumption of dietary fibre prevents the accumulation of fat mass (82, 83), increases insulin sensitivity (9, 84) and can enhance feelings of satiety (12).

Resistant starch (RS) is a type of dietary fibre that includes all starch and starch degradation products that are not absorbed in the small intestine of healthy humans (15). It is known to be fermented to a large extent by microbiota in the colon, resulting in the production of SCFAs (53, 85). These SCFAs can diffuse across the epithelial cell membrane, but SCFA absorption by the enterocytes is also mediated by the monocarboxylate transporter 1 (SLC16A1, also known as MCT1) and sodium-coupled monocarboxylate transporter 1 (SLC5A8 or SMCT1) (86).

Enhanced SCFA production provides an important link between dietary fibre consumption and health benefits. First, SCFAs lower the pH in the colon, which can prevent the overgrowth of pathogenic bacteria (87). Acetate, propionate and butyrate are the major SCFAs produced in the colon, of which butyrate is thought to be most beneficial for health. Among the health benefits observed with butyrate are the prevention and inhibition of colon carcinogenesis, protection against mucosal oxidative stress, strengthening of the colonic defence barrier and butyrate also has anti-inflammatory properties (55). Propionate has the potential to reduce cholesterol concentrations in blood (88).

In addition to these health benefits, SCFAs are thought to be involved in the increase in satiety observed with fibre consumption (25). Studies in rodents have provided evidence that fermentation of RS is an important mechanism for increased endogenous secretion of the gut hormones glucagon-like peptide 1 (GLP-1) and peptide YY (PYY) (29, 82, 89, 90). GLP-1 and PYY are satiety-stimulating hormones that are released in response to nutrient intake, mainly in the ileum and colon. SCFAs are agonists for free fatty acid receptor 2 and 3 (FFAR2 and FFAR3 respectively), 2 G protein-coupled receptors present in the gastrointestinal tract. Both of these G protein-coupled receptors are expressed in enteroendocrine cells in the gut epithelium. It has been proposed that the activation of these receptors trigger the production and release of GLP-1 and PYY by enteroendocrine L-cells (91, 92).

In the experiments described in this chapter, we investigated the effects of a diet high in RS on luminal microbiota composition, luminal SCFA concentrations and

the expression of host genes involved in SCFA uptake, SCFA signalling and satiety regulation in mucosal tissue obtained from small intestine, caecum and colon. Adult pigs were used as a model for humans because the anatomy and physiology of the gastrointestinal tract of pigs and the pig genome are similar to those of humans (66, 93). Because we recently reported that a diet high in RS decreases feeding motivation in pigs (17), special attention was given to selected genes involved in SCFA sensing and regulation of satiety.

Materials and Methods

Experimental design, pigs and housing

Two independent studies were performed. First, a pilot experiment was carried out to ascertain whether the gene expression profile along the intestine of pigs is similar to the sites of expression in humans and rodents. Three multiparous female pigs with a mean (± SEM) body weight of 273 ± 1.15 kg were included is this study.

The main study had a parallel design. Two groups of 10 female pigs (PIC Benelux B.V.), aged 22 mo, with an initial body weight of 268 ± 3.85 kg were assigned to 1 of 2 treatments. Treatments differed with regard to the type of starch in the diet: digestible starch (DS) or RS. Siblings were equally distributed between the 2 groups. Pigs were individually fed and housed in pairs that received the same diet. The area of each pen was 11 m^2 and contained 2 drinking nipples and 2 feeding troughs. Artificial lights were on from 06:30 h until 22:00 h and dimmed during the dark period. The animal protocol was approved by the Animal Care and Use Committee of Wageningen University. The same pigs were used previously for feeding motivation studies (17).

Diets and feeding

The 2 experimental diets used in the main study were identical except for type of starch. The main source of starch in the DS diet was pregelatinized potato starch (Paselli WA4; AVEBE), which was replaced on a dry matter basis in the RS diet by retrograded tapioca starch (Actistar; Cargill). According to the supplier, this starch was ≥50% resistant to digestion in the small intestine. On the basis of physical and chemical characteristics, the RS used in this study can be classified as RS type 3 (RS3) (15). Diets were isoenergetic on a gross energy basis. The detailed composition of the experimental diets is presented in **Supplemental Table 1**. Each diet was given to 10 pigs in pelleted form at 07:00 h and 17:00 h for a period of 14 d. The daily feed

allowance was 1.13 times the energy requirements for maintenance [net energy = 293 kJ/(kg$^{0.75}$ • d)], and pigs were allowed 1 h to consume the meal. All pigs had free access to water throughout the entire day.

Blood collection

Blood was collected 5 h postprandially on 2 separate days. Blood sampling was performed before the start of the treatment period when all pigs had consumed the DS diet for 2 d and at the end of the dietary intervention when pigs had been fed the DS or RS diet for 12 d. Blood was drawn from the jugular vein and collected in a BD Vacutainer EDTA tube with protease (Complete, EDTA-free; Roche) and dipeptidyl peptidase-4 (Millipore) inhibitors. Tubes were centrifuged for 10 min at 1300 *g* at 4°C immediately after blood collection. Plasma was separated into aliquots and stored at -80°C.

Collection of digesta and tissue

Digesta and tissue samples were collected 5 h after the morning meal. This time point was selected on the basis of a previous study in which an increase in SCFA concentration was observed 4-5 h after feeding (94). Pigs were stunned and exsanguinated, after which the abdominal cavity was opened. The gastrointestinal tract from stomach to anus was removed from the cavity and the length of the small intestine and colon was determined. The small intestine was divided into 10 parts of equal length, the caecum was divided into 2 parts and the colon into 4 parts. The luminal content was collected from the 4 most distal parts of the small intestine (segment 7 to 10) and from all caecal and colonic parts. For subsequent analysis of SCFA concentrations, part of the content was collected in tubes with 1 mL of H_3PO_4, after which the samples were thoroughly mixed and stored at -20°C. Luminal content was also stored in empty tubes at -20°C to determine dry matter and degradation of RS. The remaining amount of digesta was collected in 1.5 mL Eppendorf tubes to determine microbiota composition. These tubes were immediately frozen in liquid nitrogen and stored at -80°C until further analyses. In addition, a small piece from the middle of each intestinal segment was excised and rinsed in PBS. Epithelial cells were collected from these tissues by scraping the mucosal lining with a glass slide. These samples were immediately snap-frozen in liquid nitrogen and then stored at -80°C for subsequent RNA isolation.

Analysis of RS in luminal samples

RS was analysed according to methods used by Goñi et al. (95), adapted for intestinal samples, including extra washing steps and the total volume set at 35-40 mL. Impurities were removed by deionization of the sample by using equal amounts

of Q-sepharose and S-sepharose beads equilibrated with phosphate buffer, 20 mmol/L, pH 7. An aliquot (100 μL) of the sample obtained in step 9 of the procedure was combined with an equal amount of the ion exchange mix and thoroughly mixed for 5 min at room temperature. For the glucose assay, 100 μL supernatant obtained after 5 min of centrifugation at 14,000 g was used. Glucose was determined in the samples by using the Glucose Assay Kit from Sigma-Aldrich (product no. GAGO20). The amount of RS in the sample was calculated by using the method as described (95).

Microbiota analysis
Microbial DNA was extracted from 250 mg of intestinal contents by using a faecal DNA extraction protocol (96). Denaturing gradient gel electrophoresis (DGGE) analysis was performed for a preliminary scanning of the microbial profile. Briefly, universal primers S-D-Bact-0968-a-S-GC and S-D-Bact-1401-a-A-17 (97) were used to amplify the V6 to V8 variable regions of the bacterial 16S rRNA gene. The V6-V8 PCR amplicons were separated by DGGE according to the specifications of Muyzer et al. (98) by using a DCode system (Bio-Rad Laboratories). Gel images were digitally normalized by comparison with an external standard pattern by using Bionumerics software package version 4.5 (Applied MathS). Observed bands were classified across all samples, and band class information, including relative band intensity, was used for multivariate analysis.

After the preliminary scanning of microbiota composition by DGGE analysis, the luminal contents from the first part of caecum (from 9 DS-treated and 7 RS-treated pigs) and colon (from 7 DS-treated and 8 RS-treated pigs) were selected for further analysis by using the Pig Intestinal Tract Chip (PITChip). The PITChip is a phylogenetic microarray with >2900 oligonucleotides based on 16S rRNA gene sequences of 627 porcine intestinal microbial species-level phylotypes (99). The PITChip provides a very deep and reproducible phylogenetic analysis that has been compared with deep pyrosequencing of 16S rRNA gene fragments (76, 99, 100) and next-generation parallel sequencing of intestinal metagenomes (77), indicating comparable resolution and a higher sensitivity of the chip-based analysis.

The protocol for hybridization and analysis of the generated data was performed essentially as previously described for the Human Intestinal Tract Chip (101). The bacterial 16S rRNA gene was amplified by using the primers *T7prom*-Bact-27-for and Uni-1492-rev (101). The PCR products were transcribed into RNA and the purified resultant RNA was coupled with CyDye (GE Health hcare Life Sciences) before fragmentation and hybridization to the array. Microarray images were processed using Agilent's Feature Extraction Software, version 9.1 (Agilent Technologies). Data normalization and processing were performed as described (99, 101).

Dry matter and SCFA measurement

Dry matter was determined by drying the intestinal content to a constant weight at 103°C (ISO standard 6496; International Organization for Standardization, 1999).

The digesta samples collected in tubes with H_3PO_4 were thawed, mixed on a vortex and centrifuged at 20,000 g for 5 min. The supernatant was collected and diluted 1:1 with a solution containing isocaproic acid. SCFA concentrations were determined in the effluent by gas chromatography (Fisons HRGC Mega 2; CE Instruments) at 190°C by using a glass column fitted with Chromosorb 101 (Supelco). The carrier gas was N_2 saturated with methanoic acid, and isocaproic acid was used as an internal standard.

RNA isolation and quality control

Total RNA was isolated from intestinal scrapings using TRIzol reagent (Life Technologies) according to the manufacturer's instructions. Concentrations and purity of RNA samples were determined on a NanoDrop ND-1000 spectrophotometer (Isogen Life Science). RNA quality was verified with an Agilent 2100 Bioanalyzer (Agilent Technologies) by using 6000 Nano Chips (Agilent Technologies) according to the manufacturer's instructions.

qRT-PCR

Single-stranded cDNA was synthesized from 1 μg of total RNA by using the First Strand cDNA Synthesis Kit (Fermentas Life Sciences) according to the supplier's protocol. qRT-PCR was performed on a CFX384 Real-Time PCR Detection System (Bio-Rad) by using SensiMix SYBR No-ROX (Bioline). Primers were designed in Beacon Designer 7.6 by using sequences obtained from the ENSEMBL pig database. Specificity of the amplification was verified by melt curve analysis and evaluation of efficiency of PCR amplification. The primer sequences are listed in **Supplemental Table 2**. Samples were analysed in duplicate and mRNA expression of all genes reported was standardized to *RPLP0* gene expression.

Plasma measurements

All plasma measurements were performed in duplicate. Glucose was measured by using an enzymatic glucose assay (Glucose PAP SL; Elitech Group). Triglyceride (TG) and cholesterol concentrations were determined by using the enzymatic methods (Triglycerides Liquicolor, Cholesterol Liquicolor; INstruchemie). Insulin and PYY concentrations were measured by EIA [insulin: (porcine/canine) EIA; ALPCO Diagnostics; peptide YY (3-36): (rat, mouse, porcine, canine) EIA kit; Phoenix Pharmaceuticals]. GLP-1 was analysed with ELISA [Glucagon-like Peptide-1 (active) ELISA Kit; Millipore].

Statistical methods

Results are expressed as means ± SEM. The significance of differences between the 2 treatment groups of the variables determined at the end of the experimental period was evaluated by Student's *t* test. ANOVA was used to test for differences in RS content in the small intestine, caecum and colon. Significance of differences of plasma variables, which were measured before and after the experimental period, was determined by linear mixed-model analysis treating pig as a random effect. Analyses were performed in GraphPad Prism, version 5.04, and IBM SPSS Statistics, version 19. Differences were considered significant if P <0.05.

Multivariate analysis was applied for DGGE and PITChip data interpretation. To relate changes in total bacterial community composition to environmental variables, redundancy analysis (RDA) was used as implemented in the CANOCO 4.5 software package (Biometris). RDA is the canonic form of principle component analysis and is a multivariate linear regression method in which several response variables are related to the same set of environmental variables and in which the estimated matrix of regression coefficients is of reduced rank (102). The relative abundance of bands on DGGE gels and signal intensities for 144 genus-level phylogenetic groups of PITChip were used as responsive variables. Treatment class (DS or RS), SCFA concentration and gene expression values of *GCG* and *SLC16A1* were introduced as environmental (explanatory) variables. The latter were included because these variables were significantly different between the 2 treatment groups in the caecum and colon (see Results). RDA was performed by focusing on intersamples correlation, and the Monte Carlo permutation test was applied to evaluate whether treatment class, SCFA concentration and gene expression had significant influence on the microbial composition (103, 104). Because the experiment had a randomized design, we used the unrestricted permutation option that yields completely random permutations. Treatment class or other environmental variables were considered to significantly affect microbial composition with P values <0.05. Diagrams were plotted as biplots for DGGE data and as triplots for PITChip data by using CanoDraw (Biometris).

Univariate testing of differences for individual microbial groups was processed by using a Mann–Whitney *U* signed-rank test. P values were corrected for multiple testing by using Benjamini-Hochberg's approach (105).

Results

Longitudinal distribution of gene expression

In the pilot experiment, the expression of several genes involved in luminal uptake and sensing of nutrients and metabolites was measured in mucosal scrapings of 3 female pigs (**Supplemental Fig. 1**). As expected, the expression of apical sodium-dependent bile salt transporter (*SLC10A2*) was restricted to terminal ileum (106). mRNA levels of fatty acid transport protein 4 (*SLC27A4*), liver-type fatty acid binding protein (*FABP1*) and intestine-type fatty acid binding protein (*FABP2*) were highest in the proximal jejunum and resembled the pattern observed in mice (107). Furthermore, the gene expression pattern of glucagon (*GCG*; in the intestine the precursor for GLP-1 and GLP-2) and PYY (*PYY*) in the small intestine closely resembled the peptide concentrations found in pig intestine (108). Taken together, these data show the validity of our gene expression measurements in the gastrointestinal tract of pigs. Moreover, we found that the distal part of the small intestine, the caecum, and the colon showed the highest expression of genes involved in SCFA uptake (*SLC16A1*, *SLC5A8*), SCFA sensing (*FFAR2*, *FFAR3*) and satiety (*GCG*, *PYY*). Therefore, these segments were sampled in the main experiment described in this chapter.

Anthropometric variables

Body weight and fat depth were measured in all pigs at the end of the experimental period. The lengths of the small intestine and colon were determined at section. No significant differences were found between the treatment groups with respect to body weight, fat depth, and the length of the small intestine and colon (**Supplemental Table 3**).

Degradation of RS

The amount of RS was measured in the intestinal content collected at section (5 h postprandially). In RS-fed pigs, 20-40 times more RS was found in the small intestine compared with that in DS-fed pigs (**Fig. 1**). Furthermore, in the caecum of RS-fed pigs, the concentration of RS was significantly lower compared with that in the small intestine, whereas in the colon, RS concentrations were significantly lower than in the caecum and were comparable to background concentrations, i.e., those measured in DS-fed pigs (Fig. 1). From these observations we conclude that RS was fully degraded in the caecum.

2
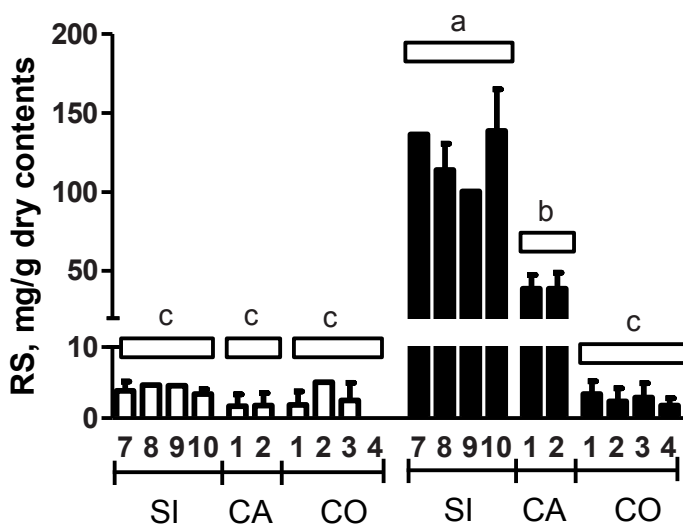
Figure 1 RS concentrations in luminal content of pigs fed the DS or RS diet for 2 wk. Values are means ± SEM, *n* = 1-4 pigs per treatment. Different letters indicate that segments differ significantly from each other, *P* <0.01 (a > b > c). From *left* to *right*, bars represent areas of the gastrointestinal tract from proximal to distal. The small intestine was divided into 10 equal parts; parts 7-10 refer to the 4 most distal segments of the small intestine, whereas the caecum and colon were divided into 2 respectively 4 segments of equal length. White horizontal bars indicate the intestinal parts that were combined for statistical analysis to determine differences between anatomic locations. CA, caecum; CO, colon; DS, digestible starch; RS, resistant starch; SI, small intestine.

Microbiota analysis

Multivariate analysis of the DGGE data revealed a significant effect of RS treatment on the composition of the microbiota in the caecum (*P* = 0.016) and colon (*P* = 0.002), whereas no significant effect of treatment was found in the small intestine (*P* = 0.18) (**Supplemental Fig. 2**).

Because treatment effects were observed in the caecum and colon, the luminal contents of the proximal part of caecum (P1 caecum) and colon (P1 colon) were selected for further analysis using the superior PITChip technique. RDA of the PITChip data showed a visual treatment effect on the microbiota in both caecum and colon. Caecal samples of RS-fed pigs were separated from those of DS-fed pigs except for pig 24 (**Fig. 2A**). The treatment-centered separation was more obvious for the colonic samples (**Fig. 2B**). Moreover, Monte Carlo Permutation testing showed that, of the environmental variables, only luminal propionate concentration

significantly (P = 0.018) contributed to explaining the observed variation in microbiota composition in the colon.

To determine which microbial groups were changed by RS treatment, univariate analysis was employed (**Tables 1** and **2**). In the caecum, we found that microbial groups of *Actinobacteria*, *Bacilli*, *Clostridium* cluster IV and XIVa, *Alphaproteobacteria*, *Betaproteobacteria* and *Spirochaetes* changed in relative abundance, albeit at corrected P values of 0.81 (Table 1). More specifically, *Streptococcus intermedius*-like group, *Streptococcus salivarius*-like group, *Streptococcus suis*-like group and *Neisseria*-like group decreased by the RS treatment, whereas the uncultured *Clostridia* cluster IV and *Rhodobacter*-like microorganisms increased in relative abundance (**Table 1**).

In the colon, 30 microbial groups were significantly changed by the RS treatment (corrected P value <0.05), whereas a trend toward significance was observed for 13 additional microbial groups (corrected P value between 0.05 and 0.07) (**Table 2**). Members of the *Actinobacteria*, *Weissella*-like group, *Clostridium* cluster IV, IX, XV,XVI and XVII, *Mollicutes*, *Fusobacteria* and *Betaproteobacteria* increased in relative abundance in pigs fed the RS diet. In contrast, groups within the classes of *Bacilli* (e.g. *Allofustis*, *Lactobacillus acidophilus*-like group and *Lactobacillus plantarum*-like group), *Clostridium* cluster XI and XIVa, *Deltaproteobacteria* and *Gammaproteobacteria* decreased upon RS consumption (**Table 2**).

Despite the change in relative abundance of several microbial groups, treatment with RS for 14 d did not significantly alter the microbial diversity in caecum and colon as indicated by Shannon's and Simpson's indices for diversity (data not shown).

2
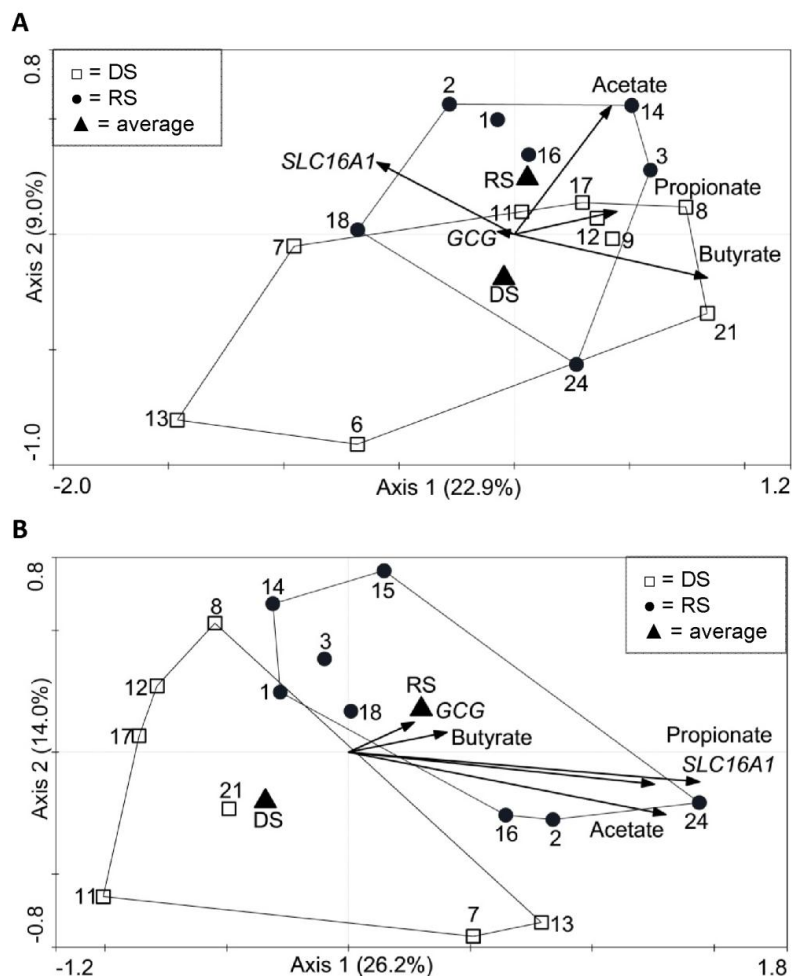
Figure 2 Triplots of RDA results, representing the principal component analysis of the microbiota composition as measured by the mean hybridization signals for 144 genus-level phylogenetic groups in the luminal content of caecum (**A**) and colon (**B**) of pigs fed the DS or RS diet for 2 wk. Samples are grouped by treatment class. Each symbol represents 1 pig, and numbers represent pig identifiers. The average of the nominal environmental variables DS and RS are represented by triangles. *GCG* (expression), *SLC16A1* (expression), acetate, propionate and butyrate concentrations are also included as environmental variables. For clarity, the microbial groups that contributed to the first 2 principal components used as explanatory axes were omitted in these triplots. Combined, both axes explain 30.9% of the total variance in the data set for (*A*) and 41.6% for (*B*). DS, digestible starch; RS, resistant starch.

Table 1 Phylogenetic groups in the luminal content of the P1 caecum of pigs fed the DS or RS diet for 2 wk that were significantly affected by diet according to univariate analysis of PITChip data[1]

Phylogenetic group	Corr. *P* value[2]	*P* value	ARC[3] DS	RS	Effect[4]
Actinobacteria					
Actinobacteria					
Bifidobacterium	0.81	0.071	0.390 ± 0.037	0.355 ± 0.031	-
Olsenella et rel.	0.81	0.091	0.007 ± 0.002	0.010 ± 0.004	+
Firmicutes					
Bacilli					
Streptococcus intermedius et rel.	0.81	0.042	0.399 ± 0.190	0.251 ± 0.077	-
Streptococcus salivarius et rel.	0.81	0.031	0.374 ± 0.178	0.244 ± 0.085	-
Streptococcus suis et rel.	0.81	0.016	0.353 ± 0.111	0.245 ± 0.047	-
Uncultured *Bacilli*	0.81	0.091	1.273 ± 0.056	1.331 ± 0.071	+
Clostridium cluster IV					
Uncultured *Clostridia* IV	0.81	0.042	1.961 ± 0.358	2.218 ± 0.283	+
Clostridium cluster XIVa					
Butyrivibrio crossotus et rel.	0.81	0.071	0.851 ± 0.108	0.763 ± 0.094	-
Clostridium sphenoides et rel.	0.81	0.091	0.820 ± 0.094	0.971 ± 0.095	+
Eubacterium rectale et rel.	0.81	0.091	0.746 ± 0.060	0.690 ± 0.060	-
Ruminococcus ganvus et rel.	0.81	0.055	0.854 ± 0.086	0.937 ± 0.080	+
Proteobacteria					
Alphaproteobacteria					
Rhodobacter et rel.	0.81	0.042	1.263 ± 0.128	1.383 ± 0.118	+
Betaproteobacteria					
Bordetella et rel.	0.81	0.091	1.052 ± 0.093	0.974 ± 0.095	-
Neisseria et rel.	0.81	0.042	0.904 ± 0.071	0.817 ± 0.081	-
Spirochaetes					
Spirochaetes					
Brachyspira	0.81	0.091	0.009 ± 0.003	0.011 ± 0.003	+
Leptospira	0.81	0.071	0.642 ± 0.071	0.728 ± 0.082	+

[1] DS, digestible starch; P1, part 1; PITChip, Pig Intestinal Tract Chip; RS, resistant starch.

[2] Corr. *P* value indicates the *P* value corrected for multiple testing according to the procedure of Benjamini-Hochberg.

[3] ARC is the Average Relative Contribution of a microbial group. Values are means ± SEM, *n* = 9 for DS-fed pigs and *n* = 7 for RS-fed pigs.

[4] "+" or "-" indicates whether the average relative contribution of the microbial group increased or decreased by the RS treatment.

Table 2 Phylogenetic groups in the luminal content of the P1 colon of pigs fed the DS or RS diet for 2 wk that were significantly affected by diet according to univariate analysis of PITChip data[1]

Phylogenetic group	Corr. *P* value[2]	*P* value	ARC[3]		Effect[4]
			DS	RS	
Actinobacteria					
Actinobacteria					
Eggerthella et rel.	0.045	0.009	0.731 ± 0.033	0.823 ± 0.081	+
Microbacterium	0.040	0.006	0.785 ± 0.057	0.911 ± 0.076	+
Micrococcus et rel.	0.045	0.009	0.806 ± 0.048	0.897 ± 0.069	+
Propionibacterium	0.069	0.021	1.258 ± 0.081	1.403 ± 0.093	+
Tonsillophilus	0.058	0.014	0.694 ± 0.035	0.791 ± 0.082	+
Firmicutes					
Bacilli					
Allofustis	0.058	0.014	0.694 ± 0.043	0.622 ± 0.052	-
Lactobacillus acidophilus et rel.	0.069	0.021	0.956 ± 0.151	0.736 ± 0.173	-
Lactobacillus plantarum et rel.	0.040	0.006	2.083 ± 0.178	1.835 ± 0.124	-
Weissella et rel.	0.045	0.009	0.660 ± 0.032	0.735 ± 0.052	+
Clostridium cluster IV					
Faecalibacterium et rel.	0.020	0.001	1.402 ± 0.188	1.748 ± 0.137	+
Faecalibacterium prausnitzii et rel.	0.020	0.001	1.648 ± 0.232	2.062 ± 0.134	+
Ruminococcus bromii et rel.	0.069	0.021	0.294 ± 0.049	0.367 ± 0.049	+
Sporobacter termitidis et rel.	0.015	0.001	3.300 ± 0.364	4.358 ± 0.283	+
Uncultured *Clostridia* IV	0.021	0.002	1.799 ± 0.107	2.232 ± 0.294	+
Clostridium cluster IX					
Phascolarctobacterium faecium et rel.	0.015	<0.001	0.896 ± 0.098	1.134 ± 0.068	+
Veilonella	0.015	0.001	0.602 ± 0.088	0.793 ± 0.066	+
Clostridium cluster XI					
Anaerovorax et rel.	0.045	0.009	1.078 ± 0.150	0.851 ± 0.111	-
Clostridium cluster XIVa					
Bryantella et rel.	0.045	0.009	2.022 ± 0.110	1.810 ± 0.172	-
Dorea et rel.	0.069	0.021	0.913 ± 0.106	0.760 ± 0.105	-
Eubacterium plexicaudatum et rel.	0.045	0.009	0.371 ± 0.033	0.324 ± 0.024	-
Eubacterium ventriosum et rel.	0.058	0.014	0.363 ± 0.032	0.321 ± 0.022	-
Roseburia intestinalis et rel.	0.040	0.006	1.047 ± 0.112	0.898 ± 0.065	-
Ruminococcus ganvus et rel.	0.045	0.009	0.934 ± 0.110	0.769 ± 0.079	-
Uncultured *Clostridia* XIVa	0.040	0.006	2.002 ± 0.127	1.744 ± 0.141	-
Clostridium cluster XV					
Eubacterium et rel.	0.015	0.001	0.604 ± 0.088	0.793 ± 0.066	+
Clostridium cluster XVI					
Eubacterium biforme et rel.	0.021	0.002	0.732 ± 0.048	0.833 ± 0.053	+
Clostridium cluster XVII					
Catenibacterium	0.021	0.002	0.274 ± 0.021	0.333 ± 0.024	+
Mollicutes					
Acholeplasma et rel.	0.045	0.009	0.690 ± 0.039	0.778 ± 0.072	+
Bulleidia moorei et rel.	0.021	0.002	0.336 ± 0.035	0.407 ± 0.032	+
Erysipelothrix	0.015	0.001	0.715 ± 0.119	0.995 ± 0.081	+
Solobacterium moorei et rel.	0.040	0.006	0.525 ± 0.091	0.714 ± 0.149	+

Fusobacteria					
Fusobacteria					
Fusobacterium	0.045	0.009	0.077 ± 0.003	0.090 ± 0.013	+
Proteobacteria					
Betaproteobacteria					
Bordetella et rel.	0.069	0.021	0.932 ± 0.105	1.076 ± 0.081	+
Neisseria et rel.	0.069	0.021	0.795 ± 0.094	0.916 ± 0.083	+
Oxalobacter et rel.	0.069	0.021	0.723 ± 0.091	0.832 ± 0.058	+
Sutterella wadsorthia et rel.	0.058	0.014	0.822 ± 0.098	0.943 ± 0.070	+
Deltaproteobacteria					
Uncultured *Deltaproteobacteria*	0.021	0.002	0.094 ± 0.019	0.067 ± 0.009	-
Gammaproteobacteria					
Escherichia coli et rel.	0.040	0.006	1.423 ± 0.108	1.161 ± 0.161	-
Pseudomonas et rel.	0.020	0.001	1.306 ± 0.154	0.975 ± 0.161	-
Psychrobacter et rel.	0.021	0.002	1.022 ± 0.062	0.870 ± 0.099	-
Uncultured *Gammaproteobacteria*	0.015	<0.001	1.314 ± 0.136	1.027 ± 0.134	-
Vibrio et rel.	0.058	0.014	0.673 ± 0.077	0.537 ± 0.098	-
Spirochaetes					
Spirochaetes					
Uncultured *Spirochaetes*	0.069	0.021	0.518 ± 0.043	0.456 ± 0.048	-

[1] DS, digestible starch; P1, part 1; PITChip, Pig Intestinal Tract Chip; RS, resistant starch.

[2] Corr. *P* value indicates the *P* value corrected for multiple testing according to the procedure of Benjamini-Hochberg.

[3] ARC is the Average Relative Contribution of a microbial group. Values are means ± SEM, *n* = 7 for DS-fed pigs and *n* = 8 for RS-fed pigs.

[4] "+" or "-" indicates whether the average relative contribution of the microbial group increased or decreased by the RS treatment.

SCFA concentrations

SCFA concentrations were measured in the intestinal contents collected at section (5 h postprandially). Total SCFA concentration was highest in the caecum and gradually decreased along the colon (**Fig. 3A**). In the caecum and colon, SCFA concentrations were significantly higher in RS-fed pigs compared with DS-fed pigs (Fig. 3A). The most abundant SCFAs in the intestine were acetate, propionate and butyrate. The increase in total SCFA concentration on RS could mainly be attributed to higher concentrations of acetate and propionate (**Fig. 3B**, **C**). Butyrate concentration was significantly higher only in RS-treated pigs in the colon part 2 (P2 colon) (**Fig. 3D**). Although concentrations of valerate were low, the values for caecum and colon were significantly higher in RS-fed pigs (**Fig. 3E**). However, in the caecum we found significantly higher concentrations of isobutyrate and isovalerate in DS-fed pigs (**Fig. 3F**, **G**).
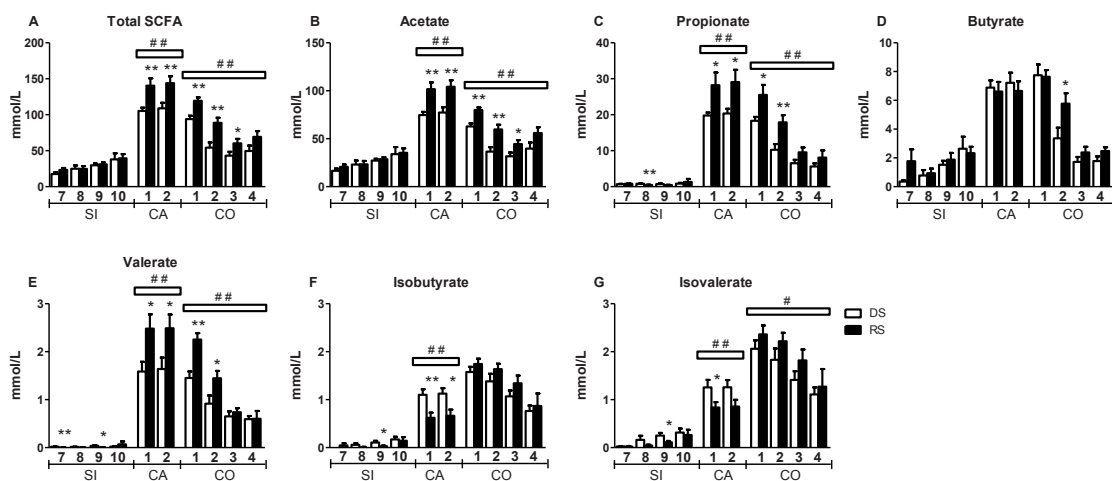
Figure 3 Total SCFAs (**A**), acetate (**B**), propionate (**C**), butyrate (**D**), valerate (**E**), isobutyrate (**F**) and isovalerate (**G**) concentrations in luminal contents of pigs fed the DS or RS diet for 2 wk. Values are means ± SEM, *n* = 6-10 pigs per treatment. *, ** DS and RS differ within the intestinal segment, *P* <0.05 and *P* <0.01, respectively. # , ## DS and RS differ within the total caecum or colon, *P* <0.05 and *P* <0.01, respectively. From *left* to *right*, bars represent areas of the gastrointestinal tract from proximal to distal. The small intestine was divided into 10 equal parts; parts 7-10 refer to the 4 most distal segments of the small intestine, whereas the caecum and colon were divided into 2 respectively 4 segments of equal length. White horizontal bars indicate the intestinal parts that were combined for statistical analysis to determine differences between treatments. CA, caecum; CO, colon; DS, digestible starch; RS, resistant starch; SI, small intestine.

Differential gene expression mucosal scrapings

The expression of several genes was determined in the mucosal scrapings collected at section (5 h postprandially). We observed a significant increase in *GCG* gene expression in RS-fed pigs in the caecum (**Fig. 4A**), whereas *PYY* gene expression was not modulated (**Fig. 4B**). In the most distal part of the small intestine, an increase in angiopoietin-like 4 (*ANGPTL4*) expression was found with RS (**Fig. 4C**). In the caecum and P2 colon, expression of *SLC16A1* was higher in RS-fed pigs compared with DS-fed pigs (**Fig. 4G**). However, the expression of the SCFA receptors *FFAR2*, *FFAR3*, G protein-coupled receptor 119 (*GPR119*) and the SCFA transporter *SLC5A8* was not different between the pigs fed RS or DS (**Fig. 4D**, **E**, **F** and **H**, respectively).
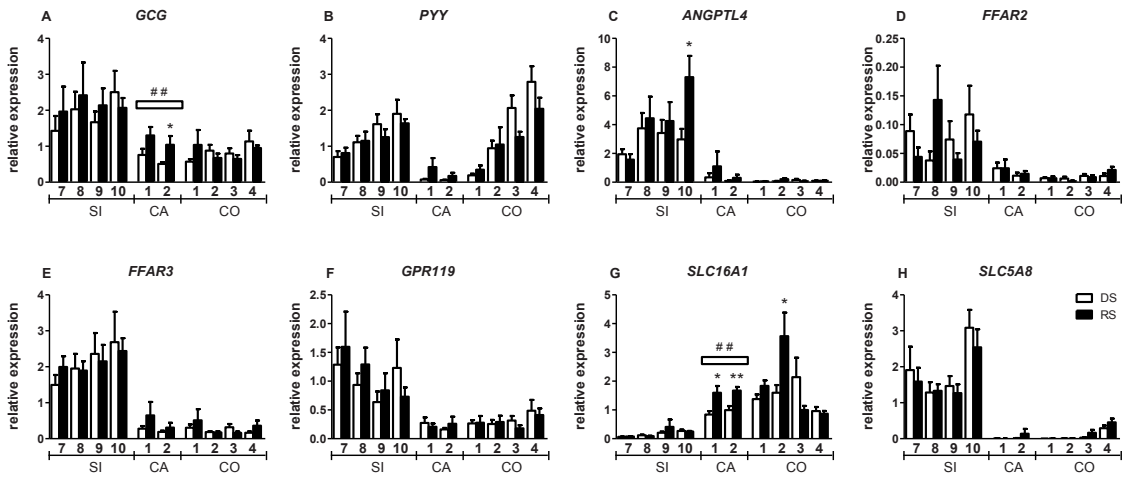
Figure 4 Relative gene expression of *GCG* (**A**), *PYY* (**B**), *ANGPTL4* (**C**), *FFAR2* (**D**), *FFAR3* (**E**), *GPR119* (**F**), *SLC16A1* (**G**) and *SLC5A8* (**H**) in mucosal scrapings along the proximal-distal axis of the intestine of pigs fed the DS or RS diet for 2 wk, as determined by qRT-PCR. Messenger RNA levels were standardized to *RPLP0*. Values are presented as means ± SEM, *n* = 6-9 pigs per treatment. *, ** DS and RS differ within the intestinal segment, *P* <0.05 and *P* <0.01, respectively; ## DS and RS differ within the total caecum, *P* <0.01. From *left* to *right*, bars represent areas of the gastrointestinal tract from proximal to distal. The small intestine was divided into 10 equal parts; parts 7-10 refer to the 4 most distal segments of the small intestine, whereas the caecum and colon were divided into 2 respectively 4 segments of equal length. White horizontal bars indicate the intestinal parts that were combined for statistical analysis to determine differences between treatments. CA, caecum; CO, colon; DS, digestible starch; RS, resistant starch; SI, small intestine.

Plasma analyses

Blood samples were taken from all pigs, both before and after the intervention. Glucose, insulin, cholesterol and GLP-1 concentrations were not affected by dietary treatment (**Supplemental Fig. 3A**, **B**, **D** and **E**, respectively). However, at the end of the intervention period, plasma TG concentrations were significantly higher in RS-fed pigs compared with pigs fed DS (**Supplemental Fig. 3C**). In addition, in DS-fed pigs, plasma PYY was significantly lower at the end of the experimental period than at the start (**Supplemental Fig. 3F**).

Discussion

In the set of experiments reported in this chapter we investigated the effects of a diet high in RS in pigs. We found that RS was completely degraded in caecum, changed caecal and colonic microbiota composition, increased caecal and colonic SCFA concentrations, and increased the expression of *SLC16A1* and *GCG* in caecum. RS had no effect on plasma concentrations of GLP-1 and PYY measured 5 h postprandially.

Our data on RS contents in intestinal segments show that RS was completely degraded in caecum, which is in line with observations on the degradation of inulin in the gastrointestinal tract of pigs (109). As a result, the composition of the microbiota differentially changed in porcine caecum and colon, as also has been reported for inulin (110). However, the RS-induced changes in the gut microbiota depend on the initial composition of an individual's gut microbiota (50), which could explain why RS-fed pigs 24 (caecum) and 1 (colon) were not clearly separated from the DS-fed pigs on the RDA triplots. Moreover, specific bacterial groups can be selectively affected by a certain type of RS (111, 112) and even by different crystalline polymorphism of the same type of RS (113) in different locations of the intestine. Young et al. (114) fed type 2 RS (RS2) to rats and found blooms of *Bacteroidetes* and *Actinobacteria* in colonic digesta. However, Martínez et al. (111) reported that type 4 RS but not RS2 significantly induced *Bacteroidetes* and *Actinobacteria* while decreasing *Firmicutes* at the phylum level. At the species level, type 4 RS increased *Bifidobacterium adolescentis* and *Parabacteroides distasonis*, whereas RS2 significantly raised the proportions of *Ruminococcus bromii* and *Eubacterium rectale*. In a study on RS3, the relatives of *R. bromii* (R-ruminococci) and *E. rectale* were found to be increased in the colon of most volunteers (50). Moreover, when the effects of structural variation of RS3 on fermentability by human gut microbiota were studied, it was found that retrograded RS3 that formed a B-type pattern induced *Bifidobacterium* spp., whereas A-type pattern RS3 induced *Atopobium* spp. (113).

In our study, the pigs were fed RS3, and we observed a clear change in caecal and colonic microbiota composition compared with pigs fed DS. The relative abundance of *R. bromii* was increased in the colonic samples of RS-fed pigs, which is consistent with previous research (50). However, *E. rectale* was not significantly changed in our study and its relative contribution in the RS group even decreased slightly. Interestingly, in addition to *E. rectale*, other bacterial groups that belong to *Clostridium* cluster XIVa showed either a significant decrease or a trend toward a decrease in RS-fed pigs, whereas bacterial groups belonging to *Clostridium* cluster IV , IX, XV, XVI and XVII increased in RS-fed pigs. This may be due to a low competitiveness of *Clostridium* cluster XIVa, because previous research indicated

the *Roseburia/E. rectale* group was particularly dependent on residual dietary carbohydrate and pH to maintain its competitiveness in the colon (115). It may also be related to the fact that we could not detect a significant effect of the RS diet on butyrate concentration in P1 colon, because several members of this group have been shown to produce butyrate (116). In turn, we found increased relative abundance of populations related to the butyrate-producing *Faecalibacterium prausnitzii*, previously suggested as a health-promoting bacterium (117). Furthermore, we found an increase in several propionate-producing microorganisms, including members of the genera *Propionibacterium*, *Veilonella* and *Phascolarctobacterium*. Propionate has previously been indicated as another health-promoting metabolite being produced in the large intestine (88). In contrast, several groups of potentially pathogenic taxa within the *Gammproteobacteria*, including *Escherichia coli* and *Pseudomonas* spp., were found to be decreased in relative abundance in the colon.

Currently, most studies focus on the colonic and faecal microbiota (50, 111, 114), whereas research on the effect of RS on caecal microbiota is limited. This study is the first to our knowledge to use comprehensive microarray-based profiling to detect the RS effect on caecal microbiota in an animal model. We observed major differences between caecum and colon with respect to microbial changes, possibly due to the change in the chemical structure of RS in colon compared with caecum, which determined the RS accessibility by groups of bacteria (111).

We found that a diet high in RS increased SCFA concentrations in the luminal content compared with a DS diet, as was also observed previously in pigs (85). However, because >95% of the SCFAs are rapidly absorbed from the colonic lumen and metabolized by the host, the total production of SCFAs is difficult to determine (60, 118). Butyrate is almost entirely used by colonocytes as their preferred energy substrate, whereas acetate and propionate move to the liver via the portal vein. Propionate is metabolized by the liver and used for gluconeogenesis, whereas acetate is a substrate for cholesterol synthesis and lipogenesis. In addition, acetate is taken up by muscle and adipose tissue (60, 62). It has been observed that RS especially results in an increased production of butyrate (53). However, our experimental setup did not allow us to quantify total butyrate production, for which preferably isotope dilution studies or direct measurements of arteriovenous differences in SCFA concentrations across the gut are required (60, 118). Moreover, it has been suggested that butyrate is taken up by the colonocytes more rapidly than acetate and propionate (60). This might explain why we did not observe a very profound increase in butyrate concentrations in pigs fed RS.

We found that *SLC16A1* was induced in pigs consuming the RS diet. This observation can be explained by the increased intestinal SCFA concentrations (119, 120). Induction of *SLC16A1* gene expression was also observed by Zhou et al (89),

who measured gene expression in epithelial cells of the gastrointestinal tract from rats fed a DS or an RS diet for 4 wk. They found that *SLC16A1*, *PYY* and *GCG* gene expression was induced in the caecum and colon. The fact that our study did not show an increase in *GCG* or *PYY* gene expression with RS consumption could be due to the different animal model used and the different duration of the dietary treatment.

The presence of SCFA-activated FFA receptors in the intestinal mucosa could provide a link between intestinal SCFAs and appetite and energy homeostasis. FFAR2 immunoreactivity was found to be almost completely colocalized with GLP-1 in terminal ileum, caecum and colon of rats (121). Furthermore, it was shown in proximal colon that the densities of FFAR2-immunoreactive enteroendocrine cells and GLP-1-producing cells were increased >2-fold by fermentable fibre supplementation compared with control (121). In addition, the activation of FFAR2 by SCFAs is suggested to facilitate or modify PYY secretion (57). In this study, no significant differences in *FFAR2* and *FFAR3* gene expression were observed between the 2 diet groups. However, this observation does not exclude the possibility that the receptors were activated in RS-fed pigs, because gene expression levels do not necessarily reflect protein levels. Our experiment showed that *GPR119*, like *GCG*, is most abundantly expressed in the distal small intestine. *GPR119* is expressed in intestinal endocrine L-cells and has been shown to stimulate the release of GLP-1 (122, 123). However, in our study the expression of *GPR119* and *GCG* was not modified upon RS feeding.

TG concentrations in plasma were found to be higher in RS-fed pigs compared with control pigs. Two mechanisms might be responsible for this increase. At first, acetate resulting from fermentation of RS in the intestine is taken up by the liver, where it can serve as a substrate for TG synthesis (60). A second explanation is that RS increases plasma ANGPTL4 concentrations, because we observed increased *ANGPTL4* gene expression in the distal part of the small intestine of RS-fed pigs. Because ANGPTL4 is an inhibitor of lipoprotein lipase, increased concentrations of ANGPTL4 result in increased plasma TG concentrations (124).

In conclusion, we showed that a diet high in RS modulates microbiota composition, SCFA concentrations and gene expression in pig intestine. These findings provide a detailed insight on the interaction between diet, microbiota, and host and may provide leads for designing functional food strategies that aim to reduce the risk of obesity and type 2 diabetes in humans. However, additional investigation is required to further elucidate the underlying molecular mechanisms and the link to satiety.

Acknowledgements

2

Supplemental Tables and Figures

Supplemental Table 1. Composition of the DS and RS diet, expressed as g/kg diet[1]

Ingredient	DS	RS
Native potato starch (Paselli WA4)	350.0	-
Retrograded tapioca starch (Actistar, Cargill)	-	338.8
Wheat	249.0	249.0
Barley	150.0	150.0
Corn gluten meal	100.0	100.0
Potato protein (Protastar)	50.0	50.0
Soy bean oil	15.0	15.0
Animal fat	15.0	15.0
Vitamin mineral premix[2]	10.0	10.0
$CaCO_3$	17.0	17.0
Monocalcium phosphate	11.0	11.0
KCl	10.0	10.0
$NaHCO_3$	15.0	15.0
NaCl	5.0	5.0
L-lysine HCl	1.5	1.5
Flavouring (Luctarom Advance Cherry Honey)	1.5	1.5
Total	1000.0	988.8

[1] DS, digestible starch; RS, resistant starch.

[2] Provided the following per kg food (of the DS diet): retinol: 3.0 mg; cholecalciferol: 50 µg; α-tocopherol: 25 mg; menadione: 1.0 mg; thiamine: 0.75 mg; riboflavin: 4.0 mg; niacin: 20 mg; pyridoxine: 1.0 mg; cyanocobalamin: 15µg; panthothenic acid: 13 mg; choline chloride: 300 mg; folic acid: 2.5 mg; biotin: 0.1 mg; Fe: 80 mg ($FeSO_4.H_2O$); Cu: 10 mg ($CuSO_4.5H_2O$); Mn: 30 mg (MnO); Zn: 60 mg ($ZnSO_4.H_2O$); Co: 0.20 mg ($CoSO_4.7H_2O$); I: 0.75 mg (KI); Se: 0.20 mg (Na_2SeO_3).

Supplemental Table 2. Primer sequences used for qRT-PCR

Gene symbol	Primer sequence (Forward)	Primer sequence (Reverse)
ALPI	CTACACATTGCGTGGAAG	ATGGAGGTATATGGCTTGA
ANGPTL4	AGATTCAGCAACTCTTCC	AATTCTGGATTCTCAAGTG
CHGA	AAGAAACAGAGCAGTTATGA	CCTCCTTCAACTCAGTCT
FFAR1	CTTGTCCTCTGTCACCTG	AGGGAGCTGGTAGTATTG
FFAR2	CGTGTTCATCGTTCAGTA	GAAGTTCTCATAGCAGGTA
FFAR3	TGGAGACCTTACGTGTTG	CGAGGATGAGAAGTAGTAGAT
GCG (glucagon)	CAAGAGGAACAAGAATAACAT	AAGAACTTACATCACTGGTA
GPR119	TATAGGCAGAAGGAGGTA	AGAGAAGGAGGAGGAATG
GPR120	TGGGATGTGTCGTTTGTT	CCTTGATGCCTTGGTGAT
FABP1(L-FABP)	TGAACTCAACGGTGACATA	ATTCTCTTGCTGATTCTCTTG
FABP2 (I-FABP)	AGATAGACCGCAATGAGA	TCCTTCTTGTGTAATTATCAGT
PYY	AGATATGCTAATACACCGAT	CCAAACCCTTCTCAGATG
RPLP0	CTTTAGGCATCACCACTA	TGTCTCCAGTCTTAATCAG
SLC5A8 (SMCT1)	CGCAGATTCCTACTAACC	GATTGTCAGTTCCACCAT
SLC10A2 (ASBT)	TGCCTCTTAATCTATACCA	GGACACAGGAACAATAAG
SLC16A1 (MCT1)	CATCAACTACCGACTTCTG	TACTGGTCTCCTCCTCTT
SLC27A4 (FATP4)	GGTTCTGGGATGATTGTG	TGGTTGAGGAGGTATCTG
VIL1	TATTATTGGTGTTCGTGCTA	TCTGGAGGAATAGGATACTAA

Supplemental Table 3. General characteristics of pigs fed the DS or RS diet for 2 wk. Values are presented as means ± SEM, *n* = 10 pigs per treatment[1]

| | Diet | | |
Measurement	DS	RS	*P* value
Body weight (kg)	274 ± 6.3	271 ± 5.0	0.68
Fat depth (mm)	29.0 ± 1.4	29.0 ± 1.1	0.98
Length small intestine (m)	16.4 ± 1.6	16.9 ± 0.8	0.77
Length colon (m)	5.8 ± 0.2	5.8 ± 0.2	1.00

[1] DS, digestible starch; RS, resistant starch.

Supplemental Figure 1.
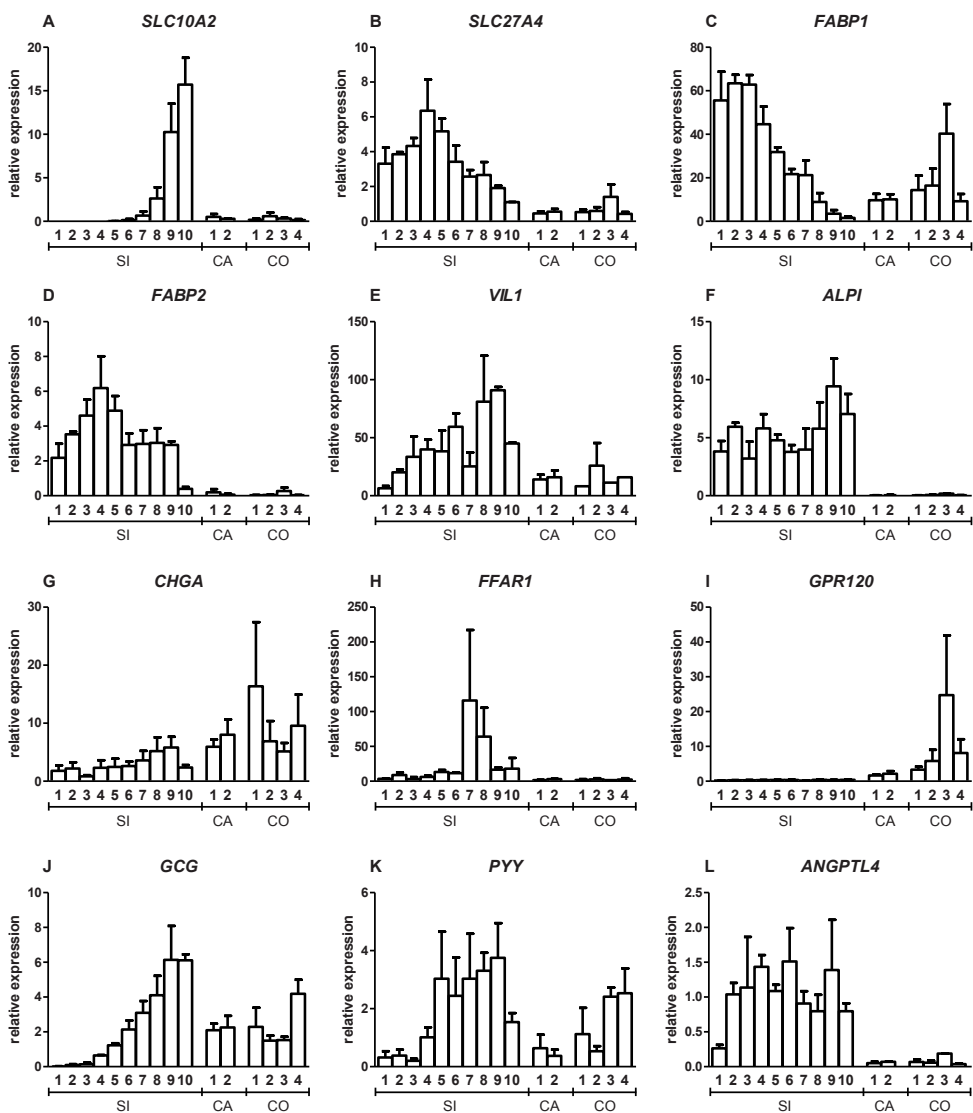
Supplemental Figure 1 (continued).
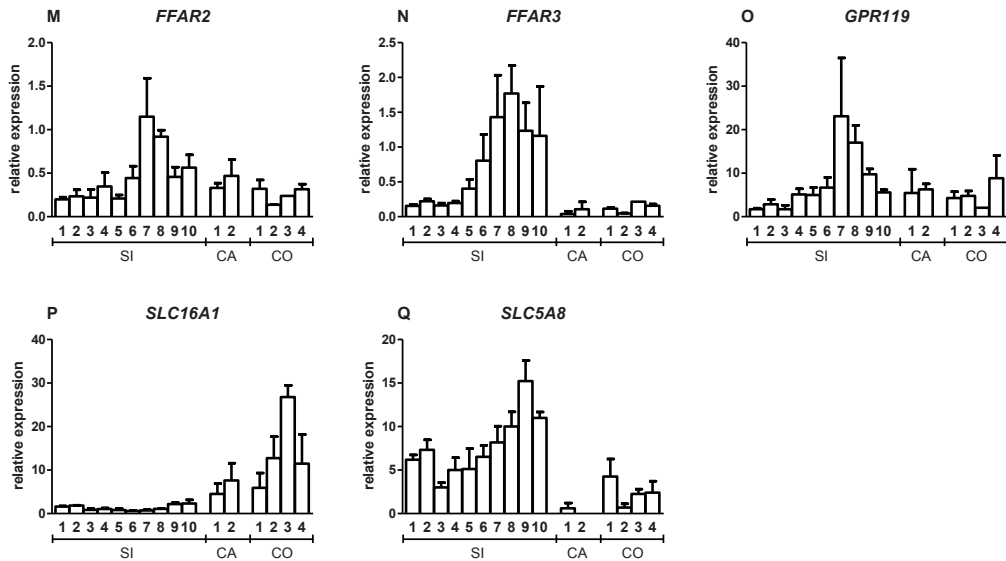
Relative gene expression of Apical sodium-dependent bile salt transporter, *SLC10A2* (**A**), Fatty acid transport protein 4, *SLC27A4* (**B**), Liver-type fatty acid binding protein, *FABP1* (**C**), Intestine-type fatty acid binding protein, *FABP2* (**D**), Villin 1, *VIL1* (**E**), Intestinal alkaline phosphatase, *ALPI* (**F**), Chromagranin A, *CHGA* (**G**), Free fatty acid receptor 1, *FFAR1* (**H**), G protein-coupled receptor 120, *GPR120* (**I**), Glucagon, *GCG* (**J**), Peptide YY, *PYY* (**K**), Angiopoietin-like 4, *ANGPTL4* (**L**), Free fatty acid receptor 2, *FFAR2* (**M**), Free fatty acid receptor 3, *FFAR3* (**N**), G protein-coupled receptor 119, *GPR119* (**O**), Monocarboxylate transporter 1, *SLC16A1* (**P**) and Sodium-coupled monocarboxylate transporter 1, *SLC5A8* (**Q**) in mucosal scrapings along the proximal-distal axis of the intestine of adult female pigs, as determined by qRT-PCR. Messenger RNA levels were standardized to *RPLP0*. Values are presented as means ± SEM, *n* = 3 pigs. From *left* to *right*, bars represent areas of the gastrointestinal tract from proximal to distal. The small intestine was divided into 10 equal parts, whereas the caecum and colon were divided into 2 respectively 4 segments of equal length. CA, caecum; C, colon; SI, small intestine.

Supplemental Figure 2.
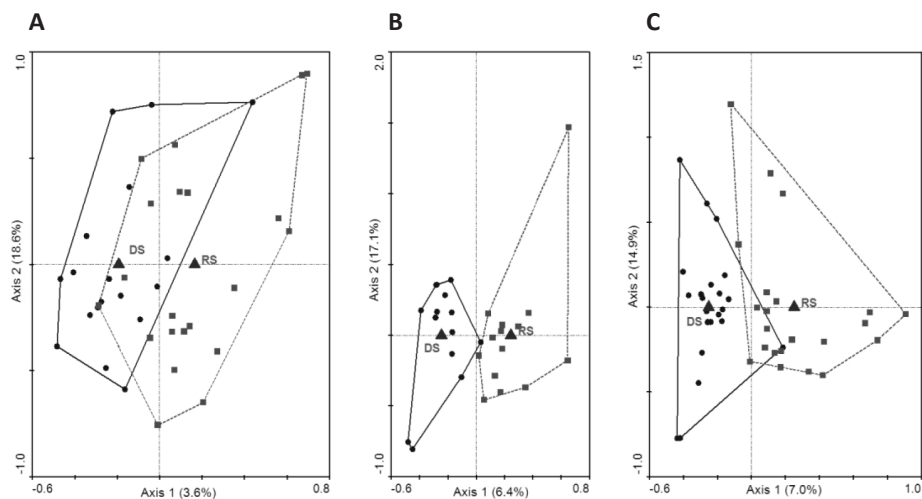
RDA analysis of DGGE profiling data of samples from small intestine (**A**), caecum (**B**) and colon (**C**). Nominal environmental variables DS and RS are represented by triangles. Samples are grouped by treatment: RS (□) and DS (●). Each symbol represents 1 pig. Combined both axes explain 22.2% of the total variance in the dataset for (A), 23.5% for (B) and 21.9% for (C). DS, digestible starch; RS, resistant starch.

Supplemental Figure 3.
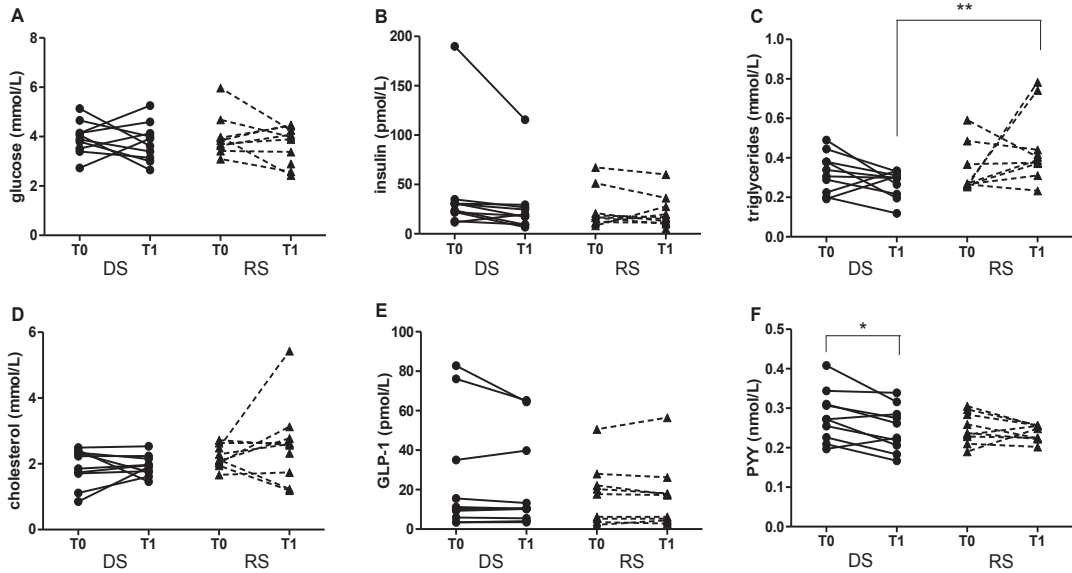
Glucose (**A**), insulin (**B**), TG (**C**), cholesterol (**D**), GLP-1 (**E**) and PYY (**F**) concentrations in plasma of pigs fed the DS or RS diet before the start of the treatment (T0) and on d12 of the treatment (T1). *n* = 10 pigs per treatment; [*], [**] DS and RS differ, *P* <0.05 and *P* <0.01, respectively. DS, digestible starch; RS, resistant starch.

Chapter 3

Dietary resistant starch improves mucosal gene expression profile and luminal microbiota composition in porcine colon

Daniëlle Haenen, Carol Souza da Silva, Jing Zhang, Sietse Jan Koopmans, Guido Bosch, Jacques Vervoort, Walter J.J. Gerrits, Bas Kemp, Hauke Smidt, Michael Müller and Guido J.E.J. Hooiveld

Abstract

Dietary resistant starch (RS) favours both colonic and whole-body metabolism and health, which has been attributed to its fermentation by microbiota in the colon that results in the production of short-chain fatty acids (SCFAs). Although the putative beneficial effects of RS have been extensively studied, knowledge on its effects on global gene expression in colon is rather limited. The main objective of the current study was to identify genes regulated by RS in the proximal colon to infer which metabolic and other pathways were modulated, and to link gene expression changes to alterations in microbiota composition and SCFA concentrations. Ten 17-wk-old male pigs, fitted with a cannula in the proximal colon for repeated collection of tissue biopsies and luminal content, were fed a digestible starch (DS) diet, or a diet high in RS (34%) for 2 consecutive periods of 14 d in a crossover design. Plasma SCFA concentrations were significantly higher with RS consumption compared to DS consumption. RS significantly (P <0.05) increased the relative abundance of several butyrate-producing microbial groups, including *Faecalibacterium prausnitzii* and *Megasphaera elsdenii*, and reduced the abundance of potentially pathogenic members of the genus *Leptospira* and the phylum of Proteobacteria. Colonic transcriptome profiling revealed that upon RS feeding oxidative metabolic pathways, such as beta-oxidation and TCA cycle, were induced, whereas many immune response pathways, including adaptive and innate immune system, were suppressed. The nuclear receptor *PPARG* was identified as a potential key upstream regulator. Overall, this study provides novel molecular insights on effects of RS in colon, and supports the believe that RS has beneficial impact on colonic health.

Introduction

Dietary resistant starch (RS) is a complex polysaccharide that resists digestion and absorption in the small intestine (SI). The effects and potential health benefits of RS have been extensively studied (15, 53, 125). In the first place, effects are found in the large intestine, i.e. caecum (CA) and colon (C), where RS is highly fermentable by microbiota, resulting in the production of short-chain fatty acids (SCFAs). Several animal studies have indeed shown that RS increases the caecal and faecal production of total SCFAs and the main individual SCFAs acetate, propionate and butyrate (53, 85, 126). Furthermore, changes in caecal and faecal microbiota composition have been demonstrated with RS (111, 112, 126), and it has been reported that RS may play a role in the prevention of colorectal cancer (127) and inflammatory bowel disease (128).

Besides its local effects on intestinal function, RS may affect whole-body metabolism and health. An increasing amount of literature provides evidence that RS improves insulin sensitivity (9, 129) and blood lipid profile (130, 131), reduces body fat (82, 83) and food intake (132) and enhances satiety (33, 133).

A large proportion of these beneficial effects is thought to be mediated through the actions of SCFAs (15). In addition to serve as metabolic substrate, both locally in the colon and in other tissues (60, 62), it is known that SCFAs can influence whole-body metabolism by acting as signalling molecules, e.g. via G protein-coupled receptors FFAR2 and FFAR3 that are expressed broadly throughout the body (134, 135).

Genome-wide transcriptional profiling, or transcriptomics, is extensively used to study how cells respond to certain stimuli or to diagnose and predict clinical outcomes (136, 137). Similarly, there is a major interest in characterizing the genes and networks that are regulated by food components, since this contributes to our understanding of a healthy diet (72, 73). Remarkably, data on the genome-wide effects of RS in the intestinal tract is scarce. It has only been reported that differential gene expression due to consumption of type 2 RS for 4 wk suggested improvement of structure and function of the GI tract in rats compared to a corn starch diet with the same energy density (138). In addition, the effect of colonic butyrate administration on gene expression profile in distal colonic mucosa has been investigated, showing that butyrate regulates fatty acid metabolism, electron transport and oxidative stress pathways in healthy humans (139).

The aim of this study was to identify genes and corresponding metabolic and other processes that are modified by RS in the mucosa of the proximal colon (pCO), and to link gene expression changes to alterations in microbiota composition and SCFA concentrations. To this end, a crossover study was performed in pigs that

3

were fitted with a permanent cannula in the pCO for repeated collection of luminal content and tissue biopsies. The full colonic gene expression profile and luminal microbiota composition were obtained by microarray techniques. Pigs were used as a model for humans, because the anatomy and physiology of the gastrointestinal tract of pigs and the pig genome bear a lot of similarities with those in humans (66, 93).

Materials and Methods

Experimental design, pigs and housing

Ten Landrace barrows (17 wk of age; initial body weight of 57.9 ±1.61 kg) from eight litters were fitted with cannulas and catheters and assigned to two dietary treatments in a 2 x 2 cross-over design. Each treatment lasted for 14d, and differed with regard to the type of starch in the diet: pregelatinized digestible starch (DS) or retrograded resistant starch (RS). Pigs were individually housed in metabolism pens of 2 m^2, equipped with a feeder. Artificial lights were on from 05:00 h until 19:00 h and dimmed during the dark period. All experimental protocols describing the management, surgical procedures, and animal care were reviewed and approved by the Animal Care and Use Committee of Wageningen University and Research Centre (Lelystad, the Netherlands).

Diets and feeding

The 2 experimental diets used were identical except for type of starch. The main source of starch in the DS diet was pregelatinized potato starch (Paselli WA4, AVEBE), which was replaced on dry matter basis in the RS diet by retrograded tapioca starch (Actistar, Cargill). According to the supplier, this starch was at least 50% resistant to digestion in the SI. Based on physical and chemical characteristics the RS used in this study can be classified as RS type 3 (15). Composition of the experimental diets is presented in **Supplemental Table 1**. Diets were fed twice a day at 07:00 h and 16:00 h as a mash, and mixed with water (ratio water:feed = 2.5:1) in the feeders immediately before feeding. The diets were isoenergetic on gross energy (GE) basis. The daily feed allowance was adjusted to 2.8 times the energy required for maintenance (MEm = 450 kJ/kg$^{0.75}$ per day) and was based on metabolic body weight (kg$^{0.75}$). Pigs were weighed every week to allow the adjustment of their feeding level in accordance to metabolic body weight. All pigs had free access to water throughout the study. During the 1-week adaptation period, before surgery, pigs were fed a 50:50 mix of the DS and RS diet, and adapted to the feeding pattern and individual housing.

Surgery

In the second week after arrival, pigs underwent surgery for the placement of a cannula in the pCO and a catheter in the carotid artery. See **Supplemental Methods** for details. The pCO was chosen as site of investigation because of the greater fermentation and higher SCFA concentrations compared to more distal colonic regions (126).

Colon biopsies

Biopsies from the intestinal wall of the pCO were collected 300 min after the morning meal on d14 of each dietary treatment. See **Supplemental Methods** for details.

Digesta collection

Digesta were collected via the gut cannula on d14 of each dietary treatment, both 30 min before and 300 min after feeding.

After sampling of digesta and biopsies on d14 of the last treatment period, pigs were anesthetized and exsanguinated, after which the abdominal cavity was opened. The gastrointestinal tract from stomach to anus was removed from the cavity and the length of the SI, CA and CO was determined. The SI was divided into 10 parts of equal length and the CO into 3 parts. Digesta were collected from 5 areas of the gastrointestinal tract: ileum (IL; SI part 7), CA, pCO, middle colon (mCO) and distal colon (dCO).

Collection and storage of the digesta samples, either taken from the cannula or at section, for determination of microbiota composition, SCFA concentration, and dry matter content was performed as described in the **Supplemental Methods**. SCFA concentrations and dry matter content were determined in the luminal content as described before (126).

Blood collection

Blood was drawn from the carotid artery on d14 of each dietary treatment, 300 min after feeding. Blood was collected in 6 mL Vacutainer EDTA tubes (Becton Dickinson) supplemented with protease (Complete, EDTA-free; Roche) and dipeptidyl peptidase-4 (Millipore) inhibitors and then placed in ice water. Tubes were centrifuged for 10 min at 1300 *g* at 4°C within 20 min after blood collection. Plasma was aliquoted and stored at -80°C.

3

RNA isolation and quality control

Total RNA was isolated from CO biopsies using TRIzol reagent (Life Technologies) according to the manufacturer's instructions, followed by RNA Cleanup using the RNeasy Micro kit (Qiagen). Concentrations, purity and quality of the RNA samples was determined as described in the **Supplemental Methods**.

Microarray hybridization and analysis

The pCO biopsies of all 10 pigs, collected on d14 of both dietary treatments, were subjected to genome-wide expression profiling. To this end, total RNA (100 ng) was used for whole transcript cDNA synthesis using the Ambion WT expression kit (Life Technologies) and subsequently labelled using the Affymetrix GeneChip WT Terminal Labelling Kit (Affymetrix). Samples were hybridized on Porcine Gene 1.0 ST arrays (Affymetrix), washed, stained, and scanned on an Affymetrix GeneChip 3000 7G scanner. Detailed protocols for array handling can be found in the GeneChip WT Terminal Labelling and Hybridization User Manual (Affymetrix; P/N 702808, Rev. 4) and are also available on request. Packages from the Bioconductor project (140), integrated in an online pipeline (141), were used to analyse the array data. Various advanced quality metrics, diagnostic plots, pseudoimages, and classification methods were used to determine the quality of the arrays prior statistical analysis (142). Array data have been submitted to the Gene Expression Omnibus under accession number GSE45554.

The approximately 600,000 probes on the Porcine Gene 1.0 ST array were redefined utilizing current genome information (143). In this study probes were reorganized based on the gene definitions as available in the NCBI Sus scrofa Entrez Gene database, build 4.1 (Sscrofa10.2 genome assembly)[1] as well as the gene predictions made by the AUGUSTUST software[2]. Since the annotation of the pig genome is still poor, the functional annotation was improved by mapping the AUGUSTUST gene predictions to the human RefSeq database[3]. Out of 17,118 pig gene predictions, 14,505 were found to have a human orthologous gene. Unless otherwise stated, the functional interpretation of the transcriptome data was performed using the human orthologs.

Normalised gene expression estimates were obtained from the raw intensity values using the robust multiarray analysis (RMA) pre-processing algorithm available in the library 'AffyPLM' using default settings (144). Differentially expressed probe sets (genes) were identified using linear models, applying moderated t-statistics that

---

[1] ftp://ftp.ncbi.nih.gov/genomes/MapView/Sus_scrofa/sequence/BUILD.4.1/

[2] http://gbi.agrsci.dk/pig/sscrofa10_2_annotation/

[3] ssc10.2.RNA.hints.augustus.gff.gffreads.fna.vs.hsa_refseqHsa_2011_10_03.txt.gz

implemented empirical Bayes regularization of standard errors (library 'limma'). To adjust for both the degree of independence of variances relative to the degree of identity and the relationship between variance and signal intensity, the moderated t-statistic was extended by a Bayesian hierarchical model to define a intensity-based moderated T-statistic (IBMT) (145). Probe sets that satisfied the criterion of $P <0.01$ were considered to be significantly regulated.

Changes in gene expression were related to functional changes using gene set enrichment analysis (GSEA) (146). The Enrichment Map plugin for Cytoscape was used for visualization and interpretation of the GSEA results (147, 148). See **Supplemental Methods** for details.

Upstream Regulator Analysis in IPA (Ingenuity Systems) was used to identify the cascade of upstream transcriptional regulators that may explain the observed gene expression changes in the dataset, and whether they are likely activated or inhibited.

To identify potentially secreted proteins, all significantly regulated genes were mapped to determine the corresponding protein IDs and peptide sequences via the UniProt database[4]. The obtained sequences were used as input for ngLOC[5] to predict the subcellular localization of these proteins.

Microbiota analysis

Microbiota composition was determined in the luminal content collected from the pCO via the cannula 300 min after feeding on d14 of each dietary treatment, essentially as described before (126). Due to technical issues, samples from only 9 of the 10 pigs could be analysed. Samples were analysed on the second generation Pig Intestinal Tract Chip (PITChip), an improved version of the original phylogenetic microarray (99) which is comprised of more than 3,200 tiled oligonucleotides targeting the 16S rRNA gene sequences of 781 porcine intestinal microbial phylotypes. PITChip images were processed using Agilent's Feature Extraction Software version 9.5 and further processed in R (library 'microbiome'[6]).

Univariate testing of differences for individual microbial groups was performed using the Mann–Whitney U signed rank test. P values were corrected for multiple testing using a false discovery rate (FDR) method (105). Groups that satisfied the criterion of $P <0.05$ were considered to be significantly affected. Multivariate analysis was applied for PITChip data interpretation as described in the **Supplemental Methods**.

---

[4] http://www.uniprot.org/

[5] http://ngloc.unmc.edu/

[6] http://microbiome.github.com/

SCFA determination by NMR spectroscopy

SCFA concentrations were determined in plasma samples obtained from the carotid artery 300 min after feeding on d14 of each dietary treatment as described in the **Supplemental Methods**.

Multivariate correlation analysis

To get insight into the mutual interactions between the gene expression, microbiota composition and plasma SCFA data, these datasets were pair-wise combined using the linear multivariate method partial least squares (PLS), taking into account the repeated measures (multilevel) structure of the data (149). We used the canonical correlation framework of multilevel-PLS since we deliberately did not want to make any prior assumption on the relationship between the 2 sets of variables that were analysed (150). Analyses were performed in R using the library mixOmics (151).

Standard statistical methods

SCFA concentrations measured in digesta were analysed using a mixed model in SAS (version 9.1; SAS Institute). For samples derived from the pCO cannula, time and individual pigs were included as repeated measurements. The model included period, diet, time, and interaction of diet and time as fixed effects, and pig as random effect. For samples taken at section, segment and individual pigs were included as repeated measurements. The model included diet, segment, and interaction of diet and segment as fixed effects, and pig as random effect. SCFA concentrations measured in plasma were analysed using a paired samples t-test in IBM SPSS Statistics 19. Differences were considered significant if $P < 0.05$. Results were expressed as means ± SEM.

Results

Anthropometric variables

All pigs remained healthy during the experiment and showed normal growth and appetite. Average body weight at the start of the experiment was 57.9 ± 1.6 kg and increased with 21.8 ± 1.1 kg during the study period. No significant effect of treatment order was found with respect to body weight development (data not shown). The average length of the SI and CO, determined at section, were similar for both treatment groups (16.1 ± 0.62 m and 3.96 ± 0.18 m respectively).

Differentially expressed genes in colon

Microarray analysis was performed to identify genes that were differentially expressed in pCO by RS compared to DS. When remapping the probes to the Sscrofa 10.2 genome assembly, the expression of 748 genes was found to be significantly changed by RS (P <0.01). Of these genes, 459 were significantly induced, whereas 289 genes were significantly suppressed by RS (**Supplemental Table 2**). The top induced gene was Intestinal-type alkaline phosphatase-like (*LOC100521756*), showing a 2.9 fold increase on RS (**Fig. 1**), whereas the most suppressed gene was Chitinase 3-like 1 (*CHI3L1*), with a 3.7 fold decrease on RS (**Fig. 1**).

Functional implications of differential gene expression

To gain insight into the underlying biological phenomena affected by RS, pig genes were mapped to human orthologous and gene set enrichment analysis (GSEA) was performed. Results of GSEA were summarized in an enrichment map to enhance the functional interpretation of enriched gene sets. Using conservative significance thresholds, an enrichment map was generated that consisted of 331 nodes (gene sets), of which 57 were positively and 274 were negatively enriched (**Supplemental Fig. 1**). These numbers demonstrated that the majority of gene sets was suppressed with RS feeding. We observed that gene sets describing processes related to *tricarboxylic acid (TCA) cycle*, *lipid metabolism*, *compound sensing*, *barrier function* and *metabolism of xenobiotics* were significantly enriched in the RS group, while gene sets involved in *immune response*, *transcription and translation*, *post-translational modification* and *intracellular processing* were enriched in the DS group (**Supplemental Fig. 1**).

Next, expression changes of genes that contributed to the differential regulation of the 3 largest clusters of processes, i.e. *lipid metabolism*, *TCA cycle* and *immune response* were visualized (**Fig. 2**). Most importantly, these results showed a modest yet consistent regulation of genes involved in the before-mentioned processes, supporting the robustness of the analysis. In addition, it revealed regulation of several key genes, including *PDK1* and *PDK4*; both involved in controlling glucose and fatty acid metabolism and homeostasis, *ANGPTL4*; regulating plasma TG levels, as well as *NFKB*, *TLR4*, *BCL6*, *ICOS* and *CR2* that all play a role in controlling the adaptive and innate immune response.

Top induced genes

Gene Description	Gene symbol	Entrez ID	Mean log2 FC	Individual log2 FC (1 2 3 4 5 6 7 8 9 10)
Intestinal-type alkaline phosphatase-like	LOC100521756	100521756	1.55	
Carbonic anhydrase II	CA2	100154873	1.35	
Uncharacterized LOC100621113	LOC100621113	100621113	1.01	
Hydroxysteroid (17-beta) dehydrogenase 2	HSD17B2	100312973	1.00	
Transmembrane 4 L6 family member 20-like	LOC100513630	100513630	0.96	
Uncharacterized protein C5orf4 homolog	LOC100525263	100525263	0.95	
Solute carrier family 30, member 10	SLC30A10	100623097	0.92	
Angiotensinogen-like	LOC100157073	100157073	0.86	
Carbonic anhydrase 12-like	LOC100152749	100152749	0.83	
Carcinoembryonic antigen-related cell adhesion molecule 7-like	LOC100524810	100524810	0.81	
ATP-binding cassette, sub-family A (ABC1), member 6	ABCA6	100520861	0.79	
Agmatinase, mitochondrial-like	LOC100519548	100519548	0.74	
ADAM metallopeptidase domain 23	ADAM23	100518044	0.74	
Claudin 10	CLDN10	100153752	0.73	
Thiopurine S-methyltransferase	TPMT	100157630	0.72	
Ubiquitin carboxyl-terminal hydrolase 2-like	LOC100520041	100520041	0.72	
Transient receptor potential cation channel subfamily M member 6-like	LOC100157775	100157775	0.71	
Transmembrane protein 117	TMEM117	100524623	0.71	
Poly (ADP-ribose) polymerase family, member 15	PARP15	100520273	0.70	
Serine palmitoyltransferase, long chain base subunit 3	SPTLC3	100519280	0.68	
Collagen alpha-6(VI) chain-like	LOC100516642	100516642	0.67	
Guanylate cyclase activator 2A (guanylin)	GUCA2A	100301560	0.66	
EGF containing fibulin-like extracellular matrix protein 1	EFEMP1	100512046	0.66	
Pancreatic lipase-related protein 2	PNLIPRP2	100462755	0.66	
Olfactory receptor 9K2-like	LOC100737562	100737562	0.66	

Top suppressed genes

Gene Description	Gene symbol	Entrez ID	Mean log2 FC	Individual log2 FC (1 2 3 4 5 6 7 8 9 10)
Chitinase 3-like 1 (cartilage glycoprotein-39)	CHI3L1	396865	-1.88	
C4b-binding protein alpha chain-like	LOC100520761	100520761	-1.42	
Secretory leukocyte peptidase inhibitor	SLPI	396886	-1.13	
C-type lectin domain family 7, member A	CLEC7A	100038025	-0.94	
Immunoresponsive 1 homolog (mouse)	IRG1	100524951	-0.93	
Chemokine (C-X-C motif) receptor 4	CXCR4	396659	-0.89	
P2Y purinoceptor 13-like	LOC100524766	100524766	-0.86	
BPI fold containing family B, member 2	BPIFB2	100113424	-0.84	
Tryptophan hydroxylase 1	TPH1	100511002	-0.80	
Chromosome 1 open reading frame 162 ortholog	C4H1orf162	100627962	-0.78	
SLAM family member 7-like	LOC100154053	100154053	-0.78	
Placenta-specific gene 8 protein-like	LOC100525175	100525175	-0.78	
Antileukoproteinase-like	LOC100512873	100512873	-0.74	
Rho GTPase activating protein 15	ARHGAP15	100520808	-0.74	
Monocarboxylate transporter 7-like	LOC100739042	100739042	-0.71	
Lymphoid enhancer-binding factor 1	LEF1	100170126	-0.70	
Transmembrane protein 156-like	LOC100525349	100525349	-0.69	
Membrane-spanning 4-domains, subfamily A, member 1	MS4A1	100627952	-0.68	
SLAM family member 6	SLAMF6	100156912	-0.67	
Sorting nexin-10-like	LOC100520876	100520876	-0.66	
Acyloxyacyl hydrolase (neutrophil)	AOAH	100522290	-0.64	
Clusterin	CLU	397025	-0.63	
CD1B antigen	PCD1B	100038007	-0.62	
Interleukin 2 receptor, gamma	IL2RG	397156	-0.60	
A-kinase anchor protein 5-like	LOC100153460	100153460	-0.60	

Figure 1 Top 25 induced genes and bottom 25 suppressed genes on the RS diet, based on the gene definitions of the NCBI Sus scrofa Entrez Gene database, build 4.1. Average log2 fold changes of the signal intensity of RS compared with DS were determined from the individual response of the 10 pigs, which are expressed as a heatmap. The intensity of the red and green colour indicates the degree of induction or suppression per pig, respectively.

Gene symbol	Mean log2 FC
COX10	0.23
HMOX2	0.21
OGDH	0.18
UQCRC1	0.16
UQCRH	0.15
PCK2	0.14
DLST	0.14
ACO1	0.13
SDHB	0.12
PCK1	0.97
PDK4	0.70
SLC16A1	0.61
PC	0.31
LDHA	-0.16
C5orf4	1.16
AGT	0.87
SPTLC3	0.68
PNLIPRP2	0.67
CYP27A1	0.63
IGF1	0.62
NR1H4	0.59
ANGPTL4	0.58
HPGD	0.56
ACSF2	0.50
HMGCS2	0.49
GPT	0.45
PLD1	0.42
THRB	0.42
FABP1	0.41
PRDX6	0.41
ACADSB	0.41
ECHDC2	0.40
UCP3	0.39
PLCE1	0.38
ADH7	0.37
FAAH	0.37
SRD5A1	0.37
CYP26B1	0.37
CES1	0.36
AGPAT2	0.36
PNPLA2	0.35
FA2H	0.35
DGAT2	0.35
STX3	0.35
ADH5	0.34
GLYCTK	0.33
HMGCL	0.33
GBA3	0.33
PPARG	0.33
SLC25A20	0.32
KDSR	0.32
GGT5	0.32
BDH1	0.31
EPHX2	0.30
RBP1	0.30
TXNIP	0.30
TNFRSF21	0.29
MGST2	0.29
CERS6	0.29
CYP2J2	0.29
CPT1A	0.28
ACAT1	0.28
ACAA2	0.27
LIPE	0.27
SGMS2	0.27
AASDH	0.26
ALDH6A1	0.26
PPM1L	0.26
DGKG	0.26
DGAT1	0.25
CYP7B1	0.25
CIDEC	0.24
DECR1	0.24

Gene symbol	Mean log2 FC
MLXIPL	0.24
ABCD3	0.24
CYP17A1	0.23
MGLL	0.23
HSD17B8	0.23
SLC35D1	0.23
PPAP2B	0.23
MBOAT1	0.22
DEGS2	0.22
GPAT2	0.22
ACADM	0.22
SLC25A1	0.21
ACOT7	0.20
ACOX1	0.20
UGDH	0.19
HNF4A	0.19
PLIN2	0.19
SGPP2	0.19
ACBD4	0.18
PCCB	0.18
KIF1B	0.17
CAB39	0.17
GPD2	0.16
HADHA	0.15
CRAT	0.15
COL4A3BP	0.15
SPTLC2	0.15
GOT2	0.14
ACADS	0.14
ADIPOR1	-0.14
MTHFS	-0.16
TNFRSF1A	-0.17
LTA4H	-0.19
DGKE	-0.20
GPX1	-0.24
LDLR	-0.28
DEGS1	-0.29
BCAT1	-0.29
SCPEP1	-0.29
FAR2	-0.29
FADS1	-0.30
FADS2	-0.32
DGKA	-0.33
ABAT	-0.38
SMPDL3A	-0.40
AKR1C1	-0.40
HAL	-0.42
IRG1	-1.07
CAV1	0.38
CREBBP	-0.14
MUC1	0.37
FZD5	0.32
ERBB2	0.23
BAD	0.23
JUN	0.23
PTPRH	0.23
JMJD6	0.22
HDAC5	0.22
BMP4	0.19
NCK2	0.19
MAPKAP1	0.17
PIK3R1	0.16
PAG1	0.15
KLF6	0.15
STIM1	0.12
ELF1	-0.11
TUBB	-0.11
KAT5	-0.13
PAK2	-0.13
FOXP1	-0.14
PPP3CA	-0.14
CD24	-0.16
PTPN6	-0.16

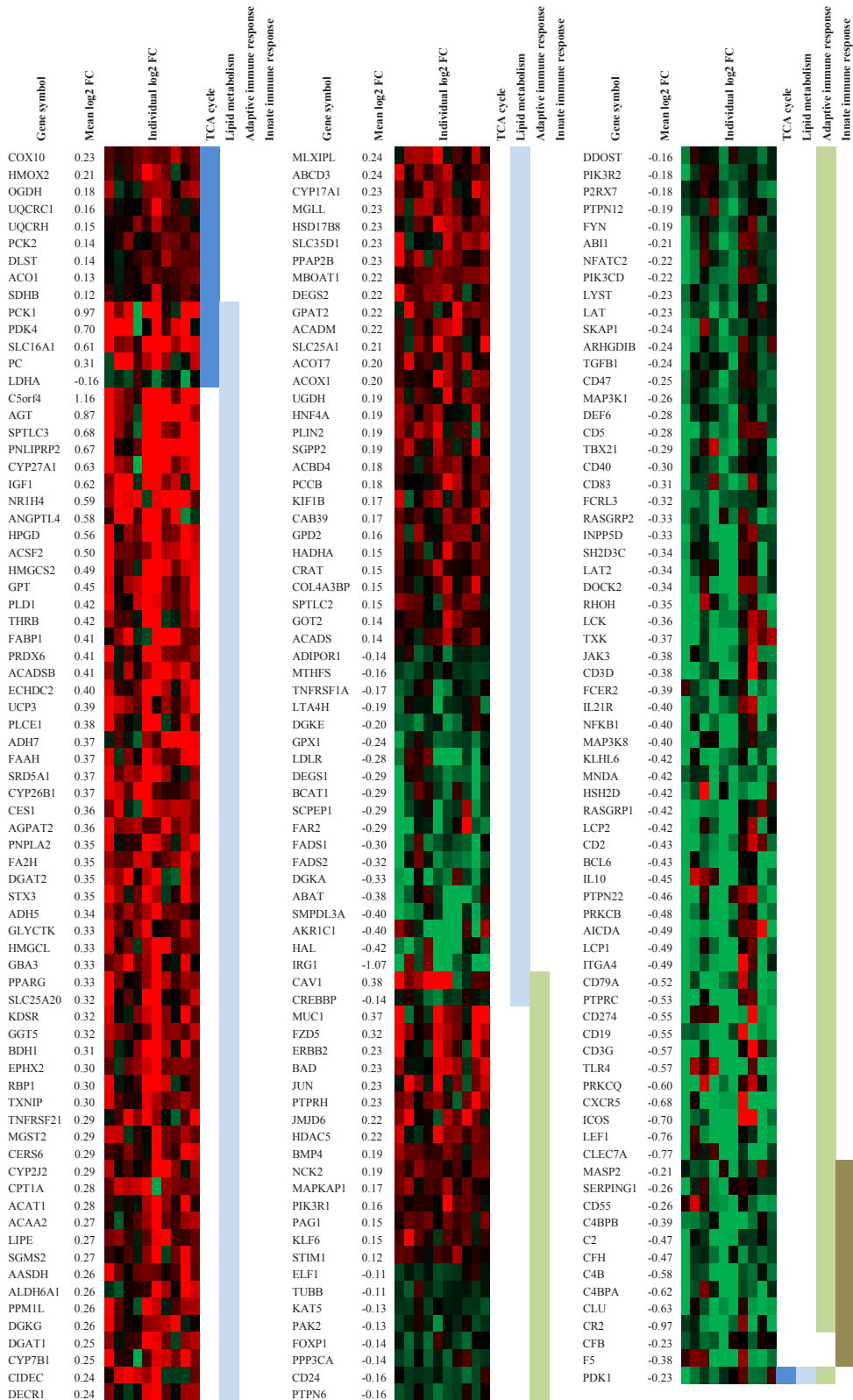| Gene symbol	Mean log2 FC
DDOST	-0.16
PIK3R2	-0.18
P2RX7	-0.18
PTPN12	-0.19
FYN	-0.19
ABI1	-0.21
NFATC2	-0.22
PIK3CD	-0.22
LYST	-0.23
LAT	-0.23
SKAP1	-0.24
ARHGDIB	-0.24
TGFB1	-0.24
CD47	-0.25
MAP3K1	-0.26
DEF6	-0.28
CD5	-0.28
TBX21	-0.29
CD40	-0.30
CD83	-0.31
FCRL3	-0.32
RASGRP2	-0.33
INPP5D	-0.33
SH2D3C	-0.34
LAT2	-0.34
DOCK2	-0.34
RHOH	-0.35
LCK	-0.36
TXK	-0.37
JAK3	-0.38
CD3D	-0.38
FCER2	-0.39
IL21R	-0.40
NFKB1	-0.40
MAP3K8	-0.40
KLHL6	-0.42
MNDA	-0.42
HSH2D	-0.42
RASGRP1	-0.42
LCP2	-0.42
CD2	-0.43
BCL6	-0.43
IL10	-0.45
PTPN22	-0.46
PRKCB	-0.48
AICDA	-0.49
LCP1	-0.49
ITGA4	-0.49
CD79A	-0.52
PTPRC	-0.53
CD274	-0.55
CD19	-0.55
CD3G	-0.57
TLR4	-0.57
PRKCQ	-0.60
CXCR5	-0.68
ICOS	-0.70
LEF1	-0.76
CLEC7A	-0.77
MASP2	-0.21
SERPING1	-0.26
CD55	-0.26
C4BPB	-0.39
C2	-0.47
CFH	-0.47
C4B	-0.58
C4BPA	-0.62
CLU	-0.63
CR2	-0.97
CFB	-0.23
F5	-0.38
PDK1	-0.23

3

Figure 2 Heatmap of significantly regulated genes (*P* <0.05) present in the positively enriched gene sets describing TCA cycle or lipid metabolism, or present in the negatively enriched gene sets describing processes involved in adaptive or innate immune response. Average and individual log2 fold changes are presented. The intensity of the red and green colour indicates the degree of induction or suppression per pig, respectively, and ranged from -0.65 (green) to 0.65 (red). Pigs are ranked based on their identifier. The vertical colour bars indicate gene set membership; dark blue: TCA cycle, light blue: lipid metabolism, olive green: adaptive immune response, tan: innate immune response.

Microbiota analysis

RS did not significantly change the microbial diversity as indicated by Shannon's index for diversity (data not shown). Principal response curves analysis showed that diet (DS or RS) explained 15.7% of the total variation in microbiota, while period and the interaction of period and diet only explained 4.8% and 6.8% respectively (data not shown). This indicated that diet was the main factor driving the microbial variation. Partial RDA of the PITChip data confirmed that diet had a significant effect on microbial variation (*P* <0.05) (**Fig. 3**).

At the phylum level, we observed a significant increase in the relative abundance of Bacteroidetes (*P* = 0.036) (**Supplemental Fig. 2A**). As a result, we found a significantly lower Firmicutes/Bacteroidetes ratio (*P* = 0.017) in RS-fed pigs (10.3 ± 2.0) compared to DS-fed pigs (20.1 ± 3.4) (**Supplemental Fig. 2B**).

At the approximate genus level (90% 16S ribosomal RNA similarity threshold), the relative abundance of several groups that include known butyrate-producing bacteria, including those related to *Faecalibacterium prausnitzii* and *Megasphaera elsdenii*, was increased upon RS feeding compared to DS feeding (*P* <0.05) (**Table 1**). Other groups that increased in relative abundance comprised *Prevotella melaninogenica*-like, uncultured *Prevotella*, *Enterococcus*-like, *Dialister*-like, *Mitsuokella multacida*-like and *Clostridium ramosum*-like bacteria. On the other hand, *Eggerthella*-like, uncultured *Bacteroidetes*, *Turicibacter*-like, *Clostridium perfringens*-like, *Anaerovorax*-like, *Peptoniphilus*-like, uncultured *Clostridia XIVa*, uncultured *Planctomycetacia*, as well as a range of potentially pathogenic microbial groups, including *Leptospira*, and several facultative bacterial groups within the *Proteobacteria*, including *Sphingomonas*-like, uncultured *Betaproteobacteria*, *Actinobacillus indolicus*-like, *Aeromonas*, *Alishewanel*-like, *Halomonas*-like, *Pasteurella*-like, *Pseudomonas*-like, *Psychrobacter*-like, *Ruminobacter amylophilus*-like, *Vibrio*-like, *Xanthomonas*-like, were found to be decreased on the RS diet (*P* <0.05) (**Table 1**).
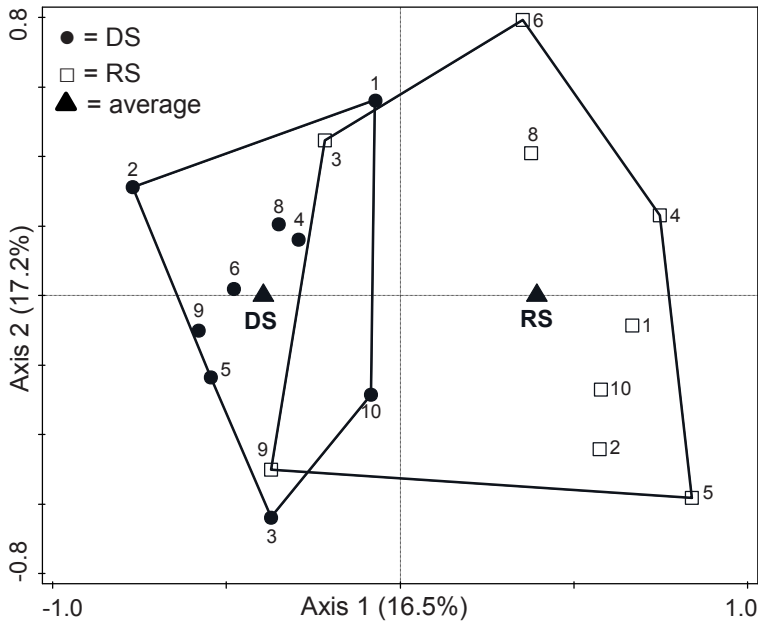
Figure 3 Biplot of partial RDA results, representing the principal component analysis of the microbiota composition as measured by the mean hybridization signals for 151 genus-level phylogenetic groups in the luminal content of proximal colon of pigs fed the DS or RS diet for 2 wk. Samples are grouped by diet. Each symbol represents 1 pig, with numbers indicating pig identifiers. The average of the nominal environmental variables DS and RS are represented by triangles. DS, digestible starch; RS, resistant starch.

Table 1 Phylogenetic groups in the luminal content of proximal colon of pigs fed DS or RS diet for 2 wk, which were significantly affected by diet according to univariate analysis of PITChip data.

Phylogenetic group	P value	FDR[1]	ARC[2] DS	ARC[2] RS	Effect[3] (RS-DS)
Actinobacteria					
Actinobacteria					
Eggerthella et rel.	0.008	0.079	0.109 ± 0.050	0.033 ± 0.043	-
Microbacterium et rel.	0.055	0.223	0.586 ± 0.100	0.709 ± 0.193	+
Bacteroidetes					
Bacteroidetes					
Parabacteroides distasonis et rel.	0.055	0.223	0.411 ± 0.278	0.622 ± 0.278	+
Prevotella melaninogenica et rel.	0.012	0.088	0.056 ± 0.055	3.079 ± 3.194	+
Uncultured *Bacteroidetes*	0.039	0.203	0.605 ± 0.934	0.080 ± 0.241	-
Uncultured *Prevotella*	0.008	0.079	0.836 ± 0.531	2.501 ± 1.679	+
Firmicutes					
Bacilli					
Enterococcus et rel.	0.039	0.203	2.480 ± 0.576	3.025 ± 0.657	+
Lactobacillus amylovorus et rel.	0.055	0.223	1.094 ± 0.963	0.400 ± 0.458	-
Lactobacillus salivarius et rel.	0.055	0.223	0.926 ± 0.356	1.267 ± 0.426	+
Turicibacter et rel.	0.004	0.079	0.197 ± 0.069	0.062 ± 0.036	-
Clostridium cluster I					
Clostridium perfringens et rel.	0.008	0.079	2.398 ± 1.763	0.403 ± 0.810	-
Clostridium cluster IV					
Faecalibacterium prausnitzii et rel.	0.020	0.123	0.969 ± 0.398	1.925 ± 1.142	+
Uncultured *Clostridia* IV	0.055	0.223	2.404 ± 0.863	1.697 ± 1.005	-
Clostridium cluster IX					
Dialister et rel.	0.004	0.079	0.453 ± 0.248	0.852 ± 0.328	+
Megasphaera elsdenii et rel.	0.008	0.079	0.850 ± 0.210	1.386 ± 0.600	+
Mitsuokella multacida et rel.	0.008	0.079	1.084 ± 0.301	1.776 ± 0.743	+
Clostridium cluster XI					
Anaerovorax et rel.	0.004	0.079	1.811 ± 0.681	0.495 ± 0.973	-
Clostridium cluster XIII					
Peptoniphilus et rel.	0.008	0.079	0.601 ± 0.350	0.176 ± 0.364	-
Clostridium cluster XIVa					
Uncultured *Clostridia* XIVa	0.039	0.203	2.412 ± 0.828	1.657 ± 0.928	-
Clostridium cluster XVIII					
Clostridium ramosum et rel.	0.008	0.079	0.213 ± 0.057	0.296 ± 0.101	+
Planctomycetes					
Planctomycetacia					
Uncultured *Planctomycetacia*	0.012	0.088	0.159 ± 0.114	0.037 ± 0.048	-
Proteobacteria					
Alphaproteobacteria					
Rhizobium et rel.	0.055	0.223	0.552 ± 0.085	0.382 ± 0.153	-
Sphingomonas et rel.	0.027	0.165	0.214 ± 0.203	0.059 ± 0.154	-
Betaproteobacteria					
Uncultured *Betaproteobacteria*	0.012	0.088	0.329 ± 0.046	0.246 ± 0.066	-
Gammaproteobacteria					
Actinobacillus indolicus et rel.	0.008	0.079	0.332 ± 0.058	0.227 ± 0.079	-
Aeromonas	0.020	0.123	0.671 ± 0.147	0.389 ± 0.268	-
Alishewanel et rel.	0.020	0.123	0.472 ± 0.093	0.255 ± 0.176	-
Escherichia coli et rel.	0.055	0.223	0.397 ± 0.190	0.166 ± 0.196	-
Halomonas et rel.	0.004	0.079	0.747 ± 0.204	0.448 ± 0.225	-
Pasteurella et rel.	0.012	0.088	0.145 ± 0.041	0.093 ± 0.037	-

Pseudomonas et rel.	0.008	0.079	0.697 ± 0.253	0.279 ± 0.340	-
Psychrobacter et rel.	0.008	0.079	0.629 ± 0.126	0.408 ± 0.173	-
Ruminobacter amylophilus et rel.	0.039	0.203	0.211 ± 0.022	0.153 ± 0.057	-
Thiocapsa et rel.	0.055	0.223	0.675 ± 0.163	0.450 ± 0.202	-
Vibrio et rel.	0.008	0.079	0.690 ± 0.149	0.438 ± 0.207	-
Xanthomonas et rel.	0.020	0.123	0.852 ± 0.063	0.682 ± 0.140	-
Spirochaetes					
Spirochaetes					
Leptospira	0.012	0.088	0.717 ± 0.172	0.402 ± 0.208	-

[1] FDR: false discovery rate.

[2] ARC: average relative contribution (%) of a microbial group. Values represented means ± SEM, *n* = 9 per treatment.

[3] "+" or "-" indicates whether the average relative contribution of the microbial group was increased or decreased by the RS treatment.

SCFA concentrations

Total SCFA concentration in the luminal content of pCO, collected 30 min before and 300 min after feeding, was not affected by dietary treatment (**Supplemental Fig. 3A**). However, the percentage of branched-chain fatty acids (BCFAs), i.e. isobutyrate and isovalerate, of total SCFAs was significantly lower in pigs fed RS (**Supplemental Fig. 3B**). Total SCFA concentration in the luminal content of CA and dCO obtained at sacrifice was significantly higher with RS consumption (**Supplemental Fig. 4A**). In pCO, mCO and dCO, significantly lower percentages of BCFAs were observed with RS consumption (**Supplemental Fig. 4B**).

     Acetate, propionate, and butyrate concentrations determined in peripheral plasma collected 300 min after feeding were significantly higher with RS consumption compared to DS consumption (**Fig. 4**).
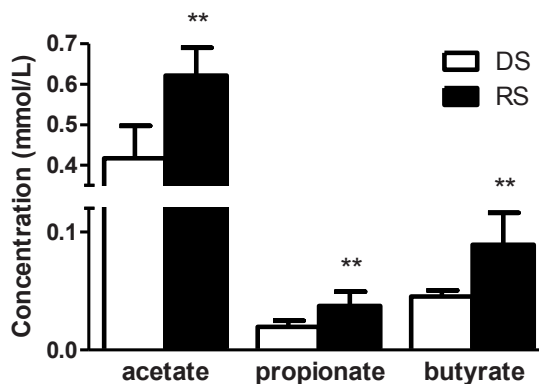

Figure 4 Acetate, propionate and butyrate concentrations in peripheral plasma of pigs fed the DS or the RS diet for 2 wk. Samples were collected 300 min after feeding. Values are means ± SEM, *n* = 10 for DS-fed pigs and *n* = 9 for RS-fed pigs. ** indicates *P* <0.01. DS, digestible starch; RS, resistant starch.

Correlation analysis

The expression of the 618 significantly regulated genes (AUGUSTUST annotation) was integrated with the relative abundance of the 37 significantly changed microbial groups using multivariate correlation analysis. A network was generated that revealed gene-microbiota combinations that were strongly correlated (correlation coefficient >0.9). This network contained 123 genes and 17 microbial groups, with each gene correlating with 1 up to 14 microbial groups (**Fig. 5A**). Most genes (i.e. 96) were significantly correlated with *Vibrio*-like bacteria, of which 75 genes were negatively correlated including the SCFA transporter *SLC16A1*, *PPARG* and the *PPARG* target gene *GPT*.

In addition, we determined which of the 618 genes correlated with concentrations of acetate, propionate and butyrate measured in peripheral plasma 300 min after feeding. The resulting network showed that 26 genes were correlated (correlation coefficient >0.9) with acetate and 48 genes were correlated with propionate and/or butyrate (**Fig. 5B**).

Correlation analysis of the 37 microbial groups with plasma acetate, propionate and butyrate (correlation coefficient >0.8) revealed 20 highly correlating microbial groups (**Fig. 5C**). Whereas the majority of correlations included negative correlations of microbial groups reduced in the presence of RS, we also observed positive correlations with known acid producing bacteria, including *Megasphaera elsdenii*, a known producer of acetate, propionate and butyrate, as well as *Mitsuokella multacida*, which has been shown to predominantly produce lactate, succinate and smaller amounts of acetate from carbohydrate fermentation. The latter compounds are in turn used as substrates by producers of propionate and butyrate (116).
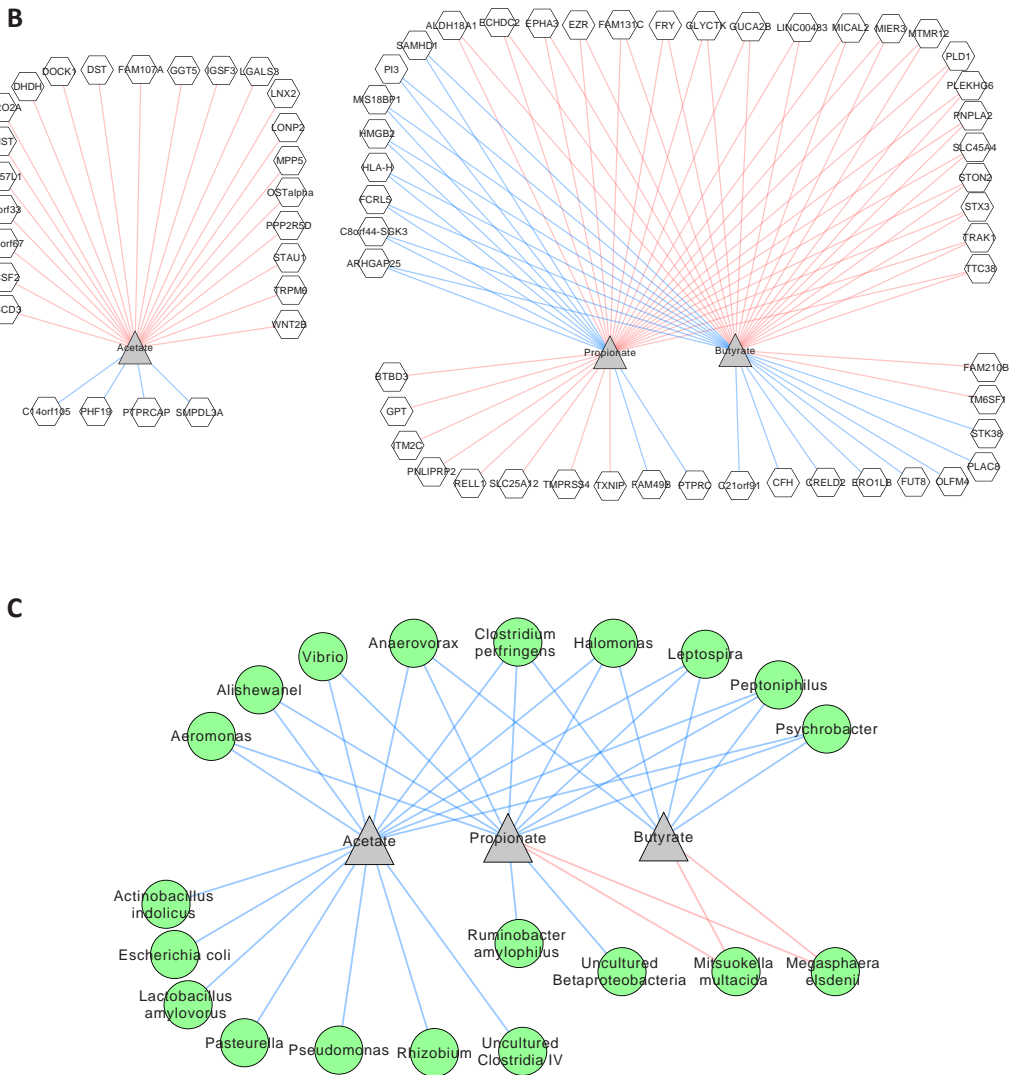
A

B

3

C
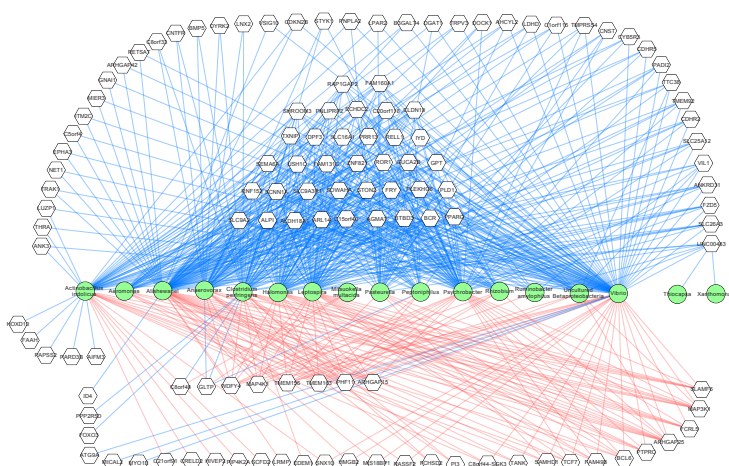
Figure 5 Correlation networks of genes correlating with microbial groups with correlation coefficient >0.9 (**A**), genes correlating with plasma acetate, propionate and butyrate concentrations with correlation coefficient >0.9 (**B**), and microbial groups correlating with plasma acetate, propionate and butyrate concentrations with correlation coefficient >0.8 (**C**). Genes are indicated as white hexagons, microbial groups as green circles, and SCFAs as grey triangles. Blue and red lines respectively represent negative and positive correlations.

Table 2 Upstream regulators, determined by Ingenuity Systems Pathway Analysis Software.

Upstream Regulator	Molecular Type	Predicted activation state	Activation z-score[1]	*P*-value of overlap[2]
PPARG	Ligand-dependent nuclear receptor	Activated	3.069	$3.10 \ 10^{-4}$
ERG	Transcription regulator	Activated	2.828	$1.33 \ 10^{-2}$
XBP1	Transcription regulator	Inhibited	-2.041	$3.96 \ 10^{-2}$

PPARG, Peroxisome proliferator-activated receptor gamma; *ERG*, V-ets erythroblastosis virus E26 oncogene homolog (avian); *XBP1*, X-box binding protein 1.

[1] Activation z-score predicts the activation state of the upstream regulator, using the gene expression pattern of its downstream genes in the dataset and takes into account the consistency of target gene activation. Upstream regulators with z-score ≥ 2 were considered to be activated, if z-score ≤ -2 the upstream regulator was considered to be inhibited.

[2] The overlap *P*-value measures the significance of overlap between the dataset genes and the genes reported to be regulated by the transcriptional activator.

Table 3 *PPARG* target genes, determined by Ingenuity Systems Pathway Analysis Software.

Name	Gene symbol	Prediction of activation state[1]	Mean log2 FC[2]	Literature Findings[3]
Transforming growth factor, beta receptor 1	*TGFBR1*	Activated	-0.25	Down
Chemokine (C-X-C motif) ligand 14	*CXCL14*	Activated	-0.26	Down
Carbonic anhydrase II	*CA2*	Activated	1.36	Up
Angiopoietin-like 4	*ANGPTL4*	Activated	0.58	Up
3-hydroxy-3-methylglutaryl-CoA synthase 2 (mitochondrial)	*HMGCS2*	Activated	0.49	Up
Uncoupling protein 3 (mitochondrial, proton carrier)	*UCP3*	Activated	0.39	Up
Caveolin 1, caveolae protein, 22kDa	*CAV1*	Activated	0.38	Up
Vascular endothelial growth factor A	*VEGFA*	Activated	0.37	Up
Peroxisome proliferator-activated receptor gamma	*PPARG*	Activated	0.33	Up
Solute carrier family 25 member 20	*SLC25A20*	Activated	0.32	Up
3-hydroxybutyrate dehydrogenase, type 1	*BDH1*	Activated	0.31	Up
Lipase, hormone-sensitive	*LIPE*	Activated	0.27	Up
Diacylglycerol O-acyltransferase 1	*DGAT1*	Activated	0.25	Up
Monoglyceride lipase	*MGLL*	Activated	0.23	Up
Acyl-CoA dehydrogenase, C-4 to C-12 straight chain	*ACADM*	Activated	0.22	Up
Phosphodiesterase 3B, cGMP-inhibited	*PDE3B*	Inhibited	-0.45	Up
Serpin peptidase inhibitor, clade A, member 1	*SERPINA1*	Inhibited	-0.60	Up
Angiotensinogen (serpin peptidase inhibitor, clade A, member 8)	*AGT*	-	0.87	Regulates
Insulin-like growth factor 1 (somatomedin C)	*IGF1*	-	0.62	Regulates
Glutamic-pyruvate transaminase (alanine aminotransferase)	*GPT*	-	0.45	Regulates
Protein tyrosine phosphatase, receptor type, F	*PTPRF*	-	0.27	Regulates

[1] Column indicates the predicted activation state of *PPARG* (either Activated or Inhibited), based on the direction of the gene expression change in the uploaded dataset.

[2] Average log2 fold change of the signal intensity of RS compared to DS.

[3] Column indicates whether literature findings support the prediction. 'Down' and 'up' indicate whether literature supports a down- or an up-regulation of the target gene by *PPARG*, respectively. 'Regulates' indicates that there is insufficient support from literature that the target gene is either up- or down-regulated by *PPARG*.

Upstream regulators

The underlying mechanisms by which RS modulated gene expression changes are not well understood. We therefore aimed to identify potential upstream transcriptional regulators that could explain the observed shift in gene expression profile. Results of this analysis predicted the transcription factors *PPARG* and *ERG* to be significantly activated on RS, while *XBP1* was predicted to be inhibited (**Table 2**). Because the highest z-score (3.069) was found for PPARG, we had a closer look at the downstream *PPARG* target genes. Out of 21 *PPARG* target genes regulated by RS, 15 genes had an expression change consistent with activation of PPARG (**Table 3**). Since *TGFBR1* and *CXCL14* are known to be down-regulated by PPARG and we indeed observed reduced expression of these target genes, this suggests that *PPARG* was activated by RS. The other 13 target genes were induced in our dataset, which corresponds with observations from literature, suggesting that *PPARG* is activated by RS.

Potentially secreted proteins

The transcriptome data were mined to identify potentially secreted proteins that may mediate effects of RS in liver or other tissues and organs. From the 655 significantly regulated genes in our dataset, we identified 849 unique encoding proteins for which the predicted locations were determined. The number of proteins is larger than the number of genes due to alternatively splicing of the mRNA molecules of the regulated gens. Fifty-three proteins were predicted to be located extracellular, and therefore secreted, with a probability above 0.20 (**Supplemental Table 3**). Of these proteins, 31 were encoded by genes induced on RS and 22 proteins were encoded by suppressed genes. Among the potentially secreted proteins that, based on the transcriptome data, are expected to increase on RS were IGF1, AGT, VEGFA and ANGPTL4. These proteins are all derived from PPARG target genes. The proteins that are expected to go down on RS include 2 more proteins derived from PPARG target genes, namely SERPINA1 and CXCL14.

3

Discussion

In the present study, we examined the effects of 2-wk-consumption of a diet high in RS on the mucosal transcriptome and luminal microbiota composition and SCFA concentrations in proximal colon of pigs. Our results showed that compared to a DS diet, the RS diet shifted colonic gene expression profile of the host from immune regulation towards metabolic regulation and reduced the abundance of several potentially pathogenic bacteria in the colonic lumen. In addition, plasma SCFA concentrations increased on the RS diet. The nuclear receptor *PPARG* was identified as a potential key upstream regulator.

Microbiota composition
Evidence suggesting that gut microbiota are highly important in the regulation of energy homeostasis and fat storage is accumulating (38, 39). Supporting this view, the Firmicutes/Bacteroidetes ratio has been linked to adiposity in humans, since obese individuals were found to have fewer Bacteroidetes compared to lean controls. In addition, the relative abundance of Bacteroidetes increased while the abundance of Firmicutes decreased with weight loss in obese subjects (42). Because we found a significantly lower Firmicutes/Bacteroidetes ratio in RS-fed pigs compared to DS-fed pigs, the microbial profile might have shifted towards a more healthy phenotype in RS-fed pigs. Although the relative abundance of Firmicutes slightly, albeit not significantly, decreased (Supplementary Fig. 2), we observed a significant increase in the relative abundance of several microbial groups previously shown to produce butyrate, including *Faecalibacterium prausnitzii* and *Megasphaera elsdenii* (116, 152, 153). Other microbial populations stimulated by RS included fermenting microorganisms such as members of the *Parabacteroides*, *Prevotella*, *Mitsuokella multacida*, and lactic acid bacteria, that produce organic acids such as acetate, lactate and succinate that are in turn used as main substrates for the production of propionate and butyrate (116).

Fermentation products
In contrast with our previous study in pigs consuming the same RS diet (126), in the current study no significant difference in SCFA concentration was observed in the pCO digesta 300 min after feeding. However, the changed percentage of BCFAs in colonic digesta confirms the applied dietary contrast. These branched-chain products are formed by amino acid fermenting microbial species that metabolize undigested and endogenous proteins, peptides, and amino acids (54), particularly when carbohydrates as preferential energy source are absent. The lower percentage of BCFAs reflects the use of RS as energy source by microbiota whereas in the DS

diet the microbiota used proteinaceous energy sources due to the digestion and fermentation of starch in the upper gastrointestinal tract and the cecum. Moreover, plasma SCFA concentrations are known to be a more reliable measure of colonic SCFA production (154). As expected, we observed increased plasma SCFA concentrations upon RS feeding.

Functional implications colon

Genome-wide expression profiling is an unbiased approach for identifying genes regulated by RS. Our microarray analysis resulted in a dataset with the expression levels of 17,118 unique genes measured in 20 colonic samples from 10 pigs on 2 dietary conditions (DS and RS). From these data we extracted the significantly regulated genes and the main processes that are expected to change based on the gene expression profile.

In RS-fed pigs, we observed an increased expression of genes involved in the TCA cycle, the pathway responsible for generating energy through the oxidization of acetyl-CoA. We previously showed that RS increases SCFA concentrations in the colonic lumen (126). These SCFAs are subsequently taken up by the colonocytes, where mainly butyrate serves as an energy source for these cells as a precursor to the TCA cycle (155). Therefore, the increased energy generation in colonocytes upon RS feeding was in line with our expectations.

In addition, genes involved in lipid metabolism were found to be induced by RS. More specifically, GSEA revealed increased uptake and release of fatty acids, fatty acid beta-oxidation and triglyceride (TG) synthesis. We hypothesize that these processes are a consequence of increased SCFA production, having a direct link with energy metabolism resulting in increased energy harvest from the diet.

Gene expression profiling also showed that RS suppressed genes involved in both the innate and the adaptive immune response, which indicates that the CO of RS-fed pigs is less exposed to potential pathogens as was confirmed by microbiota analysis of luminal content, where especially members of the Proteobacteria were found reduced in relative abundance in the RS group. This observation, combined with a less pro-inflammatory state, might thus indicate a healthier condition of RS-fed pigs as compared to DS. This observation is in line with previous studies on RS in relation to immune regulation, showing amelioration of inflammatory bowel disease upon RS feeding (156).

Microbiota are known to play a crucial role in the immune system. Therefore, it is likely that the changed microbiota composition we observed on RS directly reflects changes in expression level of genes involved in immunity. Furthermore, immune signalling can affect microbiota composition, as shown by altered gut microbiota in mice lacking toll-like receptor 5, an essential protein for pathogen

recognition and activation of innate immunity (157).

In addition to the microbiota, we hypothesize that PPARG, a ligand-activated transcription factor found to be significantly activated by RS, plays a role in the suppressed immune response. This is in line with a recent report that showed that SCFA, and especially butyrate, are agonists for PPARG (158). PPARG is also known to be involved in the prevention of inflammatory bowel disease in mice (159), pigs (160), and humans (161). Moreover, PPARG activation suppresses the activity of NF-κB, thereby blocking pro-inflammatory gene transcription (162).

Functional implications whole-body metabolism

To determine how colonic gene expression changes affect inter-organ crosstalk, we identified potentially secreted proteins. Among these proteins were angiopoietin-like 4 (ANGPTL4) and apolipoprotein D (APOD), which both play an important role in lipid metabolism. ANGPTL4 provides a link between microbiota and SCFAs in CO on one hand and adiposity on the other hand. Studies have suggested that there is a relationship between microbiota composition and ANGPTL4, as observed by strong suppression of *ANGPTL4* after conventionalization of germ free mice (40, 41). Furthermore, microbiota are able to induce ANGPTL4 production in colonocytes via production of SCFAs and subsequent activation of PPARG (158). Because we found ANGPTL4 to be a potentially secreted protein, we hypothesize that ANGPTL4 is secreted from the colonocytes into the circulation, where it inhibits lipoprotein lipase (LPL), an enzyme that hydrolyses TGs in lipoproteins into free fatty acids for uptake by tissues (124). Therefore, SCFAs may inhibit fat storage by stimulating ANGPTL4 release.

Based on the direction of the expression of its encoding gene, we expect APOD to be decreased with RS consumption. Elevated APOD production was found to significantly reduce plasma TG levels in mice, due to enhanced LPL activity and improved catabolism of TG-rich particles (163). Plasma TG levels measured in the pigs from our experiment were significantly higher after RS consumption (164). Assuming that APOD decreases and ANGPTL4 increases on RS as suggested by the transcriptome data, we expect to find a decrease in LPL activity, resulting in increased plasma TG levels.

Based on our data, TG uptake by adipose tissue is expected to be inhibited by RS, indicating that long-term RS consumption might decrease adiposity. However, the final destination of the circulating TGs is yet unknown.

Conclusion

We demonstrated that compared to an iso-caloric DS diet, a diet high in RS favoured the growth of microbial populations producing organic acids, and inhibited a range of potentially pathogenic microbial groups. We also showed that RS provoked major changes in colonic gene expression, that represent induction of oxidative metabolic pathways, and suppression of immune response pathways. Our results provide novel molecular insights on effects of RS in colon, that emphasize the resilience of the colon and support the believe that RS has beneficial impact on colonic health. Because pigs are known to be a good model for humans, our study outcomes are highly relevant to human health.

Acknowledgements

3

Supplemental Methods

Surgery

After an overnight fast, all pigs were sedated with intramuscular Ketamine 10 mg/kg (Ketamine; Alfasan) and Midazolam 0.75 mg/kg (Dormicum; Roche) and anaesthesia was intravenously induced with the anodyne Sufentanil 1 µg/kg (Sufenta; Janssen-Cilag). Pigs were intubated and anaesthesia was maintained by inhalation of 2% Sevoflurane (Abbott) combined with 40% oxygen and nitrous oxide. A Sufentanil infusion was maintained at 1 µg/kg.hour.

Pigs were surgically fitted with a simple T-cannula in the pCO 1.45 ±0.16 m distal from the ileocaecal sphincter, as was confirmed at section. The cannula was inserted in the intestinal lumen, exteriorized through a hole, fastened to the exterior part and closed with a stopper (165). In addition, pigs were fitted with a permanent blood vessel catheter (Tygon, Norton) as described previously (166). The catheter for blood sampling was placed in the carotid artery, fixed firmly at the site of insertion, tunnelled subcutaneously to the back of the pig and exteriorized between the shoulder blades. The catheters were filled and sealed off with saline containing heparin and penicillin (Procpen) and kept in a backpack which was glued to the skin.

The first 3 d after surgery, pigs were fed a restricted amount of the 50:50 mix of the DS and RS diet, i.e. 25%, 50% and 75% of their daily feed allowance on d 1, 2 and 3 respectively, to allow a gradual recovery and to avoid problems with the gut cannula. Pigs were habituated to digesta collection from the cannula and blood sampling in the first week after surgery. After 4 to 6 d of postsurgical recovery, pigs were gradually switched to one of two dietary treatments (DS and RS).

Colon biopsies

Pigs were acutely sedated by *i.v.* injection with propofol (Alfasan). The stopper was unscrewed from the cannula and digesta was removed to expose the mucosal wall of the pCO. An endoscope (OES Colonofiberscope, Olympus CF type ITIOL/1, Olympus Optical Co; LTD) was inserted via the permanent cannula into the lumen of the pCO, the intestinal wall was illuminated (OES Halogen light source with flash, Model CLE-F10, Olympus Optical Co; LTD) and visualized on a monitor (Endovision 538; Karl Storz). Biopsies were taken by an endoscopic biopsy forceps (Olympus FB-28U-1, 2 mm, 225 cm, Olympus Optical Co; LTD) and collected in screw cap tubes, after which they were immediately frozen in liquid nitrogen and stored at -80°C until further analysis.

Digesta collection

To determine microbiota composition, digesta were collected in 1.5 mL Eppendorf tubes, after which the tubes were immediately frozen in liquid nitrogen and stored at -80°C until further analyses. In addition, digesta was collected in pre-weighed 2 mL Eppendorf tubes with 0.75 mL H_3PO_4 for determining SCFA concentrations. These tubes were weighed again, thoroughly mixed on a vortex and stored at -20°C until further analysis. For measuring dry matter content, digesta were collected in empty pre-weighed Eppendorf tubes and stored at -20°C until further analysis.

RNA quality control

Concentrations and purity of RNA samples were determined on a NanoDrop ND-1000 spectrophotometer (Isogen Life Science). RNA quality was verified on an Agilent 2100 Bioanalyzer (Agilent Technologies) by using 6000 Nano Chips (Agilent Technologies) according to the manufacturer's instructions. RNA was judged as suitable for array hybridization only if samples exhibited intact bands corresponding to the 18S and 28S ribosomal RNA subunits, and displayed no chromosomal peaks or RNA degradation products (RNA Integrity Number >8.0).

GSEA analysis

GSEA has the advantage that it is unbiased, because no gene selection step is used, and a score is computed based on all genes in a gene set. Briefly, genes were ranked based on the paired IBMT-statistic and subsequently analysed for over- or underrepresentation in predefined gene sets derived from Gene Ontology, KEGG, National Cancer Institute, PFAM, Biocarta, Reactome and WikiPathways pathway databases. Only gene sets consisting of more than 15 and fewer than 500 genes were taken into account. Statistical significance of GSEA results was determined using 1,000 permutations.

SCFA determination by NMR spectroscopy

Plasma samples were diluted 1:1 in a 75 mM phosphate buffer (pH 7.4) and filtered using Nanosep centrifugal devices with Omega Membrane (Pall Corporation). The molecular weight cut-off of the filter was 10K. Subsequently, 200 µL of the eluate was transferred to a 3 mm NMR tube (Bruker match system). Samples were stored at -20 ⁰C until analysis using NMR spectroscopy. Before NMR measurements, samples were slowly warmed up to room temperature and measured at 310 K (calibrated temperature) in an Avance III NMR spectrometer operated at 600.13 MHz. After transfer of each sample into the magnet, the sample was equilibrated at 310 K for 5 min. Subsequently automated locking, automated shimming and automated 90 degree pulse angle determination was performed. ^{1}H NMR NOESY datasets were

3

acquired for each sample. In addition, each dataset was automatically processed and aligned using the alanine signal (upfield resonance of the alanine doublet signal) at 1.49 ppm. From the aligned spectra, integrals for resonances of the metabolites of interest were selected and quantified. Concentrations of metabolites were calculated based on the number of hydrogens for each metabolite selected.

Multivariate analysis microbiota

To relate changes in total bacterial community composition to diet (DS or RS), period, and the interaction of period and diet, redundancy analysis (RDA) and Principal response curves were used as implemented in the CANOCO 5 software package (Biometris). RDA is the canonical form of principle component analysis and is a multivariate linear regression method where several response parameters are related to the same set of environmental variables. The signal intensities for 151 genus-level phylogenetic groups of PITChip were used as responsive variables. Partial RDA was employed to analyse the effect of diet on microbiota. RDA was performed by centering the species and samples, using freely exchangeable whole-plot Permutations.

Supplemental Tables and Figures

Supplemental Table 1. Ingredient and nutrient composition of the experimental diets.

	DS	RS
Ingredient composition (g/kg)		
Pregelatinized purified potato starch[1]	**350.0**	0.0
Retrograded tapioca starch[2]	0.0	**342.6**
Soy oil	29.2	29.5
Wheat	200.0	202.3
Beet pulp (sugar<100 g/kg)	50.0	50.6
Barley	150.0	151.7
Wheat gluten meal	60.0	60.7
Potato protein[3]	100.0	101.1
Premix[4]	10.0	10.1
$CaCO_3$	13.5	13.7
$Ca(H_2PO_4)_2$	11.0	11.1
NaCl	3.0	3.0
L-lysine HCl	2.2	2.2
L-tryptophan	0.2	0.2
MgO (80%)	0.4	0.4
$NaHCO_3$	14.0	14.2
KCl	3.0	3.0
TiO_2	2.0	2.0
Flavor[5]	1.5	1.5
Nutrient (g/kg dry matter)		
Dry matter (g/kg)	894.5	910.0
Organic matter	941.4	941.9
Crude protein (N x 6.25)	190.9	194.3
Crude fat	16.1	28.6
Starch	524.7	477.1
Sugar	13.1	69.4
TiO_2	1.6	1.6
Energy content (MJ/kg)		
GE	16.48	16.78

DS, digestible starch diet; RS, resistant starch diet.

[1]Paselli™ WA4, Avebe Food, Veendam, the Netherlands.

[2]C*Actistar 11700, Cargill, Amsterdam, the Netherlands.

[3]Protostar, Avebe Food, Veendam, the Netherlands.

[4]Provided the following per kg of feed: vitamin A: 7500 IU; vitamin D_3: 1500 IU; vitamin E: 60 mg; vitamin K_3: 1.0 mg; vitamin B_1: 1.0 mg; vitamin B_2: 4.0 mg; vitamin B_6: 1.0 mg; vitamin B_{12}: 20 µg; niacin: 20 mg; calcium-D pantothenate: 10.5 mg; choline chloride: 100 mg; folic acid: 0.4 mg; Fe: 120 mg ($FeSO_4.H_2O$); Cu: 15 mg ($CuSO_4.5H_2O$); Mn: 60 mg (MnO); Zn: 75 mg ($ZnSO_4.H_2O$); I: 4.0 mg (KI); Se: 0.30 mg (Na_2SeO_3); anti-oxidant: 75 mg.

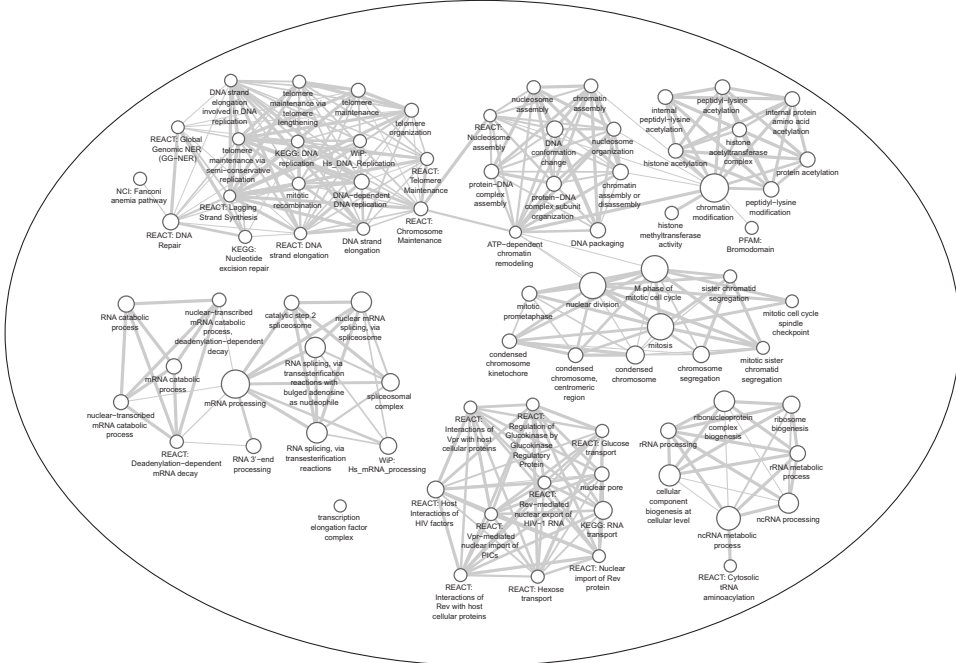[5]Luctarom Advance Cherry Honey, Lucta S.A., Barcelona, Spain.

Supplemental Table 2. An overview of all significantly regulated genes (*P* <0.01) will become available online.
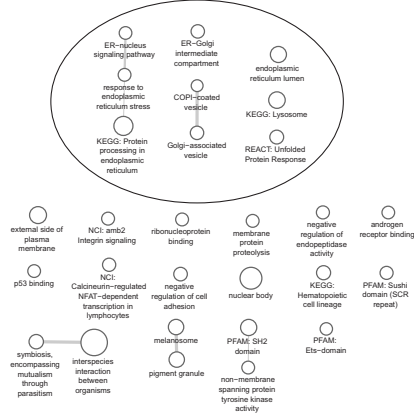
Supplemental Figure 1.
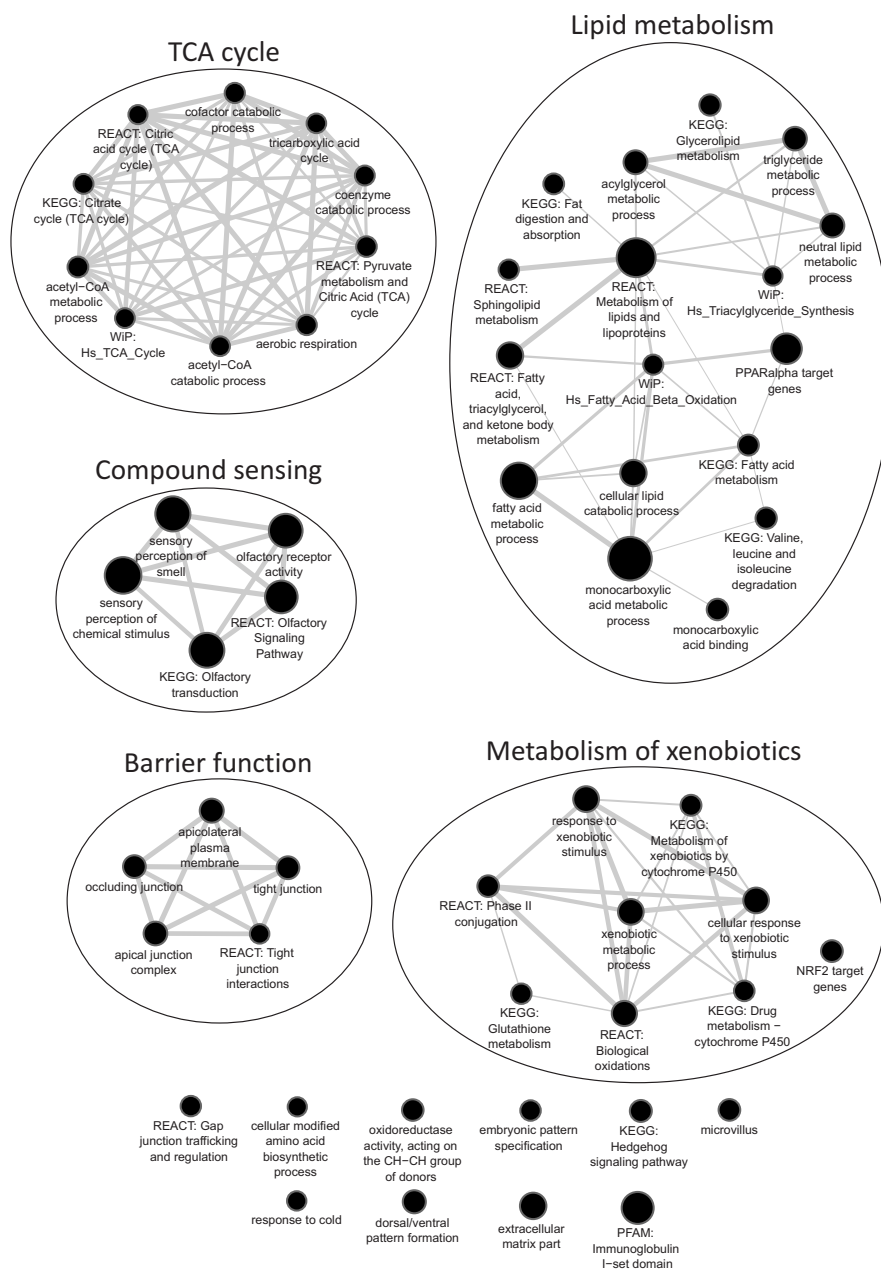
Supplemental Figure 1 (continued).

Transcription and translation

Intracellular processing

Post-translational modification

3

Supplemental Figure 1 (continued).

## Immune response
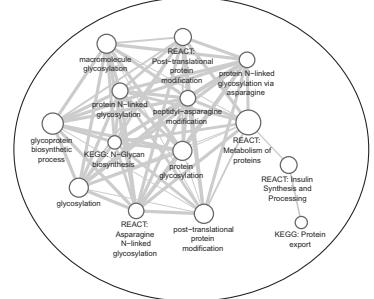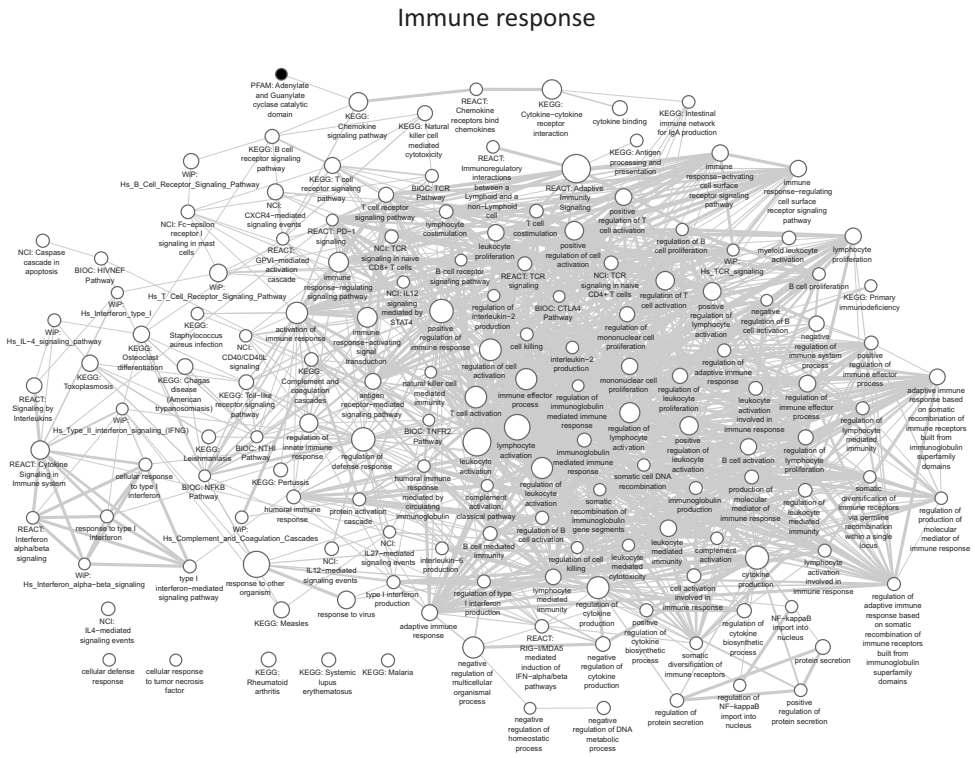
Enrichment map indicating positively and negatively enriched gene sets. Nodes represent functional gene sets, and edges between nodes their similarity. Black nodes indicate increased and white nodes indicate suppressed gene sets in the RS group compared with the DS group. Node size represents the gene set size, and edge thickness represent degree of overlap between 2 connected gene sets. Clusters were manually circled and labelled to highlight the prevalent biological functions among related gene sets.
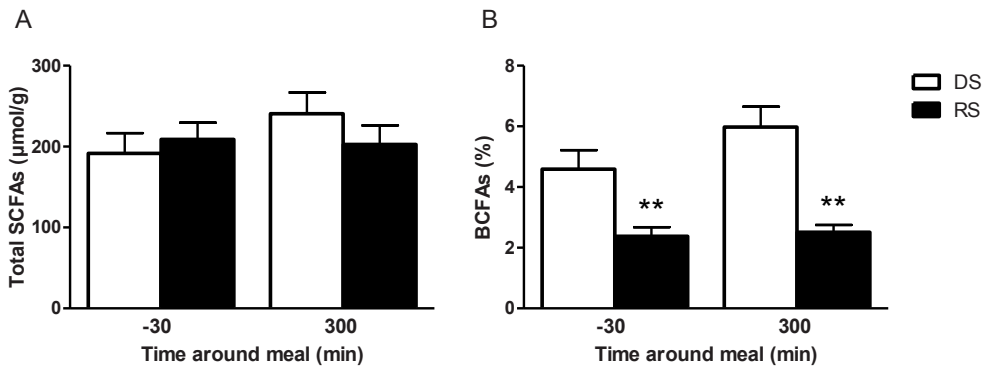
Supplemental Figure 2.
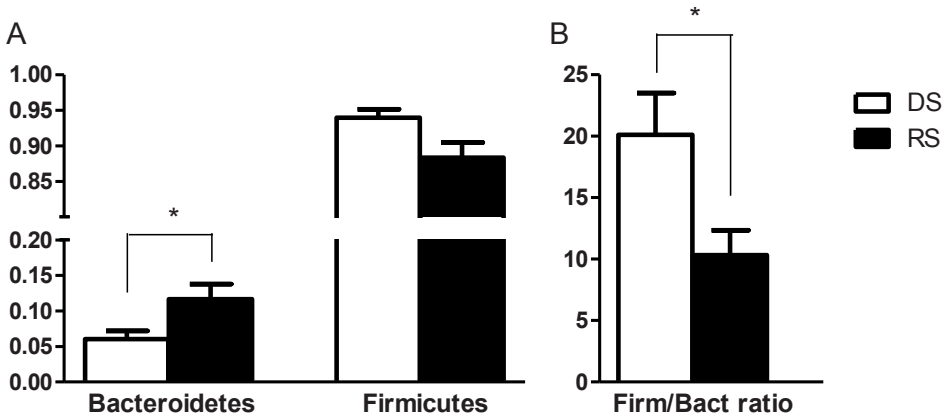
The abundance of the phyla Bacteroidetes and Firmicutes (**A**) and the ratio Firmicutes/Bacteroidetes (**B**) in pigs fed DS or RS for 2 wk, as determined by PITChip. Data are presented as means ± SEM, *n* = 9 per treatment. * indicates *P* <0.05. DS, digestible starch; RS, resistant starch.

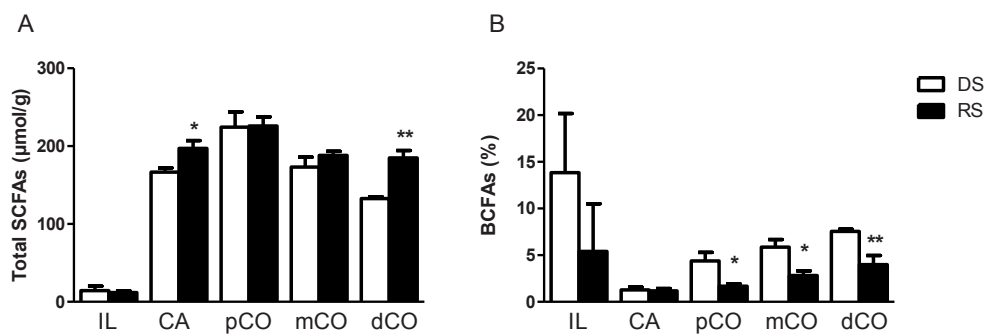**Supplemental Figure 3.**

Total SCFAs (**A**) and percentage of BCFAs from total SCFAs (**B**) measured in luminal content from proximal colon, collected 30 min before feeding (-30) and 300 min after feeding in pigs fed the DS and the RS diet. Data are presented as means ± SEM, *n* = 10 per treatment. ** indicates *P* <0.01. BCFAs, branched-chain fatty acids; DS, digestible starch; RS, resistant starch.

Supplemental Figure 4.

Total SCFAs (**A**) and percentage of BCFAs from total SCFAs (**B**) measured in luminal content from different segments of the gastrointestinal tract in pigs fed the DS or the RS diet. Data are presented as means ± SEM, *n* = 5 per treatment. * indicates *P* <0.05, ** indicates *P* <0.01. BCFAs, branched-chain fatty acids; DS, digestible starch; RS, resistant starch; ileum, IL; caecum, CA; proximal colon, pCO; middle colon, mCO; distal colon, dCO.

Supplemental Table 3. Potentially secreted proteins.

Name	Gene symbol	Entrez ID	Mean log2 FC[1]	Protein ID	Prob[2]
Insulin-like growth factor 1 (somatomedin C)	IGF1	3479	0.62	Q5U743	0.78
Bone morphogenetic protein 4	BMP4	652	0.19	P12644	0.63
Pancreatic lipase-related protein 2	PNLIPRP2	5408	0.67	P54317	0.62
Wingless-type MMTV integration site family, member 2B	WNT2B	7482	0.44	Q93097	0.61
Sema domain, immunoglobulin domain (Ig), short basic domain, secreted, 3C	SEMA3C	10512	0.36	Q99985	0.60
Dermatopontin	DPT	1805	0.58	Q07507	0.60
Bone morphogenetic protein 2	BMP2	650	0.33	P12643	0.57
Resistin like beta	RETNLB	84666	0.64	Q9BQ08	0.57
Proline/arginine-rich end leucine-rich repeat protein	PRELP	5549	0.58	P51888	0.57
Bone morphogenetic protein 5	BMP5	653	0.41	P22003	0.57
Tubulointerstitial nephritis antigen	TINAG	27283	0.52	Q9UJW2	0.54
Angiotensinogen (serpin peptidase inhibitor, clade A, member 8)	AGT	183	0.87	B2R5S1	0.54
Gastric intrinsic factor (vitamin B synthesis)	GIF	2694	0.49	P27352	0.54
ADAM metallopeptidase domain 23	ADAM23	8745	0.76	O75077	0.53
Vascular endothelial growth factor A	VEGFA	7422	0.37	P15692	0.52
Cartilage intermediate layer protein, nucleotide pyrophosphohydrolase	CILP	8483	0.56	O75339	0.51
EGF containing fibulin-like extracellular matrix protein 1	EFEMP1	2202	0.67	Q12805	0.47
Guanylate cyclase activator 2A (guanylin)	GUCA2A	2980	0.66	Q02747	0.44
Signal peptide, CUB domain, EGF-like 1	SCUBE1	80274	0.34	A0JP65	0.43
Peptidase domain containing associated with muscle regeneration 1	PAMR1	25891	0.33	Q6UXH9	0.42
Guanylate cyclase activator 2B (uroguanylin)	GUCA2B	2981	1.02	Q16661	0.42
Protocadherin-related 15	PCDH15	65217	0.40	A2A3E3	0.42
Transmembrane protease, serine 2	TMPRSS2	7113	0.35	O15393	0.37
Collagen, type VI, alpha 6	COL6A6	131873	0.85	A6NMZ7	0.33
Lysophosphatidic acid receptor 2	LPAR2	9170	0.31	Q9HBW0	0.31
Collagen, type XIV, alpha 1	COL14A1	7373	0.45	Q05707	0.31
Transmembrane protease, serine 4	TMPRSS4	56649	0.48	B7Z8C5	0.30
EPH receptor A3	EPHA3	2042	0.52	P29320	0.29
Angiopoietin-like 4	ANGPTL4	51129	0.58	Q9BY76	0.27
Thrombospondin 3	THBS3	7059	0.48	B4DQ20	0.22
Slit homolog 3 (Drosophila)	SLIT3	6586	0.41	O75094	0.20
Complement component 2	C2	717	-0.47	E9PFN7	0.66
Granulin	GRN	2896	-0.19	P28799	0.61
Complement component 4B (Chido blood group)	C4B	721	-0.58	P0C0L5	0.60
Complement factor H	CFH	3075	-0.47	F8WDX4	0.59
Serpin peptidase inhibitor, clade A, member 1	SERPINA1	5265	-0.60	P01009	0.58
Peptidase inhibitor 3, skin-derived	PI3	5266	-0.49	P19957	0.57
Lymphocyte antigen 96	LY96	23643	-0.58	Q9Y6Y9	0.57
Apolipoprotein D	APOD	347	-0.43	P05090	0.56
Complement component 4 binding protein, alpha	C4BPA	722	-0.62	P04003	0.53
Complement component 4 binding protein, beta	C4BPB	725	-0.39	P20851	0.53
Acyloxyacyl hydrolase (neutrophil)	AOAH	313	-0.63	P28039	0.50
Clusterin	CLU	1191	-0.63	P10909	0.49
Chromogranin B (secretogranin 1)	CHGB	1114	-0.55	P05060	0.46
EMI domain containing 1	EMID1	129080	-0.40	Q96A84	0.43
Olfactomedin 4	OLFM4	10562	-0.22	Q6UX06	0.42
Poliovirus receptor-related 4	PVRL4	81607	-0.75	Q96NY8	0.41
Chemokine (C-X-C motif) ligand 14	CXCL14	9547	-0.26	O95715	0.36
Polymeric immunoglobulin receptor	PIGR	5284	-0.30	P01833	0.35
Bactericidal/permeability-increasing protein	BPI	671	-0.39	P17213	0.34
Serine peptidase inhibitor, Kazal type 4	SPINK4	27290	-0.34	O60575	0.33
Cathepsin K	CTSK	1513	-0.25	P43235	0.25
ADAM metallopeptidase domain 17	ADAM17	6868	-0.22	P78536	0.23

[1] Average log2 fold changes of the signal intensity of RS compared with DS.

[2] Probability that the listed protein is present extracellularly (secreted), as determined by ngLOC. Only proteins with a probability above 0.20 are listed.

Short-chain fatty acid-induced changes in colonic gene expression depend on dietary fat content in mice

Daniëlle Haenen, Katja Lange, Shohreh Keshtkar, Michael Müller and Guido J.E.J. Hooiveld

Abstract

Acetate, propionate and butyrate are the main short-chain fatty acids (SCFAs) produced in the colon as a result of microbial fermentation of dietary fibres, and are believed to exert major health benefits. The composition of the microbiome is altered by dietary fat, which is believed to impact SCFA production. Currently it is unknown whether host gene expression responses to SCFAs are modulated by dietary fat content. The study aim was to compare changes in colonic gene expression profiles after acetate, propionate and butyrate infusions between a low fat and high fat diet, with focus on metabolic genes. Male C57BL/6J mice were fed a semi-synthetic low or high fat diet starting 2 wk before the SCFA treatment period. During treatment, mice received a rectal infusion of either an acetate, propionate, butyrate, or a saline (control) solution for 6 consecutive days, after which colon was subjected to gene expression profiling. Unsupervised visualization of the dataset was performed using Independent Principal Component Analysis. For each SCFA, similarities of effects on a low fat and a high fat diet were assessed using Rank-rank Hypergeometric Overlap. In addition, differentially expressed genes were identified, and gene set enrichment analysis was performed to determine functional implications of the regulated genes. Taking into account the complete dataset, we observed that more variation in gene expression profiles was explained by dietary fat content than by SCFA treatment. Gene expression responses to acetate and butyrate were similar on the low fat and high fat diet, but were reversed for propionate. Functionally, expression changes reflected differential modulation of several metabolic and immune processes; genes involved in oxidative phosphorylation, lipid catabolism, lipoprotein metabolism and cholesterol transport were suppressed by acetate and butyrate treatment, whereas propionate treatment resulted in changes in fatty acid and sterol biosynthesis, and in amino acid and carbohydrate metabolism. In conclusion, dietary fat content impacts the colonic gene expression response to propionate, and to a lesser extent to acetate and butyrate. Each SCFA modifies the expression of distinct, partially overlapping sets of genes. Knowledge on dietary fat content is essential when studying effects of SCFAs on metabolism.

Introduction

The gut microbiota is highly important for metabolic homeostasis and health, as it was found to play a crucial role in the regulation of energy homeostasis and fat storage (38, 39). The first evidence supporting this statement was derived from studies in germ-free mice, showing that conventionally raised mice have 42% more total body fat compared to germ-free mice, and conventionalization of germ-free mice resulted in a 57% increase in total body fat (40). Furthermore, germ-free mice were found to be protected from the development of obesity after consuming a high fat diet (41). The relationship between microbiota composition and fat storage has also been studied in humans, indicating that obese people have fewer Bacteroidetes compared to lean controls (42). In these obese subjects, the relative abundance of Bacteroidetes increased while the abundance of Firmicutes decreased with weight loss (42).

A Western-type diet typically contains high amounts of fat, and dietary fat content was shown to have a major impact on microbiota composition in the colon (43, 48). For instance, mice consuming a high fat diet displayed reduced numbers of Bacteroidetes and increased numbers of Firmicutes and Proteobacteria (48). Besides changing the microbiota composition, a high fat diet was also previously shown to alter small intestinal gene expression profile compared to a low fat diet (167).

Various studies have shown that modification of dietary patterns can have substantial impact on the development of obesity and the metabolic syndrome (6, 80). In the prevention of these metabolic abnormalities, dietary fibre is an extensively studied food component for its potential role in the management of food intake and body weight (81). The consumption of fibres was shown to prevent the accumulation of fat mass (82, 83), to increase insulin sensitivity (9, 84) and to enhance satiety (12, 14). Several types of dietary fibre, including resistant starch, pectin and inulin, are highly fermentable by the microbiota in the colon, resulting in the production of short-chain fatty acids (SCFAs). An increasing amount of evidence suggests that the health benefits observed with dietary fibre consumption are partly due to the action of these SCFAs (53). The three main SCFAs produced in the colon are acetate, propionate and butyrate, and each SCFA has distinct biological properties and can affect metabolism and health in a specific way. Butyrate is almost entirely utilized by colonocytes as their preferred energy substrate and therefore only a small proportion reaches the systemic circulation (168, 169). Butyrate was found to play an important role in the prevention and inhibition of colon carcinogenesis, the protection against mucosal oxidative stress, strengthening of the colonic defence barrier and it was found to have anti-inflammatory properties

(55). Acetate and propionate are less efficiently used by the colon and can serve as anabolic substrates in tissues other than colon (61, 62, 87).

Potential health benefits of dietary and bioactive compounds can be studied by measuring their effects on colonic gene expression profiles (73, 170). Regarding SCFAs it has been observed that colonic administration of butyrate enhances the maintenance of homeostasis in healthy humans, by regulating fatty acid metabolism, electron transport and oxidative stress pathways (139). However, the effects of acetate nor propionate, nor the potential modulating effect of dietary fat content has been investigated.

In the current study we therefore aimed to determine the effect of dietary fat content on changes in gene expression profile in colon after colonic acetate, propionate and butyrate administration. The experiment was performed in mice that were fed either a low fat or a high fat diet before and during SCFA treatment. Mice were treated with SCFAs received by rectal infusion on 6 consecutive days, after which the colonic epithelial cells were isolated to measure gene expression profiles.

This is the first experiment in which the effect of colonic SCFA administration on a low fat or a high fat diet background was studied using a comprehensive gene expression profiling approach. We demonstrate that fat content had a major impact on gene expression response to SCFAs in colon. In addition, we show which functional implications are involved in the discriminating effects of the background diets.

Materials and Methods

Ethics statement
The institutional and national guidelines for the care and use of animals were followed and the experiment was approved by the Local Committee for Care and Use of Laboratory Animals at Wageningen University.

Animals and diets
Male C57BL/6J mice were purchased from Charles River Laboratories at 8 wk of age. Mice were housed individually in a light- and temperature-controlled animal facility, with light on from 23:00 h to 11:00 h. Mice had free access to water and food, and 24h food intake was monitored in every cage. Mice received standard laboratory chow (RMH-B, Arie Blok) during the first 2 wk after arrival. Subsequently, mice were switched to semi-synthetic diets, either containing 10 en% of fat (low fat diet; LFD; *n* = 24) or 45 en% of fat (high fat diet; HFD; *n* = 24). Diets were based on Research Diets

formulas D12450B/D12451, with adaptations regarding type of fat (palm oil instead of lard) and carbohydrates to mimic the fatty acid and carbohydrate composition of the average human diet in Western societies. Diets were prepared by Research Diet Services. The complete composition of the diets is shown in **Table 1**.

Table 1 Composition of the experimental diets.

	LFD		HFD	
	g%	kcal%	g%	kcal%
Protein	19	20	24	20
Carbohydrate	67	70	41	35
Fat	4	10	24	45
Total		100		100
kcal/g	3.85		4.73	
Ingredient	g	kcal	g	kcal
Casein, lactic	200	800	200	800
L-Cystine	3	12	3	12
Corn starch	427.2	1,709	72.8	291
Maltodextrin	100	400	100	400
Sucrose	172.8	691	172.8	691
Cellulose, BW200	50	0	50	0
Soybean oil	25	225	25	225
Palm oil	20	180	177.5	1,598
Mineral mix S10026*	10	0	10	0
Dicalcium phosphate	13	0	13	0
Calcium carbonate	5.5	0	5.5	0
Potassium citrate, 1 H_2O	16.5	0	16.5	0
Vitamin mix V10001[#]	10	40	10	40
Choline bitartrate	2	0	2	0
Total	**1,055**	**4,057**	**858.1**	**4,057**

LFD, low fat diet; HFD, high fat diet. *Mineral mix S10026 contains the following (g/kg mineral mix): 41.9 magnesium oxide, 257.6 magnesium sulfate•7H_2O, 259 sodium chloride, 1.925 chromium KSO_4•12H_2O, 1.05 cupric carbonate, 0.035 potassium iodate, 21 ferric citrate, 12.25 manganous carbonate, 0.035 sodium selenite, 5.6 zinc carbonate, 0.20 sodium fluoride, 0.30 ammonium molybdate•4H_2O, 399.105 sucrose. [#]Vitamin mix V10001 contains the following (g/kg vitamin mix): 0.80 retinyl palmitate, 1.0 cholecalciferol, 10 all-rac-a-tocopheryl acetate, 0.08 menadione sodiumbisulfite, 2.0 biotin (1.0%), 1.0 cyancocobalamin (0.1%), 0.20 folic acid, 3.0 nicotinic acid, 1.6 calcium pantothenate, 0.70 pyridoxine-HCl, 0.60 riboflavin, 0.60 thiamin-HCl, and 978.42 sucrose.

SCFA infusions

After 2 wk on either the LFD or HFD, the 6-day treatment period started. Mice were assigned to one of 4 treatment groups: Control, Acetate, Propionate or Butyrate. On 6 consecutive days, the mice were mildly sedated with a mixture of isofluorane (1.5%), nitrous oxide (70%) and oxygen (30%) 2 h before the start of the dark phase, where after they received a rectal infusion of the test solutions. At time of infusion, mice were kept under sedation. Mice received an 80 µL saline solution (Control; *n*

= 6 per diet group), or an 80 μL saline solution containing 100 mM sodium acetate (Acetate; *n* = 6), 100 mM sodium propionate (Propionate; *n* = 6) or 100 mM sodium butyrate (Butyrate; *n* = 6). All solutions had a pH of 6.5 and were isotonic. The solutions were administered by inserting a gel loading tip 3 cm into the rectum and slowly pushing the solution out of the tip.

Sample collection

Four hours after the rectal infusion on day 6, colon samples were collected. To reduce the inter-individual variation in physiological state at time of tissue collection, mice were provided a restricted amount of their habitual food (approximately 20% of their average daily intake of LFD or HFD) 2 h before tissue removal. Mice were anaesthetized with isoflurane, where after the colon was excised and the length was measured. The adhering fat around the colon was carefully removed, and the colon was cut open longitudinally. The intestinal content was removed and the tissue was rinsed with phosphate buffered saline. Subsequently, the epithelial lining of the colon was scraped. These scrapings were collected in 1.5 mL Eppendorf tubes, which were immediately snap frozen in liquid nitrogen and stored at -80°C for subsequent RNA isolation.

RNA isolation and quality control

Total RNA was isolated from colon samples using TRIzol reagent (Invitrogen) according to the manufacturer's instructions, followed by RNA Cleanup using the RNeasy Micro kit (Qiagen). Concentrations and purity of RNA samples were determined on a NanoDrop ND-1000 spectrophotometer (Isogen Life Science). RNA quality was verified on an Agilent 2100 Bioanalyzer (Agilent Technologies) using 6000 Nano Chips according to the manufacturer's instructions. RNA was judged as suitable for array hybridization only if samples exhibited intact bands corresponding to the 18S and 28S ribosomal RNA subunits, and displayed no chromosomal peaks or RNA degradation products (RNA Integrity Number >8.0).

Microarray hybridization

Samples were subjected to genome-wide expression profiling using Affymetrix Mouse Gene 1.1 ST arrays (Affymetrix). Total RNA (100 ng) was used for whole transcript cDNA synthesis using the Ambion WT expression kit (Life Technologies) and subsequently labelled using the Affymetrix GeneChip WT Terminal Labeling Kit (Affymetrix). Samples were hybridized, washed, stained and scanned on an Affymetrix GeneTitan instrument. Detailed protocols for array handling can be found in the GeneChip WT Terminal Labeling and Hybridization User Manual (Affymetrix; P/N 702808, Rev. 4) and are also available on request.

Microarray analysis

Packages from the Bioconductor project (140), integrated in an online pipeline (141), were used to analyse the array data. Various advanced quality metrics, diagnostic plots, pseudoimages, and classification methods were used to determine the quality of the arrays prior statistical analysis (142, 171). One colon sample, derived from a mouse on the LFD in the Acetate group, was excluded from analyses because the array was of insufficient quality. The 828,268 probes on the Mouse Gene 1.1 ST array were redefined utilizing current genome information from the Entrez Gene database (custom CDF v16) (143). Array data have been submitted to the Gene Expression Omnibus, a database repository for gene expression data hosted at the NCBI, under accession number GSE48856.

Normalized gene expression estimates were obtained from the raw intensity values using the Robust Multi-array Average (RMA) preprocessing algorithm available in the library 'AffyPLM' using default settings (144).

The Mouse Gene 1.1 ST array probes the expression of 21,225 unique genes. Differentially expressed genes (probe sets) were identified using linear models, applying moderated t-statistics that implemented empirical Bayes regularization of standard errors (library 'limma'). The moderated t-test statistic has the same interpretation as an ordinary t-test statistic, except that the standard errors have been moderated across genes, i.e. shrunk to a common value, using a Bayesian model (172). To adjust for both the degree of independence of variances relative to the degree of identity and the relationship between variance and signal intensity, the moderated t-statistic was extended by a Bayesian hierarchical model to define an intensity-based moderated T-statistic (IBMT) (145). IBMT improves the efficiency of the Empirical Bayes moderated t-statistics and thereby achieves greater power while correctly estimating the true proportion of false positives. Probe sets that satisfied the criterion of $P < 0.01$ were considered to be significantly regulated.

Unsupervised visualization of the full dataset was performed using Independent Principal Component Analysis (IPCA), a variant of the classical tool PCA that better reflects the internal structure of the data generated of noisy omics experiments (173).

Similarity of the effects of each SCFA on the LFD and HFD was assessed using the Rank-rank Hypergeometric Overlap (RRHO) algorithm (174). RRHO is a threshold-free method which visualizes the overlap between 2 ranked lists of differentially expressed genes. In brief, genes differentially expressed between SCFA infusion and the control treatment were ranked according to their IBMT t-statistic. The hypergeometric P value of overlap was calculated to determine the significance of overlapping genes between 2 datasets which is visualized in a matrix. On the x-axis of the matrix, genes were ranked by their degree of differential regulation

(top up to bottom down) between SCFA infusion on the LFD and the control infusion on the LFD. On the y-axis genes were ranked based on their expression change with SCFA treatment on the HFD compared to control.

Analysis of functional implications

Changes in gene expression were related to functional changes using gene set enrichment analysis (GSEA) (146). GSEA has the advantage that it is unbiased, because no gene selection step is used, and a score is computed based on all genes in a gene set. Briefly, genes were ranked based on the IBMT-statistic and subsequently analysed for over- or underrepresentation in predefined gene sets derived from Gene Ontology, KEGG, National Cancer Institute, PFAM, Biocarta, Reactome and WikiPathways pathway databases. Only gene sets consisting of more than 15 and fewer than 500 genes were taken into account. Statistical significance of GSEA results was determined using 1,000 permutations. The Enrichment Map plugin for Cytoscape was used for visualization and interpretation of the GSEA results (147, 148).

To identify the cascade of upstream transcriptional regulators that may explain the observed gene expression changes in the dataset, Upstream Regulator Analysis was performed using Ingenuity Pathway Analysis (IPA; Ingenuity Systems).

Statistics

Results on food intake and body weight were expressed as means ± SEM, regarding *P* <0.05 as statistically significant.

Results

Food intake and body weight development

At the start of the 2-wk intervention on the LFD and HFD, mice were stratified into 2 groups based on body weight, that averaged 22.7 g in both groups. Mice fed the HFD consumed the same amount of food as mice receiving the LFD (3.11 ± 0.08 versus 3.09 ± 0.04 g per day, respectively). However, since the HFD contained more energy per gram, the caloric intake was significantly higher in mice fed the HFD compared to mice fed the LFD (14.8 ± 0.36 versus 11.9 ± 0.14 kcal per day, respectively; *P* <0.0001). During the treatment period, caloric intake of mice on the HFD remained significantly higher compared to mice fed the LFD (**Table 2**). SCFA treatment did not significantly affect caloric intake within both diet groups.

After the 2-wk intervention, body weight of mice fed the HFD was significantly higher compared to mice fed the LFD (26.6 ± 0.31 versus 23.9 ± 0.24

g respectively; *P* <0.0001), which is in line with the observed difference in caloric intake between the 2 diet groups. During the SCFA treatment period, body weight change was similar with all SCFA treatments (data not shown).

Table 2 Daily food intake during the SCFA treatment period in mice fed the LFD or the HFD.

		Daily food intake (g)	Daily food intake (kcal)
LFD	Control	3.03 ± 0.076	11.67 ± 0.294
	Acetate	2.98 ± 0.118	11.48 ± 0.453
	Propionate	3.08 ± 0.114	11.84 ± 0.439
	Butyrate	2.89 ± 0.076	11.14 ± 0.293
	Average all treatments	3.00 ± 0.049	11.54 ± 0.188
HFD	Control	2.71 ± 0.095	12.80 ± 0.450
	Acetate	2.70 ± 0.097	12.77 ± 0.457
	Propionate	2.57 ± 0.084	12.17 ± 0.400
	Butyrate	2.48 ± 0.100	11.73 ± 0.474
	Average all treatments	2.61 ± 0.047**	12.37 ± 0.224**

Values are means ± SEM, *n* = 6 per diet group, ** indicates a significant difference between average daily food intake in mice fed the LFD compared to mice fed HFD (*P* <0.01). LFD, low fat diet; HFD, high fat diet.

4

Dietary fat drives variation in SCFA-induced gene expression changes
After the SCFA treatment period, gene expression in colonic scrapings was profiled on microarrays. IPCA revealed that most variation in the dataset was due to fat content of the diet, since on the first dimension LFD and HFD samples clustered together (**Fig. 1**). The IPCA plot did not show a clear clustering based on SCFA treatment, indicating that dietary fat content was the major factor driving differences in gene expression profiles.
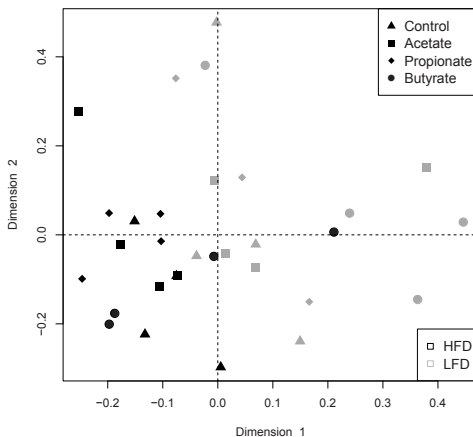

Figure 1 IPCA plot colonic gene expression profile. Independent principle component analysis (IPCA) was used to plot the variation of normalized gene expression among the samples. The first 2 dimensions, explaining the highest variation, are shown.

Characterization of overlap between LFD and HFD

To characterize the similarity of the transcriptional responses to SCFA treatment on the LFD and HFD, RRHO analysis was applied. As indicated by the RRHO P value heatmaps, the response to acetate or butyrate was rather similar on both diets (**Fig. 2A** and **2C** respectively). For acetate we noticed in the RRHO heatmap a significant (yellow-red) area across the bottom left to top right diagonal of the map (**Fig. 2A**). This showed that the gene ranking in both lists was similar, indicating that the genes regulated by acetate on either the LFD or HFD were the same, even in case of a different extent of regulation. For butyrate treatment a comparable RRHO heatmap was observed, although the significance area was more pronounced in the top-right area (**Fig. 2C**), which suggested a higher similarity between the LFD and the HFD for genes suppressed by butyrate than for genes induced by butyrate. In contrast, for propionate treatment a completely different RRHO heatmap was observed (**Fig. 2B**). A significant (blue-purple) area was observed mainly in the upper left quarter of the heatmap that further extended to bottom right of the diagonal. Since RRHO conventions state a strong negative signal should be interpreted as a strong positive trend in the opposite sense (174), these results showed that genes induced by propionate on the LFD were suppressed on the HFD. For the inversely regulated genes (i.e. suppressed on the LFD and increased on the HFD) this effect was less pronounced. In summary, the global, cutoff-free RRHO analysis indicated that dietary fat content mostly impacted the regulation of propionate-responsive genes, and to a lesser extent genes regulated by acetate and butyrate.

Next we used a significance cut-off (P <0.01) to determine the number of genes regulated by acetate, propionate or butyrate treatment as compared to the control infusion. Because we were interested in the modulatory role of dietary fat, Venn diagrams were created to compare regulation on LFD and HFD. Acetate treatment resulted in the differential expression of 151 genes in mice fed the LFD, and 138 genes were changed in mice fed the HFD (**Fig. 2D**). Two genes were regulated on both the LFD and the HFD (*Cnih2* and *Zfp367*). Propionate treatment modified the expression of 214 genes in the LFD group, whereas almost twice as many genes, i.e. 440, were changed in mice fed the HFD (**Fig. 2E**). Of the 29 overlapping genes, 25 were changed in opposite direction when comparing HFD with LFD, which is in line with the result of RRHO analysis. Among the 12 genes that were induced in the LFD group and suppressed in the HFD group were genes involved in energy homeostasis (*Echs1*, *Gcdh*, *Hibadh*, *Ndufs7* and *Nmnat1*). Vice versa, among the 13 genes that were suppressed by propionate in the LFD group and induced in the HFD group were small nuclear RNAs (snRNAs; *Rnu12* and *Rnu3a*) and small nucleolar RNAs (snoRNAs; *Snora31*, *Snora7a* and *Snord35b*). Butyrate treatment resulted in 250 regulated genes on the LFD, and 267 genes on the HFD, with 8 genes (*Apoa2*,

Apoc2, *Cd19*, *Cd22*, *Cd72*, *Fcer2a*, *Gpx4* and *Rnu3a*) being regulated on both diets (**Fig. 2F**). In addition, Venn diagrams showed that both on the LFD and HFD, the number of overlapping genes between SCFA treatments was limited (**Supplemental Fig. 1**).

Taken together, these results showed that the effects of the SCFAs on gene expression were dependent on dietary fat, and that each SCFA modifies the expression of a distinct, partially overlapping set of genes.
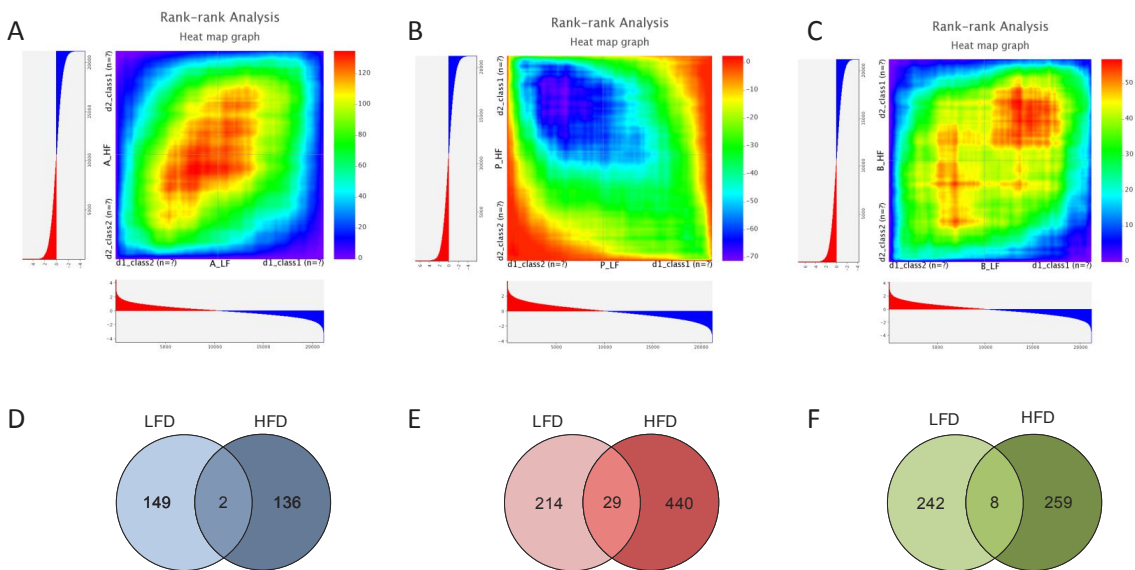

Figure 2 Effects of dietary fat on colonic gene expression. Heatmaps of Rank–rank Hypergeometric Overlap (RRHO) analysis of the effect of 6-day acetate (**A**), propionate (**B**) and butyrate (**C**) infusion on colonic gene expression, and Venn diagrams showing the number of significantly regulated genes (*P* <0.01) in the colon of mice after 6 d of rectal infusion of acetate (**D**), propionate (**E**) or butyrate (**F**). For RRHO analysis the full dataset was used to determine the overlap between the transcriptional responses on the LFD and the HFD after SCFA infusion. The plots indicate the pattern of overlap between the LFD and the HFD background. Differentially regulated genes for each SCFA infusion on HFD versus LFD background were ranked based on IBMT t value and plotted along the axis, with the X-axis representing the LFD and the Y-axis representing the HFD. Colour represents the degree of hypergeometric distribution (Benjamini and Yekutieli-corrected signed log10 transformed *P* value of overlap). Each Venn diagram shows the number of regulated genes on a LFD background, on a HFD background and the number of genes regulated on both dietary backgrounds. Effects of SCFA infusion were compared with effects after saline infusion in mice fed the same background diet (LFD or HFD).

Functional implications of gene expression changes

GSEA was performed to determine which biological processes were affected by the SCFA treatments. Results on the LFD and HFD were jointly visualized in enrichment maps (**Supplemental Fig. 2**).

Acetate infusion changed gene sets in the same direction in the LFD and the HFD group (**Supplemental Fig. 2A**). Immune response (e.g. *lymphocyte activation*, *cytokine production*, *positive regulation of immune response* and *antigen processing and presentation*) was induced by acetate and among the suppressed processes were cell cycle (e.g. *mitosis* and *KEGG: DNA Replication*), lipid metabolism (e.g. *cholesterol transport*, *lipoprotein metabolic process*, *lipid homeostasis* and *acylglycerol catabolic process*), and oxidative phosphorylation (e.g. *mitochondrial respiratory chain*).

With propionate treatment, the direction of gene set enrichment was highly dependent on the fat content of the diet (**Supplemental Fig. 2B**). Processes increased on the LFD and suppressed on the HFD include *DNA replication*, *DNA repair*, *WiP: Mm_Fatty_Acid_Biosynthesis*, amino acid metabolism (e.g. *WiP: Mm_Tryptophan_metabolism*, *KEGG: Histidine metabolism*, and *KEGG: Valine, leucine, and isoleucine degradation*) and carbohydrate metabolism (*REACT: Glucose metabolism* and *REACT: Metabolism of carbohydrates*). Translation (e.g. *REACT: Translation* and *KEGG: Ribosome*) and oxidoreductase activity (e.g. heme-copper terminal oxidase activity) were suppressed in the LFD and induced in the HFD group. In addition, immune-related processes (e.g. *lymphocyte activation*, c*ytokine binding* and *B cell receptor signaling pathway*) were increased by propionate with both diets.

Similarly, in both diet groups butyrate treatment resulted in induction of the immune response (e.g. *positive regulation of immune system process*, *T cell activation*, *B cell activation* and *antigen processing and presentation*). Furthermore, *mRNA processing* and *chromatin modification* were increased by butyrate, whereas lipid metabolism (e.g. *lipid homeostasis*, *regulation of cholesterol transport* and *triglyceride-rich lipoprotein particle*) and oxidative phosphorylation (e.g. *KEGG: Oxidative phosphorylation* and *REACT: Respiratory electron transport*) were suppressed by butyrate (**Supplemental Fig. 2C**).

Metabolic implications

After studying all biological processes changed by SCFA treatment, we focused on the metabolic processes altered by the different treatments (**Fig. 3A**). In general, oxidative phosphorylation, digestive processes (e.g. *digestion*, *digestive system process* and *intestinal absorption*), and lipid-related processes were suppressed by acetate and butyrate treatment. Regarding the lipid-related processes, on both dietary

backgrounds acetate and butyrate inhibit lipid catabolism (e.g. *neutral lipid catabolic process* and *acylglycerol catabolic process*), lipoprotein metabolism (e.g. *protein-lipid complex remodeling* and *triglyceride-rich lipoprotein particle*) and *cholesterol transport*. Propionate treatment resulted in increased fatty acid biosynthesis on the LFD background, while suppressing this process on a HFD background. On the HFD, propionate also decreased sterol biosynthesis. Furthermore, propionate was shown to affect amino acid metabolism and carbohydrate metabolism, with an induction on the LFD and suppression in the HFD group.

Subsequently we determined which of the genes present in the enriched metabolic gene sets were robustly regulated (P <0.01). In total 121 genes were changed in at least one treatment condition. These genes were clustered on expression rations, and this revealed 2 main clusters that separated according to LFD and HFD (data not shown). Within these diet clusters, acetate and butyrate were most similar to each other and differed from propionate. To further compare the metabolic genes responsive to SCFAs independent of the dietary background, overlap analysis was performed for genes robustly regulated by each SCFA on either the LFD or the HFD (**Fig. 3B**). Overlap between all 3 SCFAs was found for 2 genes (*Fabp1* and *Slc2a2*) which were suppressed with SCFAs on the LFD. In addition, 11 genes were commonly regulated by acetate and butyrate on the LFD. Acetate and propionate shared only one gene (*Bckdhb*) and propionate and butyrate commonly regulated 9 genes. Overall, the 23 commonly regulated genes are mainly involved in lipid transport (*Apoa4*, *Apoa1*, *Apoc3*, *Apoc2*, *Npc1l1*, *Mttp*, *Plb1*, *Mogat2* and *Rbp2*), glucose homeostasis (*G6pc* and *Slc2a2*) and, in particular with propionate and butyrate treatment, in the generation of energy, i.e. mitochondrial metabolism (*Idh3b*, *Acaa2*, *Echdc2*, *Hibadh*, *H2-Ke6*, *Ndufs7*, *Uqcr10* and *Cox6a1*). No overlapping genes between SCFAs were found on the HFD.

Besides metabolic genes commonly regulated by SCFAs, we identified metabolic genes specifically regulated by one SCFA (highlighted in **Fig. 3B**). The highest proportion of specifically regulated genes was found for propionate. These genes were only changed on the HFD and were mainly involved in fatty acid metabolism (*Acaa1b* and *Acot7*), mitochondrial metabolism (*Cox4i1*, *Ndufa7*, *Atp6v1d*, *Atp6v1a*, *Atp6v0d1*, *Cyc1*, *Slc25a1* and *Slc25a11*) and amino acid metabolism (*Maob*, *Lap3*, *Aldh9a1*, *Got1* and *Tdh*). Similarly, on the LFD propionate specifically regulated genes involved in fatty acid metabolism (*Acsl1* and *Acot2*) and amino acid metabolism (*Hnmt*, *Bhmt*, *Aldh7a1* and *Alas2*). However, whereas the majority of genes changed with propionate on the HFD were suppressed (25 vs. 9 genes induced), most genes were induced (9 vs. 2 genes suppressed) in the LFD group. Four of the propionate-specific genes were commonly regulated in opposite direction depending on the fat content of the diet (*Gcdh*, *Echs1*, *Cyb5r3* and *Nmnat*).

Taken together, although we observed more overlap of effects of SCFAs infused on the LFD, a more divergent set of genes was induced by SCFAs when infused on the HFD. These results support an important role of dietary fat content in determining the transcriptional response to SCFA infusion.

Next we aimed to identify upstream regulators that potentially could explain the observed shift in gene expression profile for each SCFA treatment (**Table 3**). On the LFD, acetate and butyrate treatment were predicted to significantly inhibit HNF4A, whereas propionate might activate the proinflammatory cytokine TNF. For butyrate on a HFD, many regulators were expected to change. A number of regulators involved in immunity, such as the transcription regulator CEBPB and the cytokines CSF2 and IL6, were predicted to be activated.
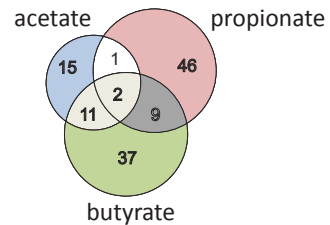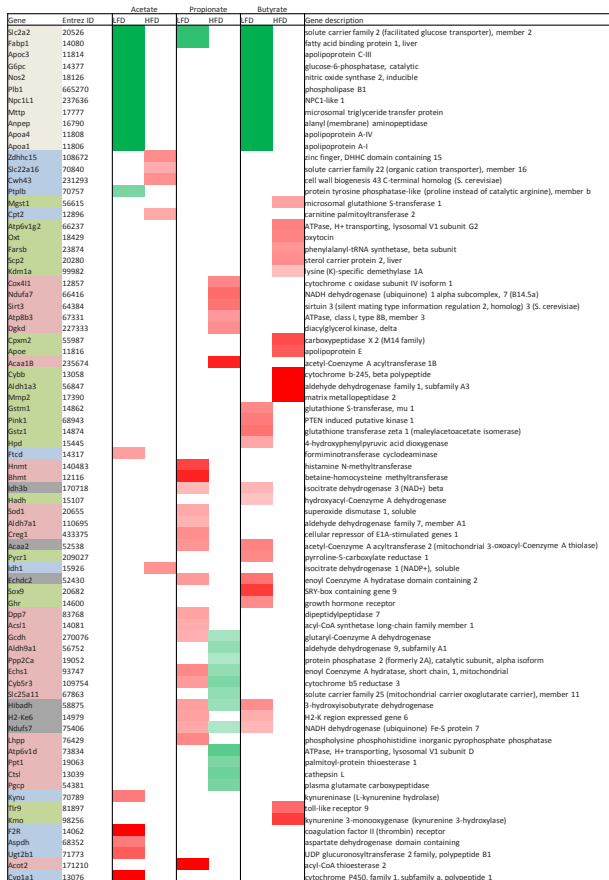
A

Process	Control HFD vs LFD	Acetate LFD	Acetate HFD	Propionate LFD	Propionate HFD	Butyrate LFD	Butyrate HFD
Lipid metabolism							
TG metabolism		down					
Lipid catabolism		down	down			down	down
Lipid biosynthesis	down			up	down		
Membrane lipid biosynthesis						up	
Lipid transport						down	
Mitochondrial LCFA beta oxidation			up				
Lipoprotein metabolism		down	down			down	
Cholesterol biosynthesis	down				down		
Cholesterol transport		down	down			down	down
Amino acid metabolism							
Amino acid metabolism				up	down		
Tryptophan metabolism				up	down		
Histidine metabolism				up	down		
Phenylalanine metabolism					down		
Lysine degradation				up	down	up	
BCAA degradation				up	down	up	
Carbohydrate metabolism							
Carbohydrate metabolism				up	down		
Glycolysis and gluconeogenesis					down		
Glucose metabolism				up	down		
Energy metabolism							
Oxidative phosphorylation	down	down	down			down	down
NAD metabolism				up	down		
Propanoate metabolism				up	down		
Beta-alanine metabolism					down		

Process	Control HFD vs LFD	Acetate LFD	Acetate HFD	Propionate LFD	Propionate HFD	Butyrate LFD	Butyrate HFD
Digestion							
Digestive process		down	down			down	down
Intestinal absorption	down						
Fat digestion and absorption	down	down	down			down	down
Vitamin digestion and absorption		down	down			down	down
Others							
Monoamine transport		up					
Glutathione metabolism				up	down	up	
Exopeptidase activity					down		
Aminopeptidase activity					down		
Collagen metabolic process							up
PPAR signaling pathway	down						

B

Gene	Entrez ID	Gene description
Slc2a2	20526	solute carrier family 2 (facilitated glucose transporter), member 2
Fabp1	14080	fatty acid binding protein 1, liver
Apoc3	11814	apolipoprotein C-III
G6pc	14377	glucose-6-phosphatase, catalytic
Nos2	18126	nitric oxide synthase 2, inducible
Plb1	665270	phospholipase B1
Npc1l1	237636	NPC1-like 1
Mttp	17777	microsomal triglyceride transfer protein
Anpep	16790	alanyl (membrane) aminopeptidase
Apoa4	11808	apolipoprotein A-IV
Apoa1	11806	apolipoprotein A-I
Zdhhc15	108672	zinc finger, DHHC domain containing 15
Slc22a16	70840	solute carrier family 22 (organic cation transporter), member 16
Cwh43	231293	cell wall biogenesis 43 C-terminal homolog (S. cerevisiae)
Ptplb	70757	protein tyrosine phosphatase-like (proline instead of catalytic arginine), member b
Mgst1	56615	microsomal glutathione S-transferase 1
Cpt2	12896	carnitine palmitoyltransferase 2
Atp6v1g2	66237	ATPase, H+ transporting, lysosomal V1 subunit G2
Oxt	18429	oxytocin
Farsb	23874	phenylalanyl-tRNA synthetase, beta subunit
Scp2	20280	sterol carrier protein 2, liver
Kdm1a	99982	lysine (K)-specific demethylase 1A
Cox4i1	12857	cytochrome c oxidase subunit IV isoform 1
Ndufa7	66416	NADH dehydrogenase (ubiquinone) 1 alpha subcomplex, 7 (B14.5a)
Sirt3	64384	sirtuin 3 (silent mating type information regulation 2, homolog) 3 (S. cerevisiae)
Atp8b3	67331	ATPase, class I, type 8B, member 3
Dgkd	227333	diacylglycerol kinase, delta
Cpxm2	55987	carboxypeptidase X 2 (M14 family)
Apoe	11816	apolipoprotein E
Acaa1B	235674	acetyl-Coenzyme A acyltransferase 1B
Cybb	13058	cytochrome b-245, beta polypeptide
Aldh1a3	56847	aldehyde dehydrogenase family 1, subfamily A3
Mmp2	17390	matrix metallopeptidase 2
Gstm1	14862	glutathione S-transferase, mu 1
Pink1	68943	PTEN induced putative kinase 1
Gstz1	14874	glutathione transferase zeta 1 (maleylacetoacetate isomerase)
Hpd	15445	4-hydroxyphenylpyruvic acid dioxygenase
Ftcd	14317	formiminotransferase cyclodeaminase
Hnmt	140483	histamine N-methyltransferase
Bhmt	12116	betaine-homocysteine methyltransferase
Idh3b	170718	isocitrate dehydrogenase 3 (NAD+) beta
Hadh	15107	hydroxyacyl-Coenzyme A dehydrogenase
Sod1	20655	superoxide dismutase 1, soluble
Aldh7a1	110695	aldehyde dehydrogenase family 7, member A1
Creg1	433375	cellular repressor of E1A-stimulated genes 1
Acaa2	52538	acetyl-Coenzyme A acyltransferase 2 (mitochondrial 3-oxoacyl-Coenzyme A thiolase)
Pycr1	209027	pyrroline-5-carboxylate reductase 1
Idh1	15926	isocitrate dehydrogenase 1 (NADP+), soluble
Echdc2	52430	enoyl Coenzyme A hydratase domain containing 2
Sox9	20682	SRY-box containing gene 9
Ghr	14600	growth hormone receptor
Dpp7	83768	dipeptidylpeptidase 7
Acsl1	14081	acyl-CoA synthetase long-chain family member 1
Gcdh	270076	glutaryl-Coenzyme A dehydrogenase
Aldh9a1	56752	aldehyde dehydrogenase 9, subfamily A1
Ppp2ca	19052	protein phosphatase 2 (formerly 2A), catalytic subunit, alpha isoform
Echs1	93747	enoyl Coenzyme A hydratase, short chain, 1, mitochondrial
Cyb5r3	109754	cytochrome b5 reductase 3
Slc25a11	67863	solute carrier family 25 (mitochondrial carrier oxoglutarate carrier), member 11
Hibadh	58875	3-hydroxyisobutyrate dehydrogenase
H2-Ke6	14979	H2-K region expressed gene 6
Ndufs7	75406	NADH dehydrogenase (ubiquinone) Fe-S protein 7
Lhpp	76429	phospholysine phosphohistidine inorganic pyrophosphate phosphatase
Atp6v1d	73834	ATPase, H+ transporting, lysosomal V1 subunit D
Ppt1	19063	palmitoyl-protein thioesterase 1
Ctsl	13039	cathepsin L
Pgcp	54381	plasma glutamate carboxypeptidase
Kynu	70789	kynureninase (L-kynurenine hydrolase)
Tlr9	81897	toll-like receptor 9
Kmo	98256	kynurenine 3-monooxygenase (kynurenine 3-hydroxylase)
F2R	14062	coagulation factor II (thrombin) receptor
Aspdh	68352	aspartate dehydrogenase domain containing
Ugt2b1	71773	UDP glucuronosyltransferase 2 family, polypeptide B1
Acot2	171210	acyl-CoA thioesterase 2
Cyp1a1	13076	cytochrome P450, family 1, subfamily a, polypeptide 1

Venn diagram:

acetate — propionate — butyrate

- acetate only: 15
- acetate ∩ propionate: 1
- propionate only: 46
- acetate ∩ butyrate: 11
- center (all three): 2
- propionate ∩ butyrate: 9
- butyrate only: 37

4

Figure 3 Metabolic processes changed in colon of mice after 6 days of SCFA treatment. **A.** Overview of the metabolic processes changed in colon as observed with gene set enrichment analysis (GSEA). Each process name represents a cluster of gene sets describing similar processes. Positive or negative enrichment of the gene sets according to conservative criteria ($P <0.001$, False Discovery Rate <0.05, and Jaccard + Overlap Combined 0.375) is indicated with 'up' and 'down' respectively.
B. List of all significantly regulated genes ($P <0.01$) present in the gene sets describing the metabolic processes in Fig. 3A. Relative expression of genes is indicated for SCFA vs. control treatment, with red indicating an increase and green indicating a decrease in expression. The Venn diagram shows the number of genes regulated by each SCFA. The colour of each gene name on the list corresponds to the area of the Venn diagram the gene belongs to.

Table 3 Potential upstream regulators in colon of mice after 6 days of SCFA treatment.

	Upstream Regulator	Average Fold Change[1]	Molecule Type	Activation z-score[2]
LFD				
Acetate	HNF4A	-1.03	transcription regulator	-2.60
	KDM5B	1.03	transcription regulator	2.00
	NUPR1	1.16	transcription regulator	2.00
	TP53	1.14	transcription regulator	2.93
Propionate	PAX5	1.53	transcription regulator	2.17
	NFE2L2	-1.02	transcription regulator	2.24
	TNF	1.19	cytokine	2.43
Butyrate	HNF4A	1.05	transcription regulator	-2.45
	PKD1	1.04	ion channel	-2.00
	ZBTB20	1.13	other	2.00
	MAPK1	1.04	kinase	2.24
HFD				
Acetate	SRF	-1.07	transcription regulator	-2.34
	MKL1	-1.02	transcription regulator	-2.22
	TNF	1.00	cytokine	2.23
Propionate	TP53	-1.05	transcription regulator	-2.12
	BNIP3L	1.08	other	2.00
Butyrate	Alpha catenin		group	-3.26
	Estrogen receptor		group	-2.45
	HOXA10	-1.07	transcription regulator	-2.00
	CEBPB	-1.00	transcription regulator	2.00
	HBB	-1.29	transporter	2.00
	HBD		transporter	2.00
	LTBR	-1.01	transmembrane receptor	2.00
	TCR		complex	2.00
	PRL	1.07	cytokine	2.02
	CSF2	1.06	cytokine	2.18
	Cg		complex	2.20
	TGFB1	1.25	growth factor	2.26
	IL6	1.01	cytokine	2.49
	CEBPA	1.02	transcription regulator	2.60

Upstream regulators were determined by Ingenuity Systems Pathway Analysis Software.

[1] Average fold changes of the signal intensity after SCFA infusion compared with saline infusion in mice fed the same background diet (LFD or HFD).

[2] Activation z-score predicts the activation state of the upstream regulator, using the gene expression pattern of its downstream genes. Upstream regulators with z-score ≥ 2 are considered to be significantly activated, if z-score ≤ -2 the upstream regulator is significantly inhibited.

4

SCFA infusion reverses effects of high fat feeding

A stemmed heatmap was created to determine whether the genes significantly regulated (*P* <0.01) by the HFD after control infusion were also significantly regulated by SCFA infusion. As observed from the colour coding of the regulated genes, SCFA infusion on a LFD background tended to have the same effects on gene expression as the control infusion on a HFD background (**Fig. 4A**). However, SCFA infusion on the HFD changed gene expression in opposite direction compared with the control infusion on the HFD, indicating that SCFAs in combination with a HFD might shift gene expression profile towards the control, LFD situation.

When using a fold change cut-off of 1.5, the expression of 47 genes was increased on the HFD compared to the LFD with the control treatment. Of these genes, 8 were suppressed with at least one SCFA treatment on the HFD, including *Cnn1*, *Klb*, *Tagln*, *Col8a1* and 4 genes encoding for transporters (*Scnn1g*, *Slc24a3*, *Scnn1b* and *Best2*) (**Fig. 4B**). In addition, with the control treatment the expression of 73 genes was decreased with the HFD compared to the LFD (**Fig. 4C**). Seven of these genes (*Glo1*, *Psma3*, *Mir18*, *Ang4*, *Snord35b*, *Retnlb* and *Snora75*) were induced with propionate and one gene (*Apol9b*) was induced with acetate on the HFD.

These results indicate that SCFAs on a HFD background might reverse the gene expression changes induced by HFD feeding without SCFA infusion.

A
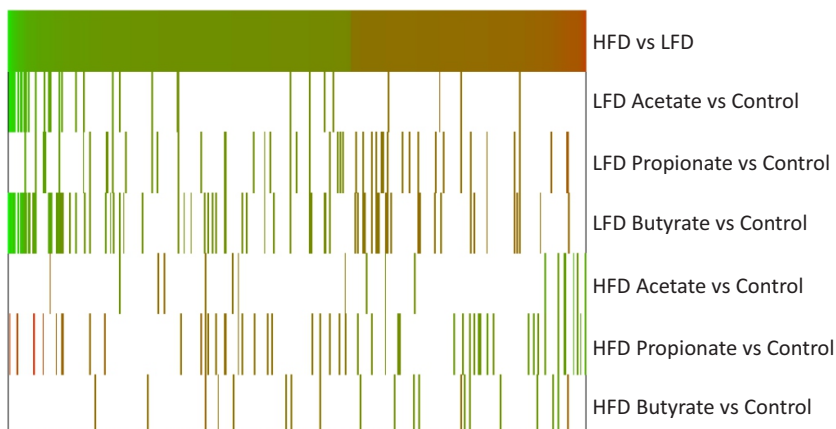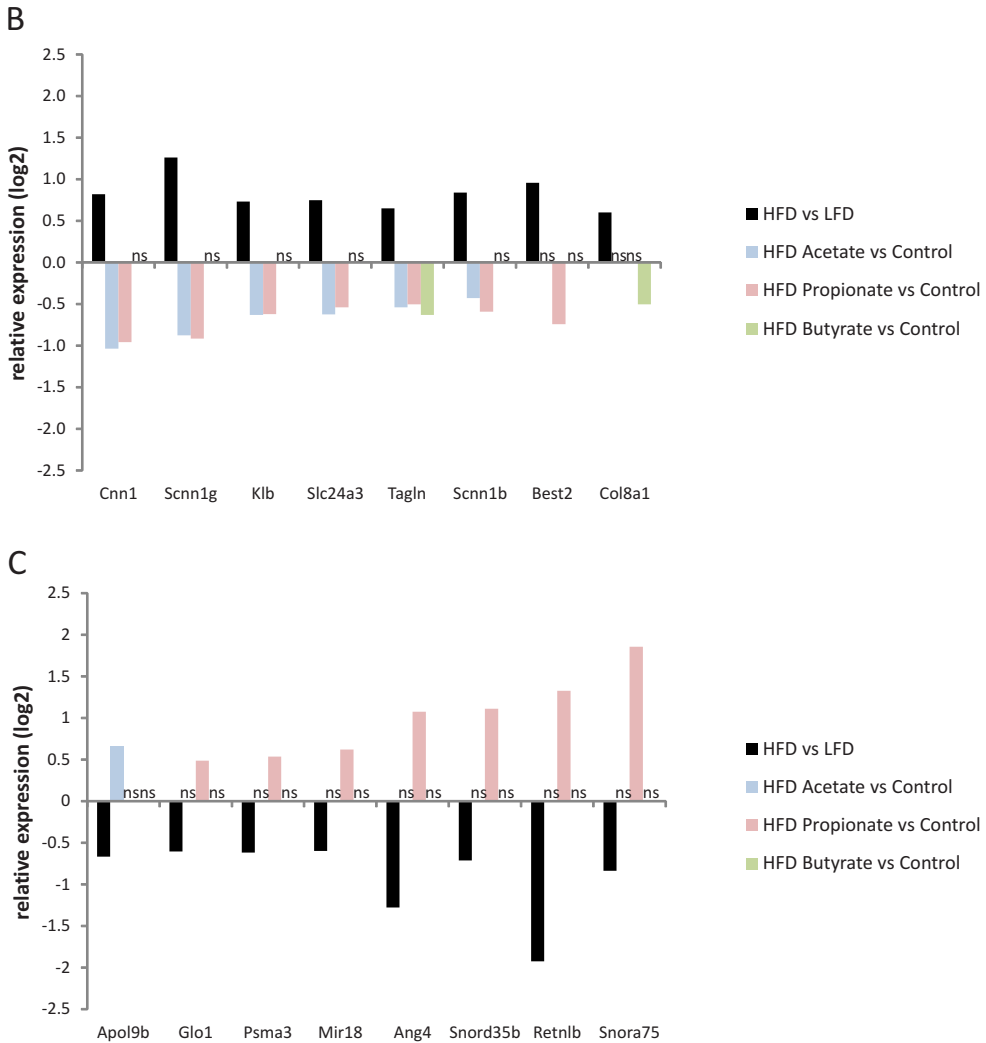
Figure 4 Effects SCFA infusion in combination with HFD. **A.** Heat diagram showing the co-regulation of genes under HFD conditions (Control) in comparison to SCFA infusions under LFD and HFD conditions. Significantly regulated genes (*P* <0.01) are shown and only genes regulated with HFD compared to LFD (Control) were included in the analysis. **B.** Bar chart showing the effect of SCFAs on genes highly induced (*P* <0.01 and fold change >1.5) with HFD compared to LFD; values are given as log2 of the relative expression. Effects of SCFAs are only plotted if effects are significant (*P* <0.01), with ns indicating non-significant effects. **C.** Bar chart showing the effect of SCFAs on genes highly suppressed (*P* <0.01 and fold change <-1.5) with HFD compared to LFD; values are given as log2 of the relative expression. Effects of SCFAs are only plotted if effects are significant (*P* <0.01), with ns indicating non-significant effects.

Discussion

To our knowledge, this is the first experiment in which the impact of fat content in the diet on gene expression changes induced by colonic SCFAs was investigated. We showed that dietary fat is an important factor determining the metabolic implications of SCFA administration. Although a HFD combined with colonic SCFA treatment has not been studied before, experiments have been conducted to determine the effect of diets both high in fibres and fat. A mouse study reported that fermentable fibre decreased energy intake, body weight gain and fat mass when added to a high fat diet (175). A similar effect was observed in pigs fed diets differing in fat level (5% or 17.5%) and fibre type (fermentable or non-fermentable fibre) (176). The fermentable fibre inulin resulted in an attenuation of the body weight development and fat mass accumulation induced by high fat feeding, suggesting a strong interplay between dietary fat and fibre type. We speculate this interaction might be, at least partially, attributed to an increased SCFA production resulting from fermentation of fibres by bacteria in the colon, as we showed here on gene expression level that SCFAs reverse the changes induced by HFD feeding.

It was previously shown that the colonic microbiota composition is affected by dietary fat content (43). Although our experiment did not allow the measurement of microbiota composition, we assume the 2-wk run-in period on either a low or high fat diet might have resulted in a stable change in microbiota composition, as has been reported (46, 177, 178). Therefore, it is very likely that part of the colonic gene expression changes observed on the HFD background are the result of changed microbial composition. Interestingly, a number of studies showed that animals fed a HFD have lower intestinal concentrations of acetate, propionate and butyrate than animals on a LFD (176, 179). It appears that HFD feeding reduces the fermentation capacity of the microbiota compared with a LFD, which might be explained by the lower amount of carbohydrates in the HFD compared to LFD (179). In our study, the amount of colonic SCFAs that was infused was kept constant both in mice fed the LFD and in mice fed the HFD.

Functional implications

In general, the main metabolites produced by the microbiota are SCFAs which induce a wide array of gene expression changes. In particular these changes relate to metabolic and immune-related processes, but SCFAs are also suggested to have regulatory functions.

Metabolic impact of SCFAs in colon

Acetate, propionate and butyrate have very distinct properties and are known to affect health and metabolism in a specific way. To have a closer look at the metabolic effects of each individual SCFA, we administered the SCFAs separately in this experiment.

Acetate is known to serve as a substrate for cholesterol synthesis and lipogenesis (60), and the gene expression changes suggest this also occurs in colon.

Propionate is known for its potential to reduce cholesterol levels in blood (180, 181). This effect is supported by the current study, as colonic gene expression changes indicate that propionate suppresses cholesterol biosynthesis on the HFD background. Furthermore, propionate was shown to affect amino acid metabolism, which might be explained by the fact that propionate can be metabolized by the TCA cycle, thereby contributing to the generation of TCA-derived amino acids (182).

Butyrate is generally believed to be the preferred energy substrate for colonocytes (60). Indeed, butyrate was shown to have a very high impact on oxidative phosphorylation. In addition, butyrate has been reported to restore energy homeostasis and prevent autophagy which mainly can be attributed to its metabolic effects (155).

Effects of acetate and butyrate on the expression of genes involved in lipid and lipoprotein metabolism were highly comparable, whereas propionate induced very distinct changes in gene expression profile. It is known that both acetate and butyrate enter the TCA cycle as acetyl-CoA, whereas propionate enters as succinyl-CoA (182). This pattern of SCFA utilization might explain the similar effects of acetate and butyrate on gene expression level.

In general, the metabolic implications of lipoprotein and lipid metabolic processes are not well described for colonic tissue. Dietary fat is assumed to be taken up by the small intestine and effects on colonic tissue remain unclear. However, the changes on gene expression level suggest a role for colonic tissue in lipid metabolism.

Immune response

The consumption of dietary fibres was previously shown to attenuate the development of inflammatory bowel disease and irritable bowel syndrome (183). It has been hypothesized that this beneficial effect can mainly be attributed to the production of SCFAs as a result of fermentation of the fibres by colonic bacteria (184). With acetate, propionate and butyrate treatment, we observed an increase in immune response, both on a LFD and a HFD background. The upstream regulator analysis suggests that these processes can in part be attributed to the transcription factor CEBPB and the cytokines CSF2, IL6 and TNF.

4

SCFAs were previously found to regulate immune-related processes via the chemoattractant receptor GPR43 (45). Besides the regulation of inflammatory responses by Gpr43, metabolic implications of Gpr43 were demonstrated by Kimura et al. (179). In this study, adipose tissue specific transgenic Gpr43 mice remained lean, whereas GPR43 -/- mice exhibited obesity. The effects were seemingly mediated by microbial metabolites, i.e. SCFAs. In addition to our observation that SCFAs regulate genes involved in both immunity and metabolism, dietary fibre was also shown to modulate immune-related processes and metabolism in opposite direction (185). The effects of SCFAs on gene expression therefore point to GPR43-activated signalling. However, it remains unclear to what extend this signalling results in the suppression of genes involved in lipid-related process in colonic tissue.

Regulatory role SCFAs via non-coding RNAs

We observed that several non-coding RNAs were regulated by SCFA infusion. In the top 50 of genes induced by propionate treatment in mice fed the HFD, 25 small nucleolar RNAs (snoRNAs) were present. snoRNAs are non-coding RNA molecules of about 60-300 nucleotides, which form a new class of RNA species putatively involved in the regulation of gene expression. A recent study provided evidence for a role of snoRNAs in palmitate-induced oxidative stress, as shown by resistance to lipotoxic and oxidative stress *in vitro* and prevention of propagation of oxidative stress *in vivo* as a result of loss of snoRNAs U32a, U33 and U35a (186). The HFD used in our study contained high amounts of palm oil. However, in mice receiving the control infusion we did not observe any snoRNAs induced with HFD consumption. Therefore, it appears that snoRNAs are particularly induced on the HFD in combination with propionate treatment. Since studies on the effect of propionate on snoRNAs have not been performed, we could only speculate which specific characteristic of propionate caused this effect. Furthermore, it has been observed that butyrate regulates non-coding RNAs, among others snoRNAs (187).

Altogether, we believe that the observed changes in the expression of snoRNAs are a highly relevant finding for the function of SCFAs as regulatory molecules. In future research, the impact of snoRNAs on metabolism should be further elucidated.

Conclusion

We showed that dietary fat content has a major impact on gene expression response to SCFAs in colon, an important metabolic organ. Based on the study outcomes, we conclude that standardization of the fat content in the background diet is essential for studying effects of colonic SCFAs, because there appears to be a close interplay between dietary fat and colonic SCFAs. The HFD used in this experiment, containing

45 en% of fat, closely represents the human diet and therefore results obtained from mice consuming the HFD might best reflect what would happen in humans. More research is required to further elucidate how diet composition, in particular the amount of fat and dietary fibre, can improve human health.

Acknowledgements

4

Supplemental Tables and Figures

Supplemental Figure 1.
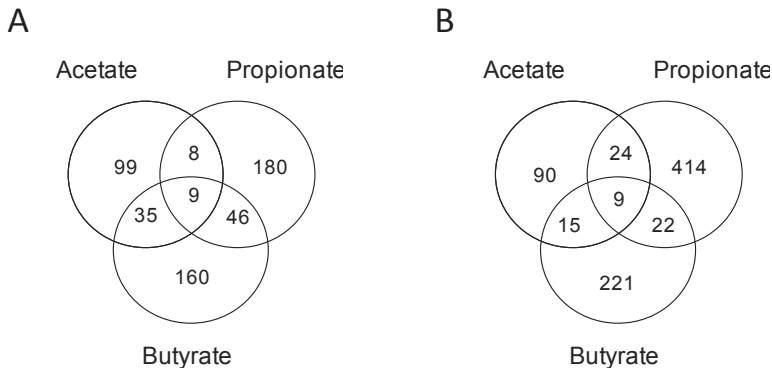
Venn diagrams of significantly regulated genes in colon. Each Venn diagram shows the number of significantly regulated genes (*P* <0.01) in the colon of mice fed the LFD (**A**) or the HFD (**B**) after 6 days of rectal infusion of acetate, propionate and butyrate. Effects of SCFA infusion were compared with effects after saline infusion in mice fed the same background diet (LFD or HFD).

Supplemental Figure 2.
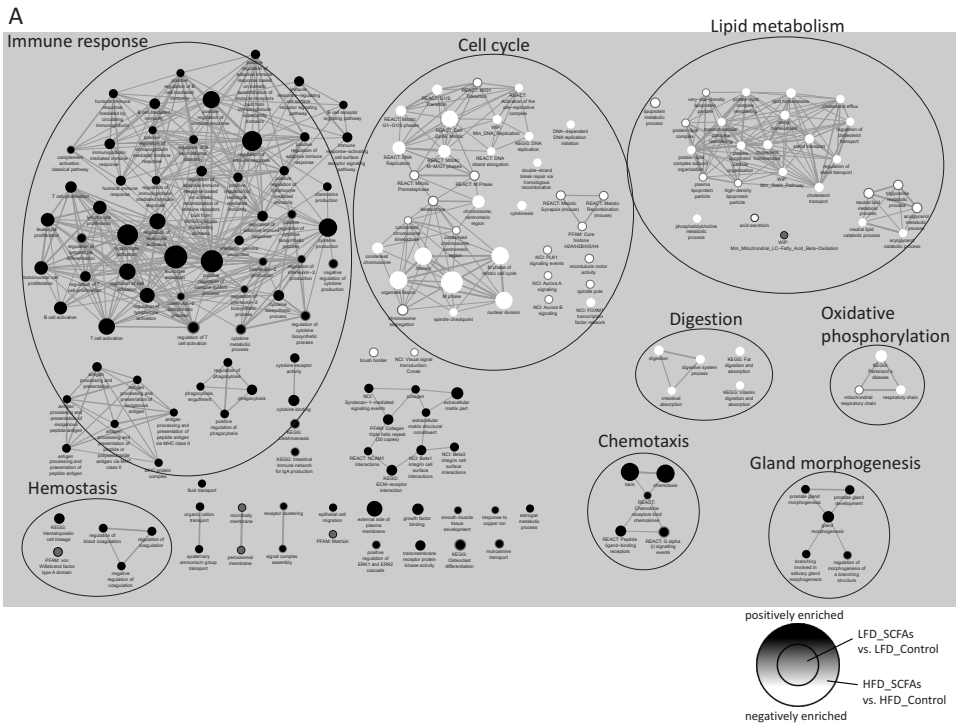
Supplemental Figure 2 (continued).
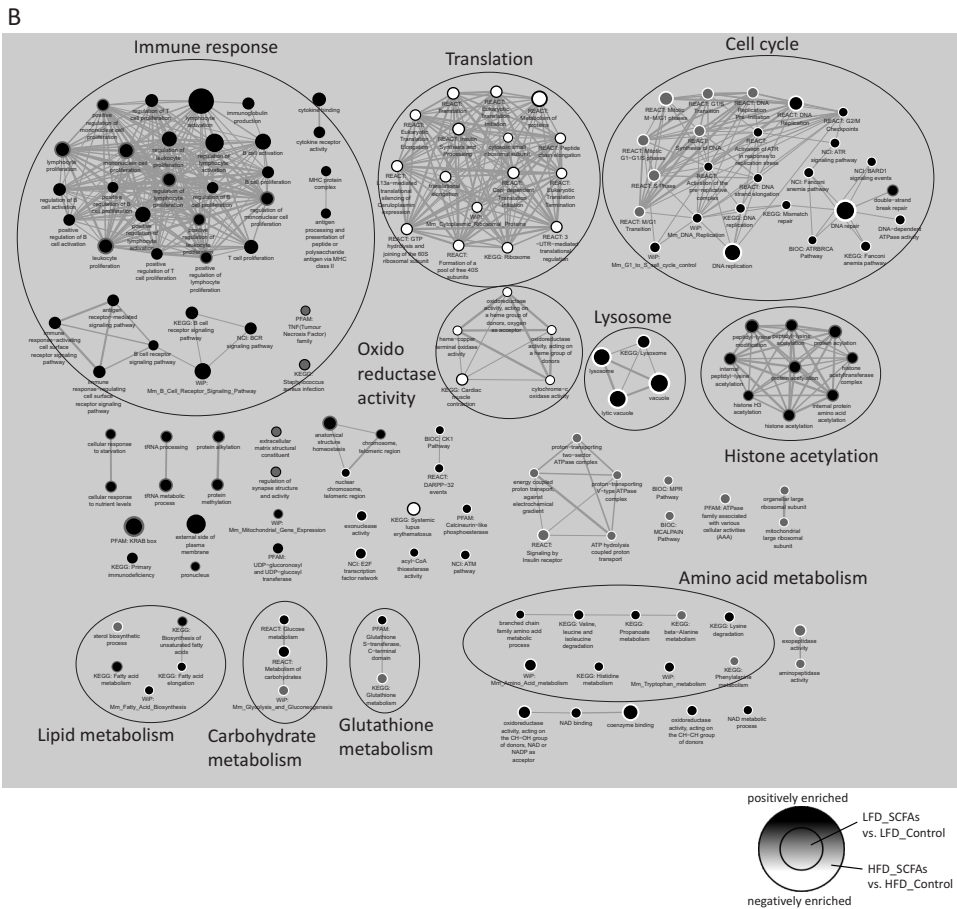
Supplemental Figure 2 (continued).
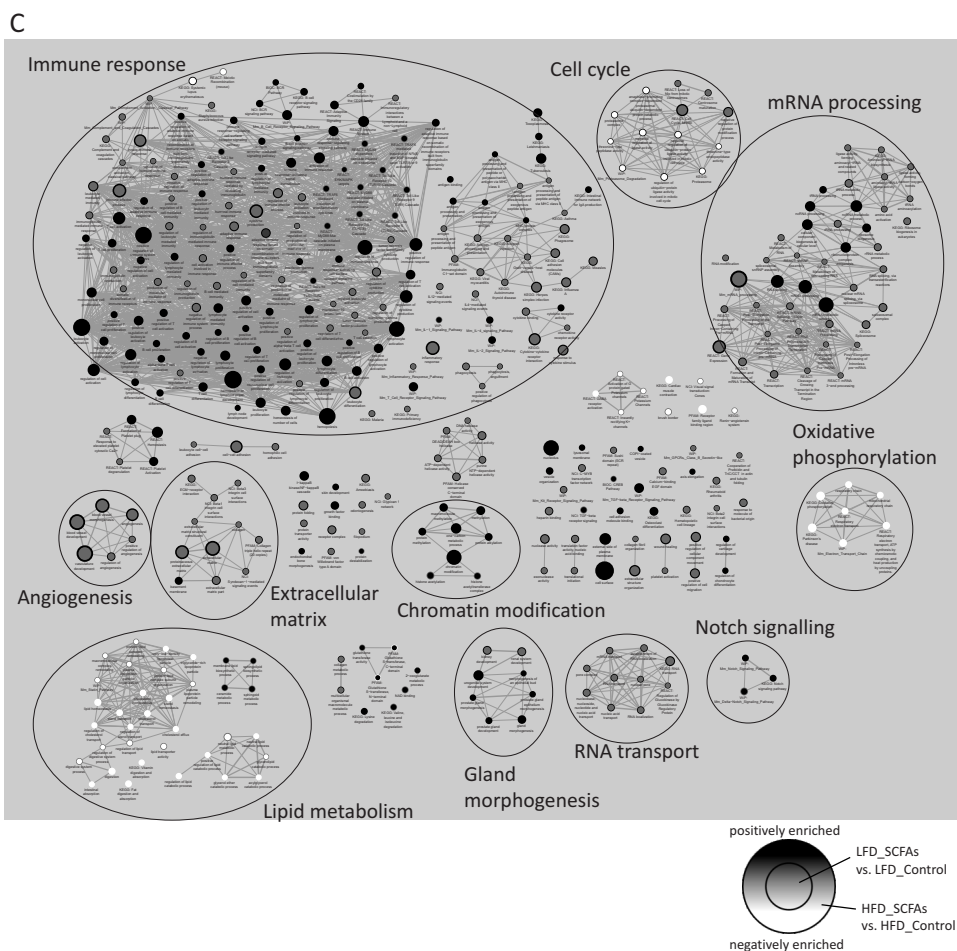
Enrichment maps indicating positively and negatively enriched gene sets. Enrichment maps were created to visualize gene expression changes in colon after acetate (**A**), propionate (**B**) and butyrate (**C**) treatment. Nodes represent functional gene sets, and edges between nodes represent their similarity. The inner part of each node indicates the effect on a LFD background; the outer part of each node indicates the effect on a HFD background. Black indicates induction and white indicates suppression of gene sets with SCFA infusion compared with saline infusion. A grey colour indicates that the gene set was not enriched. Node size represents the gene set size, and edge thickness represents the degree of overlap between 2 connected gene sets. The significance thresholds used were *P* <0.001, False Discovery Rate <0.05 and Jaccard + Overlap Combined 0.375. Clusters were manually circled and labelled to highlight the prevalent biological functions among related gene sets.

4

Effects of resistant starch on behaviour, satiety-related hormones and metabolites in growing pigs

Carol Souza da Silva, Daniëlle Haenen, Sietse Jan Koopmans, Guido J.E.J. Hooiveld, Guido Bosch, J. Elizabeth Bolhuis, Bas Kemp, Michael Müller and Walter J.J. Gerrits

Abstract

Resistant starch (RS) has been suggested to prolong satiety in adult pigs. The present study investigated the RS-induced changes in behaviour, satiety-related hormones and metabolites in catheterised growing pigs to explore the possible underlying mechanisms for RS-induced satiety. In a cross-over design with two 14d periods, 10 pigs (approximately 58 kg) were assigned to two dietary treatments comprising diets containing either 35% of pregelatinized potato starch (PS) or 34% of retrograded tapioca starch (RS). Diets were isoenergetic on gross energy basis. Pigs were fed at 2.8 × maintenance. The postprandial plasma response of satiety-related hormones and metabolites was measured at the end of each period using frequent blood sampling. Faecal and urinary energy losses were measured. Behaviour was scored from video recordings using instantaneous scan sampling for 24 h. Energy digestibility and metabolisability were ~6% lower in the RS compared with the PS diet (P <0.001), and metabolizable energy (ME) intake was ~3% lower in RS-fed than in PS-fed pigs (P <0.001). RS-fed pigs showed less feeder-directed (P =0.001) and drinking (P =0.10) behaviours than PS-fed pigs, and higher peripheral short-chain fatty acid (SCFA) levels (P <0.001) throughout the day. Postprandial glucose and insulin responses were lower in RS-fed than in PS-fed pigs (P <0.001). Triglyceride (TG) levels were higher in RS-fed than in PS-fed pigs (P <0.01), and nonesterified fatty acids (NEFAs) levels did not differ between diets (P =0.90). Glucagon-like peptide-1 (GLP-1) levels were lower in RS-fed than in PS-fed pigs (P <0.001), and peptide tyrosine tyrosine (PYY) levels did not differ between diets (P =0.90). Blood serotonin levels were lower (P <0.001), whereas monoamine oxidase activity (P <0.05) and tryptophan (P <0.01) levels were higher in RS-fed than in PS-fed pigs. Despite a lower ME intake, RS seemed to enhance satiety based on behavioural observations. Possible underlying mechanisms for RS-induced satiety include increased 24 h plasma SCFA levels, and decreased postprandial glucose and insulin responses. GLP-1 and PYY seemed not to play a role in RS-induced satiety. Low blood serotonin levels suggested a difference in intestinal serotonin release between treatments. The role of intestinal serotonin on motility and transit, and immunity in relation to RS requires additional research. It is unknown if higher plasma tryptophan levels led to higher brain serotonin levels in RS-fed pigs, which could support the reduced feeder-directed behaviours after the RS diet. Increased postprandial plasma TG levels corresponded with increased SCFA levels, but it is unclear if TGs may have signalled satiety in RS-fed pigs.

Implications

In this study, resistant starch seemed to enhance satiety, to increase 24 h short-chain fatty acid and TG concentrations, to reduce postprandial glucose, insulin, and serotonin, but not to affect some putative hormonal regulators of satiety such as GLP-1 and PYY. Increased knowledge about the underlying mechanisms by which resistant starch induces satiety could facilitate a deliberate and effective application of resistant starch in animal and human diets. Resistant starch may potentially be used for improving welfare in restrictedly-fed sows, which may experience hunger. Moreover, resistant starch may be used for reducing energy intake and body weight gain in humans.

Introduction

Resistant starch (RS) escapes enzymatic digestion in the small intestine and is largely fermented in the caecum and colon into short-chain fatty acids (SCFAs) (188). Behavioural studies in pigs suggest that RS prolongs the duration of satiety (17, 133, 189). For adult pigs, RS appeared to be more satiating than other types of fermentable fibre, likely due to its slow rate of fermentation, which may impact feelings of satiety (133).

In humans, however, studies on the satiating properties of RS have yielded inconsistent results (12, 125), which could be related to the difficulty to standardize external factors affecting satiety regulation (age, body weight, gender, food intake) and the time required for microbial adaptation to fermentable fibre. Therefore, pigs, which are also omnivorous colonic fermenters (53) are increasingly used as models for human digestive function. Moreover, the fat content of a meal influences satiety regulation, as consumption of high fat diets reduces plasma glucose levels (125). Most RS diets used in human studies had a low fat content (0-5%) or were not matched for fat content, which may influence satiating effects of RS (125).

Putative mechanisms for the satiating effects of RS are related to the increased microbial production of SCFAs. First, increased intestinal absorption of SCFAs may prolong postprandial energy supply to the body (188, 190), which may cover energy requirements particularly after intestinal absorption of glucose is completed, and thereby, prolong satiety (190). It has been shown that exchange of enzymatically digestible starch by RS in the diet, indeed, resulted in stabilized postprandial levels of glucose and insulin, which prolongs satiety likely by preventing drops in glucose levels below basal levels (94, 190). Second, SCFAs may stimulate the release of the satiety-related hormones peptide tyrosine tyrosine

5

(PYY) and glucagon-like peptide-1 (GLP-1) from entero-endocrine cells (138). Both hormones affect satiety via an effect in the brain (either through the circulation or through vagal afferent signals, or both) and via the 'ileal brake' (25). Finally, SCFAs may stimulate the release of serotonin (5-hydroxytryptamine, 5-HT) in the colon through activation of free fatty acid 2 receptors expressed in 5-HT-containing cells, which affects colonic motility and overall transit time of digesta, thus contributing to satiety regulation, independently of PYY and GLP-1 (25).

Postprandial changes in metabolic and hormonal profiles and physical activity induced by RS are not well characterized over time, and are important to study the mechanisms by which RS promotes long-term satiety. Therefore, the present study aimed to assess the time-course of RS-induced changes in general physical activity and behaviour (as an indicator of hunger/satiety), satiety-related hormones and metabolites in growing pigs, and relate those to feeding behaviour and meal size during an *ad libitum* meal. In addition, satiating effects of RS were evaluated in the presence of extra dietary fat.

Materials and methods

Animals and housing

Ten Landrace barrows (initial body weight: 58 ± 1.6 kg; age: 4 months) from 8 litters (1-2 pigs per litter) were assigned to 2 dietary treatments in a 2 × 2 crossover design with 2 identical 14d experimental periods. Treatments differed in the type of starch in the diet: pregelatinized potato starch (PS) or retrograded tapioca starch (RS). Pigs were individually housed in metabolism pens (2 × 1 m) within a temperature controlled room (20 ± 2°C). Lights were on from 05:00 h until 19:00 h and dimmed during the night. Pens were equipped with a feeder and cleaned daily. A metal tray and funnel system beneath a rubberized metal-grid floor (0.5 cm oval holes) allowed urine collection with minimal faecal contamination. The Animal Care and Use Committee of Wageningen University and Research Centre (Lelystad, The Netherlands) approved the experiment.

Diets, feeding and surgery

The two experimental diets contained either 35% PS (Paselli™ WA4, Avebe Food) or 34% RS (C*Actistar 11700, Cargill), and were designed to meet nutrient requirements according to the Dutch feed evaluation system for pigs (191). Diets were formulated to provide equal amounts of gross energy (GE) (~17 MJ GE/kg diet). **Table 1** shows the ingredient and analysed chemical composition of the diets. Diets were produced as a single batch of a basal diet to which starch sources were

added. Diets were flavoured to mask differences in palatability, and TiO_2 was added as an indigestible marker. Two isocaloric high-fat (HF) diets were formulated with wheat and barley starch being exchanged for 20% soy oil resulting in a HF-PS and a HF-RS diet (Table 1). Diets were fed as mash, and mixed with water (water:feed = 2.5:1) in the feeders just before feeding. Pigs were fed at 07:00 h and 16:00 h at 2.8 × the energy requirements for maintenance (MEm = 450 kJ/kg$^{0.75}$ per day). The amount of feed was adjusted daily according to the metabolic body weight (kg$^{0.75}$) of the pigs and an anticipated daily gain of about 500 g. Water was continuously available.

During 1-week habituation, pigs were fed a 50:50 mix of the PS and RS diets, and adapted to individual housing and feeding regime. Furthermore, each of the two HF diets was fed twice to prevent feed neophobia during the experiment. After the habituation period, pigs were provided with two permanent blood vessel catheters in the carotid artery for blood sampling and in the jugular vein for back-up in case of a malfunctioning arterial catheter (see (166) for details). In the week after surgery, pigs were habituated to blood sampling. After 4 to 6 days of postsurgical recovery, pigs were gradually switched to the experimental diets. In each experimental period (d1 to d14), pigs were daily fed a restricted meal of the PS and RS diets, with the exception of the morning meal on d8, when a restricted meal of the HF-PS and HF-RS diets was provided, and the morning meal on d10, when an *ad libitum* meal of the PS and RS diets was provided.

Table 1 Ingredient and analysed chemical composition of experimental diets.

	Experimental diet			
	PS	RS	HF-PS	HF-RS
Ingredient composition (g/kg)				
Pregelatinized purified potato starch[1]	350.0	0.0	452.0	0.0
Retrograded tapioca starch[2]	0.0	342.6	0.0	444.0
Soy oil	29.2	29.5	198.2	201.2
Wheat	200.0	202.3	0.0	0.0
Beet pulp (sugar<100 g/kg)	50.0	50.6	64.6	65.5
Barley	150.0	151.7	0.0	0.0
Wheat gluten meal	60.0	60.7	77.5	78.6
Potato protein[3]	100.0	101.1	129.1	131.0
Premix[4]	10.0	10.1	12.9	13.1
$CaCO_3$	13.5	13.7	17.4	17.7
$Ca(H_2PO_4)_2$	11.0	11.1	14.2	14.4
NaCl	3.0	3.0	3.9	3.9
L-lysine HCL	2.2	2.2	2.8	2.9
L-tryptophan	0.2	0.2	0.3	0.3
MgO (80%)	0.4	0.4	0.5	0.5

5

NaHCO$_3$	14.0	14.2	18.1	18.3
KCl	3.0	3.0	3.9	3.9
TiO$_2$	2.0	2.0	2.6	2.6
Flavour[5]	1.5	1.5	1.9	2.0
Chemical composition (g/kg dry matter)				
Dry matter (g/kg as is)	894.5	910.0	924.3	952.1
Organic matter	941.4	941.9	937.4	936.9
Crude protein (N × 6.25)	190.9	194.3	186.2	188.7
Crude fat	16.1	28.6	197.0	201.0
Starch	524.7	477.1	411.1	337.5
Sugar	13.1	69.4	6.0	70.7
Ti	1.6	1.6	-	-
Energy content (MJ/kg)				
GE	16.48	16.78	-	-

PS=pregelatinized potato starch diet; RS=retrograded tapioca starch diet; HF-PS=high-fat pregelatinized potato starch diet; HF-RS=high-fat retrograded tapioca starch diet.

[1]Paselli^{TM} WA4, Avebe Food, Veendam, The Netherlands.

[2]C*Actistar 11700, Cargill, Amsterdam, The Netherlands.

[3]Protostar, Avebe Food, Veendam, The Netherlands.

[4]Provided the following per kg of feed: vitamin A: 7500 IU; vitamin D$_3$: 1500 IU; vitamin E: 60 mg; vitamin K$_3$: 1.0 mg; vitamin B$_1$: 1.0 mg; vitamin B$_2$: 4.0 mg; vitamin B$_6$: 1.0 mg; vitamin B$_{12}$: 20 µg; niacin: 20 mg; calcium-D pantothenate: 10.5 mg; choline chloride: 100 mg; folic acid: 0.4 mg; Fe: 120 mg (FeSO$_4$.H$_2$O); Cu: 15 mg (CuSO$_4$.5H$_2$O); Mn: 60 mg (MnO); Zn: 75 mg (ZnSO$_4$.H$_2$O); I: 4.0 mg (KI); Se: 0.30 mg (Na$_2$SeO$_3$); anti-oxidant: 75 mg.

[5]Luctarom Advance Cherry Honey, Lucta S.A., Barcelona, Spain.

Measurements and sample collection

Body weight was measured weekly. Faeces (for GE and Ti analyses) and urine (for GE analysis) were collected quantitatively per pig during the last 2 and 3 days, respectively, of each experimental period. Faecal samples were collected directly from the pen floor twice daily and urine samples were collected daily from the total urine output of each pig, and stored at -20°C until analysis. In each period, satiating effects of the diets were assessed when pigs were fed a restricted morning meal of the HF-PS and HF-RS diets (d8), an *ad libitum* morning meal (d10) and a restricted morning meal (d14), both of the PS and RS diets. An additional *ad libitum* meal of a 50:50 mix of the PS and RS diets was provided 7 h after the HF morning meals. During the *ad libitum* meals (d8 and d10), feeding behaviour and voluntary feed intake were measured.

Blood samples (6 mL) were collected in EDTA tubes with protease and dipeptidyl peptidase-IV inhibitors before (at -30 and 0 min) and after (at 20, 40, 60, 90, 120, 180, 240 and 300 min) the restricted meal of the PS and RS diets on d14,

placed in ice water and centrifuged at 1300 *g* for 10 min at 4°C within 20 min after collection. Plasma was stored at -80°C until analysis. Extra blood samples (9 mL) were collected in EDTA tubes before (at -30 min) and after (at 20 and 300 min) the restricted meal on d14. For measuring 5-HT levels, tubes with blood were placed in ice water and centrifuged at 160 *g* for 10 min at room temperature to obtain platelet-rich plasma (PRP). The extracted PRP (1 mL) was centrifuged at 13000 *g* for 15 min at room temperature to obtain platelet pellets. The washed (with 1 mL of 0.9% NaCl solution, followed by centrifugation at 13000 *g* for 5 min) pellets were stored at -80°C until analysis. For measuring monoamine oxidase (MAO) activity, blood samples (1.2 mL) were stored at -80°C until analysis.

Chemical analyses and calculations
Diets were analysed for dry matter, ash, starch, sugar, crude protein, crude fat, GE and Ti as previously described (26), see **Supplemental Material** for details. Blood plasma was analysed for glucose, insulin, TGs, NEFAs, active GLP-1, active PYY, tryptophan (Trp), large neutral amino acids (LNAA) and SCFAs. Blood platelet pellets were analysed for 5-HT, and whole blood for MAO activity (see **Supplemental Material** for details). Apparent faecal energy digestibility coefficient was calculated as previously described (26) and the digestible energy (DE) content of the diet as its GE content multiplied by this coefficient. The metabolizable energy (ME) content was calculated as GE intake minus energy lost in faeces and urine.

Behavioural observations
On d12 of each experimental period, the pigs' postures and behaviours were scored from video recordings using 10 min-instantaneous scan sampling for 24 h and expressed as percentages of observation time. Postures were standing and walking, kneeling and sitting, lateral lying, and ventral lying (133). Behavioural oral activities were explorative behaviour (rooting or nosing floor or pen fixtures), chewing (repetitively chewing of pen fixtures or sham chewing) (189), feeder-directed behaviour (eating, and sniffing, licking or touching the feeder with the snout), drinking, and other (all other behavioural activities).

Furthermore, pigs were observed continuously for 1 h during the *ad libitum* meal of a 50:50 mix of the PS and RS diets 7 h after the HF-PS and HF-RS diets (d8) and during the *ad libitum* meal of the PS and RS diets (d10). Behaviours and postures scored were the same as described above, except that eating was scored separately, and used to determine the duration of the first bout of eating. The Observer software package (Noldus Information Technology B.V.) was used for all behavioural recordings.

5

Statistical analyses

Data were analysed using a mixed model in SAS (version 9.1; SAS Institute) with values in time and treatment of individual pigs taken as repeated measurements. For feed intake and body weight data, the model included period and diet as fixed effects and pig as random effect. For the behaviours (d8, d10 and d12), plasma hormones and metabolites (d14) the model included period, diet, (sampling or observation) time, and interaction of diet and time as fixed effects, and pig and pig (diet) as random effects. Sequence of treatments effect was removed from the final model if not significant (P >0.10). Data are presented as least-square means ± SEM.

Results

Catheters functioned well during the experiment and were accurately placed as confirmed after section. None of the diets offered was refused during the experiment. All pigs remained healthy, and had a normal growth throughout the experiment. Pigs' body weight at the start (57.9 ± 1.6 kg) and end (79.7 ± 2.0 kg) of the experiment did not differ between diets.

Diets and feed intake

Energy digestibility (DE:GE) and metabolisability (ME:GE) were approximately 6% lower (P <0.001, **Table 2**), and ME intake was approximately 27 kJ//kg$^{0.75}$ per day (~3%) lower in the RS compared with the PS diet (P <0.001, Table 2). When a mixture of the PS and RS diets was provided *ad libitum* 7 h after providing a restricted meal of either HF-PS and HF-RS diets in the morning of d8, pigs consumed 70.3 and 58.9 g/kg$^{0.75}$ (SEM = 5.1), respectively, corresponding to a difference in ME intake of 165 kJ/kg$^{0.75}$ (P =0.12, Table 2). When the PS and RS diets were fed *ad libitum* in the morning of d10, feed intake was about twice the normal meal size: 70.3 and 68.8 g/kg$^{0.75}$ (SEM=5.0) in PS- and RS-fed pigs, respectively, with no difference between diets (P =0.83). ME intake of the *ad libitum* meal was 69 kJ/kg$^{0.75}$ lower in RS-fed than in PS-fed pigs (P =0.52, Table 2). There was an effect of the sequence of treatments on the size of the *ad libitum* meal consumed on d8 and d10. Pigs receiving the PS-RS sequence ate 23 and 15 g/kg$^{0.75}$ less compared with pigs receiving the RS-PS sequence (P <0.05 and P =0.07 on d8 and d10, respectively). This corresponded to a difference in ME intake of 332 kJ/kg$^{0.75}$ and 214 kJ/kg$^{0.75}$ (P <0.05 and P =0.08 on d8 and d10, respectively).

Table 2 Digestible and metabolizable energy intake (in kJ//kg$^{0.75}$ per day, unless indicated otherwise) in growing pigs fed an ad libitum meal of a 50:50 mix of the pregelatinized potato starch (PS) and retrograded tapioca starch (RS) diets at 7 h after a restricted high fat (HF) meal of either PS or RS (d8), an ad libitum morning meal (d10), and a restricted morning meal (d14), both of the PS and RS diets[1].

	Diet			Effects[2]	
	PS	RS	s.e.[3]	D	S
Day 8 (kJ/kg$^{0.75}$ per meal)[4]					
ME intake	1015.3	850.2	73.8	ns	*
Day 10 (kJ/kg$^{0.75}$ per meal)					
ME intake	1039.0	970.1	72.9	ns	#
Day 14					
GE intake	1095.3	1137.3	4.0	***	ns
DE intake	988.9	963.1	3.5	***	ns
ME intake	982.3	955.6	3.5	***	ns
DE:GE, %	90.1	84.5	0.3	***	ns
ME:GE, %	89.6	84.0	0.3	***	ns

DE=digestible energy; GE=gross energy; ME=metabolizable energy.

[1]Throughout the experiment, pigs were daily fed a restricted meal of the PS and RS diets, with the exception of the morning meals on d8 and d10.

[2]Statistical significance of effects of diet (D), and sequence of treatment (S) is indicated: #P <0.10, *P <0.05, **P <0.01, ***P <0.001, ns=non-significant. Period (P) did not influence energy intake.

[3]Pooled standard error of the least-square means.

[4]Pigs were fed a HF meal containing PS or RS in the morning of d8, and ME intake corresponds to the consumption of a 50:50 mix of the PS and RS diets 7 h after each HF meal.

5

Physical activity (24 h)

Behaviours on d12 were affected by time of the day (all P <0.001; **Table 3**), except for drinking behaviour. Generally, pigs showed a daily activity pattern characterized by peaks of activity around feeding in the morning (between 07:00 h and 09:00 h) and in the afternoon (between 16:00 h and 18:00 h), interspersed by resting periods. Lying did not differ between diets (P =0.30). RS-fed pigs spent more time lying ventrally (45% vs. 37%) and less time lying laterally (44% vs. 51%, SEM=2) than PS-fed pigs (both P <0.05, Table 3). PS-fed pigs performed more feeder-directed behaviours (5% vs. 3%, SEM=1, P =0.001), and tended to spend more time drinking (1.3% vs. 0.6%, SEM=0.3, P =0.10) than RS-fed pigs (Table 3).

Table 3 Daily physical activity (in % of observation time) of growing pigs fed a restricted meal of a diet containing either pregelatinized potato starch (PS) or retrograded tapioca starch (RS), based on video observations using 10 min-instantaneous scan sampling.

Behaviour	Diet			Effects[1]	
	PS	RS	s.e.[2]	D	T
Posture					
Lying	88.0	90.0	1.0	ns	***
Ventrally	37.0	45.0	2.0	*	***
Laterally	51.0	44.0	2.0	*	***
Standing and walking	9.0	8.0	1.0	ns	***
Kneeling and sitting	3.0	3.0	1.0	ns	***
Behavioural oral activities	23.0	19.0	2.0	ns	***
Explorative behaviour	10.0	10.0	2.0	ns	***
Chewing	7.0	6.0	2.0	ns	***
Feeder-directed behaviour	5.0	3.0	1.0	**	***
Drinking	1.3	0.6	0.3	#	ns

[1]Statistical significance of effects of diet (D) and observation time (T) is indicated: #P <0.10, *P <0.05, **P <0.01, ***P <0.001, ns=non-significant. Interaction between diet and time (D × T) and period (P) did not influence daily physical activity.

[2]Pooled standard error of the least-square means.

Behaviour during ad libitum meals

During the *ad libitum* meal of the PS and RS diets (d10), all behaviours were affected by time (all P <0.001). Generally, activity of the pigs decreased after the first 15 min of the meal. The duration of the first bout of eating was shorter (P <0.01) in RS-fed (452 s) than in PS-fed pigs (957 s, SEM=109). RS-fed pigs spent more time on non-feeder directed explorative behaviour (77 s vs. 42 s, SEM=13, P <0.05), and less time on feeder-directed behaviour, including eating, than PS-fed pigs (74 s vs. 130 s, SEM=11, P <0.01). RS-fed pigs (63 s) spent less time eating than PS-fed pigs (116 s, SEM=9, P <0.001), and this effect tended to be most pronounced during the first 30 min of the meal (diet × time interaction, P =0.06). During the *ad libitum* meal of a 50:50 mix of the PS and RS diets provided 7 h after the HF-PS and HF-RS diets (d8), all behaviours were affected by time (all P <0.001), but were unaffected by diet (data not shown).

Blood parameters

Plasma SCFA, glucose, insulin, TG, NEFA, GLP-1 and PYY levels around ingestion of the restricted PS and RS meals on d14 are presented in **Figures 1-4**. 5-HT, MAO, Trp, LNAA and Trp:LNAA ratio are given in **Table 4**. Plasma SCFA levels were higher in RS-fed than in PS-fed pigs (all P <0.001). Basal glucose and insulin levels did not

differ between diets. When pigs were fed the restricted meal, plasma glucose levels were affected by diet (P <0.001), sampling time (P <0.001) and their interaction (P <0.01), with lower levels in RS-fed than in PS-fed pigs, particularly at 20, 40, 60, 120 and 240 min postprandial. The peak in glucose levels at approximately 20 min postprandial was lower in RS-fed than in PS-fed pigs (P <0.01). Plasma insulin levels were affected by diet (P <0.001), sampling time (P <0.001) and their interaction (P <0.001), with lower levels in RS-fed than in PS-fed pigs, particularly at 20, 40 and 60 min postprandial. The peak in insulin at approximately 40 min postprandial was lower in RS-fed than in PS-fed pigs (P <0.01). Plasma TG levels were higher in RS-fed pigs than in PS-fed pigs (P <0.01). TG levels differed between sampling times (P <0.001), with higher levels at 90 min postprandial than at 0 min. Plasma NEFA levels were unaffected by diet (P =0.90), but were affected by sampling time (P <0.05), with higher levels at 90, 120, 180 and 240 min than at 40 min postprandial. Plasma GLP-1 levels were lower in RS-fed than in PS-fed pigs (P <0.001). GLP-1 levels differed between sampling times (P <0.001), with higher levels at 60 min than at 90, 120 and 180 min postprandial. Plasma PYY levels were unaffected by diet (P =0.90), but tended to be affected by sampling time (P =0.06), with higher levels at -30 min than at 120 min postprandial.

Platelet 5-HT was affected by sampling time (P <0.05) with higher levels at -30 min than at 20 min postprandial, and tended to be lower in RS-fed pigs (P =0.08). Blood 5-HT levels were lower (P <0.001) and MAO activity was higher in RS-fed than in PS-fed pigs (P <0.05). Plasma Trp levels were affected by diet (P <0.01), sampling time (P <0.001) and there was a trend for the effect of their interaction (P =0.07). Trp levels were higher in RS-fed than in PS-fed pigs, particularly at 300 min postprandial. Plasma LNAA levels and Trp:LNAA ratio tended to be higher in RS-fed than in PS-fed pigs (P =0.08 and P =0.07, respectively). LNAA levels were affected by sampling time (P <0.001), with higher levels at 300 min postprandial than at -30 min. The Trp:LNAA ratio was affected by sampling time (P =0.001), with higher levels at -30 min than at 20 and 300 min postprandial.

5
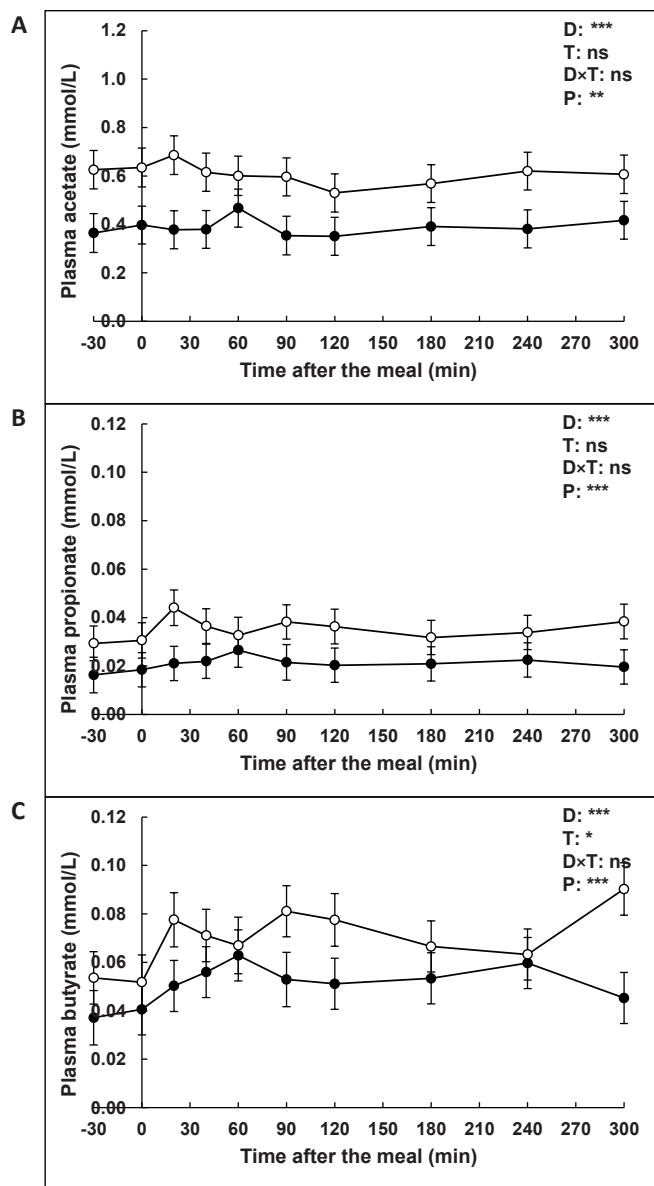
Figure 1 Plasma concentrations of SCFAs: acetate (**A**), propionate (**B**) and butyrate (**C**), in peripheral blood collected before (-30 min), during (0 min) and after (20 to 300 min) feeding growing pigs a restricted meal of the pregelatinized potato starch (PS) diet (●) and retrograded tapioca starch (RS) diet (○) in the morning of d14. Statistical significance of effects of diet (D), sampling time (T), their interaction (D × T), and period (P) is indicated: #P <0.10, *P <0.05, **P <0.01, ***P <0.001, ns=non-significant.
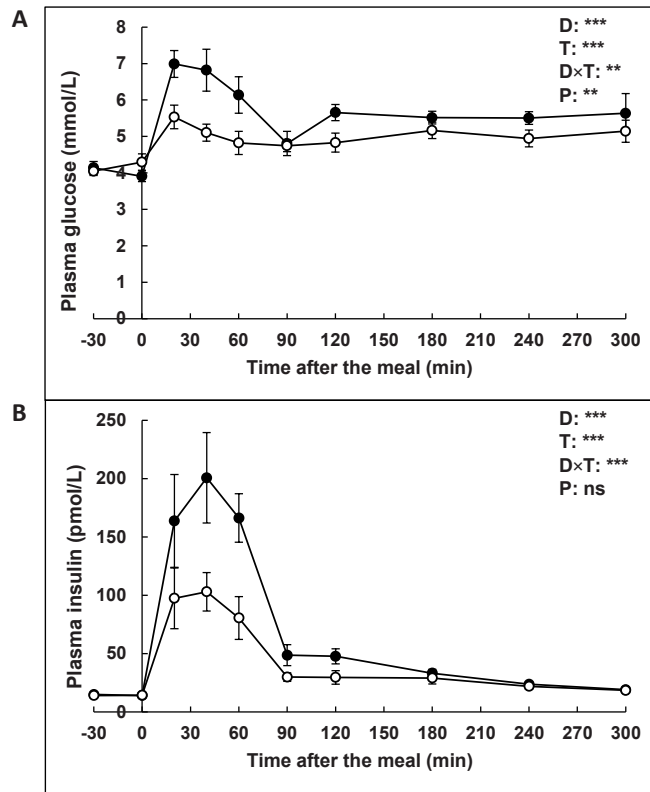
Figure 2 Plasma concentrations of glucose (**A**) and insulin (**B**) in peripheral blood collected before (-30 min), during (0 min) and after (20 to 300 min) feeding growing pigs a restricted meal of the pregelatinized potato starch (PS) diet (●) and retrograded tapioca starch (RS) diet (o) in the morning of d14. Statistical significance of effects of diet (D), sampling time (T), their interaction (D × T), and period (P) is indicated:
#P <0.10, *P <0.05, **P <0.01, ***P <0.001, ns=non-significant.

5
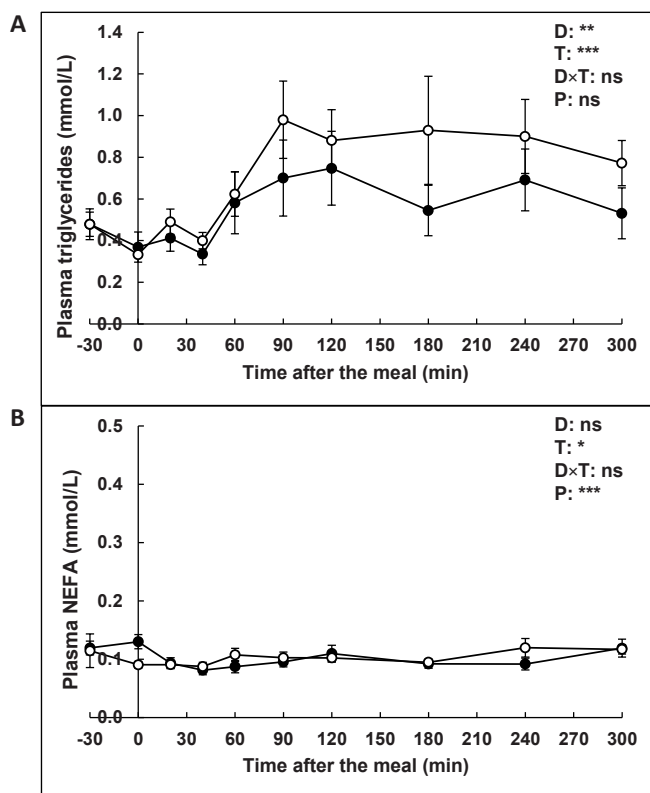
Figure 3 Plasma concentrations of TGs (**A**) and NEFAs (**B**) in peripheral blood collected before (-30 min), during (0 min) and after (20 to 300 min) feeding growing pigs a restricted meal of the pregelatinized potato starch (PS) diet (●) and retrograded tapioca starch (RS) diet (○) in the morning of d14. Statistical significance of effects of diet (D), sampling time (T), their interaction (D × T), and period (P) is indicated: #*P* <0.10, **P* <0.05, ***P* <0.01, ****P* <0.001, ns=non-significant.
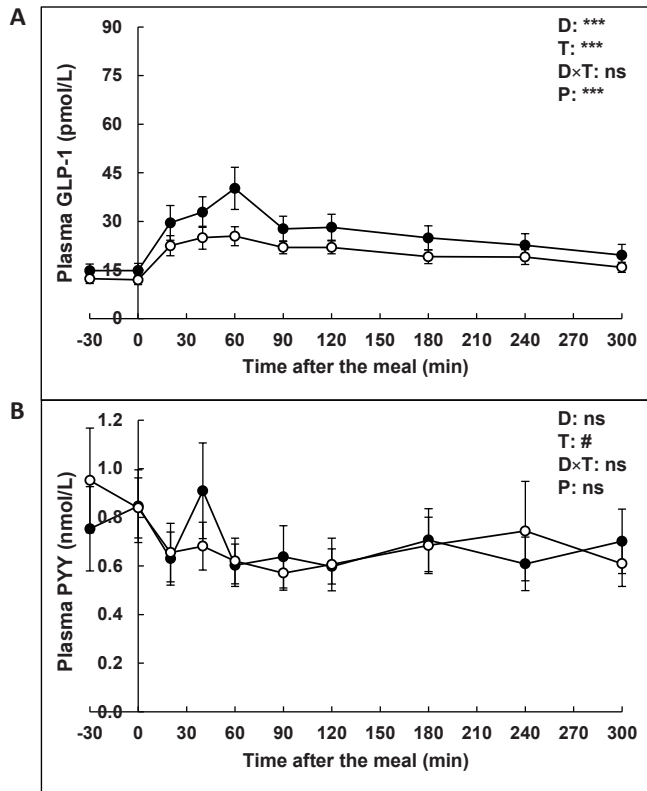
Figure 4 Plasma concentrations of GLP-1 (**A**) and PYY (**B**) in peripheral blood collected before (-30 min), during (0 min) and after (20 to 300 min) feeding growing pigs a restricted meal of the pregelatinized potato starch (PS) diet (●) and retrograded tapioca starch (RS) diet (○) in the morning of d14. Statistical significance of effects of diet (D), sampling time (T), their interaction (D × T), and period (P) is indicated: #P <0.10, *P <0.05, **P <0.01, ***P <0.001, ns=non-significant.

5

Table 4 Platelet serotonin (platelet 5-HT, in µmol/10^9 platelets), whole blood serotonin (blood 5-HT, in µmol/L), monoamine oxidase activity (MAO, in µmol/L/h), tryptophan (Trp, in mmol/L), large neutral amino acids (LNAA, in mmol/L), and Trp:LNAA ratio in peripheral blood of growing pigs fed a restricted meal of a diet containing either pregelatinized potato starch (PS) or retrograded tapioca starch (RS).

	Diet			Effects[1]			
	PS	RS	s.e.[2]	D	T	D × T	P
Average over sampling times							
Platelet 5-HT	0.024	0.021	0.002	#	*	ns	***
Blood 5-HT	6.46	5.03	0.46	***	ns	ns	ns
MAO activity	82.94	89.34	7.70	*	ns	ns	ns
Trp	0.060	0.068	0.002	**	***	#	ns
LNAA	1.22	1.32	0.05	#	***	ns	ns
Trp:LNAA	0.050	0.053	0.002	#	**	ns	ns
30 min before the meal							
Platelet 5-HT	0.026	0.023	0.003	ns	-	-	**
Blood 5-HT	5.95	4.91	0.58	#	-	-	#
MAO activity	84.78	85.93	8.29	ns	-	-	ns
Trp	0.043	0.046	0.003	#	-	-	ns
LNAA	0.80	0.79	0.08	ns	-	-	ns
Trp:LNAA	0.054	0.059	0.002	ns	-	-	ns
20 min after the meal							
Platelet 5-HT	0.021	0.018	0.003	ns	-	-	**
Blood 5-HT	6.86	5.18	0.58	*	-	-	ns
MAO activity	79.81	91.78	8.29	*	-	-	ns
Trp	0.070	0.074	0.003	ns	-	-	ns
LNAA	1.46	1.50	0.08	ns	-	-	ns
Trp:LNAA	0.048	0.050	0.002	ns	-	-	ns
300 min after the meal							
Platelet 5-HT	0.023	0.020	0.003	ns	-	-	*
Blood 5-HT	6.56	5.01	0.58	**	-	-	ns
MAO activity	84.23	90.31	8.29	ns	-	-	ns
Trp	0.067	0.084	0.003	*	-	-	ns
LNAA	1.39	1.66	0.08	#	-	-	ns
Trp:LNAA	0.049	0.051	0.002	ns	-	-	ns

[1]Significance of effects of diet (D), sampling time (T), their interaction (D × T), and period (P) is indicated: #P <0.10, *P <0.05, **P <0.01, ***P <0.001, ns=non-significant.
[2]Pooled standard error of the least-square means.

Discussion

To assess satiating effects of RS, we studied general physical activity during 24 h, and feeding behaviour and meal size during an *ad libitum* meal in growing pigs. In addition, we studied the effect of feeding HF diets containing RS and PS on feeding behaviour and meal size 7 h postprandial, to test whether satiating effects of RS are dependent on fat intake. RS-fed pigs showed less feeder-directed and drinking behaviours than PS-fed pigs over 24 h, indicating a long-term satiating effect of RS, which corresponds with studies reporting reduced signs of hunger such as decreased feeding motivation (17, 133), reduced physical activity and preprandial restlessness, and enhanced satiety with dietary RS in restrictedly-fed pigs (189).

When the PS and RS diets were fed *ad libitum*, RS-fed pigs decreased duration of the first bout of eating and reduced feeder-directed behaviour (including eating), suggesting that RS enhanced also short-term satiety in pigs, likely reflecting an effect of the previous RS meal (133). These effects of RS were found with RS-fed pigs having a 3% lower ME intake than PS-fed pigs. During *ad libitum* meal, however, feed intake was similar for RS-fed and PS-fed pigs. Voluntary feed intake of a mixed diet (PS:RS=50:50) 7 h after digestion of a HF diet was numerically reduced in the HF-RS-fed compared with the HF-PS-fed pigs, although the ME supply from the HF-RS diet was expected to be lower than that of the HF-PS diet. Thus, satiating effects of RS diets successfully compensated for a reduced ME content of the diet, but were apparently not able to further reduce voluntary feed intake during an *ad libitum* meal. Possibly, the drive for lean growth in the growing pigs used in the present study partly overruled the satiety-enhancing effect of RS previously observed in adult pigs (133). Alternatively, the *ad libitum* meal test may be less sensitive after a prolonged period of restricted feeding (~9 h inter-meal interval), resulting in temporary over-feeding and large variation in voluntary feed intake. Remarkably, feed intake during *ad libitum* meals on d8 and d10 was lower for pigs receiving PS in period 1 followed by RS in period 2, than for pigs receiving RS-PS (sequence effect), which could be due to a decrease in the time needed for adaptation to the RS after feeding PS. Adaptation of the intestinal microbiota composition may occur more rapidly when pigs are changed from a low to a high fibre diet, which is accompanied with increased fermentation capacity (192). This increased fermentation likely contributed to the decreased voluntary feed intake in pigs receiving RS as last treatment.

5

Mechanisms for satiating effects of RS

To explore mechanisms by which RS may promote long-term satiety, we evaluated the effect of dietary RS on postprandial satiety-related hormones and metabolites. Mechanisms for the satiating effects of RS may be related to increased production of SCFAs (188, 190), which can prolong energy supply to the body (190). In the present study, peripheral SCFA levels were elevated throughout the day (both pre- and postprandial) in RS-fed pigs compared to PS-fed pigs, in accordance with previous studies (53, 193). Moreover, postprandial glucose and insulin responses were lower in RS-fed pigs than in PS-fed pigs, reflecting a decreased influx of glucose by enzymatic digestion of RS as compared with PS, in line with other studies (193, 194).

In rats, SCFAs from RS stimulate the release of satiety-related hormones, such as GLP-1 and PYY from entero-endocrine cells (138), which could be a biological mechanism by which RS promotes satiety. In the present study, however, postprandial GLP-1 levels were lower for RS-fed than for PS-fed pigs, and PYY levels were similar for both diets throughout the day. The effect found on GLP-1 could be attributed to the lower amount of glucose released from the RS diet as compared with the PS diet, as it has been shown in pigs that GLP-1 secretion is maintained by glucose until 4 h postprandial, and thereafter by SCFAs until up to 10 h postprandial (193). In our pigs it was only possible to relate GLP-1 secretion to the differences in glucose response, and not to the differences in SCFA levels. SCFAs and glucose can stimulate PYY secretion in rat intestine, but both to a smaller extent than fatty acids, which are considered the most potent stimulators of PYY secretion (195). In the present study, the intake of long-chain fatty acids was identical between diets, thus the similar postprandial PYY levels likely resulted from reduced glucose and increased SCFA concentrations in RS-fed pigs. It is unknown whether the PYY stimulating potential of SCFAs equals that of glucose in pigs, but studies in rats suggest that the PYY response may be less strong with normal luminal physiological SCFA concentrations than with supra-physiological intestinal infusions (195). The absence of a preprandial treatment difference in plasma PYY implies that the influence of SCFAs on plasma PYY is limited, as preprandial SCFA uptake likely exceeds that of glucose in RS-fed pigs (196). Alternatively, a negative feedback of GLP-1 on PYY secretion may exist, as also demonstrated in humans (197), and may have contributed to the PYY responses observed in our study.

Over the three sampling times, blood 5-HT levels were lower, whereas MAO activity and Trp levels were higher in RS-fed than in PS-fed pigs, indicating dietary effects on 5-HT metabolism. In the present study 5-HT was quantified in blood platelets, which possess a high-affinity uptake system and accumulate high concentrations of excess 5-HT produced by the intestine (198). Dietary manipulation

can influence intestinal 5-HT release (e.g. (199)), which in turn changes intestinal motility and transit (200), and thereby potentially affects satiety (25). Intestinal motility could be reduced in RS-fed pigs, possibly leading to a reduced passage rate of digesta in the colon, in line with a previous study demonstrating increased full weights of the caecum and colon in pigs fed native potato starch (201). It should be noted though, that the relationship between intestinal 5-HT release and motility is not always in the same direction (199). The role of locally produced 5-HT on colonic motility, transit time and satiety in relation to dietary RS remains to be elucidated.

Intestinal 5-HT release may also be related to the activity of the gastrointestinal immune system. Some of the 5-HT secreting cells (e.g. enterochromaffin and mucosal mast cells) and 5-HT itself are involved in pro-inflammatory immune responses in the gastrointestinal tract (202). The low blood 5-HT levels found in the RS-fed pigs could be associated with a downregulation of genes involved in both innate and adaptive immune responses found in the colon of RS-fed pigs in this study (185). Changes in microbiota composition likely also play a role in the downregulated immune response observed in RS-fed pigs (185).

The increased plasma Trp levels (5-HT precursor) and Trp:LNAA ratios in RS-fed pigs, combined with the reduced blood 5-HT levels found in RS-fed pigs may reflect a decreased uptake of Trp into peripheral tissues. Plasma Trp:LNAA ratio has been shown to be a major determinant of brain 5-HT concentration (203), which has been reported to be involved in the regulation of feeding behaviour (204). For instance, it has been demonstrated that food-seeking and food-taking behaviours are usually reduced in non-human primates with increased brain 5-HT turnover (205). Although it is unknown whether the higher Trp levels and Trp:LNAA ratios in the RS-fed pigs resulted in higher brain 5-HT levels, this would be consistent with the lower level of feeder-directed behaviours in these pigs.

NEFA levels measured in blood reflect mobilized fatty acids from adipose tissues, and were expected to be increased just before the morning meal, particularly in PS-fed pigs, likely coinciding with a drop in respiration quotient (RQ) (206) due to increased fatty acid oxidation. There were no differences, though, in NEFA levels between treatments, likely because in growing animals the majority of nutrients is used for muscle and adipose tissue growth, with minimal rates of lipolysis. Particularly in pigs, most body lipids originate from *de novo* fatty acid synthesis, and mainly glucose is used as substrate by adipose tissue (major site of fatty acid synthesis) for *de novo* lipogenesis (207).

Plasma TG levels were increased after feeding RS-diets, particularly between 90 and 300 min postprandial, corresponding with our previous observations in pigs fed similar diets (126). An explanation is that RS may have increased plasma levels of angiopoietin-related protein 4 (Angptl4), which is related to an upregulated

5

expression of Angptl4 in the distal small intestine of RS-fed pigs (126). Angptl4 inhibits lipoprotein lipase (LPL), which is responsible for the hydrolysis of TGs, thereby increasing plasma TG levels (208). The large difference in postprandial glucose and insulin responses between treatments occurred predominantly before 90 min postprandial. It is generally assumed that insulin stimulates TG uptake in peripheral tissues and inhibits TG production by the liver (209). Consequently this would have led to reduced plasma TG responses in PS fed pigs, particularly in the first 90 min postprandial. Such a response was not observed. Moreover, no inverse relationship between the area under the curve (AUC) was observed between plasma TGs and insulin until 300 min postprandial (r =0.04, *P* =0.88). In contrast, AUC for TGs and SCFAs (particularly acetate) were highly correlated (r =0.62, *P* <0.01), which suggests that increased plasma TG levels are mainly driven by increased SCFA levels. The expression of two genes responsible for fatty acid transport (fatty acid-binding protein 1, FABP1) and fatty acid synthesis (Acetyl-CoA carboxylase alpha, ACACA) were indeed found to be upregulated in the liver of RS-fed pigs (both *P* <0.05, 2.58 and 1.33 fold increase, respectively) ((185), unpublished results). Inhibition of hepatic fatty acid oxidation seems to increase food intake in rats, mice and humans, although a suppressive effect of an enhanced hepatic fatty acid oxidation on feeding has not been demonstrated (210). Further studies are required to investigate whether TG levels signal satiety.

In conclusion, although RS-fed pigs showed behavioural signs of increased satiety and reduced postprandial glucose and insulin responses as compared with PS-fed pigs, we did not find an increase in GLP-1 and PYY plasma levels. Dietary RS did, however, affect SCFA and TG plasma levels throughout the day, and 5-HT metabolism. The involvement of these in the satiating effects of RS merits further research.

Acknowledgements

Supplemental Material

Chemical analyses

Diets were analysed for dry matter (ISO 6469/NEN 3332), ash (ISO 5984/NEN 3329), Kjeldahl nitrogen (ISO 5983/NEN 3145), crude fat (ISO-DIS 6492), starch and sugars (NIKO637MEMO 93–302) as previously described (211), and for gross energy (GE) using an adiabatic bomb calorimetry (IKA-C700, Janke & Kunkel). Ti was analysed using a method based on Short et al. (212) and Myers et al. (213). Faeces were dried at 70°C and ground in a centrifugal mill to pass a 1.0-mm mesh screen (ZM100, Retsch B.V.) prior to analyses. Faeces and urine were analysed for GE and faeces for Ti as described above. All analyses were carried out in duplicate.

Blood plasma was analysed for glucose (Glucose PAP SL; ELITech Group), insulin (Porcine/Canine Insulin EIA kit; ALPCO Diagnostics), TGs (Triglycerides liquicolor kit; Instruchemie), NEFAs (NEFAc-kit, Wako; Instruchemie), active GLP-1 (GLP-1 ELISA kit; Millipore, Linco Research), active PYY (PYY EIA kit; Phoenix Pharmaceuticals), tryptophan (Trp) (^{1}H-NMR spectroscopy), large neutral amino acids (LNAA; sum of isoleucine, leucine, valine, phenylalanine, and tyrosine) (^{1}H-NMR spectroscopy) and SCFAs (^{1}H-NMR spectroscopy).

For NMR measurements, plasma samples were filtered using Nanosep® Centrifugal Devices with Omega™ Membrane (Pall Corporation) with a 10K molecular weight cut-off. To remove trace amounts of glycerine and sodium azide, all filters were washed 6 times (centrifuged at 14000 *g* for 5 min) with MQ water (500 µL), and centrifuged for 10 min after the 6th wash to make sure the filters were water free. Plasma samples were diluted 1:1 in a 75 mM phosphate buffer (pH 7.4). The diluted plasma (300 µL) was transferred to the filter and centrifuged at 14000 *g* for 60 min at 4°C. The extracted solution (200 µL) was transferred to a 3 mm NMR tube (Bruker match system), and samples were stored at -20°C until analysis. For ^{1}H-NMR spectroscopy, samples were slowly warmed up to room temperature and measured at 310K (calibrated temperature) in an Avance III NMRspectrometer operated at 600.13 MHz. Each sample was transferred into the magnet, and equilibrated at 310K for 5 min. Subsequently, automated locking, shimming and 90° pulse angle determination was performed. For each sample ^{1}H NMR NOESY datasets were acquired, and processed and aligned using the alanine signal (upfield resonance of the alanine doublet signal) at 1.49 ppm. From the aligned spectra, integrals for resonances of the metabolites of interest were selected and quantified. Concentrations of metabolites were calculated based on the number of hydrogen atoms for each metabolite selected.

The 5-HT concentration in platelet pellets was determined using a protocol adapted from Kluge *et al.* (214). Results were expressed in µmol/10[9] platelets (i.e.

platelet 5-HT) and subsequently over total blood platelets in whole blood in µmol/L (i.e. blood 5-HT) by multiplying platelet 5-HT by the number of platelets counted in whole blood using a Sysmex (10^9 platelets/L).

MAO activity in whole blood was determined using a protocol adapted from Van Kempen *et al.* (215), which represents MAO activity that is almost completely (>95%) found on blood platelets. Results were expressed as total amount of formed 4-hydroxyquinoline in whole blood in µmol/L/h.

5

Postprandial kinetics of the plasma proteome and metabolome in pigs consuming fibres with different physicochemical properties

Daniëlle Haenen, Sietse Jan Koopmans, Leo Kruijt, Mari Smits, Jacques Vervoort, Michael Müller and Guido J. E. J. Hooiveld

Abstract

Dietary fibres are extensively studied for their potential role in the management of food intake and body weight. One of the mechanisms via which fibres can help in the prevention of obesity is by enhancing satiety. Fibres with different physicochemical properties, e.g. bulkiness, viscosity and fermentability, affect satiety in different ways. The aim of this study was to determine the effect of fibres with different physicochemical properties on *ad libitum* food intake and on postprandial plasma protein and metabolite profiles in minipigs. Therefore, 5 minipigs were assigned to a control (C) diet or a diet containing lignocellulose (LC), pectin (PEC) or resistant starch (RS) for periods of 8 d in a 4 x 4 Latin square design. Fibre types were selected based on their different physicochemical properties; LC is a bulky fibre, RS is a fermentable fibre and PEC is both a viscous and a fermentable fibre. Portal and carotid blood samples were collected from catheters on day 8 of each treatment, both before and at several time points after the *ad libitum* morning meal. Plasma protein profiles were measured by surface enhanced laser desorption/ionization time-of-flight mass spectrometry (SELDI-TOF-MS) and used to determine differentially expressed proteins. The abundance of 973 peptides and proteins with different physicochemical properties could be determined. Plasma protein profiles were found to be most similar between the C and LC diet, and between the PEC and RS diet. With all diets, the most pronounced shift in the abundance of plasma proteins occurred between 240 and 480 min postprandially. Sparse multilevel partial least squares-discriminant analysis identified 44 and 65 proteins that were differentially expressed in portal and carotid plasma samples, respectively, depending on both fibre diet and postprandial time. Furthermore, NMR-based metabolomics was applied to identify a set of metabolites in portal plasma. A total of 24 metabolites was measured, including the short-chain fatty acids (SCFAs) acetate, propionate and butyrate. The concentrations of all SCFAs were significantly higher after RS consumption than after C, LC and PEC consumption. This study showed that the consumption of diets with fermentable fibres results in a different plasma protein and metabolite profile compared to a diet containing a non-fermentable fibre or a diet without fibre.

Introduction

Dietary fibres are an extensively studied food component, because of their potential role in the management of food intake and body weight. Several studies have shown that consumption of dietary fibre increases insulin sensitivity (8, 9) and that it can help with the reduction of body weight in overweight and obese subjects (10, 11). Part of these observations can be attributed to effects on appetite control, since dietary fibre consumption is suggested to enhance satiety (12-14).

Knowledge on the underlying mechanisms responsible for an increase in satiety following consumption of a diet high in dietary fibre is limited. A major factor complicating the elucidation of these mechanisms is the large variety in fibre types, all having different physicochemical properties. These properties, including bulkiness, viscosity, and fermentability, should be taken into account, because they are expected to influence digestive physiology and feelings of satiety in different ways (17).

Bulky fibres have a high water-binding capacity, resulting in increased gastric distension thereby enhancing feelings of satiety (216). Viscous fibres can form a gel in the stomach and the nutrients trapped within this viscous matrix will more slowly exit the stomach and therefore delay gastric emptying (217). In addition, in the small intestine the presence of viscous fibres and unabsorbed macronutrients delays gastric emptying and prolongs transit time, a mechanism known as the 'ileal brake', which enhances digestion and absorption of food (218). The ileal brake increases the time that the chyme stays in contact with intestinal absorption surfaces, resulting in increased secretion of satiety-related hormones such as glucagon-like peptide 1 (GLP-1) and peptide tyrosine-tyrosine (PYY). The secretion of these hormones can ultimately contribute to the enhancement of feelings of satiety (217). Fermentable fibres are highly fermentable by bacteria in the large intestine, resulting in the production of short-chain fatty acids (SCFAs), which may also increase satiety (25). SCFAs may induce satiety mainly via 2 mechanisms. SCFAs can stabilise levels of glucose and insulin in blood (125), and SCFAs are suggested to stimulate the production and release of GLP-1 and PYY by enteroendocrine L-cells present in the colon, possibly via G-protein coupled receptors (56-58).

Plasma proteomics is a technique for measuring the entire set of proteins, referred to as the proteome, expressed in plasma. Plasma proteomics has been successfully applied in both human and animal studies for the identification of new biomarkers of disease and nutritional status (74, 219, 220). Along the same line, all metabolites present in a biological sample can be determined using an approach called metabolomics. Because metabolomics can be used to determine alterations in metabolism under different conditions, the use of this technique in nutrition

6

research is increasing. For instance, metabolomics has been applied in intervention studies to assess novel biomarkers of dietary intake (75).

The objective of the present study was to identify proteins in plasma that were differentially expressed in minipigs fed different fibre diets using a plasma proteomics approach. Minipigs, in this experiment used as a model for humans, were assigned to a control (C) diet or a diet containing pectin (PEC), lignocellulose (LC) or resistant starch (RS) for periods of 8 d in a 4 x 4 Latin square design. Fibre types were selected based on their different physicochemical properties. From all pigs, portal and carotid blood samples were taken from catheters on d 8 of each treatment, both before and at several time points after the *ad libitum* morning meal. To determine the plasma proteome, plasma samples were analysed using surface-enhanced laser desorption/ionization time-of-flight mass spectrometry (SELDI-TOF-MS). In addition, ^{1}H-NMR spectroscopy-based metabolomics was applied to increase our understanding of how different fibres can modulate the plasma profile of small metabolites. Data sets were subjected to multivariate data analysis to identify proteins and metabolites that were differentially regulated after feeding the fibre diets.

Materials and methods

Experimental design, pigs and housing

Five (4 + 1) 2-year-old female Göttingen minipigs (Ellegaard, Denmark) with an initial body weight of 44 ± 1.5 kg were fitted with catheters and assigned to 4 dietary treatments in a 4 x 4 Latin square design. An extra pig was included in the study as back-up in case of complications due to surgery or blood sampling, and this pig (p5) was randomly assigned to one of the treatment orders (p2) (**Table 1**). Each treatment lasted for 8 d, and differed with respect to the type of starch in the diet: highly methylated citrus pectin (PEC), lignocellulose (LC), resistant starch from native potato starch (RS) or a high-starch control (C). Pigs were individually housed in metabolism pens of 2 m^2 equipped with a feeder. Artificial lights were on from 6:00 h until 22:00 h and dimmed during the dark period. The performed research was in compliance with the ARRIVE guidelines on animal research (221). Experimental protocols describing the management, surgical procedures, and animal care were reviewed and approved by the Animal Care and Use Committee of Wageningen University and Research Centre (Lelystad, the Netherlands).

Table 1 Overview Latin square design experimental diets.

		Pig				
		1	2	3	4	5
Period 1	d 1-4	C	C + PEC	C + LC	C + RS	C + PEC
	d 5-8	C	PEC	LC	RS	PEC
Period 2	d 1-4	C + PEC	PEC + RS	LC + C	RS + LC	PEC + RS
	d 5-8	PEC	RS	C	LC	RS
Period 3	d 1-4	PEC + LC	RS + C	C + RS	LC + PEC	RS + C
	d 5-8	LC	C	RS	PEC	C
Period 4	d 1-4	LC + RS	C + LC	RS + PEC	PEC + C	C + LC
	d 5-8	RS	LC	PEC	C	LC

C, control; LC, lignocellulose; PEC, pectin; RS, resistant starch

Diets and feeding

The 4 experimental diets used were identical except for type of starch. Fibres were selected based on different physicochemical properties that were expected to have distinct effects in the gastrointestinal tract: LC is a bulky fibre, RS is a fermentable fibre and PEC is both a viscous and a fermentable fibre. The different fibres were exchanged for pregelatinized potato starch from the control (C) diet based on GE content (**Table 2**). Diets were produced as a single batch of a basal diet to which starch sources were added.

Diets were fed twice a day at 7:00 h and 15:00 h as a mash by mixing the diets with water in the feeders immediately before feeding (ratio water:feed = 1.5:1). The first 4 d of each treatment period, pigs received a 1:1 mix of the diet consumed in the previous period and the experimental diet of the new period to allow habituation to the new diet (**Table 1**). On the last 4 d of each period, pigs consumed only one of the experimental diets. From d 1 to d 7 of each period, pigs were fed a restricted amount of feed. The feeding level was gradually increased during each period. On d 8 of the treatment period, both the morning and afternoon meal were provided *ad libitum*. During the 1-wk adaptation period before surgery, pigs were fed the control diet and adapted to the feeding pattern and individual housing.

6

Table 2 Ingredient composition of the experimental diets.

Ingredient, g/kg[1]	Diet			
	control	lignocellulose	pectin	resistant starch
Pregelatinized potato starch[2]	350	250	200	-
Lignocellulose[3]	-	100	-	-
Pectin[4]	-	-	149	-
Native potato starch[5]	-	-	-	394
Potato protein	50	50	50	50
Maize gluten meal	100	100	100	100
Wheat	249	249	249	249

Barley	150	150	150	150
Soy oil	15	15	15	15
Animal fat	15	15	15	15
Vitamin and mineral premix[6]	10	10	10	10
$CaCO_3$	17	17	17	17
$Ca(H_2PO_4)_2$	11	11	11	11
NaCl	5	5	5	5
L-lysine HCl	1.5	1.5	1.5	1.5
$NaHCO_3$	15	15	15	15
KCl	10	10	10	10
Flavour[7]	1.5	1.5	1.5	1.5
Total	1000	1000	999	1044

[1]Ingredients are expressed in g/kg of the Control diet and sum up to 1000 for all diets in which the gross energy (GE) content of the fibre sources is identical to that of the pregelatinized potato starch.

[2]Paselli™ WA 4 (AVEBE FOOD).

[3]ARBOCEL® RC Fine (J. RETTENMAIER & SÖHNE).

[4]UNIPECTINE™ RS 150 CITRUS (CARGILL).

[5]Native potato starch (AVEBE FOOD).

[6]Provided the following per kg of feed: vitamin A: 7500 IU; vitamin D_3: 1500 IU; vitamin E: 60 mg; vitamin K_3: 1.0 mg; vitamin B_1: 1.0 mg; vitamin B_2: 4.0 mg; vitamin B_6: 1.0 mg; vitamin B_{12}: 20 µg; niacin: 20 mg; calcium-D pantothenate: 10.5 mg; choline chloride: 100 mg; folic acid: 0.4 mg; Fe: 120 mg ($FeSO_4.H_2O$); Cu: 15 mg ($CuSO_4.5H_2O$); Mn: 60 mg (MnO); Zn: 75 mg ($ZnSO_4.H_2O$); I: 4.0 mg (KI); Se: 0.30 mg (Na_2SeO_3); anti-oxidant: 75 mg.

[7]Luctarom Advance Cherry Honey, Lucta S.A., Barcelona, Spain.

Surgery

Pigs underwent surgery for the placement of catheters in the external jugular vein, the carotid artery and the portal vein. The catheters in the carotid artery and the portal vein were used for blood sampling and the catheter in the jugular vein was placed as a back-up in case of a malfunctioning arterial catheter.

After an overnight fast, all pigs were sedated with intramuscular Ketamine 10 mg/kg (Ketamine, Alfasan) and Midazolam 0.75 mg/kg (Dormicum, Roche) and anaesthesia was intravenously induced with the anodyne Sufentanil 1 µg/kg (Sufenta, Janssen-Cilag). Pigs were intubated and anaesthesia was maintained by inhalation of 2% Sevoflurane (Abbott) combined with 40% oxygen and nitrous oxide. A Sufentanil infusion was maintained at 1 µg/kg/hour. All pigs were equipped with 3 permanent polyethylene blood vessel catheters (Tygon, Norton) as described previously (166). The catheters for blood sampling were placed in the external jugular vein, in the carotid artery and in the portal vein, fixed firmly at the site of insertion, tunnelled subcutaneously to the back of the pig and exteriorized between the shoulder blades. The catheters were filled and sealed off with saline containing heparin and penicillin (Procpen) and kept in a backpack which was glued to the skin.

The first 4 d after surgery, pigs were fed a restricted amount of the control diet, i.e. 50, 100, 200 and 300 g per meal on d 1, 2, 3 and 4 respectively, to allow a gradual recovery. After that, 300 g per meal was continued into the onset of the experimental diets. Pigs were habituated to blood sampling in the first week after surgery. After 5 to 7 days of postsurgical recovery, experimental period 1 started. On the first 4 d of this period, all pigs received a 1:1 mix of the control diet and the experimental diet (**Table 1**).

Blood sampling
Blood was drawn from the carotid artery and the portal vein on d 8 of each dietary treatment before (at -30 and 0 min) and after (at 30, 60, 120, 180, 240 and 480 min) the morning meal. Blood was collected in 6 mL Vacutainer EDTA tubes (Becton Dickinson) supplemented with protease (Complete, EDTA-free; Roche) and dipeptidyl peptidase-4 (Millipore) inhibitors and then placed in ice water. Tubes were centrifuged for 10 min at 1300 *g* at 4°C immediately after blood collection. Plasma was aliquoted and stored at -80 °C until further analysis.

Due to experimental errors or the malfunctioning of some of the catheters during the course of the study, not all blood samples could be collected.

SELDI-TOF-MS analysis
SELDI-TOF-MS analysis was performed on both carotid and portal plasma samples derived from 5 pigs on 4 different dietary treatments (C, LC, PEC and RS), collected at 2 time points before and at 6 time points after feeding. First, samples were enriched for medium- and low abundance proteins with Proteominer beads according to the manufacturer's instructions (Bio-Rad Laboratories Inc.). In short, filter plates (AcroPrep, PALL) were loaded with Proteominer beads, after which 200 µL of each plasma sample was transferred to the wells of the filter plate and incubated for 2 hr (4 °C, on a platform shaker). Subsequently, the unbound proteins were removed by performing 3 washing steps and discarded. The retained proteins were fractionated by incubating the filter plate with different elution reagents. Elution reagent 1 (1 M NaCl 20 mM HEPES pH 7.5), elution reagent 2 (200 mM glycine pH 2.4), elution reagent 3 (60% ethylene glycol) and elution reagent 4 (33% isopropylalcohol, 16.7% acetonitril, 0.1% trifluoracetic acid) were loaded to the wells of the plate, resulting in 4 different eluates.

The 4 fractions of each sample were then separately applied to protein chip arrays. These arrays are composed of different chromatographic surfaces that are designed to retain, not elute, proteins of interest. Each chemically surface is designed to retain proteins according to a general or specific physicochemical property of the proteins. The weak cation exchanger (CM10), reverse phase (H50)

6

and immobilized metal affinity capture (IMAC30) ProteinChip arrays and binding buffer combinations were prepared according to the manufacturer's instructions (Bio-Rad). The different ProteinChip arrays were equilibrated with the respective binding buffers. Samples were analysed on 2 different CM10 arrays, one for which a low-stringency binding/washing buffer (0.1 M sodium acetate, pH 4.0) was used, whereas the other array was treated with a high-stringency binding/washing buffer (50 mM HEPES, pH 7.0). Before applying the samples, the active spots of the H50 array were preactivated with 75 µL 50% methanol, and the active spots of the IMAC30 array were preactivated with 100 µL of 0.1 M copper sulfate solution according to the manufacturer's instructions (Bio-Rad). Samples (10 µL of the eluate combined with 90 µL binding buffer) were loaded to each well of the array and were allowed to bind (60 min, room temperature, on a platform shaker) to the array. After the binding step, the entire array was washed 3 times with the respective binding buffers (5 min, with agitation) and then twice with deionized water. After briefly drying the arrays, 1 µL of a saturated solution of sinapinic acid (Sigma) dissolved in 50% (vol/vol) acetonitrile and 0.5% (vol/vol) trifluoracetic acid was applied twice to each of the active spots of the array, and was allowed to thoroughly dry.

Subsequently, the different ProteinChip arrays were placed in the SELDI ProteinChip Biology System Reader 4,000 (Bio-Rad) and scanned with a laser energy of 3500 nJ. The SELDI ProteinChip spectra were analysed by using the ProteinChip Data Manager Client 3.5 software (Bio-Rad). The instrument was calibrated by using the All-in-One ProteinStandard II (Bio-Rad). Spectrum alignment was performed on the calibrated spectra to reduce mass variations of peaks within a group of similar spectra. Subsequently, baseline subtraction was conducted. Baseline subtraction offsets in the spectra set the result of electrical noise and the noise from energy absorbing molecules (222). Spectra were normalised to standardise the intensities of the spectra. The normalization process involved taking the total ion current used for all the spots, averaging the intensity (µA), and adjusting the intensity scales for all the spots so that all spectra could be displayed on the same scale (222). The peaks ranging from 1,500 to 200,000 mass-to-charge-ratio (*m/z*) were detected and extracted by the ProteinChip 3.5 software. The spectral region from 0 to 1,500 *m/z* was unreliable for normalization and peak detection due to matrix interference and was therefore excluded from the analyses. The spectral region above 200,000 *m/z* was also not included in the analyses because the intensity of the laser was too small for this region.

The first step for the initial peak detection was the creation of clusters by the ProteinChip 3.5 software. Within a designated mass-to-charge ratio, the program grouped peaks that were present across multiple spectra at the same

narrow window of 0.3% *m/z* value. Each cluster was then treated as a single protein. Mass spectral data were exported as a profile matrix and used to evaluate the effect of diet and time of sampling on the protein profile.

¹H-NMR spectroscopy

All portal plasma samples were diluted 1:1 in a 75 mM phosphate buffer (pH 7.4) and filtered by using Nanosep centrifugal devices with Omega Membrane (Pall Corporation). The molecular weight cut-off of the filter was 10K. In order to remove trace amounts of glycerin and sodium azide, all filters were pre-treated with 500 µL of MQ water, followed by centrifugation at 14.000 *g* for 5 min. This step was repeated 5 times, with a 10 min centrifugation step after the 6th wash, to ensure the filters were free of water. Then 300 µL of the diluted plasma was transferred to the filter, and centrifuged for 55 min at 14.000 *g* at 4 °C. Subsequently, 170 µL of the eluate was transferred to a 3 mm NMR tube (Bruker match system). Samples were stored at -20 °C until analysis by using NMR spectroscopy.

Before NMR measurements, samples were slowly warmed up to room temperature and measured at 310 K (calibrated temperature) in an Avance III NMR spectrometer operated at 600.13 MHz. After transfer of each sample into the magnet, the sample was equilibrated at 310 K for 5 min. Subsequently automated locking, automated shimming and automated 90 degree pulse angle determination was performed. ¹H NMR NOESY datasets were acquired for each sample. In addition, each dataset was automatically processed and aligned using the alanine signal (upfield resonance of the alanine doublet signal) at 1.49 ppm. From the aligned spectra, integrals for resonances of the metabolites of interest were selected and quantified. Concentrations of metabolites were calculated based on the number of hydrogen atoms of each metabolite selected.

Multivariate data analysis

Multivariate analysis and visualization of the SELDI-TOF-MS and ¹H-NMR data sets were performed in R using the library mixOmics (151). Samples derived from portal and carotid blood were analysed separately. Due to problems with the catheter, only one carotid blood sample could be obtained from one pig (p2), and this pig was therefore excluded from the analysis of the carotid blood samples. The sparse form of multilevel partial least squares-discriminant analysis (PLS-DA) was used to select proteins that were differentially expressed between diets and time points (149). Due to the relatively small size of the dataset, the portal metabolomics dataset was analysed using (regular) multilevel PLS-DA. For both forms of multilevel PLS-DA the number of discriminant vectors (dimensions) *H* was set at 3, equalling number of treatments minus 1, as recommended (223). The number of proteins to select

for sparse multilevel PLS-DA was determined by applying tuning criterion 2, i.e. maximized correlation between the 2 factors (fibre and postprandial time) on each dimension (149).

Statistical methods

Food intake was analysed using One-Way ANOVA in IBM SPSS Statistics 19. SCFA concentrations determined in portal plasma were analysed using a linear mixed model in IBM SPSS Statistics 19. The model included diet, time and interaction of diet and time as fixed effects, and pig as random effect. Differences were considered significant if P <0.05.

Results

Food intake

On d 8 of each treatment period, meals were provided *ad libitum*. In the morning, pigs fed the RS diet had a significantly higher food intake than pigs consuming the C (P = 0.031) or the PEC diet (P = 0.006) (**Fig. 1**). When adding up food intake in the morning with food intake in the afternoon, RS-fed pigs consumed significantly more than PEC-fed pigs (P = 0.012) (Fig. 1).
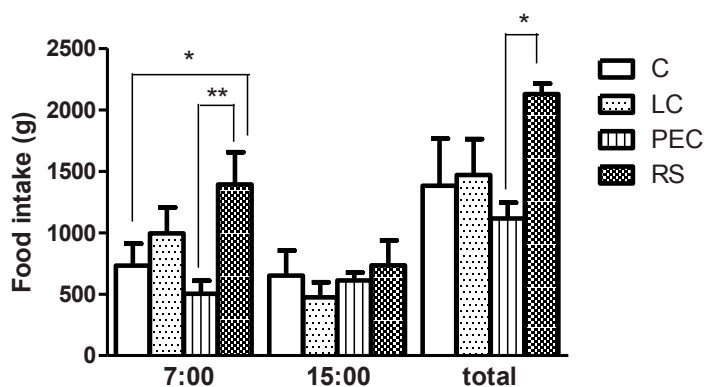
Figure 1 Food intake on d 8 of each treatment period during the morning meal (7:00), the afternoon meal (15:00) and during both meals. Values are means ± SEM, n = 5 pigs per diet. * and ** indicate that 2 diets differ from each other with P <0.05 and P <0.01, respectively. C, control diet; LC, lignocellulose diet; PEC, pectin diet; RS, resistant starch diet.

Proteomics analysis

A total of 973 proteins could be determined in both portal and carotid plasma samples using SELDI-TOF-MS analysis, with 232, 245, 265 and 231 proteins being measured on the CM10 high stringent, CM10 low stringent, H50 and the IMAC30 array respectively. We were mainly interested to identify the proteins whose postprandial expression was different between both time point and the fibre type consumed. To this end the sparse multilevel PLS-DA was used.

Protein profile portal blood

The expression of the 973 proteins in 116 portal plasma samples derived from all 5 pigs was used as input for sparse multilevel PLS-DA. The analysis revealed that 44 proteins (27 in dimension 1, 14 in dimension 2 and 3 in dimension 3) explained most of the variation in the 2 factor dataset (fibre and postprandial time). The sparse multilevel PLS-DA plot showed that, based on the expression levels of these 44 proteins, some diets and time points cluster together (**Fig. 2A**). Samples taken after consumption of the C or the LC diet are mainly located on the right side of the plot, with samples taken before (-30 and 0 min) and 30 and 60 min after feeding in the upper part of the plot and samples collected after 120, 180 and 240 min present in the lower part of the figure. Samples corresponding to PEC and RS consumption cluster together in the middle of the plot, with samples collected 180 and 240 min post-feeding located below the samples taken at earlier time points. For all diets, samples obtained 480 min after feeding were mainly located on the upper left side of the figure. This observed clustering pattern was confirmed with a clustered heatmap of the 44 proteins, showing that the C diet clustered with the LC diet whereas the PEC diet clustered with the RS diet (**Fig. 2B**). Furthermore, the earlier time points (-30, 0, 30, 60 and 120 min) clustered together, and the late time points, most clearly 480 min, also clustered together. The intensity of the colour of the proteins measured at later time points indicates that the most extreme (either highest or lowest) peak intensities occurred more than 180 min after feeding. The expression pattern of representative proteins from the 3 main protein clusters in the heatmap are visualised in **Fig. 2C**. The expression of C217172_H50 from protein cluster 1 increased over time, especially with the PEC diet. On the other hand, the intensity of C34169_6_CM10low from protein cluster 2 decreased over time and the expression of this protein appeared to be unaffected by diet. C36297_5_H50, representing cluster 3, did show a highly diet-dependent expression pattern.

Overall, these data indicate that the protein expression pattern in response to dietary fibre is similar between the C and LC diet, and between the PEC and RS diet. The major shift in the proteome starts 120 min after feeding, with the most pronounced shift between 240 and 480 min postprandially.
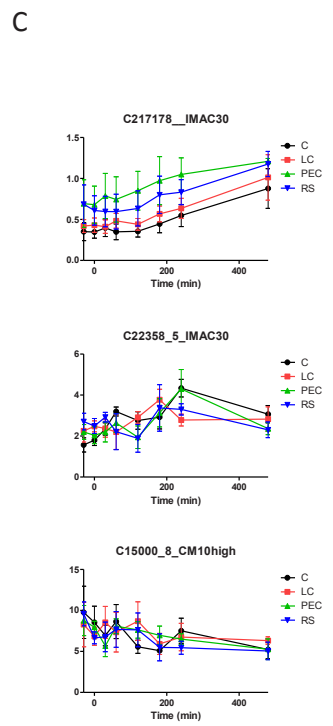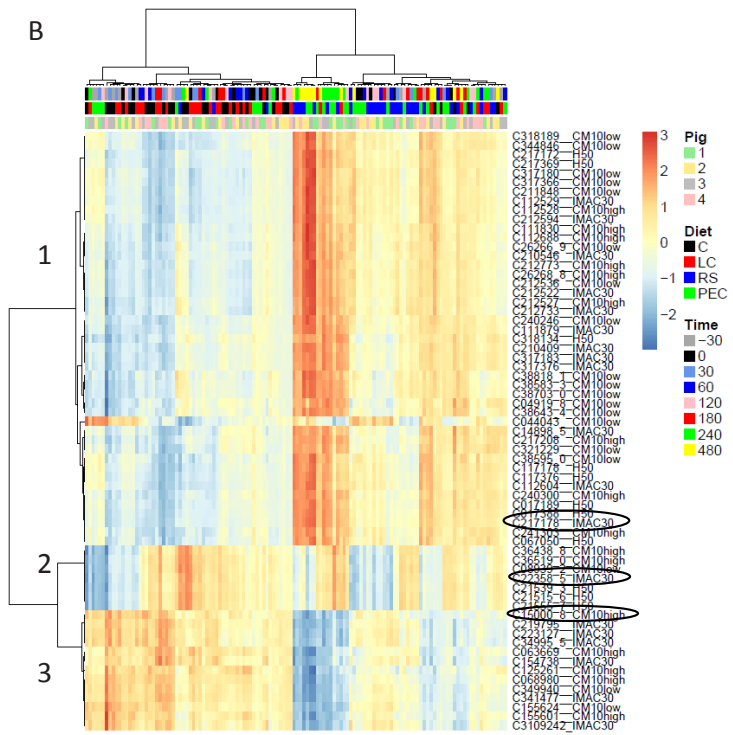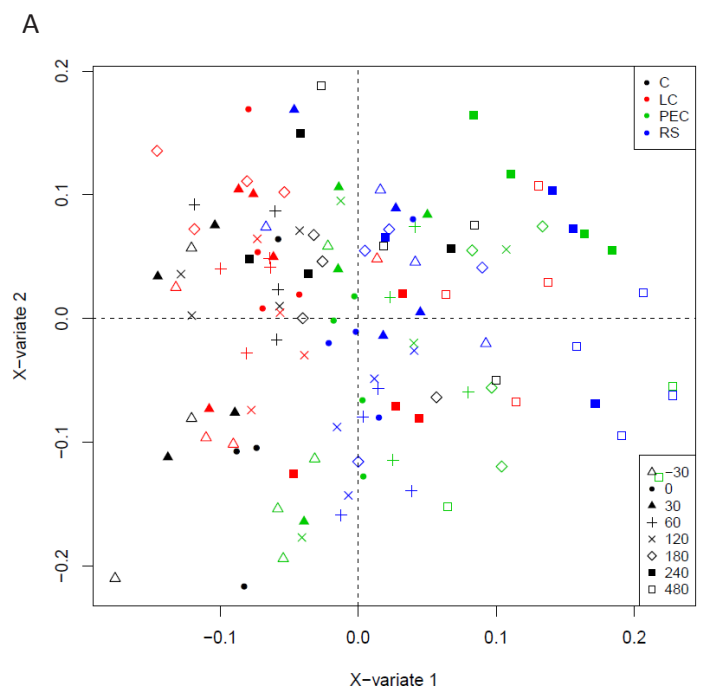
6
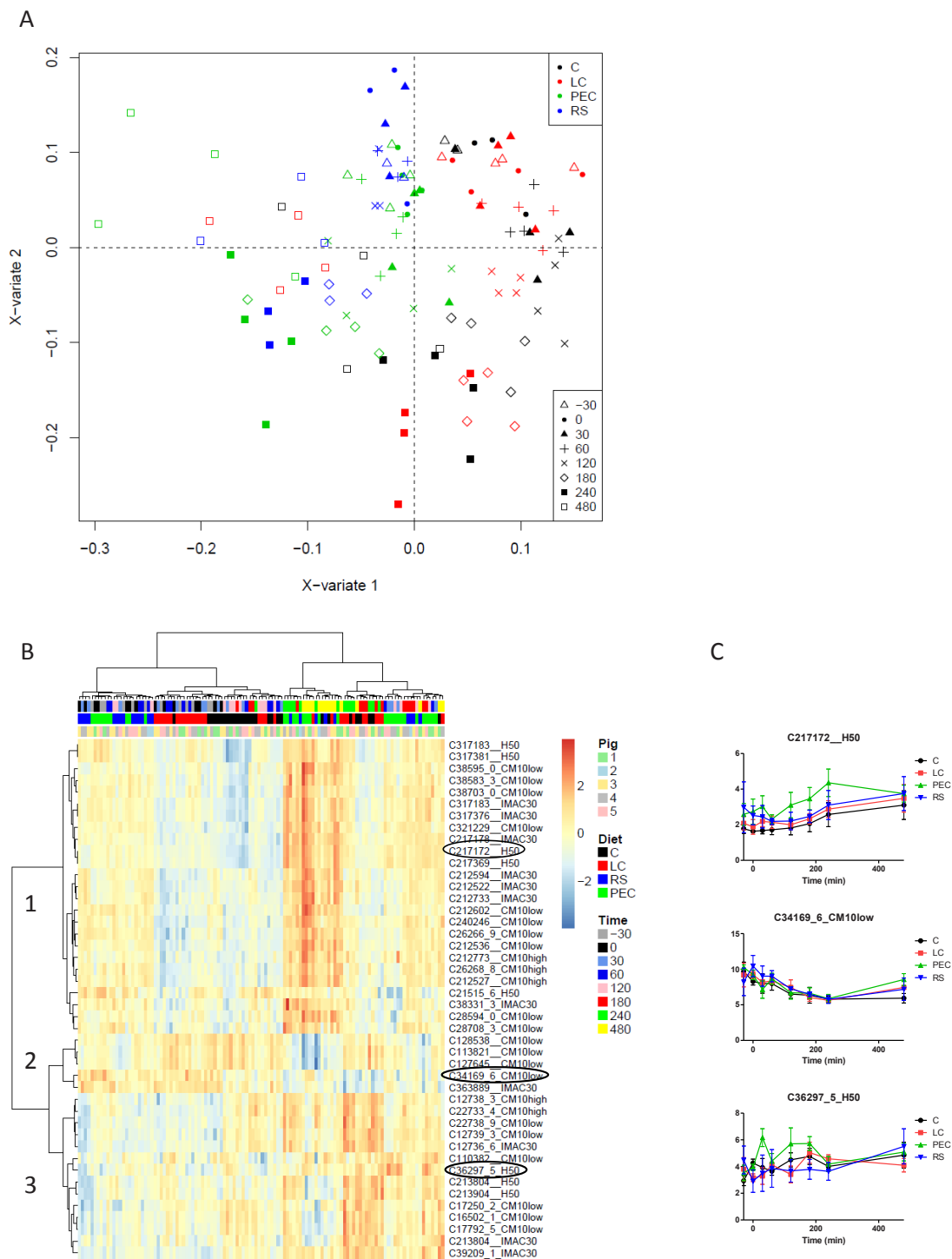
Figure 2 Sparse multilevel PLS-DA analysis of portal plasma samples visualised in a scatter plot (**A**) and a clustered heatmap (**B**) and the expression pattern of three representative proteins (**C**). **A.** Sparse multilevel PLS-DA sample representation for dimensions 1-3 of all 116 portal plasma samples, with symbols indicating different time points and colours indicating different diets. X and Y axis represent the subspace to project the samples. **B.** Unsupervised clustering analysis with Euclidian distance and Ward method of the 44 proteins selected by sparse multilevel PLS-DA. Samples are represented in columns and proteins in rows. Protein identifiers indicate fraction (C0 to C3 for fraction 1 to 4), followed by mass-to-charge-ratio and array type. For visualization purposes the data were row normalized. Samples with an intensity above average are marked red and samples with an intensity below average are marked blue (colour gradient). The 3 main protein clusters were arbitrarily labelled 1, 2 and 3. **C.** Typical expression pattern of 3 proteins from the 3 different clusters on the heatmap (B; circled) before feeding (-30 and 0 min) and after feeding (30 to 480 min) pigs an *ad libitum* meal of the control (C), lignocellulose (LC), pectin (PEC) or resistant starch (RS) diet in the morning of d 8. C, control diet; LC, lignocellulose diet; PEC, pectin diet; RS, resistant starch diet.

Protein profile carotid blood

The same analysis was performed on plasma derived from the carotid artery. The expression of all proteins in 126 carotid plasma samples, derived from 4 pigs, was used as input for sparse multilevel PLS-DA analysis. A total of 65 proteins was found to be most discriminating between the diets and time points (57 in dimension 1 and 8 in dimension 2). The resulting sparse multilevel PLS-DA plot showed that the C and LC samples are in general located on the left side of the plot, whereas the PEC and RS samples are located on the right side of the figure (**Fig. 3A**). However, the clustering according to diet was less pronounced than the clustering observed with portal plasma. Samples taken 240 and 480 min after feeding were mainly located on the right side of the plot, indicating that the major shift in the proteome occurred at these time points. A clustered heatmap of the 65 proteins revealed that samples mainly clustered according to diet, and to a smaller extent according to time point (**Fig. 3B**). The highest and lowest peak intensities were observed in plasma collected 480 min postprandial. The intensity of C217178_IMAC30, a typical protein from protein cluster 1 on the clustered heatmap, increased over time with the highest expression 480 min after feeding (**Fig. 3C**). The expression patterns were similar in all diets, although the basal levels before feeding were different. C22358_5_IMAC30, representing cluster 2, showed a diet-dependent expression pattern, with the highest expression observed either 180 or 240 min postprandially. The intensities of the proteins from cluster 3, as visualised for C15000_8_CM10high, slightly decreased over time.

Figure 3 Sparse multilevel PLS-DA analysis of carotid plasma samples visualised in a scatter plot (**A**) and a clustered heatmap (**B**) and the expression pattern of three representative proteins (**C**). **A.** Sparse multilevel PLS-DA sample representation for dimensions 1-2 of all 126 carotid plasma samples, with symbols indicating different time points and colours indicating different diets. X and Y axis represent the subspace to project the samples. **B.** Unsupervised clustering analysis with Euclidian distance and Ward method of the 65 proteins selected by sparse multilevel PLS-DA. Samples are represented in columns and proteins in rows. Protein identifiers indicate fraction (C0 to C3 for fraction 1 to 4), followed by mass-to-charge-ratio and array type. For visualization purposes the data were row normalized. Samples with an intensity above average are marked red and samples with an intensity below average are marked blue (colour gradient). The 3 main protein clusters were arbitrarily labelled 1, 2 and 3. **C.** Typical expression pattern of 3 proteins from the 3 different clusters on the heatmap (B; circled) before feeding (-30 and 0 min) and after feeding (30 to 480 min) pigs an *ad libitum* meal of the control (C), lignocellulose (LC), pectin (PEC) or resistant starch (RS) diet in the morning of d 8. C, control diet; LC, lignocellulose diet; PEC, pectin diet; RS, resistant starch diet.

Comparison portal and carotid blood

Subsequently we were interested to know the degree of overlap between the differentially expressed proteins observed in portal blood and in carotid blood. Out of the 44 proteins identified in portal blood by multilevel PLS-DA, only 19 proteins were also found to be differentially regulated in carotid blood, suggesting hepatic clearance of these proteins (**Fig. 4**). Similarly, the liver and extra-hepatic tissues may also play a role in regulating the abundance of the 46 proteins that were only differentially regulated in carotid plasma.
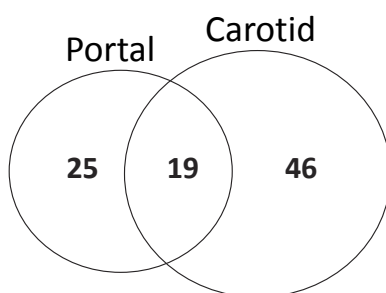
Figure 4 Venn diagram showing the overlap of proteins identified by sparse multilevel PLS-DA in portal and carotid plasma.

Metabolites portal blood

In addition to the proteome analysis, NMR-based metabolomics was performed on portal plasma samples. In total, 24 metabolites were measured in these samples. The identity of 21 metabolites was determined, whereas 3 metabolites could not be identified solely by their ^{1}H-NMR peak pattern. The clustered heatmap resulting from multilevel PLS-DA analysis showed the clustering pattern of the metabolites (**Fig. 5**). The branched-chain amino acids (valine, leucine and isoleucine), the SCFAs (acetate, propionate, butyrate and butyrate-derivative) and the 3 unknown metabolites (unknown 1, 2 and 3) formed separate clusters. Furthermore, a slight clustering according to diet was observed, whereas time appeared to have no impact on the clustering pattern. The highest concentrations were found for the branched-chain amino acids and unknown metabolites 1, 2 and 3 after consumption of the LC diet.

Because the SCFAs resulted from the fermentation of fibres, we had a closer look at the postprandial pattern of these metabolites (**Fig. 6**). The concentrations of acetate, propionate and butyrate were significantly higher with the RS diet than the concentrations after C, LC and PEC consumption. The highest concentrations with RS were observed 480 min post-feeding. In addition, acetate concentrations were significantly higher with PEC consumption compared to C and LC consumption (*P* values 0.016 and 0.012 respectively).
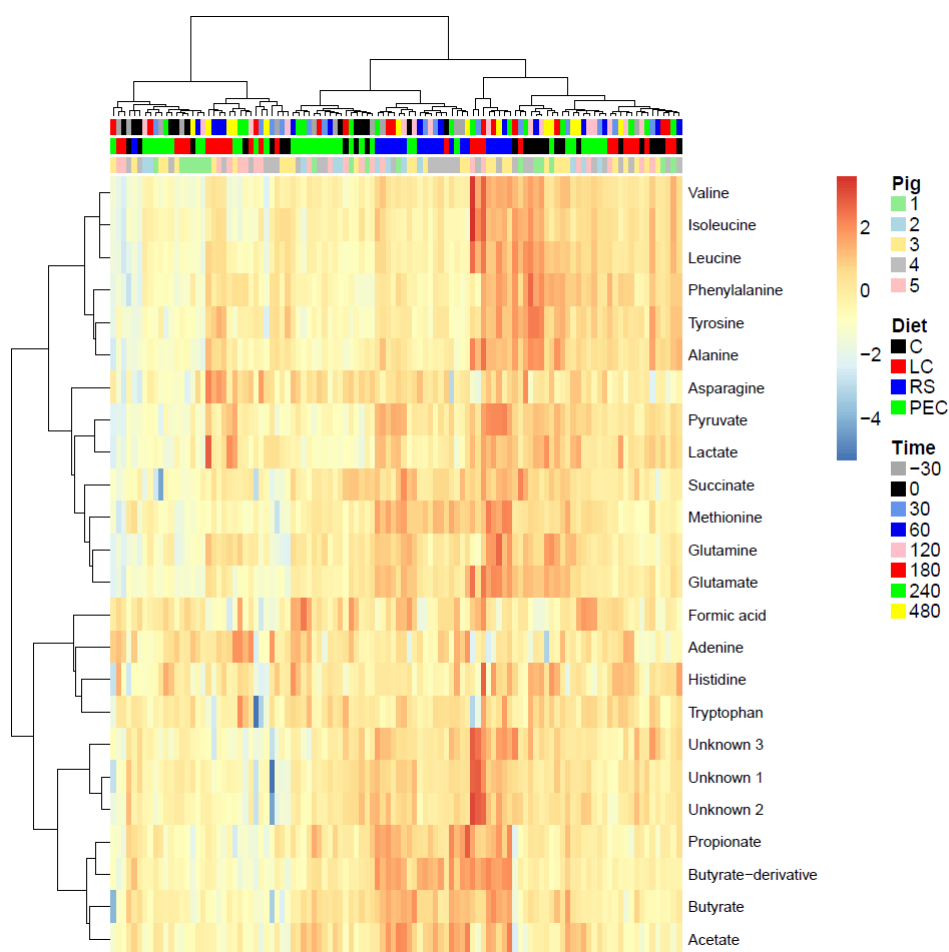
Figure 5 Unsupervised clustering analysis with Euclidian distance and Ward method of the 24 metabolites determined in 108 samples by ^{1}H-NMR based metabolomics as analysed by multilevel PLS-DA. Samples are represented in columns and metabolites in rows. For visualization purposes the data was row normalized. Samples with concentrations above average are marked red and samples with concentrations below average are marked blue (colour gradient).
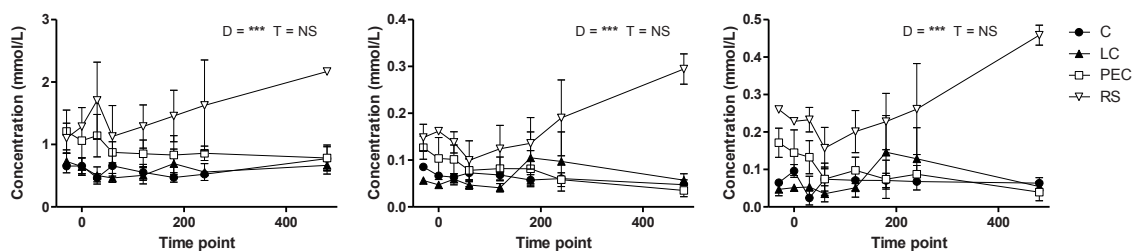
Figure 6 Plasma concentrations of acetate (**A**), propionate (**B**) and butyrate (**C**) in portal blood collected before feeding (-30 and 0 min) and after feeding (30 to 480 min) pigs an *ad libitum* meal of the control (C), lignocellulose (LC), pectin (PEC) or resistant starch (RS) diet in the morning of d 8. Statistical significance of effects of diet (D) and sampling time (T) is shown with *** indicating *P* <0.001 and NS indicating non-significant effects. C, control diet; LC, lignocellulose diet; PEC, pectin diet; RS, resistant starch diet.

Discussion

In this study we have shown that protein expression profiles of portal and carotid plasma depend on the fibre diet consumed, with a clear distinction between samples collected after PEC and RS consumption and samples taken after C and LC consumption. With all diets, a pronounced shift in the proteome was observed between 240 and 480 min post-feeding.

Changes in protein expression were observed at a later time point in carotid than in portal plasma samples (around 240 and 180 min after feeding respectively). This observation may partially be explained by hepatic clearance and conversion of both nutrients and plasma proteins in portal plasma until reaching a threshold, resulting in a delayed response in carotid plasma. The proteins exclusively present in carotid plasma may be produced by the liver or secreted by extra-hepatic tissues.

We observed that protein profiles were highly similar between PEC and RS consumption. PEC, besides being a viscous fibre, is fermentable by bacteria in the large intestine, although to a slightly smaller extent than RS (224). The fermentability of the PEC and RS diet is supported by the SCFA concentrations measured in portal blood, showing that RS consumption significantly increased concentrations of all SCFAs compared to the 3 other diets, and acetate levels were significantly higher after PEC consumption compared to the C and LC diet. However, more similar SCFA concentrations were expected in the PEC and the RS diet (224), which might be due to the significantly higher food intake of RS-fed pigs compared to pigs consuming the PEC diet. Despite the different SCFA concentrations in PEC-fed pigs compared

to RS-fed pigs, the plasma protein profile was highly similar between these diets, indicating that the protein profile might be SCFA-independent.

The reason for studying 3 different fibre types is because these fibres each have their own physicochemical properties, which might result in differences in degree and mechanism of satiety regulation. Interestingly, the 4 different diets tested in our study have previously been used in an experiment on feeding motivation in another group of pigs (17), showing that PEC was the least satiating fibre and LC and RS were the most satiating fibres. It could be speculated that the similarities between LC and RS regarding effects on satiety are reflected at the plasma proteome level. However, the protein profiles were very different after LC consumption than after RS feeding. If a substantial part of the proteome describes what happens with satiety regulation, the mechanisms via which these changes occur are very different for RS compared to LC. This is supported by the very distinct physicochemical properties of these fibre types, with LC being a bulky fibre and RS being a fermentable fibre.

The identification of the measured proteins is a great challenge and beyond the scope of this chapter. A limitation of the SELDI-TOF MS technology is that its spectrum reports a low-resolution profile of protein species that bound to the protein chip arrays, which is due to the relatively low resolution and hence mass accuracy of its mass analyser, and lack of tandem MS capabilities (225, 226). Furthermore, proteins can be post-translationally modified, e.g. by glycosylation, which also obscures the identification of the protein.

However, although it is not possible to name the measured proteins, the proteins in our dataset do provide a number of interesting leads. Among the 973 proteins we determined, some proteins had a similar mass-to-charge-ratio (*m/z*) and showed a similar postprandial expression pattern, suggesting that 2 forms of the same protein may be detected. Moreover, a view proteins with an identical *m/z* ratio were determined on multiple arrays. These observations suggest that the number of unique proteins measured was in fact lower than 973.

The *m/z* of a protein can help us determine which metabolic function each protein might have. The *m/z* determined in this experiment varied from 1,504.7 to 195,739. Usually a compound with a molecular weight below 5,000 Da is defined as a peptide, meaning some compounds that we defined as proteins were in fact peptides. Examples of peptides are GLP-1 and PYY, with a mass of approximately 3,298 Da and 4,310 Da respectively.

6

In addition, the type of protein array to which the plasma fractions were hybridized may provide clues on the physicochemical property of the proteins. For example, CM10 arrays bind molecules with a positive charge on the surface, H50 arrays capture large proteins through hydrophobic interactions and IMAC30 arrays capture molecules that bind polyvalent metal ions.

The intensities of the peaks measured using SELDI-TOF-MS are indicative of the concentration of the proteins in plasma. In our dataset, large differences in intensity were observed between the proteins, ranging from almost 0 to over 600. Because the proteins that are usually present at high concentrations in plasma are largely known, the relative abundance of the proteins may also provide evidence about the protein identity.

Analysis of the ^{1}H-NMR-based metabolomics data revealed a mild effect of diet on the postprandial concentrations of a variety of amino acids. This suggests that the type of fibre may influence protein digestion, which may be due to shifts in the composition and activity of the microbiota.

In conclusion, this study showed that the consumption of diets with fermentable fibres results in different postprandial plasma protein and metabolite profiles compared to a diet containing non-fermentable fibres or a diet without fibres. Among the proteins that explained the majority of the variation between diets and time points, potential biomarkers for intake of fermentable fibre or gut-derived mediators of satiety may be identified. However, this will require further investigation.

Acknowledgements

6

General discussion

Motivation and aim of the research

The objective of the research described in this thesis was to reveal the effects of fermentation in the large intestine using a comprehensive approach with focus on metabolism and satiety. In order to investigate this, experiments were performed in pigs to determine the effect of a diet high in resistant starch (RS) on microbiota composition, short-chain fatty acid (SCFA) concentrations and gene expression in colon, and on several plasma variables including glucose, insulin, satiety-related hormones, SCFAs and serotonin. Results from these studies are described in **Chapter 2**, **3** and **5**. **Chapter 6** shows the result of a proteomics analysis of portal and carotid plasma of minipigs fed different fibre diets. In addition, we used a mouse model to determine the effect of dietary fat content on colonic gene expression profile after colonic administration of SCFAs. In **Chapter 4** the main findings from this experiment are reported.

Main findings of the research

Essentially 3 major findings are reported in this thesis. First, we showed that the consumption of RS changed the microbiota composition in the caecal and colonic lumen. The abundance of several potentially pathogenic bacteria was decreased, whereas the SCFA-producing populations increased in abundance. Second, colonic gene expression changes were observed after RS consumption and after colonic administration of SCFAs. With both treatments, among the changes in the transcriptional profile of the host were changes in metabolic processes, such as energy and lipid metabolism, and immune response. Third, we showed that fat content in the background diet had a major impact on gene expression responses to SCFAs in colon. Dietary fat appeared to be is an important factor determining the metabolic implications of SCFA administration. These main findings will be discussed in more detail in the next paragraphs.

<u>*RS consumption modulates microbiota composition*</u>

We determined caecal and colonic microbiota composition of pigs after 2 wk of RS consumption (**Chapter 2** and **3**). In colon, diet was found to be the main factor driving the microbial variation. Among the microbial groups increased in relative abundance by RS treatment were the healthy gut-associated butyrate-producing *Faecalibacterium prausnitzii* bacteria, whereas potentially pathogenic members of the *Gammaproteobacteria*, including *Escherichia coli*, *Pseudomonas*, *Psychrobacter* and *Vibrio* spp., were reduced in relative abundance.

As has been shown in literature, 2 wk of intervention should be sufficient for the establishment of a new stable microbial composition (46, 178). Because we did not have the opportunity to follow changes in microbiota composition over time, it

was impossible to predict in which order colonic changes occurred. In RS-fed pigs, we observed an increase in SCFA concentrations in the colonic lumen (**Chapter 2** and **3**). These SCFAs were produced by the microbiota. However, consumption of RS for a prolonged period resulted in changes in the microbial composition. Determining the main factor(s) driving this change is rather difficult. The increased availability of substrate for fermentation, in this case RS, might have required a change in microbial composition, because the initial microbiota composition did not allow all substrate to be fermented. In that case the fibre itself was directly driving the microbial shift. In addition, it might be possible that the fermentation products, i.e. SCFAs, have resulted in microbial changes. The shift in microbiota composition can in turn result in changes in both the total SCFA production and the relative production of the individual SCFAs, indicating there is an interaction between SCFAs and microbiota.

During the experiment described in **Chapter 3**, luminal content was collected to isolate microbial RNA. Recently developed techniques allow the determination of the so-called metatranscriptome, which is the gene expression profile of all gut microbiota. Information on the microbial activity, for which the analysis is currently in progress, in addition to the microbial composition, could increase our understanding of the causal relationships. For example, these data could help answering the question whether RS consumption enhances the microbial fermentation capacity independent of the composition.

Although the causal relationships remain to be elucidated, the observed shift in microbial profile with RS consumption supports the general believe that fermentable fibres have a beneficial impact on colonic health.

Fermentation modulates colonic gene expression profile

Comparing genome-wide expression profiles is an unbiased approach for identifying genes and processes that are affected by a compound or diet. Both in pigs and mice, the whole-genome expression profile of colon was studied (**Chapter 3** and **4**). In the mouse study, we investigated the effects of colonic administration of SCFAs, whereas the pig study described the effects of fermentable dietary fibre (RS) consumption. Although the experimental set-up and aim of the study performed in mice were different from those of the pig studies, the fact that SCFAs are products of the fermentation of fibres, allows some comparison to be made between the results derived from mice and the results derived from pigs. Interestingly, we observed a general induction of lipid-related processes after RS consumption in pigs, whereas these processes were generally suppressed by SCFA treatment in mice. This opposite direction of change was also found for immune response, which appeared to be suppressed in pigs and induced in mice.

In RS-fed pigs, we observed an increased expression of genes involved in the

7

TCA cycle, the pathway responsible for generating energy through the oxidization of acetyl-CoA. The increased energy generation in colonocytes upon RS feeding was in line with our expectations, as we also observed that RS increases SCFA concentrations in the colonic lumen. These SCFAs are taken up by the colonocytes, where they serve as a precursor to the TCA cycle. These data are supported by the mouse experiment, showing that SCFAs, mainly acetate and butyrate, affect energy metabolism. The similarities in gene expression pattern observed between acetate and butyrate might be due to the fact that both acetate and butyrate enter the TCA cycle as acetyl-CoA, whereas propionate enters as succinyl-CoA (182). **Chapter 4** also showed that propionate affects amino acid metabolism, which could be explained by the fact that propionate can be metabolized by the TCA cycle, thereby contributing to the generation of TCA-derived amino acids (182). In mice receiving acetate or butyrate infusions, highly comparable changes in lipid and lipoprotein metabolism were observed, whereas propionate induced very distinct changes in gene expression profile.

Within our research group a study was performed, in which C57BL/6J mice were fed diets containing different fibre types for 10d (Lange *et al.*, unpublished data). Among the fibre types included in this study was RS, which was the same fibre also added to the pig diets used in **Chapter 3**. The colonic gene expression data showed that RS resulted in positive enrichment of genes involved in immune response, whereas metabolic processes such as fatty acid oxidation, oxidative phosphorylation, glutathione metabolism, glycolysis, gluconeogenesis and branched-chain amino acid processes, were negatively enriched with RS. This mouse study revealed that RS consumption induced opposite colonic changes compared to the studies performed in pigs. However, the direction in which colonic gene expression profile was modulated with RS in mice was quite similar as observed with SCFA infusion in mice (**Chapter 4**).

In pigs, the transcription factor *PPARG* was predicted to be significantly activated with RS consumption in pigs, indicating that this upstream regulator could explain part of the observed shift in gene expression profile. In addition, the transcriptome data were used to identify potentially secreted proteins that may mediate effects of RS in liver or other tissues and organs. Among the potentially secreted proteins that were expected to increase with RS were IGF1, AGT, VEGFA and ANGPTL4, proteins which are all derived from PPARG target genes. These data suggest that changes in colonic gene expression can affect whole-body metabolism and health.

Based on these results we assume that the animal model played a major role in the observed effects on gene expression level. Differences in microbiota composition could partly explain the large discrepancy between the results, as

microbial composition is known to be highly different among species (227) and dependent on the diet. In addition, it should be noted that colonic gene expression is a complex variable. Gene expression changes could have been induced by the microbiota or the SCFAs, but also less well characterised factors might be involved.

Dietary fat modulates colonic gene expression profile

In the study described in **Chapter 4**, mice received rectal SCFA infusions on a low fat or a high fat diet background. Dietary fat content was shown to have a major impact on colonic gene expression response to SCFAs, especially after propionate treatment. For instance, the direction of the changes in fatty acid biosynthesis, amino acid metabolism and carbohydrate metabolism induced by propionate was highly dependent on background diet. These metabolic processes were induced on a low fat diet background, whereas suppression of these processes was observed with high fat feeding. Furthermore, SCFA infusion on the high fat diet background appeared to partially reverse the gene expression changes induced by high fat feeding without SCFA infusion.

Overall we observed that dietary fat is an important factor determining the metabolic implications of SCFA administration. Part of the colonic gene expression changes observed on the high fat diet background are likely to be the result of a change in microbial composition (43, 48). Based on our findings, it can be concluded that standardization of the fat and carbohydrate content in the background diet is essential for studying effects of colonic SCFAs, because there appears to be a close interplay between dietary fat and colonic SCFAs. The high fat diet used in this experiment, containing 45 en% of fat, closely represents the human diet and therefore results obtained from mice consuming the high fat diet might best reflect what would happen in humans.

SCFA concentrations after RS consumption

In the pig studies described in this thesis, SCFA concentrations were measured after RS consumption at different locations of the intestinal lumen (**Chapter 2** and **3**), and in portal (**Chapter 6**) and peripheral (**Chapter 3/5**) plasma at several time points. Although the studies differed with respect to experimental set-up and the location and time of sample collection for SCFA measurement, comparison of the SCFA ratios provides some relevant information (**Table 1**).

Knowledge about the ratio in which the individual SCFAs are produced is mainly derived from *in vitro* fermentation studies. *In vitro* fermentation of RS using faecal inocula from pigs resulted in a SCFA composition of 65:22:14 (acetate:propionate:butyrate) (224). This composition is comparable to the ratios calculated from the results described in **Chapter 3**, showing an

7

acetate:propionate:butyrate ratio of 58:31:12 in colon (**Table 1**). However, the relative concentration of butyrate found in **Chapter 2** was much lower (i.e. 6%), whereas the relative acetate concentration was much higher compared to the study described in **Chapter 3** (75 vs. 58%). Since diet composition and time of sampling were the same in both experiments, the discrepancy between the results might be due to difference in age (4 vs. 22 months), body weight (60 vs. 270 kg) and gender of the pigs. It should also be noted that concentrations do not necessarily reflect production rates, as the rate of SCFA absorption could have differed between the individual SCFAs and between the pigs.

SCFAs are taken up by the colonocytes, after which they can either be used as an energy source for the colonocytes, or they are transported to the liver via the portal vein to serve as anabolic substrates in tissues other than colon (61, 62). SCFA levels were determined in portal plasma collected from minipigs (**Chapter 6**), showing that around 75% of the measured SCFAs was acetate. When comparing this number with the 58% measured in the colonic lumen (**Chapter 3**), this indicates that propionate and butyrate are metabolised by the colonocytes to a higher extent than acetate. Surprisingly, butyrate levels were slightly higher compared to propionate levels, although butyrate is assumed to mainly serve as an energy source for the colonocytes (169). In peripheral plasma, collected in the study described in **Chapter 3/5**, approximately 85% of the measured SCFAs was acetate. Relative plasma concentrations of propionate and butyrate were lower in peripheral plasma than in portal plasma, with again butyrate levels being slightly higher compared to propionate levels. Other studies have shown as well that acetate is by far the most abundant SCFA in peripheral plasma (228, 229). However, since peripheral blood is a complex matrix, it is not possible to explain where the circulating SCFAs were derived from or by which organ they will be metabolised.

It should be taken into account that extensive interconversion between acetate and butyrate takes place in the intestinal tract (230), which further complicates the determination of acetate, propionate and butyrate production resulting from colonic fermentation.

Animal models

Pigs
In this thesis, effects of dietary fibres were tested in pigs. This model was selected because the anatomy and physiology of the gastrointestinal tract of pigs is highly similar to those in humans (66), making pigs a suitable invasive model for the digestive function in humans. Furthermore, extensive conservation exists between

Table 1 SCFA composition measured in intestinal lumen and plasma of pigs after RS consumption.

Study	Location	Hours after feeding	Acetate:propionate:butyrate[1]
	Intestinal lumen		
Chapter 2	Distal small intestine	5	91:3:6
	Caecum	5	75:21:5
	Colon	5	75:19:6
Chapter 3	Distal small intestine	5	94:3:3
	Caecum	5	56:33:11
	Proximal colon[2]	5	53:34:13
	Colon[3]	5	58:31:12
	Plasma		
Chapter 6	Portal	4	78:9:13
	Portal	8	74:10:16
Chapter 3/5	Peripheral	4	86:5:9
	Peripheral	5	83:5:12

[1]Relative concentrations are expressed as proportion of the sum of acetate, propionate and butyrate concentration.

[2]SCFAs measured in luminal content collected from the location of the cannula.

[3]SCFAs measured in luminal content collected at section.

the pig and human genome sequence (67, 70). Another advantage is that research findings in pigs can be used to improve the welfare of restrictedly fed animals, such as adult pigs, which may suffer from hunger and related welfare problems (14).

However, the use of pig models has some limitations. In pig breeding, remarkable progress in reducing backfat and improving growth rate was made during the last 100 years (231). It is very likely that the long history of pig breeding had a large impact on the genetics of these animals. Domestic pigs can be a suitable model for increasing our understanding of mechanisms of fibre-induced satiety, but on the level of metabolism, pigs have adapted to rapid growth, which might complicate the translation of data obtained from pig experiments to the human situation.

As observed from the pig studies on the effects of RS (**Chapter 2** and **3**), the inter-individual variation between pigs regarding colonic microbiota composition, SCFA concentrations and gene expression was rather high, although pigs were genetically related (i.e. siblings were included) in both experiments. This high degree of variation is also observed in human intervention studies, underlining the similarity between pigs and humans. However, large differences in observations between pigs make it more difficult to find robust effects of diet.

7

Mice

To determine the effect of rectally administered SCFAs on colonic gene expression profile, C57BL/6J mice were the animal model of choice. Among the advantages of a mouse model are the low costs, small size and high reproduction rate of mice. In addition, mice are relatively easy to house and to handle and inbred strains to limit inter-individual genetic variation and transgenic mouse models are available (63, 64). To understand basal mechanisms of metabolism and the role of nutrition and specific transcription factors in metabolic regulation, mouse models have been proven to be very valuable.

However, data obtained from mouse experiments should be translated to humans with caution, because of large contributions of the genetic background caused by the breeding selection (65). In addition, a number of highly important differences between metabolism in mice and humans exist, for instance regarding cholesterol metabolism.

Furthermore, collection of a sufficient amount of blood from mice in order to measure hormones or metabolites may in some cases be challenging. On the other hand, the small size of mice makes organ collection relatively simple, because a complete organ, such as colon or liver, can be collected at section.

Relevance to humans

In this thesis, both mice and pigs were used as models for humans, as we were interested to know how fermentation of fibres can improve human health. These animal studies have been valuable in the identification of metabolic changes resulting from fermentation, which could not have been achieved with human intervention studies.

However, we have shown that identical fibres can induce distinct metabolic effects in different species, indicating that species differences should not be underestimated. These differences could be attributed to differences in fermentation capacity. As shown by *in vitro* fermentation, human faecal inoculum has a higher ability to ferment RS than faecal inoculum of pigs, and human inoculum is able to ferment a broader variety of fibres than pig inoculum (224). This difference between pig and human inoculum could be due to the consumption of a more heterogeneous and uncontrolled diet by humans, resulting in the adaptation of the human gut microbiota to a larger variety of fibres. For future research, standardisation of the microbiota composition between animals is recommended. Human gut microbiota have been successfully transplanted into germfree piglets and mice, resulting in a human-like microbial community (48, 232), which seems very promising.

A highly relevant question is which animal model best reflects what would happen in humans. Because higher similarities exist between the anatomy,

physiology and metabolism of the gastrointestinal tract of pigs and humans than between the intestine of mice and humans, pigs would be the preferred model. However, the exact research question largely determines which model would be most suitable and most feasible to use. Also, in addition to animal studies, *in vitro* studies or human intervention studies can be performed in parallel to enhance mechanistic knowledge and to obtain a clear picture of the actual implications for humans.

Implications for human health

The previous paragraphs of this chapter mainly focussed on colonic changes induced by fermentation, but eventually these changes are expected to affect whole-body metabolism and health. Importantly, RS is suggested to contribute to the prevention of obesity (125, 233). This might seem rather contradictory, because the fermentation products, i.e. SCFAs, also serve as an energy source for the body, suggesting that these fibres would increase body weight and adiposity. However, studies showed that RS can enhance satiety (17, 132, 133), which was also supported by this thesis (**Chapter 5**), resulting in decreased food intake. Furthermore, studies have shown that RS can reduce weight gain and adiposity (82, 83, 234). These beneficial effects are thought to be largely mediated by SCFAs.

Satiety and food intake

Essentially, fermentable fibres can enhance satiety via 3 mechanisms. First, SCFAs resulting from fermentation can stabilise glucose and insulin levels, as supported by the findings described in **Chapter 5**. A more gradual increase in glucose and insulin levels after a meal is believed to enhance satiety (216). Second, fermentable fibres can affect the secretion of satiety-related hormones such as glucagon-like peptide 1 (GLP-1) and peptide YY (PYY) (29, 82). SCFAs are agonists for free fatty acid receptors (FFA2 and FFA3), which are expressed in enteroendocrine cells in the gut epithelium. The activation of these receptors was suggested to trigger the production and release of GLP-1 and PYY by enteroendocrine L-cells (91, 92). In **Chapter 5** we measured a significant decrease in GLP-1 levels after RS consumption, which is in line with the changes in glucose and insulin levels. The exact implications of this decrease in GLP-1 are however largely unknown. Third, RS was found to decrease blood serotonin levels (**Chapter 5**). Diet was previously shown to influence intestinal serotonin release (199), which in turn changes intestinal motility and transit (200), thereby potentially affects satiety (25). Intestinal motility could be reduced in RS-fed pigs, possibly leading to a reduced passage rate of digesta in the colon.

7

Several factors influence the outcome of studies on the satiating properties of fermentable fibres. Two of these factors concern the experimental design. First, the duration of the intervention can have a major impact on study outcome. In our studies, pigs consumed the RS diet for 2 wk. However, experiments have been performed with very different study durations, also showing slightly different study results (83, 132). In an accompanying project, an experiment was performed in which long-term effects of an RS diet on feeding patterns and growth performance in growing pigs fed *ad libitum* for 12 wk were studied (235). Pigs fed RS were shown to change feeding patterns compared to DS-fed pigs, i.e RS consumption increased feed intake per meal, meal duration and inter-meal intervals, and reduced the number of meals per day. However, daily dry matter intake was not affected.

Second, the selection of an adequate control diet is highly important when studying effects of fibres. In the pig studies described in this thesis, we decided to exchange DS for RS on gross energy basis. DS is broken down and absorbed in the small intestine, resulting in rapid nutrient uptake, a rapid glucose peak and therefore also rapidly available energy. On the other hand, RS escapes digestion in the small intestine and is fermented by microbiota in the large intestine resulting in the production of SCFAs. Although the amount of gross energy was similar in both diets, metabolizable energy was 4.8% lower in the RS diet (14.10 MJ/kg) compared to the DS diet (14.78 MJ/kg) (**Chapter 3/5**). Despite the lower caloric value of the RS diet, this diet seemed to be more satiating compared to the DS diet (**Chapter 5**). Therefore, comparison of diets with the same amount of gross energy might result in an underestimation of the satiating effects of a fermentable fibre diet, because the metabolizable energy is usually slightly lower in these diets. It is important to note that the amount of energy that can be obtained from fermentable fibres is highly dependent on the fibre type and the species in which the study was performed.

Body weight development
It is important to know whether changes in satiety and/or food intake are reflected in changes in body weight or adiposity. The study on the effects of *ad libitum* consumption of RS for 12 wk in growing pigs showed that RS-fed pigs had a reduced intake of digestible energy (DE) compared to DS-fed pigs (235). Despite the reduced DE intake, RS-fed pigs had similar growth rates as pigs fed DS and at the end of the study body weight was similar in all pigs. However, intestinal weights of RS-fed pigs were higher compared to DS-fed pigs, which could be explained by the high fermentation level with RS. This observation is highly relevant to humans, as in most human intervention studies no effect of long term fibre consumption on body weight can be observed (12). In research on fermentable fibres, determining

body composition or intestinal weight in addition to body weight alone, could yield completely different conclusions about the effects of fibres on body weight development.

Conclusion and recommendations

The main findings of this thesis are summarised in **Fig. 1**, showing how fermentable dietary fibres may ultimately induce satiety and reduce body weight. In this thesis, a nutrigenomics approach was used to investigate the effects of fermentable dietary fibres, taking full advantage of the current state of art in genomics research (72, 73).

This thesis supports the implementation of fermentable dietary fibres into the human diet to improve colonic health and to reduce energy intake and body weight gain, which ultimately may prevent obesity and type 2 diabetes. Increased knowledge about the underlying mechanisms by which resistant starch induces satiety could facilitate the effective application of resistant starch in human diets. More research is required to further elucidate how diet composition, in particular the presence of fermentable dietary fibres, can improve human health.
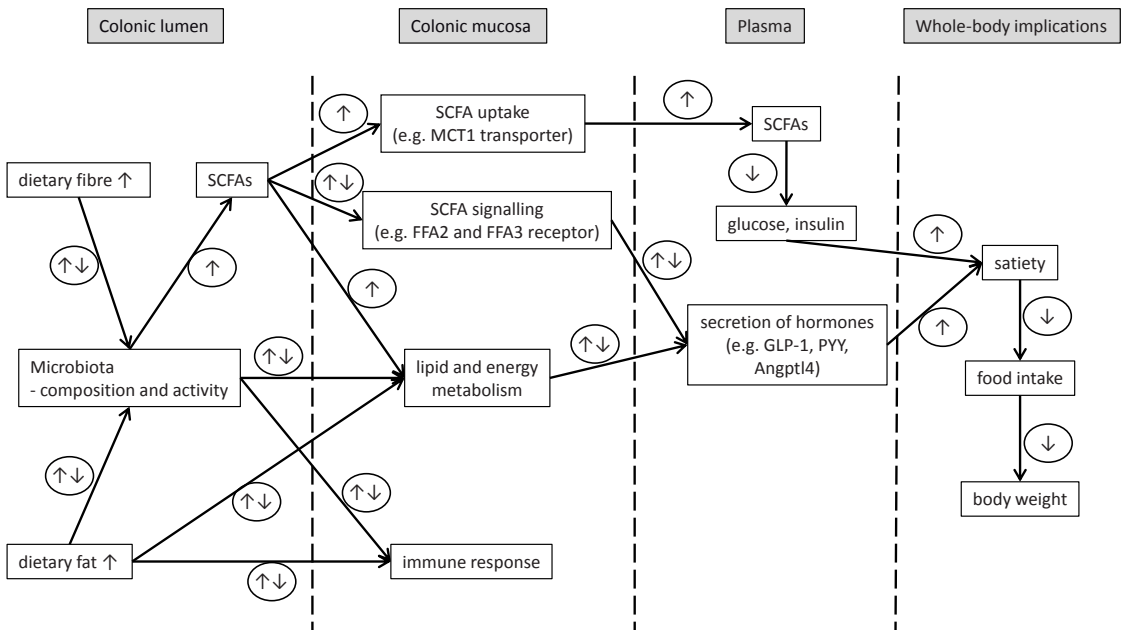
Figure 1 Overview of the variables changed in the colonic lumen, the colonic mucosa and in plasma as a result of fermentable dietary fibre consumption, and its ultimate implications on satiety, food intake and body weight regulation.

References

1.   WHO. Obesity and overweight. 2013 [cited 2013 March 25]; Available from: http://www.who.int/mediacentre/factsheets/fs311/en/

2.   WHO. Obesity europe. 2013 [cited 2013 March 25]; Available from: http://www.euro.who.int/en/what-we-do/health-topics/noncommunicable-diseases/obesity/facts-and-figures

3.   WHO. The challenge of obesity in the who european region and the strategies for response - summary. 2007 [cited 2013 April 11]; Available from: http://www.euro.who.int/__data/assets/pdf_file/0008/98243/E89858.pdf

4.   Flegal KM, Carroll MD, Ogden CL, Curtin LR. Prevalence and trends in obesity among us adults, 1999-2008. JAMA. 2010 Jan 20;303:235-41.

5.   Mozumdar A, Liguori G. Persistent increase of prevalence of metabolic syndrome among u.S. Adults: Nhanes iii to nhanes 1999-2006. Diabetes Care. 2011 Jan;34:216-9.

6.   Feldeisen SE, Tucker KL. Nutritional strategies in the prevention and treatment of metabolic syndrome. Appl Physiol Nutr Metab. 2007 Feb;32:46-60.

7.   Slavin J. Fiber and prebiotics: Mechanisms and health benefits. Nutrients. 2013;5:1417-35.

8.   Breneman CB, Tucker L. Dietary fibre consumption and insulin resistance - the role of body fat and physical activity. Br J Nutr. 2012 Dec 7:1-9.

9.   Robertson MD, Bickerton AS, Dennis AL, Vidal H, Frayn KN. Insulin-sensitizing effects of dietary resistant starch and effects on skeletal muscle and adipose tissue metabolism. Am J Clin Nutr. 2005 Sep;82:559-67.

10.   Grube B, Chong PW, Lau KZ, Orzechowski HD. A natural fiber complex reduces body weight in the overweight and obese: A double-blind, randomized, placebo-controlled study. Obesity (Silver Spring). 2013 Jan;21:58-64.

11.   Liu S, Willett WC, Manson JE, Hu FB, Rosner B, Colditz G. Relation between changes in intakes of dietary fiber and grain products and changes in weight and development of obesity among middle-aged women. Am J Clin Nutr. 2003 Nov;78:920-7.

12.   Wanders AJ, van den Borne JJ, de Graaf C, Hulshof T, Jonathan MC, Kristensen M, Mars M, Schols HA, Feskens EJ. Effects of dietary fibre on subjective appetite, energy intake and body weight: A systematic review of randomized controlled trials. Obes Rev. 2011 Jun 16.

13.   Kristensen M, Jensen MG. Dietary fibres in the regulation of appetite and food intake. Importance of viscosity. Appetite. 2011 Feb;56:65-70.

14.   de Leeuw JA, Bolhuis JE, Bosch G, Gerrits WJ. Effects of dietary fibre on behaviour and satiety in pigs. Proc Nutr Soc. 2008 Nov;67:334-42.

15.   Nugent AP. Health properties of resistant starch. Nutr Bull. 2005;30:27-54.

16.   AACC. Dietary fiber. 2000 [cited 2013 March 25]; Available from: http://www.aaccnet.org/initiatives/definitions/Pages/DietaryFiber.aspx

17.   Souza da Silva C, van den Borne JJ, Gerrits WJ, Kemp B, Bolhuis JE. Effects of dietary fibers with different physicochemical properties on feeding motivation in adult female pigs. Physiol Behav. 2012 Jul 10;107:218-30.

18.   Centers for Disease C, Prevention. Trends in intake of energy and macronutrients--united states, 1971-2000. MMWR Morb Mortal Wkly Rep. 2004 Feb 6;53:80-2.

19.   Cummings DE, Overduin J. Gastrointestinal regulation of food intake. J Clin Invest. 2007 Jan;117:13-23.

20.   Wren AM, Bloom SR. Gut hormones and appetite control. Gastroenterology. 2007 May;132:2116-30.

21.   Drewnowski A. Energy density, palatability, and satiety: Implications for weight control. Nutr Rev. 1998 Dec;56:347-53.

22.   Zijlstra N, de Wijk RA, Mars M, Stafleu A, de Graaf C. Effect of bite size and oral processing time of a semisolid food on satiation. Am J Clin Nutr. 2009 Aug;90:269-75.

23.   Dikeman CL, Fahey GC. Viscosity as related to dietary fiber: A review. Crit Rev Food Sci Nutr. 2006;46:649-63.

24.   Kristensen M, Damgaard TW, Sorensen AD, Raben A, Lindelov TS, Thomsen AD, Bjergegaard C, Sorensen H, Astrup A, Tetens I. Whole flaxseeds but not sunflower seeds in rye bread reduce apparent digestibility of fat in healthy volunteers. Eur J Clin Nutr. 2008 Aug;62:961-7.

25.   Sleeth ML, Thompson EL, Ford HE, Zac-Varghese SE, Frost G. Free fatty acid receptor 2 and nutrient sensing: A proposed role for fibre, fermentable carbohydrates and short-chain fatty acids in appetite regulation. Nutr Res Rev. 2010 Jun;23:135-45.

26.   Bosch G, Verbrugghe A, Hesta M, Holst JJ, van der Poel AF, Janssens GP, Hendriks WH. The effects of dietary fibre type on satiety-related hormones and voluntary food intake in dogs. Br J Nutr. 2009 Jul;102:318-25.

27.   Reimer RA, Pelletier X, Carabin IG, Lyon M, Gahler R, Parnell JA, Wood S. Increased plasma pyy levels following supplementation with the functional fiber polyglycoplex in healthy adults. Eur J Clin Nutr. 2010 Jul 28.

28.   Weickert MO, Spranger J, Holst JJ, Otto B, Koebnick C, Mohlig M, Pfeiffer AF. Wheat-fibre-induced changes of postprandial peptide yy and ghrelin responses are not associated with acute alterations of satiety. Br J Nutr. 2006 Nov;96:795-8.

29.   Zhou J, Martin RJ, Tulley RT, Raggio AM, McCutcheon KL, Shen L, Danna SC, Tripathy S, Hegsted M, Keenan MJ. Dietary resistant starch upregulates total glp-1 and pyy in a sustained day-long manner through fermentation in rodents. Am J Physiol Endocrinol Metab. 2008 Nov;295:E1160-6.

30.   Freeland KR, Wilson C, Wolever TM. Adaptation of colonic fermentation and glucagon-like peptide-1 secretion with increased wheat fibre intake for 1 year in hyperinsulinaemic human subjects. Br J Nutr. 2010 Jan;103:82-90.

31.   Karhunen LJ, Juvonen KR, Huotari A, Purhonen AK, Herzig KH. Effect of protein, fat, carbohydrate and fibre on gastrointestinal peptide release in humans. Regul Pept. 2008 Aug 7;149:70-8.

32. Field BC, Chaudhri OB, Bloom SR. Bowels control brain: Gut hormones and obesity. Nat Rev Endocrinol. 2010 Aug;6:444-53.

33. Raben A, Tagliabue A, Christensen NJ, Madsen J, Holst JJ, Astrup A. Resistant starch: The effect on postprandial glycemia, hormonal response, and satiety. Am J Clin Nutr. 1994 Oct;60:544-51.

34. Raben A, Christensen NJ, Madsen J, Holst JJ, Astrup A. Decreased postprandial thermogenesis and fat oxidation but increased fullness after a high-fiber meal compared with a low-fiber meal. Am J Clin Nutr. 1994 Jun;59:1386-94.

35. Musso G, Gambino R, Cassader M. Obesity, diabetes, and gut microbiota: The hygiene hypothesis expanded? Diabetes Care. 2010 Oct;33:2277-84.

36. Whelan K, Quigley EM. Probiotics in the management of irritable bowel syndrome and inflammatory bowel disease. Curr Opin Gastroenterol. 2013 Mar;29:184-9.

37. Aroniadis OC, Brandt LJ. Fecal microbiota transplantation: Past, present and future. Curr Opin Gastroenterol. 2013 Jan;29:79-84.

38. Grootaert C, Marzorati M, Van den Abbeele P, Van de Wiele T, Possemiers S. Prebiotics to manage the microbial control of energy homeostasis. Benef Microbes. 2011 Dec 1;2:305-18.

39. Delzenne NM, Neyrinck AM, Cani PD. Modulation of the gut microbiota by nutrients with prebiotic properties: Consequences for host health in the context of obesity and metabolic syndrome. Microb Cell Fact. 2011 Aug 30;10 Suppl 1:S10.

40. Backhed F, Ding H, Wang T, Hooper LV, Koh GY, Nagy A, Semenkovich CF, Gordon JI. The gut microbiota as an environmental factor that regulates fat storage. Proc Natl Acad Sci U S A. 2004 Nov 2;101:15718-23.

41. Backhed F, Manchester JK, Semenkovich CF, Gordon JI. Mechanisms underlying the resistance to diet-induced obesity in germ-free mice. Proc Natl Acad Sci U S A. 2007 Jan 16;104:979-84.

42. Ley RE, Turnbaugh PJ, Klein S, Gordon JI. Microbial ecology: Human gut microbes associated with obesity. Nature. 2006 Dec 21;444:1022-3.

43. Hildebrandt MA, Hoffmann C, Sherrill-Mix SA, Keilbaugh SA, Hamady M, Chen YY, Knight R, Ahima RS, Bushman F, Wu GD. High-fat diet determines the composition of the murine gut microbiome independently of obesity. Gastroenterology. 2009 Nov;137:1716-24 e1-2.

44. Martins dos Santos V, Muller M, de Vos WM. Systems biology of the gut: The interplay of food, microbiota and host at the mucosal interface. Curr Opin Biotechnol. 2010 Aug;21:539-50.

45. Maslowski KM, Vieira AT, Ng A, Kranich J, Sierro F, Yu D, Schilter HC, Rolph MS, Mackay F, Artis D, et al. Regulation of inflammatory responses by gut microbiota and chemoattractant receptor gpr43. Nature. 2009 Oct 29;461:1282-6.

46.   Murphy EF, Cotter PD, Healy S, Marques TM, O'Sullivan O, Fouhy F, Clarke SF, O'Toole PW, Quigley EM, Stanton C, et al. Composition and energy harvesting capacity of the gut microbiota: Relationship to diet, obesity and time in mouse models. Gut. 2010 Oct 6.

47.   Scarpellini E, Campanale M, Leone D, Purchiaroni F, Vitale G, Lauritano EC, Gasbarrini A. Gut microbiota and obesity. Intern Emerg Med. 2010 Oct;5 Suppl 1:S53-6.

48.   Turnbaugh PJ, Ridaura VK, Faith JJ, Rey FE, Knight R, Gordon JI. The effect of diet on the human gut microbiome: A metagenomic analysis in humanized gnotobiotic mice. Sci Transl Med. 2009 Nov 11;1:6ra14.

49.   Delzenne NM, Cani PD. Interaction between obesity and the gut microbiota: Relevance in nutrition. Annu Rev Nutr. 2011 Aug 21;31:15-31.

50.   Walker AW, Ince J, Duncan SH, Webster LM, Holtrop G, Ze X, Brown D, Stares MD, Scott P, Bergerat A, et al. Dominant and diet-responsive groups of bacteria within the human colonic microbiota. ISME J. 2011 Feb;5:220-30.

51.   de Wit N, Derrien M, Bosch-Vermeulen H, Oosterink E, Keshtkar S, Duval C, de Vogel-van den Bosch J, Kleerebezem M, Muller M, van der Meer R. Saturated fat stimulates obesity and hepatic steatosis and affects gut microbiota composition by an enhanced overflow of dietary fat to the distal intestine. Am J Physiol Gastrointest Liver Physiol. 2012 Sep 1;303:G589-99.

52.   Arumugam M, Raes J, Pelletier E, Le Paslier D, Yamada T, Mende DR, Fernandes GR, Tap J, Bruls T, Batto JM, et al. Enterotypes of the human gut microbiome. Nature. 2011 May 12;473:174-80.

53.   Topping DL, Clifton PM. Short-chain fatty acids and human colonic function: Roles of resistant starch and nonstarch polysaccharides. Physiol Rev. 2001 Jul;81:1031-64.

54.   Hendriks WH, van Baal J, Bosch G. Ileal and faecal protein digestibility measurement in humans and other non-ruminants - a comparative species view. Br J Nutr. 2012 Aug;108 Suppl 2:S247-57.

55.   Hamer HM, Jonkers D, Venema K, Vanhoutvin S, Troost FJ, Brummer RJ. Review article: The role of butyrate on colonic function. Aliment Pharmacol Ther. 2008 Jan 15;27:104-19.

56.   Tazoe H, Otomo Y, Kaji I, Tanaka R, Karaki SI, Kuwahara A. Roles of short-chain fatty acids receptors, gpr41 and gpr43 on colonic functions. J Physiol Pharmacol. 2008 Aug;59 Suppl 2:251-62.

57.   Karaki S, Mitsui R, Hayashi H, Kato I, Sugiya H, Iwanaga T, Furness JB, Kuwahara A. Short-chain fatty acid receptor, gpr43, is expressed by enteroendocrine cells and mucosal mast cells in rat intestine. Cell Tissue Res. 2006 Jun;324:353-60.

58.   Cuche G, Cuber JC, Malbert CH. Ileal short-chain fatty acids inhibit gastric motility by a humoral pathway. Am J Physiol Gastrointest Liver Physiol. 2000 Nov;279:G925-30.

59.   Roediger WE. Role of anaerobic bacteria in the metabolic welfare of the colonic mucosa in man. Gut. 1980 Sep;21:793-8.

60. Bergman EN. Energy contributions of volatile fatty acids from the gastrointestinal tract in various species. Physiol Rev. 1990 Apr;70:567-90.

61. Wong JM, de Souza R, Kendall CW, Emam A, Jenkins DJ. Colonic health: Fermentation and short chain fatty acids. J Clin Gastroenterol. 2006 Mar;40:235-43.

62. Bloemen JG, Venema K, van de Poll MC, Olde Damink SW, Buurman WA, Dejong CH. Short chain fatty acids exchange across the gut and liver in humans measured at surgery. Clin Nutr. 2009 Dec;28:657-61.

63. Peters LL, Robledo RF, Bult CJ, Churchill GA, Paigen BJ, Svenson KL. The mouse as a model for human biology: A resource guide for complex trait analysis. Nat Rev Genet. 2007 Jan;8:58-69.

64. Beckers J, Wurst W, de Angelis MH. Towards better mouse models: Enhanced genotypes, systemic phenotyping and envirotype modelling. Nat Rev Genet. 2009 Jun;10:371-80.

65. Parks BW, Nam E, Org E, Kostem E, Norheim F, Hui ST, Pan C, Civelek M, Rau CD, Bennett BJ, et al. Genetic control of obesity and gut microbiota composition in response to high-fat, high-sucrose diet in mice. Cell Metab. 2013 Jan 8;17:141-52.

66. Guilloteau P, Zabielski R, Hammon HM, Metges CC. Nutritional programming of gastrointestinal tract development. Is the pig a good model for man? Nutr Res Rev. 2010 Jun;23:4-22.

67. Hart EA, Caccamo M, Harrow JL, Humphray SJ, Gilbert JG, Trevanion S, Hubbard T, Rogers J, Rothschild MF. Lessons learned from the initial sequencing of the pig genome: Comparative analysis of an 8 mb region of pig chromosome 17. Genome Biol. 2007;8:R168.

68. Meyers SN, Rogatcheva MB, Larkin DM, Yerle M, Milan D, Hawken RJ, Schook LB, Beever JE. Piggy-bacing the human genome ii. A high-resolution, physically anchored, comparative map of the porcine autosomes. Genomics. 2005 Dec;86:739-52.

69. Rogatcheva MB, Chen K, Larkin DM, Meyers SN, Marron BM, He W, Schook LB, Beever JE. Piggy-bacing the human genome i: Constructing a porcine bac physical map through comparative genomics. Anim Biotechnol. 2008;19:28-42.

70. Groenen MA, Archibald AL, Uenishi H, Tuggle CK, Takeuchi Y, Rothschild MF, Rogel-Gaillard C, Park C, Milan D, Megens HJ, et al. Analyses of pig genomes provide insight into porcine demography and evolution. Nature. 2012 Nov 15;491:393-8.

71. Tuggle CK, Wang Y, Couture O. Advances in swine transcriptomics. Int J Biol Sci. 2007;3:132-52.

72. Afman L, Muller M. Nutrigenomics: From molecular nutrition to prevention of disease. J Am Diet Assoc. 2006 Apr;106:569-76.

73. Muller M, Kersten S. Nutrigenomics: Goals and strategies. Nat Rev Genet. 2003 Apr;4:315-22.

74. Ganesh V, Hettiarachchy NS. Nutriproteomics: A promising tool to link diet and diseases in nutritional research. Biochim Biophys Acta. 2012 Oct;1824:1107-17.

75. Brennan L. Metabolomics in nutrition research: Current status and perspectives. Biochem Soc Trans. 2013 Apr 1;41:670-3.

76. Claesson MJ, O'Sullivan O, Wang Q, Nikkila J, Marchesi JR, Smidt H, de Vos WM, Ross RP, O'Toole PW. Comparative analysis of pyrosequencing and a phylogenetic microarray for exploring microbial community structures in the human distal intestine. PLoS One. 2009;4:e6669.

77. Qin J, Li R, Raes J, Arumugam M, Burgdorf KS, Manichanh C, Nielsen T, Pons N, Levenez F, Yamada T, et al. A human gut microbial gene catalogue established by metagenomic sequencing. Nature. 2010 Mar 4;464:59-65.

78. Wang Z, Gerstein M, Snyder M. Rna-seq: A revolutionary tool for transcriptomics. Nat Rev Genet. 2009 Jan;10:57-63.

79. May C, Brosseron F, Chartowski P, Schumbrutzki C, Schoenebeck B, Marcus K. Instruments and methods in proteomics. Methods Mol Biol. 2011;696:3-26.

80. Amine E, Baba N, Belhadj M, Deurenberg-Yap M, Djazayery A, Forrester T, Galuska D, Herman S, James W, M`Buyamba J, et al. Diet, nutrition and the prevention of chronic diseases. Geneva, Switzerland.: World Health Organization; 2003. Report No.: 0512-3054

81. Lattimer JM, Haub MD. Effects of dietary fiber and its components on metabolic health. Nutrients. 2010 Dec;2:1266-89.

82. Keenan MJ, Zhou J, McCutcheon KL, Raggio AM, Bateman HG, Todd E, Jones CK, Tulley RT, Melton S, Martin RJ, et al. Effects of resistant starch, a non-digestible fermentable fiber, on reducing body fat. Obesity (Silver Spring). 2006 Sep;14:1523-34.

83. So PW, Yu WS, Kuo YT, Wasserfall C, Goldstone AP, Bell JD, Frost G. Impact of resistant starch on body fat patterning and central appetite regulation. PLoS One. 2007;2:e1309.

84. Weickert MO, Mohlig M, Schofl C, Arafat AM, Otto B, Viehoff H, Koebnick C, Kohl A, Spranger J, Pfeiffer AF. Cereal fiber improves whole-body insulin sensitivity in overweight and obese women. Diabetes Care. 2006 Apr;29:775-80.

85. Bird AR, Vuaran M, Brown I, Topping DL. Two high-amylose maize starches with different amounts of resistant starch vary in their effects on fermentation, tissue and digesta mass accretion, and bacterial populations in the large bowel of pigs. Br J Nutr. 2007 Jan;97:134-44.

86. Halestrap AP, Meredith D. The slc16 gene family-from monocarboxylate transporters (mcts) to aromatic amino acid transporters and beyond. Pflugers Arch. 2004 Feb;447:619-28.

87. Roy CC, Kien CL, Bouthillier L, Levy E. Short-chain fatty acids: Ready for prime time? Nutr Clin Pract. 2006 Aug;21:351-66.

88. Hosseini E, Grootaert C, Verstraete W, Van de Wiele T. Propionate as a health-promoting microbial metabolite in the human gut. Nutr Rev. 2011 May;69:245-58.

89. Zhou J, Hegsted M, McCutcheon KL, Keenan MJ, Xi X, Raggio AM, Martin RJ. Peptide yy and proglucagon mrna expression patterns and regulation in the gut. Obesity (Silver Spring). 2006 Apr;14:683-9.

90. Cherbut C, Ferrier L, Roze C, Anini Y, Blottiere H, Lecannu G, Galmiche JP. Short-chain fatty acids modify colonic motility through nerves and polypeptide yy release in the rat. Am J Physiol. 1998 Dec;275:G1415-22.

91. Samuel BS, Shaito A, Motoike T, Rey FE, Backhed F, Manchester JK, Hammer RE, Williams SC, Crowley J, Yanagisawa M, et al. Effects of the gut microbiota on host adiposity are modulated by the short-chain fatty-acid binding g protein-coupled receptor, gpr41. Proc Natl Acad Sci U S A. 2008 Oct 28;105:16767-72.

92. Miyauchi S, Hirasawa A, Ichimura A, Hara T, Tsujimoto G. New frontiers in gut nutrient sensor research: Free fatty acid sensing in the gastrointestinal tract. J Pharmacol Sci. 2010 Jan;112:19-24.

93. Miller ER, Ullrey DE. The pig as a model for human nutrition. Annu Rev Nutr. 1987;7:361-82.

94. Serena A, Jorgensen H, Bach Knudsen KE. Absorption of carbohydrate-derived nutrients in sows as influenced by types and contents of dietary fiber. J Anim Sci. 2009 Jan;87:136-47.

95. Goñi I, García-Diz L, Mañas E, Saura-Calixto F. Analysis of resistant starch: A method for foods and food products. Food Chem. 1996;56:445-9.

96. Salonen A, Nikkila J, Jalanka-Tuovinen J, Immonen O, Rajilic-Stojanovic M, Kekkonen RA, Palva A, de Vos WM. Comparative analysis of fecal DNA extraction methods with phylogenetic microarray: Effective recovery of bacterial and archaeal DNA using mechanical cell lysis. J Microbiol Methods. 2010 May;81:127-34.

97. Konstantinov SR, Awati A, Smidt H, Williams BA, Akkermans AD, de Vos WM. Specific response of a novel and abundant lactobacillus amylovorus-like phylotype to dietary prebiotics in the guts of weaning piglets. Appl Environ Microbiol. 2004 Jul;70:3821-30.

98. Muyzer G, de Waal EC, Uitterlinden AG. Profiling of complex microbial populations by denaturing gradient gel electrophoresis analysis of polymerase chain reaction-amplified genes coding for 16s rrna. Appl Environ Microbiol. 1993 Mar;59:695-700.

99. Pérez Gutiérrez O, van den Bogert B, Derrien M, Koopmans SJ, Molenaar D, de Vos WM, Smidt H. Design of a high-throughput diagnostic microarray for the characterization of pig gastrointestinal tract microbiota (chapter 3). Unraveling piglet gut microbiota dynamics in response to feed additives (phd thesis). Wageningen: Ponsen & Looijen; 2010. p. 40-67 (http://library.wur.nl/WebQuery/wda/lang/1939249).

100. van den Bogert B, de Vos WM, Zoetendal EG, Kleerebezem M. Microarray analysis and barcoded pyrosequencing provide consistent microbial profiles depending on the source of human intestinal samples. Appl Environ Microbiol. 2011 Mar;77:2071-80.

101. Rajilic-Stojanovic M, Heilig HG, Molenaar D, Kajander K, Surakka A, Smidt H, de Vos WM. Development and application of the human intestinal tract chip, a phylogenetic microarray: Analysis of universally conserved phylotypes in the abundant microbiota of young and elderly adults. Environ Microbiol. 2009 Jul;11:1736-51.

102. Velu R, Reinsel GC. Multivariate reduced-rank regression: Theory and applications. New York, USA: Springer; 1998.

103. ter Braak CJF. Canonical correspondence analysis: A new eigenvector technique for multivariate direct gradient analysis. Ecology. 1986 Oct;67:1167-79.

104. Lepš J, Šmilauer P. Multivariate analysis of ecological data using canoco. Cambridge, UK: Cambridge University Press; 2003.

105. Benjamini Y, Hochberg Y. Controlling the false discovery rate: A practical and powerful approach to multiple testing. J R Stat Soc Ser B. 1995;57:289-300.

106. Wong MH, Oelkers P, Craddock AL, Dawson PA. Expression cloning and characterization of the hamster ileal sodium-dependent bile acid transporter. J Biol Chem. 1994 Jan 14;269:1340-7.

107. Bunger M, van den Bosch HM, van der Meijde J, Kersten S, Hooiveld GJ, Muller M. Genome-wide analysis of pparalpha activation in murine small intestine. Physiol Genomics. 2007 Jul 18;30:192-204.

108. Mortensen K, Christensen LL, Holst JJ, Orskov C. Glp-1 and gip are colocalized in a subset of endocrine cells in the small intestine. Regul Pept. 2003 Jul 15;114:189-96.

109. Yasuda K, Maiorano R, Welch RM, Miller DD, Lei XG. Cecum is the major degradation site of ingested inulin in young pigs. J Nutr. 2007 Nov;137:2399-404.

110. Patterson JK, Yasuda K, Welch RM, Miller DD, Lei XG. Supplemental dietary inulin of variable chain lengths alters intestinal bacterial populations in young pigs. J Nutr. 2010 Dec;140:2158-61.

111. Martinez I, Kim J, Duffy PR, Schlegel VL, Walter J. Resistant starches types 2 and 4 have differential effects on the composition of the fecal microbiota in human subjects. PLoS One. 2010;5:e15046.

112. Kleessen B, Stoof G, Proll J, Schmiedl D, Noack J, Blaut M. Feeding resistant starch affects fecal and cecal microflora and short-chain fatty acids in rats. J Anim Sci. 1997 Sep;75:2453-62.

113. esmes U, Beards EJ, Gibson GR, Tuohy KM, Shimoni E. Effects of resistant starch type iii polymorphs on human colon microbiota and short chain fatty acids in human gut models. J Agric Food Chem. 2008 Jul 9;56:5415-21.

114. Young W, Roy NC, Lee J, Lawley B, Otter D, Henderson G, McCann MJ, Tannock GW. Changes in bowel microbiota induced by feeding resistant starch stimulate transcriptomic and physiological responses in the weanling host. Appl Environ Microbiol. 2012 Jul 13.

115. Louis P, Scott KP, Duncan SH, Flint HJ. Understanding the effects of diet on bacterial metabolism in the large intestine. J Appl Microbiol. 2007 May;102:1197-208.

116. Flint HJ, Scott KP, Louis P, Duncan SH. The role of the gut microbiota in nutrition and health. Nat Rev Gastroenterol Hepatol. 2012 Oct;9:577-89.

117. Sokol H, Pigneur B, Watterlot L, Lakhdari O, Bermudez-Humaran LG, Gratadoux JJ, Blugeon S, Bridonneau C, Furet JP, Corthier G, et al. Faecalibacterium prausnitzii is an anti-inflammatory commensal bacterium identified by gut microbiota analysis of crohn disease patients. Proc Natl Acad Sci U S A. 2008 Oct 28;105:16731-6.

118. Cummings JH. The large intestine in nutrition and disease. Brussels, Belgium: Danone Institute; 1997.

119. Cuff MA, Lambert DW, Shirazi-Beechey SP. Substrate-induced regulation of the human colonic monocarboxylate transporter, mct1. J Physiol. 2002 Mar 1;539:361-71.

120. Borthakur A, Saksena S, Gill RK, Alrefai WA, Ramaswamy K, Dudeja PK. Regulation of monocarboxylate transporter 1 (mct1) promoter by butyrate in human intestinal epithelial cells: Involvement of nf-kappab pathway. J Cell Biochem. 2008 Apr 1;103:1452-63.

121. Kaji I, Karaki S, Tanaka R, Kuwahara A. Density distribution of free fatty acid receptor 2 (ffa2)-expressing and glp-1-producing enteroendocrine l cells in human and rat lower intestine, and increased cell numbers after ingestion of fructo-oligosaccharide. J Mol Histol. 2011 Feb;42:27-38.

122. Chu ZL, Carroll C, Alfonso J, Gutierrez V, He H, Lucman A, Pedraza M, Mondala H, Gao H, Bagnol D, et al. A role for intestinal endocrine cell-expressed g protein-coupled receptor 119 in glycemic control by enhancing glucagon-like peptide-1 and glucose-dependent insulinotropic peptide release. Endocrinology. 2008 May;149:2038-47.

123. Lan H, Vassileva G, Corona A, Liu L, Baker H, Golovko A, Abbondanzo SJ, Hu W, Yang S, Ning Y, et al. Gpr119 is required for physiological regulation of glucagon-like peptide-1 secretion but not for metabolic homeostasis. J Endocrinol. 2009 May;201:219-30.

124. Yoshida K, Shimizugawa T, Ono M, Furukawa H. Angiopoietin-like protein 4 is a potent hyperlipidemia-inducing factor in mice and inhibitor of lipoprotein lipase. J Lipid Res. 2002 Nov;43:1770-2.

125. Higgins JA. Resistant starch: Metabolic effects and potential health benefits. J AOAC Int. 2004 May-Jun;87:761-8.

126. Haenen D, Zhang J, da Silva CS, Bosch G, van der Meer IM, van Arkel J, van den Borne JJ, Perez Gutierrez O, Smidt H, Kemp B, et al. A diet high in resistant starch modulates microbiota composition, scfa concentrations, and gene expression in pig intestine. J Nutr. 2013 Jan 16;143:274-83.

127. Conlon MA, Kerr CA, McSweeney CS, Dunne RA, Shaw JM, Kang S, Bird AR, Morell MK, Lockett TJ, Molloy PL, et al. Resistant starches protect against colonic DNA damage and alter microbiota and gene expression in rats fed a western diet. J Nutr. 2012 May;142:832-40.

128. Jacobasch G, Schmiedl D, Kruschewski M, Schmehl K. Dietary resistant starch and chronic inflammatory bowel diseases. Int J Colorectal Dis. 1999 Nov;14:201-11.

129. Johnston KL, Thomas EL, Bell JD, Frost GS, Robertson MD. Resistant starch improves insulin sensitivity in metabolic syndrome. Diabet Med. 2010 Apr;27:391-7.

130. Park OJ, Kang NE, Chang MJ, Kim WK. Resistant starch supplementation influences blood lipid concentrations and glucose control in overweight subjects. J Nutr Sci Vitaminol (Tokyo). 2004 Apr;50:93-9.

131. Lopez HW, Levrat-Verny MA, Coudray C, Besson C, Krespine V, Messager A, Demigne C, Remesy C. Class 2 resistant starches lower plasma and liver lipids and improve mineral retention in rats. J Nutr. 2001 Apr;131:1283-9.

132. Bodinham CL, Frost GS, Robertson MD. Acute ingestion of resistant starch reduces food intake in healthy adults. Br J Nutr. 2010 Mar;103:917-22.

133. Souza da Silva C, Bolhuis JE, Gerrits WJJ, Kemp B, Van den Borne JJGC. Effects of dietary fibers with different fermentation characteristics on feeding motivation in adult female pigs. Physiology & Behavior. 2013.

134. Ichimura A, Hirasawa A, Hara T, Tsujimoto G. Free fatty acid receptors act as nutrient sensors to regulate energy homeostasis. Prostaglandins Other Lipid Mediat. 2009 Sep;89:82-8.

135. Layden BT, Angueira AR, Brodsky M, Durai V, Lowe WL, Jr. Short chain fatty acids and their receptors: New metabolic targets. Transl Res. 2013 Mar;161:131-40.

136. Quackenbush J. Microarray analysis and tumor classification. N Engl J Med. 2006 Jun 8;354:2463-72.

137. Schadt EE. Molecular networks as sensors and drivers of common human diseases. Nature. 2009 Sep 10;461:218-23.

138. Keenan MJ, Martin RJ, Raggio AM, McCutcheon KL, Brown IL, Birkett A, Newman SS, Skaf J, Hegsted M, Tulley RT, et al. High-amylose resistant starch increases hormones and improves structure and function of the gastrointestinal tract: A microarray study. J Nutrigenet Nutrigenomics. 2012;5:26-44.

139. Vanhoutvin SA, Troost FJ, Hamer HM, Lindsey PJ, Koek GH, Jonkers DM, Kodde A, Venema K, Brummer RJ. Butyrate-induced transcriptional changes in human colonic mucosa. PLoS One. 2009;4:e6759.

140. Gentleman RC, Carey VJ, Bates DM, Bolstad B, Dettling M, Dudoit S, Ellis B, Gautier L, Ge Y, Gentry J, et al. Bioconductor: Open software development for computational biology and bioinformatics. Genome Biol. 2004;5:R80.

141. Lin K, Kools H, de Groot PJ, Gavai AK, Basnet RK, Cheng F, Wu J, Wang X, Lommen A, Hooiveld GJ, et al. Madmax - management and analysis database for multiple ~omics experiments. J Integr Bioinform. 2011;8:160.

142. Heber S, Sick B. Quality assessment of affymetrix genechip data. OMICS. 2006 Fall;10:358-68.

143. Dai M, Wang P, Boyd AD, Kostov G, Athey B, Jones EG, Bunney WE, Myers RM, Speed TP, Akil H, et al. Evolving gene/transcript definitions significantly alter the interpretation of genechip data. Nucleic Acids Res. 2005;33:e175.

144. Irizarry RA, Hobbs B, Collin F, Beazer-Barclay YD, Antonellis KJ, Scherf U, Speed TP. Exploration, normalization, and summaries of high density oligonucleotide array probe level data. Biostatistics. 2003 Apr;4:249-64.

145. Sartor MA, Tomlinson CR, Wesselkamper SC, Sivaganesan S, Leikauf GD, Medvedovic M. Intensity-based hierarchical bayes method improves testing for differentially expressed genes in microarray experiments. BMC Bioinformatics. 2006;7:538.

146. Subramanian A, Tamayo P, Mootha VK, Mukherjee S, Ebert BL, Gillette MA, Paulovich A, Pomeroy SL, Golub TR, Lander ES, et al. Gene set enrichment analysis: A knowledge-based approach for interpreting genome-wide expression profiles. Proc Natl Acad Sci U S A. 2005 Oct 25;102:15545-50.

147. Merico D, Isserlin R, Stueker O, Emili A, Bader GD. Enrichment map: A network-based method for gene-set enrichment visualization and interpretation. PLoS One. 2010;5:e13984.

148. Smoot ME, Ono K, Ruscheinski J, Wang PL, Ideker T. Cytoscape 2.8: New features for data integration and network visualization. Bioinformatics. 2011 Feb 1;27:431-2.

149. Liquet B, Le Cao KA, Hocini H, Thiebaut R. A novel approach for biomarker selection and the integration of repeated measures experiments from two assays. BMC Bioinformatics. 2012 Dec 6;13:325.
      150.   Le Cao KA, Martin PG, Robert-Granie C, Besse P. Sparse canonical methods for biological data integration: Application to a cross-platform study. BMC Bioinformatics. 2009;10:34.

150. Le Cao KA, Martin PG, Robert-Granie C, Besse P. Sparse canonical methods for biological data integration: Application to a cross-platform study. BMC Bioinformatics. 2009;10:34.

151. Le Cao KA, Gonzalez I, Dejean S. Integromics: An r package to unravel relationships between two omics datasets. Bioinformatics. 2009 Nov 1;25:2855-6.

152. Tsukahara T, Koyama H, Okada M, Ushida K. Stimulation of butyrate production by gluconic acid in batch culture of pig cecal digesta and identification of butyrate-producing bacteria. J Nutr. 2002 Aug;132:2229-34.

153. Louis P, Flint HJ. Diversity, metabolism and microbial ecology of butyrate-producing bacteria from the human large intestine. FEMS Microbiol Lett. 2009 May;294:1-8.

154. Cummings JH, Pomare EW, Branch WJ, Naylor CP, Macfarlane GT. Short chain fatty acids in human large intestine, portal, hepatic and venous blood. Gut. 1987 Oct;28:1221-7.

155. Donohoe DR, Garge N, Zhang X, Sun W, O'Connell TM, Bunger MK, Bultman SJ. The microbiome and butyrate regulate energy metabolism and autophagy in the mammalian colon. Cell Metab. 2011 May 4;13:517-26.

156. Bassaganya-Riera J, DiGuardo M, Viladomiu M, de Horna A, Sanchez S, Einerhand AW, Sanders L, Hontecillas R. Soluble fibers and resistant starch ameliorate disease activity in interleukin-10-deficient mice with inflammatory bowel disease. J Nutr. 2011 Jul;141:1318-25.

157. Vijay-Kumar M, Aitken JD, Carvalho FA, Cullender TC, Mwangi S, Srinivasan S, Sitaraman SV, Knight R, Ley RE, Gewirtz AT. Metabolic syndrome and altered gut microbiota in mice lacking toll-like receptor 5. Science. 2010 Apr 9;328:228-31.

158. Alex S, Lange K, Amolo T, Grinstead JS, Haakonsson AK, Szalowska E, Koppen A, Mudde K, Haenen D, Al-Lahham S, et al. Short chain fatty acids stimulate angiopoietin-like 4 synthesis in human colon adenocarcinoma cells by activating ppary. Mol Cell Biol. 2013;33:1303-16.

159. Hontecillas R, Bassaganya-Riera J. Peroxisome proliferator-activated receptor gamma is required for regulatory cd4+ t cell-mediated protection against colitis. J Immunol. 2007 Mar 1;178:2940-9.

160. Bassaganya-Riera J, Hontecillas R. Cla and n-3 pufa differentially modulate clinical activity and colonic ppar-responsive gene expression in a pig model of experimental ibd. Clin Nutr. 2006 Jun;25:454-65.

161. Lewis JD, Lichtenstein GR, Deren JJ, Sands BE, Hanauer SB, Katz JA, Lashner B, Present DH, Chuai S, Ellenberg JH, et al. Rosiglitazone for active ulcerative colitis: A randomized placebo-controlled trial. Gastroenterology. 2008 Mar;134:688-95.

162. Bassaganya-Riera J, Reynolds K, Martino-Catt S, Cui Y, Hennighausen L, Gonzalez F, Rohrer J, Benninghoff AU, Hontecillas R. Activation of ppar gamma and delta by conjugated linoleic acid mediates protection from experimental inflammatory bowel disease. Gastroenterology. 2004 Sep;127:777-91.

163. Perdomo G, Kim DH, Zhang T, Qu S, Thomas EA, Toledo FG, Slusher S, Fan Y, Kelley DE, Dong HH. A role of apolipoprotein d in triglyceride metabolism. J Lipid Res. 2010 Jun;51:1298-311.

164. Souza da Silva C, Haenen D, Koopmans SJ, Hooiveld GJEJ, Bosch G, Bolhuis JE, Kemp B, Müller M, Gerrits WJJ. Effects of resistant starch on behaviour, satiety-related hormones and metabolites in growing pigs. Animal (submitted manuscript). 2013.

165. Mroz Z, Bakker GC, Jongbloed AW, Dekker RA, Jongbloed R, van Beers A. Apparent digestibility of nutrients in diets with different energy density, as estimated by direct and marker methods for pigs with or without ileo-cecal cannulas. J Anim Sci. 1996 Feb;74:403-12.

166. Koopmans SJ, van der Meulen J, Dekker R, Corbijn H, Mroz Z. Diurnal variation in insulin-stimulated systemic glucose and amino acid utilization in pigs fed with identical meals at 12-hour intervals. Horm Metab Res. 2006 Sep;38:607-13.

167.   de Wit NJ, Bosch-Vermeulen H, de Groot PJ, Hooiveld GJ, Bromhaar MM, Jansen J, Muller M, van der Meer R. The role of the small intestine in the development of dietary fat-induced obesity and insulin resistance in c57bl/6j mice. BMC Med Genomics. 2008;1:14.

168.   Roediger WE. Utilization of nutrients by isolated epithelial cells of the rat colon. Gastroenterology. 1982 Aug;83:424-9.

169.   Fleming SE, Fitch MD, DeVries S, Liu ML, Kight C. Nutrient utilization by cells isolated from rat jejunum, cecum and colon. J Nutr. 1991 Jun;121:869-78.

170.   Kussmann M, Rezzi S, Daniel H. Profiling techniques in nutrition and health research. Curr Opin Biotechnol. 2008 Apr;19:83-99.

171.   Brettschneider J, Collin F, Bolstad BM, Speed TP. Quality assessment for short oligonucleotide microarray data. Technometrics. 2008 Aug;50:241-64.

172.   Smyth GK. Linear models and empirical bayes methods for assessing differential expression in microarray experiments. Stat Appl Genet Mol Biol. 2004;3:Article3.

173.   Yao F, Coquery J, Le Cao KA. Independent principal component analysis for biologically meaningful dimension reduction of large biological data sets. BMC Bioinformatics. 2012;13:24.

174.   Plaisier SB, Taschereau R, Wong JA, Graeber TG. Rank-rank hypergeometric overlap: Identification of statistically significant overlap between gene-expression signatures. Nucleic Acids Res. 2010 Sep;38:e169.

175.   Delmee E, Cani PD, Gual G, Knauf C, Burcelin R, Maton N, Delzenne NM. Relation between colonic proglucagon expression and metabolic response to oligofructose in high fat diet-fed mice. Life Sci. 2006 Aug 1;79:1007-13.

176.   Yan H, Potu R, Lu H, Vezzoni de Almeida V, Stewart T, Ragland D, Armstrong A, Adeola O, Nakatsu CH, Ajuwon KM. Dietary fat content and fiber type modulate hind gut microbial community and metabolic markers in the pig. PLoS One. 2013;8:e59581.

177.   Cani PD, Amar J, Iglesias MA, Poggi M, Knauf C, Bastelica D, Neyrinck AM, Fava F, Tuohy KM, Chabo C, et al. Metabolic endotoxemia initiates obesity and insulin resistance. Diabetes. 2007 Jul;56:1761-72.

178.   Cani PD, Neyrinck AM, Fava F, Knauf C, Burcelin RG, Tuohy KM, Gibson GR, Delzenne NM. Selective increases of bifidobacteria in gut microflora improve high-fat-diet-induced diabetes in mice through a mechanism associated with endotoxaemia. Diabetologia. 2007 Nov;50:2374-83.

179.   Kimura I, Ozawa K, Inoue D, Imamura T, Kimura K, Maeda T, Terasawa K, Kashihara D, Hirano K, Tani T, et al. The gut microbiota suppresses insulin-mediated fat accumulation via the short-chain fatty acid receptor gpr43. Nat Commun. 2013;4:1829.

180.   Cheng HH, Lai MH. Fermentation of resistant rice starch produces propionate reducing serum and hepatic cholesterol in rats. J Nutr. 2000 Aug;130:1991-5.

181.   Demigne C, Morand C, Levrat MA, Besson C, Moundras C, Remesy C. Effect of propionate on fatty acid and cholesterol synthesis and on acetate metabolism in isolated rat hepatocytes. Br J Nutr. 1995 Aug;74:209-19.

182.   Black AL, Kleiber M. The transfer of carbon from propionate to amino acids in intact cows. J Biol Chem. 1958 May;232:203-9.

183.   Hallert C, Bjorck I, Nyman M, Pousette A, Granno C, Svensson H. Increasing fecal butyrate in ulcerative colitis patients by diet: Controlled pilot study. Inflamm Bowel Dis. 2003 Mar;9:116-21.

184.   Albenberg LG, Lewis JD, Wu GD. Food and the gut microbiota in inflammatory bowel diseases: A critical connection. Curr Opin Gastroenterol. 2012 Jul;28:314-20.

185.   Haenen D, Souza da Silva C, Zhang J, Koopmans SJ, Bosch G, Vervoort J, Kemp B, Smidt H, Muller M, Hooiveld GJEJ. Dietary resistant starch improves mucosal gene expression profile and luminal microbiota composition in porcine colon. 2013.

186.   Michel CI, Holley CL, Scruggs BS, Sidhu R, Brookheart RT, Listenberger LL, Behlke MA, Ory DS, Schaffer JE. Small nucleolar rnas u32a, u33, and u35a are critical mediators of metabolic stress. Cell Metab. 2011 Jul 6;14:33-44.

187.   Wu S, Li RW, Li W, Li CJ. Transcriptome characterization by rna-seq unravels the mechanisms of butyrate-induced epigenomic regulation in bovine cells. PLoS One. 2012;7:e36940.

188.   Darzi J, Frost GS, Robertson MD. Do scfa have a role in appetite regulation? Proc Nutr Soc. 2011 Feb;70:119-28.

189.   Bolhuis JE, van den Brand H, Bartels AC, Oostindjer M, van den Borne JJGC, Kemp B, Gerrits WJJ. Effects of fermentable starch on behaviour of growing pigs in barren or enriched housing. Applied Animal Behaviour Science. 2010 Mar;123:77-86.

190.   de Leeuw JA, Jongbloed AW, Spoolder HAM, Verstegen MWA. Effects of hindgut fermentation of non-starch polysaccharides on the stability of blood glucose and insulin levels and physical activity in empty sows. Livestock Production Science. 2005 Sep 30;96:165-74.

191.   Bureau CV. Cvb table pigs. Product Board Animal Feed. The Hague, The Netherlands; 2007.

192.   Sappok MA. In vitro fermentation capacity of hindgut microbiota in pigs in relation to dietary fibre.: Wageningen University, The Netherlands; 2012.

193.   Regmi PR, van Kempen TA, Matte JJ, Zijlstra RT. Starch with high amylose and low in vitro digestibility increases short-chain fatty acid absorption, reduces peak insulin secretion, and modulates incretin secretion in pigs. J Nutr. 2011 Jan 19.

194.   Giuberti G, Gallo A, Masoero F. Plasma glucose response and glycemic indices in pigs fed diets differing in in vitro hydrolysis indices. Animal. 2012 Jul;6:1068-76.

195.   Onaga T, Zabielski R, Kato S. Multiple regulation of peptide yy secretion in the digestive tract. Peptides. 2002 Feb;23:279-90.

196. Gerrits WJ, Bosch MW, van den Borne JJ. Quantifying resistant starch using novel, in vivo methodology and the energetic utilization of fermented starch in pigs. J Nutr. 2012 Feb;142:238-44.

197. Naslund E, Bogefors J, Skogar S, Gryback P, Jacobsson H, Holst JJ, Hellstrom PM. Glp-1 slows solid gastric emptying and inhibits insulin, glucagon, and pyy release in humans. Am J Physiol. 1999 Sep;277:R910-6.

198. Keszthelyi D, Troost FJ, Masclee AA. Understanding the role of tryptophan and serotonin metabolism in gastrointestinal function. Neurogastroenterol Motil. 2009 Dec;21:1239-49.

199. Bertrand RL, Senadheera S, Markus I, Liu L, Howitt L, Chen H, Murphy TV, Sandow SL, Bertrand PP. A western diet increases serotonin availability in rat small intestine. Endocrinology. 2011 Jan;152:36-47.

200. Kemperman RFJ, Bruins S, Te Lintelo JTV, Van der Dijs FPL, Erwich JJHM, Landman H, Muskiet FD, Kema IP, Muskiet FAJ. Relation between platelet serotonin and feeding mode in newborns suggests that gut motor activity is a determinant of platelet serotonin content. Biog Amines. 2007;21:260-72.

201. Bolhuis JE, van den Brand H, Staals S, Gerrits WJJ. Effects of pregelatinized vs. Native potato starch on intestinal weight and stomach lesions of pigs housed in barren pens or on straw bedding. Livest Sci. 2007 May 15;109:108-10.

202. Manocha M, Khan WI. Serotonin and gi disorders: An update on clinical and experimental studies. Clin Transl Gastroenterol. 2012;3:e13.

203. Fernstrom JD, Wurtman RJ. Brain serotonin content: Physiological regulation by plasma neutral amino acids. Science. 1972 Oct 27;178:414-6.

203. Fernstrom JD, Wurtman RJ. Brain serotonin content: Physiological regulation by plasma neutral amino acids. Science. 1972 Oct 27;178:414-6.

204. Magalhaes CP, de Freitas MF, Nogueira MI, Campina RC, Takase LF, de Souza SL, de Castro RM. Modulatory role of serotonin on feeding behavior. Nutr Neurosci. 2010 Dec;13:246-55.

205. Foltin RW. Effects of amphetamine, dexfenfluramine, diazepam, and other pharmacological and dietary manipulations on food "seeking" and "taking" behavior in non-human primates. Psychopharmacology (Berl). 2001 Oct;158:28-38.

206. Bolhuis JE, van den Brand H, Staals ST, Zandstra T, Alferink SJ, Heetkamp MJ, Gerrits WJ. Effects of fermentable starch and straw-enriched housing on energy partitioning of growing pigs. Animal. 2008 Jul;2:1028-36.

207. O'Hea EK, Leveille GA. Significance of adipose tissue and liver as sites of fatty acid synthesis in the pig and the efficiency of utilization of various substrates for lipogenesis. J Nutr. 1969 Nov;99:338-44.

208. Delzenne NM, Neyrinck AM, Backhed F, Cani PD. Targeting gut microbiota in obesity: Effects of prebiotics and probiotics. Nat Rev Endocrinol. 2011 Nov;7:639-46.

209. Morand C, Remesy C, Levrat MA, Demigne C. Replacement of digestible wheat starch by resistant cornstarch alters splanchnic metabolism in rats. J Nutr. 1992 Feb;122:345-54.

210. Leonhardt M, Langhans W. Fatty acid oxidation and control of food intake. Physiol Behav. 2004 Dec 30;83:645-51.

211. Goelema JO, Spreeuwenberg MAM, Hof G, van der Poel AFB, Tamminga S. Effect of pressure toasting on the rumen degradability and intestinal digestibility of whole and broken peas, lupins and faba beans and a mixture of these feedstuffs. Anim Feed Sci Tech. 1998;76:35-50.

212. Short FJ, Gorton P, Wiseman J, Boorman KN. Determination of titanium dioxide added as an inert marker in chicken digestibility studies. Anim Feed Sci Tech. 1996 Jun 15;59:215-21.

213. Myers WD, Ludden PA, Nayigihugu V, Hess BW. Technical note: A procedure for the preparation and quantitative analysis of samples for titanium dioxide. J Anim Sci. 2004 Jan;82:179-83.

214. Kluge H, Bolle M, Reuter R, Werner S, Zahlten W, Prudlo J. Serotonin in platelets: Comparative analyses using new enzyme immunoassay and hplc test kits and the traditional fluorimetric procedure. J Lab Med. 1999;23:360-4.

215. Van Kempen GMJ, van Brussel JL, Pennings EJM. Assay of platelet monoamine oxidase in whole blood. Clin Chim Acta. 1985;153:197-202.

216. de Graaf C, Blom WA, Smeets PA, Stafleu A, Hendriks HF. Biomarkers of satiation and satiety. Am J Clin Nutr. 2004 Jun;79:946-61.

217. Howarth NC, Saltzman E, Roberts SB. Dietary fiber and weight regulation. Nutr Rev. 2001 May;59:129-39.

218. Maljaars PW, Peters HP, Mela DJ, Masclee AA. Ileal brake: A sensible food target for appetite control. A review. Physiol Behav. 2008 Oct 20;95:271-81.

219. Hu S, Dong TS, Dalal SR, Wu F, Bissonnette M, Kwon JH, Chang EB. The microbe-derived short chain fatty acid butyrate targets mirna-dependent p21 gene expression in human colon cancer. PLoS One. 2011;6:e16221.

220. Thadikkaran L, Siegenthaler MA, Crettaz D, Queloz PA, Schneider P, Tissot JD. Recent advances in blood-related proteomics. Proteomics. 2005 Aug;5:3019-34.

221. Kilkenny C, Browne WJ, Cuthill IC, Emerson M, Altman DG. Improving bioscience research reporting: The arrive guidelines for reporting animal research. PLoS Biol. 2010;8:e1000412.

222. Hong H, Dragan Y, Epstein J, Teitel C, Chen B, Xie Q, Fang H, Shi L, Perkins R, Tong W. Quality control and quality assessment of data from surface-enhanced laser desorption/ionization (seldi) time-of flight (tof) mass spectrometry (ms). BMC Bioinformatics. 2005 Jul 15;6 Suppl 2:S5.

223. Le Cao KA, Boitard S, Besse P. Sparse pls discriminant analysis: Biologically relevant feature selection and graphical displays for multiclass problems. BMC Bioinformatics. 2011;12:253.

224. Jonathan MC, van den Borne JJGC, van Wiechen P, da Silva CS, Schols HA, Gruppen H. In vitro fermentation of 12 dietary fibres by faecal inoculum from pigs and humans. Food Chem. 2012 Aug 1;133:889-97.

225. Seibert V, Wiesner A, Buschmann T, Meuer J. Surface-enhanced laser desorption ionization time-of-flight mass spectrometry (seldi tof-ms) and proteinchip technology in proteomics research. Pathol Res Pract. 2004;200:83-94.

226. Issaq HJ, Conrads TP, Prieto DA, Tirumalai R, Veenstra TD. Seldi-tof ms for diagnostic proteomics. Anal Chem. 2003 Apr 1;75:148A-55A.

227. Ley RE, Lozupone CA, Hamady M, Knight R, Gordon JI. Worlds within worlds: Evolution of the vertebrate gut microbiota. Nat Rev Microbiol. 2008 Oct;6:776-88.

228. Bloemen JG, Olde Damink SW, Venema K, Buurman WA, Jalan R, Dejong CH. Short chain fatty acids exchange: Is the cirrhotic, dysfunctional liver still able to clear them? Clin Nutr. 2010 Jun;29:365-9.

229. Fernandes J, Vogt J, Wolever TM. Inulin increases short-term markers for colonic fermentation similarly in healthy and hyperinsulinaemic humans. Eur J Clin Nutr. 2011 Jun 29.

230. Duncan SH, Holtrop G, Lobley GE, Calder AG, Stewart CS, Flint HJ. Contribution of acetate to butyrate formation by human faecal bacteria. Br J Nutr. 2004 Jun;91:915-23.

231. Merks JW, Mathur PK, Knol EF. New phenotypes for new breeding goals in pigs. Animal. 2012 Apr;6:535-43.

232. Pang X, Hua X, Yang Q, Ding D, Che C, Cui L, Jia W, Bucheli P, Zhao L. Inter-species transplantation of gut microbiota from human to pigs. ISME J. 2007 Jun;1:156-62.

233. Higgins JA, Brown MA, Storlien LH. Consumption of resistant starch decreases postprandial lipogenesis in white adipose tissue of the rat. Nutr J. 2006;5:25.

234. Belobrajdic DP, King RA, Christophersen CT, Bird AR. Dietary resistant starch dose-dependently reduces adiposity in obesity-prone and obesity-resistant male rats. Nutr Metab (Lond). 2012;9:93.

235. Souza da Silva C, Bosch G, Bolhuis JE, Stappers LJN, van Hees HMJ, Gerrits WJJ, Kemp B. Potential of alginate and resistant starch to modify feeding patterns and performance in ad libitum-fed growing pigs. J Anim Sci. 2013.

Samenvatting

Obesitas is wereldwijd uitgegroeid tot een groot probleem voor de volksgezondheid, omdat het geassocieerd is met het zogenaamde metabool syndroom, een combinatie van risicofactoren die tegelijk aanwezig zijn en die het risico op hart- en vaatziekten en type 2 diabetes verhogen. Er is aangetoond dat voedingsvezels, de eetbare bestanddelen van planten die niet verteerd en geabsorbeerd worden in de dunne darm van de mens, belangrijk zijn ter preventie van obesitas en het metabool syndroom. Dit verband kan deels worden verklaard door de toegenomen mate van verzadiging als gevolg van de consumptie van vezels. Voedingsvezels kunnen worden gefermenteerd door de bacteriën, ook wel de microbiota genoemd, die aanwezig zijn in de dikke darm (caecum en colon), wat leidt tot de productie van korte-keten vetzuren. De invloed van voedingsvezels op verzadiging kan deels worden toegeschreven aan de productie van deze korte-keten vetzuren. Het doel van het onderzoek beschreven in dit proefschrift was om de effecten van fermentatie in de dikke darm in kaart te brengen, met daarbij een specifieke focus op de gevolgen voor metabolisme en verzadiging. Gedetailleerde achtergrondinformatie en een beschrijving van de zogeheten 'omics technieken' die zijn toegepast voor het verkrijgen van de resultaten staan beschreven in **Hoofdstuk 1**.

Resistent zetmeel (RS) is een voedingsvezel die in hoge mate wordt gefermenteerd door de microbiota in de dikke darm. **Hoofdstuk 2** beschrijft een experiment waarin volwassen zeugen gedurende 2 weken een dieet met veel RS consumeerden. Monsters afkomstig uit verschillende darmdelen werden verzameld om de microbiota samenstelling en de concentraties van de korte-keten vetzuren in het lumen te bepalen, en om de expressie van genen die betrokken zijn bij de opname en signalering van korte-keten vetzuren en de regulatie van verzadiging in het darmweefsel te meten. We laten zien dat RS volledig wordt afgebroken in het caecum. Zowel in het caecum als in het colon zagen we verschillen in de microbiota samenstelling tussen RS-gevoede varkens en varkens die een verteerbaar zetmeel (DS) dieet hadden geconsumeerd. In het colon van RS-gevoede varkens namen onder andere de butyraat-producerende *Faecalibacterium prausnitzii* toe, die zijn geassocieerd met een gezonde darm, terwijl potentieel pathogene *Gammaproteobacteria* in verminderde mate aanwezig waren. In RS-gevoede varkens waren de korte-keten vetzuurconcentraties in caecum en colon en de genexpressie van glucagon (*GCG*; voorloper van verzadigingshormoon GLP-1) en de korte-keten vetzuur transporter SLC16A1 in het caecum significant hoger. Alles bij elkaar heeft deze studie laten zien dat RS de microbiota samenstelling, korte-keten vetzuurconcentraties en genexpressie in de varkensdarm beïnvloedt.

De effecten van RS zijn tevens onderzocht in een experiment in jonge groeiende

varkens. Deze dieren hadden een canule in het voorste deel van het colon voor herhaalde afname van weefselbiopten (voor bepaling genexpressieprofielen) en voor verzameling van de darminhoud (voor bepaling korte-keten vetzuurconcentraties en microbiota samenstelling). Om de interindividuele variatie zo klein mogelijk te houden, werden het DS en het RS dieet in een cross-over studie aan de varkens verstrekt gedurende 2 weken per dieet. **Hoofdstuk 3** beschrijft welke genen en metabole processen worden beïnvloed door RS in het voorste deel van het colon, zoals gemeten met behulp van microarray analyse. We zagen een verschuiving in het genexpressieprofiel van immuun regulatie naar vet- en energiemetabolisme als gevolg van RS consumptie. De nucleaire receptor *PPARG* werd geïdentificeerd als een potentiële centrale regulator. Bovendien verhoogde RS de aanwezigheid van bacteriën die geassocieerd zijn met een gezonde darm, terwijl de aanwezigheid van potentieel pathogene microbiële groepen verminderde.

Daarnaast is er een experiment uitgevoerd in muizen (**Hoofdstuk 4**), met als doel het vaststellen van het effect van het vetgehalte in de voeding op genexpressieprofielen in het colon na rectale toediening van de korte-keten vetzuren acetaat, propionaat en butyraat. Aan mannelijke C57BL/6J muizen werd een semisynthetisch laag vet of hoog vet dieet gevoerd vanaf 2 weken voor de start van de interventieperiode. Gedurende de interventie kregen de muizen een acetaat, propionaat, butyraat of een controle zoutoplossing rectaal geïnfundeerd op 6 opeenvolgende dagen, waarna het colon werd verzameld voor bepaling van de genexpressieprofielen. We hebben geconstateerd dat het vetgehalte van het voer een zeer grote invloed heeft op de verandering in genexpressie als gevolg van korte-keten vetzuren in het colon, voornamelijk na het toedienen van propionaat. Bovendien wijzen de dieet- en korte-keten vetzuur-afhankelijke veranderingen in genexpressie op de modulatie van diverse metabole processen. Genen betrokken bij oxidatieve fosforylering, vetafbraak, lipoproteïne metabolisme en cholesterol transport werden onderdrukt door acetaat en butyraat, terwijl propionaat leidt tot veranderingen in vetzuur- en sterol-biosynthese, en in aminozuur- en koolhydraat-metabolisme. Daarnaast lijkt een infusie met korte-keten vetzuren de genexpressieveranderingen geïnduceerd door een hoog vet dieet deels terug te draaien. Samengevat hebben we laten zien dat het vetgehalte in het dieet een belangrijke factor is die de metabole effecten na toediening van korte-keten vetzuren beïnvloedt.

Hoofdstuk 5 beschrijft de resultaten verkregen uit de studie die ook wordt beschreven in Hoofdstuk 3, waarbij echter de nadruk ligt op de tijdsafhankelijke veranderingen in gedrag, verzadigingshormonen en metabolieten als gevolg van RS. De postprandiale plasmaconcentraties van verzadigingshormonen en metabolieten

werden aan het eind van elke 2 weken durende periode gemeten door middel van herhaalde perifere bloedafnames via katheters. RS-gevoede varkens vertoonden minder voerbak-gericht gedrag en drinkgedrag dan DS-gevoede varkens en hadden hogere korte-keten vetzuurconcentraties in het plasma gedurende de dag. De postprandiale glucose, insuline en glucagon-like peptide-1 (GLP-1) responsen waren lager in RS-gevoede dan in DS-gevoede varkens, terwijl triglyceride concentraties hoger waren. Plasma serotonine concentraties, die gezien worden als een indicator voor de regulatie van verzadiging, waren lager in RS-gevoede dan in DS-gevoede varkens. Ondanks een lagere inname van metaboliseerbare energie, lijkt RS op basis van de gedragsobservaties verzadiging te verhogen. Verhoogde korte-keten vetzuurconcentraties en een verlaagde postprandiale glucose en insuline respons in plasma behoren tot de mogelijke onderliggende mechanismen voor RS-geïnduceerde verzadiging.

Het doel van de studie die wordt beschreven in **Hoofdstuk 6** was het achterhalen van de effecten van verschillende vezels op postprandiale eiwit- en metabolietprofielen in plasma. Minipigs kregen een controle (C) dieet toegewezen of een dieet dat lignocellulose (LC), pectine (PEC) of RS bevatte voor een periode van 8 dagen in een 4 x 4 Latijns vierkant. Er was gekozen voor vezels met verschillende physico-chemische eigenschappen; LC is een bulkvormende vezel, RS is een fermenteerbare vezel en PEC is zowel een visceuze als een fermenteerbare vezel. Op dag 8 van elke periode werden bloedmonsters uit de poortader en de carotus verzameld via katheters, zowel voor als op diverse tijdstippen na een *ad libitum* ochtendmaaltijd. In plasma zijn 973 peptiden en eiwitten gemeten. De eiwitprofielen na consumptie van het C en het LC dieet en de eiwitprofielen na consumptie van het PEC en het RS dieet kwamen het meest met elkaar overeen. Met alle diëten vond de grootste verschuiving in de aanwezige plasmaeiwitten plaats tussen 240 en 480 min na de maaltijd. In plasmamonsters uit de poortader en de carotus kwamen 44 respectievelijk 65 eiwitten differentieel tot expressie, afhankelijk van het vezeldieet en het postprandiale tijdstip. Verder zijn 24 metabolieten gemeten in portaal plasma, waaronder de korte-keten vetzuren acetaat, propionaat en butyraat. De concentraties van alle korte-keten vetzuren waren significant hoger na RS consumptie dan na C, LC en PEC consumptie. Dit experiment heeft laten zien dat de consumptie van diëten met fermenteerbare vezels resulteert in een ander plasma eiwitprofiel dan een dieet zonder vezels of een dieet dat een niet-fermenteerbare vezel bevat.

Drie belangrijke bevindingen worden beschreven in dit proefschrift. Ten eerste hebben we aangetoond dat de consumptie van RS de microbiota samenstelling

in het lumen van het colon verandert, met een afname in potentieel pathogene bacteriën en een toename in korte-keten vetzuur-producerende populaties. Ten tweede hebben we laten zien dat zowel na RS consumptie als na rectale toediening van korte-keten vetzuren veranderingen optreden in de genexpressie in het colon. Beide behandelingen induceerden veranderingen in metabole processen zoals energie-en vetmetabolisme en in immuun respons. Tot slot zagen we dat het vetgehalte in het dieet een grote invloed heeft op de veranderingen in genexpressie als gevolg van rectale toediening van korte-keten vetzuren. Deze belangrijkste resultaten worden in detail bediscussieerd in **Hoofdstuk 7**, evenals de voordelen en beperkingen van de gebruikte diermodellen en de betekenis van de bevindingen voor de humane gezondheid. Alles bij elkaar ondersteunt dit proefschrift de implementatie van fermenteerbare voedingsvezels in het humane eetpatroon met als doel het verbeteren van de darmgezondheid en het beperken van energie-inname en gewichtstoename, wat uiteindelijk kan helpen bij de preventie van obesitas en type 2 diabetes. Aanvullend onderzoek is echter noodzakelijk om de mechanismen te achterhalen die ten grondslag liggen aan de verbetering van de humane gezondheid door consumptie van fermenteerbare voedingsvezels.

Dankwoord

Vol trots presenteer ik jullie mijn proefschrift! Het was hard werken, maar gelukkig stond ik er niet alleen voor. Graag zou ik daarom alle mensen willen bedanken die me de afgelopen jaren hebben geholpen met het tot stand komen van dit proefschrift. Jullie steun was onmisbaar!

Allereerst wil ik mijn promotor en co-promotoren bedanken. Michael, dankzij je kritische houding wist je mijn onderzoek in de juiste richting te duwen. Bovendien heb ik veel van je geleerd en heeft je visie op de voedingswetenschap me geïnspireerd. Bas Kemp, hoewel we elkaar niet heel regelmatig zagen, kijk ik met een goed gevoel terug op de samenwerking binnen ons interdisciplinaire project. Je inbreng tijdens vergaderingen is de voortgang van het project sterk ten goede gekomen. Guido, als mijn directe begeleider wil ik je bedanken voor alle tijd en energie die je hebt gestoken in mijn project. Hoewel je altijd druk in de weer bent met duizend verschillende dingen kon ik op je rekenen wanneer ik je input echt nodig had. Ook tijdens de experimenten en op het lab heb je me geholpen, terwijl dat absoluut niet de fijnste klusjes waren. Je energie en optimisme hebben me gemotiveerd op de momenten dat ik dreigde vast te lopen. Ik weet niet hoever ik zou zijn gekomen zonder jouw inzet, ik ben je heel erg dankbaar!

Graag wil ik alle andere mensen bedanken die betrokken waren bij het IP/OP project. Bedankt voor de samenwerking! Liesbeth Bolhuis, Walter Gerrits, Monica Mars en Henk Schols wil ik in het bijzonder bedanken voor de relevante input tijdens project meetings. Carol, thank you so much for the nice collaboration in the past years! I could always count on quick replies to my e-mails whenever I had a question, and I'm happy you taught me a lot about pigs. I was particularly happy to have you around during the study in Lelystad, where we stayed over in the middle of the Flevopolder, seemingly disconnected from the world outside. Good luck in your future career! Joost, ik vond het erg jammer dat je zo vroeg het project moest verlaten, want je had altijd een duidelijk overzicht van wat er zich afspeelde binnen het project en je brede kennis van mijn onderwerp heeft me echt geholpen tijdens de opstartfase. Guido Bosch, bedankt voor het leveren van een belangrijke bijdrage aan de voorbereiding, uitvoering en de data analyse (korte-keten vetzuren, statistiek) van de varkensproeven! Bovendien was je inzet essentieel voor het plannen van meetings en het op elkaar afstemmen van papers. Anne and Melliana, it was very nice collaborating with you as fellow PhD students on the same project.

Graag bedank ik iedereen die betrokken was bij de experimenten in Lelystad. Sietse Jan, heel erg bedankt voor je hulp tijdens de voorbereidingen, de uitvoering en de dataverwerking. Jan van der Meulen, bedankt dat we gebruik konden maken van je expertise. Leo Kruijt, jou wil ik bedanken voor het uitvoeren van de SELDI-

TOF-MS analyses. Je was een goede begeleider op het lab van wie ik veel heb geleerd. Je nam de tijd om alles goed uit te leggen en ik vond het fantastisch dat je bereid was om flink door te pakken in de decembermaand om alle analyses voor de jaarwisseling af te krijgen.

I'd also like to thank Jing, Hauke and Odette from the Microbiology Department for the fruitful collaboration. The results on microbiota composition have become an essential part of my thesis, which I could not have imagined beforehand. Thanks for your efforts!

Daarnaast wil ik graag de mensen van het CKP bedanken, in het bijzonder Judith, Bert, Wilma en Rene. Bedankt voor jullie hulp bij de voorbereiding en de uitvoering van de muizenexperimenten!

Van IP/OP en het CKP door naar NMG. Ik wil graag al mijn (oud) NMG collega's bedanken voor hun hulp, de input tijdens lab meetings, maar natuurlijk ook voor de gezelligheid tijdens de lunch en uitjes wat maakt dat ik met een fijn gevoel terugkijk op mijn aio-tijd.

In het bijzonder wil ik mijn (oud)kamergenoten bedanken. Ageeth, Sandra, Maryam en Noortje, het was erg gezellig om met jullie de kamer te delen. Juri, je werkt nog niet zo heel lang bij ons, maar ik waardeer je ontspannen houding die zorgt voor wat rust op de kamer. Veel succes de komende jaren! Rinke, fijn dat ik zo vaak op je aanwezigheid kon rekenen als ik in het weekend moest doorwerken. Diederik, de kamer zou een stuk minder levendig zijn geweest zonder jou. Het was bovendien erg handig dat je 3 weken eerder promoveert dan ik, zodat ik alles een beetje van je kon afkijken. Bedankt voor het delen van documenten, ideeën en promotiestress! De tijd zal nu moeten leren of ik bepaalde gewoonten waar onze kamer zo berucht om is ga overnemen. Maar aangezien ik dit alles al jaren heb weten te verdragen, denk ik toch echt dat ik immuun ben ;-).

Graag bedank ik ook de andere aio's van NMG en Pharma. Frits, Fenni, Ya, Parastoo, Wieneke and Neeraj, it was nice to get to know you and good luck during the rest of your PhD project! Nikkie, Jvalini en Inge, jullie wil ik bedanken voor de prettige sfeer iedere keer als ik een bezoekje bracht aan jullie kamer, maar ook voor de gezelligheid buiten de werkuren. Katja, it was nice collaborating with you. Your sense of humour really helped me through my moments of doubt and stress. I think we can be proud of our joint paper, which really improved thanks to your ideas and knowledge. Keep up the good work! I'm already curious about your propositions ;-).

I'd also like to thank the students who helped me during my project. Ingrid, thanks for your help with the pilot mouse experiment. Marlene and Natasa, thank you for helping me in the lab with the data collection.

Dan zijn er nog meer mensen die ik zeker niet wil vergeten te noemen. Sander, bedankt voor je interesse in mijn project. Ik ben blij dat mijn resultaten van waarde waren voor een prachtige publicatie. Shohreh, thank you for performing an enormous amount of lab work for me. I could always count on you and you gave me confidence in my lab work. Jenny en Mechteld, bedankt voor het uitvoeren van de microarray-analyses. Jessica, bedankt voor het delen van je ideeën over mijn data, je hulp bij de varkensproef en voor de gezelligheid tijdens de iets minder werk-gerelateerde activiteiten.

Daarnaast wil ik graag mijn opponenten bedanken voor het plaatsnemen in mijn promotiecommissie en voor de tijd die ze hebben gestoken in het lezen van mijn proefschrift.

Uiteraard wil ik ook mijn paranimfen Rianne en Milène bedanken. Ik ben heel blij dat jullie allebei meteen enthousiast waren toen ik vroeg of jullie aan mijn zij wilden staan tijdens mijn verdediging. Rianne, bedankt voor de vele goede gesprekken tijdens onze duurloopjes en etentjes over de ups en downs waar elke aio mee te maken krijgt. Ik vind het ook heel fijn dat je inmiddels hebt meegemaakt hoe het is om te promoveren. Je hebt me echt het vertrouwen gegeven dat het mij ook zal lukken. Milène, als kamergenootje wil ik je bedanken voor de gesprekken als we allebei even geen zin hadden om te werken. Helemaal in de meest recente samenstelling van de kamer was ik blij dat je zo goed tegen de bizarre uitlatingen in kon gaan ;-). Bovendien ben je altijd heel behulpzaam geweest, of het nu ging om het oplossen van een computerprobleem of een lift naar Hoofddorp. Thanks!

Graag wil ik ook mijn vrienden bedanken die de afgelopen jaren veel interesse hebben getoond in het verloop van mijn aio-project. Jullie zijn heel belangrijk voor me geweest! Ik wil ook de mensen bedanken die ik heb leren kennen bij WSKOV en die ervoor gezorgd hebben dat de repetities voor mij een perfecte manier waren om te ontspannen. Al mijn hardloopmaatjes bij Tartlétos en Pallas: dankzij jullie ging ik altijd met plezier naar de trainingen! In het bijzonder wil ik de dames uit de lustrumcommissie (Hannie, Esther, Carolien, Mieke, Paulien en Imke) bedanken voor hun betrokkenheid en de gezellige etentjes, feestjes en uitjes.

Dit laatste paragraafje heb ik gereserveerd voor het bedanken van mijn familie. Ik wil mijn oma's bedanken voor de goede zorgen en voor hun interesse in hoe het op mijn werk gaat. Mark, fantastisch dat je bereid was me te helpen met de lay-out van mijn boekje en met het ontwerpen van de cover! Het kostte alles bij elkaar nog best veel tijd, maar het resultaat is prachtig. Bedankt, ik ben super trots op je! Pap en mam, op jullie onvoorwaardelijke steun heb ik altijd kunnen rekenen. Wanneer de zaken iets anders liepen dan ik had gehoopt dan waren jullie er voor me met bemoedigende woorden, advies of gewoon een luisterend oor. Jullie vertrouwen in mij heeft me de afgelopen jaren gemotiveerd om door te zetten. Jullie betekenen alles voor me.

Daniëlle

About the author

Curriculum vitae

Daniëlle Haenen was born on the 26th of July 1985 in Heemstede, the Netherlands. After completing secondary school at the KSH in Hoofddorp in 2003, she started the Bachelor's programme Nutrition and Health at Wageningen University. After receiving her Bachelor's degree in 2006, she continued with the Master's programme Nutrition and Health and specialised in Molecular Nutrition. During her Master she performed a thesis at the chair of Nutrition, Metabolism and Genomics on the effect of DNA demethylation on the differentiation of osteoblasts and adipocytes. She carried out her second thesis at Numico Research, where she studied ectopic fat accumulation in liver. Under supervision of Prof. dr. K.H. Herzig, Daniëlle performed her internship at the Molecular Physiology group of the A.I. Virtanen Institute for Molecular Sciences in Kuopio (Finland), where she studied the effects of orexin A and glucose level on insulin secretion in pancreatic beta cell lines. She received her Master's degree in September 2008, and in December 2008 she was appointed as a PhD researcher at the Division of Human Nutrition of Wageningen University. Her project was part of the IP/OP project *Satiety and Satisfaction* and entitled *Fermentation in the gut prolongs satiety*. She performed her PhD project at the chair of Nutrition, Metabolism and Genomics, supervised by Prof. dr. M. Müller and dr. G.J.E.J. Hooiveld. The results of the research, focussing on the impact of fermentable dietary fibre consumption on metabolism and satiety, are described in this thesis. In addition, Daniëlle attended several (international) conferences and courses during her PhD project, and she was involved in teaching.

List of publications

Haenen D, Zhang J, Souza da Silva C, Bosch G, van der Meer IM, van Arkel J, van den Borne JJ, Pérez Gutiérrez O, Smidt H, Kemp B, Müller M, Hooiveld GJ. A Diet High in Resistant Starch Modulates Microbiota Composition, SCFA Concentrations, and Gene Expression in Pig Intestine. *The Journal of Nutrition* **2013**; 143: 274–283.

Jonathan MC, **Haenen D**, Souza da Silva C, Bosch G, Schols HA, Gruppen H. Influence of a diet rich in resistant starch on the degradation of non-starch polysaccharides in the large intestine of pigs. *Carbohydrate Polymers* **2013**; 93: 232-239.

Alex S, Lange K., Amolo T, Grinstead JS, Haakonsson AK, Szalowska E, Koppen A, Mudde K, **Haenen D**, Al-Lahham S, Roelofsen H, Houtman R, van der Burg B, Mandrup S, Bonvin AM, Kalkhoven E, Muller M, Hooiveld GJ, Kersten S. Short chain fatty acids stimulate Angiopoietin-like 4 synthesis in human colon adenocarcinoma cells by activating PPARgamma. *Molecular and Cellular Biology* **2013**, 33(7): 1303-16.

Haenen D, Souza da Silva C, Zhang J, Koopmans SJ, Bosch G, Vervoort J, Gerrits WJ, Kemp B, Smidt H, Müller M, Hooiveld GJ. Resistant Starch Induces Catabolic but Suppresses Immune Pathways, and Changes the Microbiome in Porcine Proximal Colon. *Submitted for publication*

Haenen D, Lange K, Keshtkar S, Müller M, Hooiveld GJ. Short-chain fatty acid-induced changes in colonic gene expression depend on dietary fat content in mice. *Submitted for publication*

Souza da Silva C, **Haenen D**, Koopmans SJ, Hooiveld GJ, Bosch G, Bolhuis JE, Kemp B, Müller M, Gerrits WJ. Effects of resistant starch on behaviour, satiety-related hormones and metabolites in growing pigs. *Submitted for publication*

Haenen D, Koopmans SJ, Kruijt L., Smits M., Vervoort J., Müller M., Hooiveld GJ. Postprandial kinetics of the plasma proteome and metabolome in pigs consuming fibres with different physicochemical properties. *Manuscript in preparation*

Overview of completed training activities

Discipline specific activities
Wageningen Nutritional Sciences Forum, Arnhem, 2009
NuGO course microarray analysis, Maastricht, 2009
8th Masterclass Nutrigenomics, Wageningen, 2009
NuGO week, Montecatini Terme, 2009
Symposium Pigs: 'The missing link?', Lelystad, 2010
NWO Nutrition Meeting, Deurne, 2010
Proteomics course, Wageningen, 2011
Excursion Technical University of Munich, Freising, 2011
NuGO week, Wageningen, 2011
NWO Nutrition Meeting, Deurne, 2011
13th Gut Day Symposium, Wageningen, 2011
Masterclass 'Analysis using R', Wageningen, 2012
5th International Dietary Fibre Conference, Rome, 2012
NWO Nutrition Meeting, Deurne, 2012

General courses
VLAG PhD week, Bilthoven, 2009
Laboratory Animal Science Course, Wageningen, 2009
Effective behaviour in your professional surroundings, Wageningen, 2010
Scientific writing, Wageningen, 2011
Career Orientation, Wageningen, 2012

Optional activities
Preparation of research proposal, 2009
PhD tour Human Nutrition, Scandinavia, 2009
Journal club of Human Nutrition and NMG group, 2008-2010
NMG group weekly scientific meetings, 2008-2012

Cover and layout design: Mark Haenen
Printing: GVO drukkers en vormgevers B.V. | Ponsen & Looijen, Ede, the Netherlands